Identification of regulatory factors that control the synthesis of the small regulatory RNA CsrC in *Yersinia pseudotuberculosis*

Von der Fakultät für Lebenswissenschaften

der Technischen Universität Carolo-Wilhelmina

zu Braunschweig

zur Erlangung des Grades einer

Doktorin der Naturwissenschaften

(Dr. rer. nat.)

genehmigte

D i s s e r t a t i o n

von Stephanie Christine Seekircher

aus Neuss

1. Referentin: Prof. Dr. Petra Dersch
2. Referent: Prof. Dr. André Fleißner
eingereicht am: 31.03.2014
mündliche Prüfung (Disputation) am: 13.06.2014

Druckjahr 2014

Vorveröffentlichungen der Dissertation

Teilergebnisse aus dieser Arbeit wurden mit Genehmigung der Fakultät für Lebenswissenschaften, vertreten durch die Mentorin der Arbeit, in folgenden Beiträgen vorab veröffentlicht:

Tagungsbeiträge

Seekircher S., Böhme K., Heroven A.K., Dersch P.: Synthesis of the regulatory RNA CsrC in *Yersinia pseudotuberculosis* is mediated by the nucleoid –associated protein YmoA (Poster). II. Summer School on Pathogen-Host interactions, Münster (2011).

Böhme K., Heroven A.K., Seekircher S., Dersch P.: Synthesis of the regulatory RNA CsrC in *Yersinia pseudotuberculosis* is mediated by the RNA-binding protein CsrA, the nucleoid-associated proteins YmoA, H-NS and the RNA-chaperon Hfq (Poster). 62. Mosbacher Kolloquium, Mechanisms of RNA-mediated regulation, Mosbach (2011).

Heroven A.K., Böhme K., Seekircher S., Dersch P.: sRNA-mediated control of the primary invasion factor invasin in *Yersinia pseudotuberculosis* (Vortrag). Schwerpunkttreffen des SPP 1258, Sensorische und regulatorische RNAs in Prokaryoten, Kassel (2011).

Seekircher S., Böhme K., Heroven A.K., Dersch P.: sRNA-mediated control of the primary invasion factor invasin in *Yersinia pseudotuberculosis* (Poster). Jahrestagung der Vereinigung Allgemeiner und Angewandter Mikrobiologie, Tübingen (2012).

Seekircher S., Böhme K., Heroven A.K., Dersch P.: sRNA-mediated control of the primary invasion factor invasin in *Yersinia pseudotuberculosis* (Poster). 3. Nationale *Yersinia* Konferenz, Tübingen (2012).

Seekircher S., Böhme K., Heroven A.K., Dersch P.: sRNA-mediated control of the primary invasion factor invasin in *Yersinia pseudotuberculosis* (Poster). Schwerpunkttreffen des SPP 1258, Sensorische und regulatorische RNAs in Prokaryoten, Bochum (2012).

Seekircher S., Böhme K., Heroven A.K., Thiermann T., Dersch P.: New regulators of the *Yersinia* Csr System (Poster). 3rd Conference on Regulating with RNA in Bacteria, Würzburg (2013).

Table of contents

List of Tables

List of Figures

List of Abbreviations

A	adenine
A_{xx}	absorption$_{nm}$
ad.	to (lat.)
AHT	anhydrotetracyclin
Amp	ampicillin
appr.	approximately
ATP	adenosin-triphosphate
B.	*Burkholderia*
bp	base pairs
BLAST	basic local alignment search tool
BHI	brain-heart-infusion
°C	degree Celsius
C	cytosine
cAMP	cyclic adenosine monophosphate
Cb	carbeniciliin
Cm	chloramphenicol
cm	centi meter
Cy	cyanine
Δ	deletion
dem.	demineralised
DF	dilution factor
DIG	digoxygenin
DMEM	Dulbecco's modified eagle medium
DNA	desoxyribonucleic acid
DNAse	desoxyribonuclease
DMF	dimethylformamide
dNTP	desoxyribonucleosid-triphosphate
dsDNA	double-stranded DNA
DTT	dithiothreitol
E.	*Escherichia* or *Erwinia*
EDTA	ethylenediaminetetraacetate
e.g.	exempli gratia (lat.)
et al.	et alit (lat.)
EtOH	ethanol
exp	exponential
F	Farad
F12	nutrient mixture
fig.	figure
g	gram

G	Guanin
HCl	hydrochloric acid
His	histidin
HPI	high pathogenicity island
ID	identity
IM	innermMembrane
IPTG	isopropyl-β-D-1-thiogalacto-pyranoside
Kan	kanamycin
kb	kilo bases
kDA	kilo Dalton
l	liter
L.	*Legionella*
lacZ	reporter gene encoding for β-galactosidase
LB	Luria-Bertani
LPS	mipopolysaccharide
µ	micro (1×10^{-6})
m	milli (1×10^{-3}) or meter
M	molar (mol/L)
MF	multiplication factor
min	minutes
MLN	mesenteric lymph node
mol	amount of substance ($6.022*10^{23}$ particles)
MOPS	3-(N-Morpholino)-propanesulfonic acid
N	any nucleotide
n	nano (1×10^{-9})
ng	nanogram
Ni-NTA	nickel-nitrilotriacetic acid
nm	nano meter
ns	not significant
nt	nucleotide
Ω	Ohm
OD	optical density
OM	outer membrane
ONPG	ortho-Nitrophenyl-β-D-galactopyranosid
ORF	open reading frame
ori	origin of replication
P.	*Pseudomonas*
p	pico
PAA	polyacrylamide
PAGE	polyacrylamide gel electrophoresis
PCR	polymeras chain reaction
pH	negative logarithm of H+ ions

PP	Peyer’s patches
QS	quorum sensing
RBS	ribosomal binding site
RNA	ribonucleic acid
RNase	ribonuclease
rpm	rotations per minute
RT	room temperature
RT-PCR	Reverse transcribed polymerase chain reaction
S	subunit
S.	*Salmonella*
SD	Shine-Dalgarne
SDS	sodiumdodecyl sulfate
sec	cecond
spp	species
SSC	saline-sodium citrate
ssDNA	single-stranded DNA
stat	stationary
Strep	streptactin
T	reaction time
T	Thymin
Tab.	table
Tet	tetracyclin
TAE	Tric-acetate
TBE	Tris-borate-EDTA
TEMED	tetramethylethylenediamine
Tris	Tris-(hydroxymethyl)-aminoethane
U	units
U	uridine
UTR	untranlsated region
UV	ultra violett
V	volume
V.	*Vibrio*
(v/v)	volume per volume
(w/v)	weight per volume
w/o	without
wt	wildtype
X-Gal	5-bromo-4-chloro-3-indoyl-β-D-galactopyranosid
Y.	*Yersinia*

1. Introduction

Over the last century infectious diseases were declining. Unfortunately since the 1980ies deaths by infectious diseases are re-emerging (Hughes, 2001). Bacteria were able to develop drug-resistance strategies and as a consequence of the global interconnection their genetic pool is interchanged more rapidly, evolving new and highly infectious diseases that challenge mankind (NRC, 1992; NRC, 2010).

In order to survive and compete in natural habitats, bacteria need to adapt their physiological state to their rapidly changing environments. In case of pathogenic bacteria the prompt acclimatization to host-conditions is crucial for a successful infection. Such global changes are governed by complex regulatory networks that control the expression of virulence factors necessary for colonization of and persistence within the host. Recently it became more and more evident that post-transcriptional control systems play a central role in host-pathogen interactions (Lucchetti-Miganeh *et al.*, 2008). One important representative of these post-transcriptional systems is the Csr (carbon storage regulator) system, which is found throughout the prokaryotes (Mercante *et al.*, 2006). It encompasses the RNA-binding protein CsrA that blocks ribosome binding at or near the Shine-Dalgarno sequence (SD) of its target mRNAs. Function of the CsrA protein is antagonized by two non-coding RNAs, CsrB and CsrC, constituting an sRNA-based regulon (Romeo, 1998; Baker *et al.*, 2002; Dubey *et al.*, 2003). During the past decades gene regulation by small RNAs (sRNAs) is considered as an emerging field with versatile regulatory mechanisms.

1.1. The genus *Yersinia*

The genus *Yersinia* was named after the Swiss-French bacteriologist Alexandre Émile Jean Yersin, who first described the plague bacillus in 1894 (Yersin, 1894). Yersiniae belong to the family of *Enterobacteriaceae*, which are Gram-negative, rod-shaped coccobacilli that bear a facultative anaerobic lifestyle. They grow at temperatures between 4°C and 43°C, but their optimal growth conditions are moderate temperatures between 20°C and 30°C. Due to the peritrichous flagella bacteria are motile under these conditions. Among the 18 different *Yersinia* species, three are human-specific pathogens - *Y. pestis*, *Y. enterocolitica* and *Y. pseuodtuberculosis* (Bottone, 1997; Drummond *et al.*, 2012; Carniel *et al*., 2006; Savin *et*

al., 2014). Although the routes of infection and clinical manifestations differ significantly among the three species, they all share a tropism for lymphoid tissue during the infectious process. Inside the host all three species have evolved weapons that enable the escape from the hosts immune defence system, in particular uptake and clearance by macrophages and neutrophils is prevented (Perry and Fetherston, 1997).

Y. pestis is the most infamous member of the genus as it is the causative agent of pneumonic and bubonic plague. It was responsible for three human pandemics (Justinian plague 5th - 7th century; Black death 13th - 15th century and modern plague 19th century) that drastically reduced the European population. *Y. pestis* evolved from *Y. pseudotuberculosis* only 1,500 to 20,000 years ago (Achtman *et al.*, 1999; Wren, 2003; Morelli *et al.*, 2010). In contrast to the enteropathogenic *Yersinia* species it causes highly infectious and severe diseases, which are manifested by fever, swollen buboes (which arise from bacteria that multiply within the draining lymph nodes) as well as haemorrhages, pneumonic and septicemic plague. Rodents (rats) are the primary reservoirs for this pathogenic agent, which is further transmitted to humans by the flea vector (Brubaker, 1991; Perry and Fetherston, 1997). Within the 21st century rare cases of plague occurred in the USA, whereas severe plague outbreaks challenged especially the African population. World-wide over 1,600 people died from the black death within the last ten years (Butler, 2013).

Besides *Y. pestis* also *Y. enterocolitica* and *Y. pseudotuberculosis* exhibit a zoonotic life-style. The latter two are found in soil and water reservoirs and are transmitted to humans via the fecal-oral route by contaminated food (milk-products, raw meat, plants) or drinking water. In case of *Y. enterocolitica* wildlife and domestic animals, especially pigs, serve as natural reservoirs (Bockemuhl and Roggentin, 2004; Fredriksson-Ahomaa *et al.*, 2007; de Boer *et al.*, 2008). Those two enteropathogenic species cause gut-associated diseases (yersiniosis) ranging from mild gastroenteritis to mesenteric lymphadenitis, enterocolitis and terminal ileitis and pseudoappendicitis; often accompanied by fever, vomiting and acute diarrhoea. In most cases such yersiniosis are self-limiting and only in rare cases sequelae of systemic infections lead to focal abscess formation in liver and kidney or to manifestations like the erythema nodosum and reactive arthritis (Paff, 1976; Naktin and Beavis, 1999; Oellerich *et al.*, 2007). Clinical manifestations strongly depend on the age and physical state of the patient. Young children are mainly faced by enterocolitis whereas older children and young adults mainly develop ileitis (Bottone, 1997). Specific virulence factors of all three

pathogenic species are encoded in so-called pathogenicity islands (PAIs) throughout the genome or are plasmid-derived. The enteropathogenic species carry the chromosomally encoded *inv* locus (renamed *invA*), which encodes for the adhesion and invasion factor invasin that mediates bacterial penetration of the epithelium (Marra and Isberg, 1997; Schubert *et al.*, 2004). The key virulence trait for a sophisticated defence strategy is the virulence plasmid (*Y. pestis* pCD1; *Y. pseudotuberculosis* pIB1). It encodes the type III secretion system, effector molecules essential for host-defence and the adhesin YadA. In contrast to the enteropathogenic *Yersinia* species, *Y. pestis* additionally harbours two more plasmids (pFRA, pPLA), which are essential for transmission and survival in the flea (Cornelis, 2002a; Chain *et al.*, 2004).

1.1.1. Pathogenesis and important virulence determinants of *Yersinia*

With regard to the most dramatic changes in virulence-gene expression one can distinguish between two major infection processes: the early infection phase and the ongoing infection phase. The early phase is characterized by bacterial survival in the environment and expression of so-called early virulence genes like invasin, which are needed for the initial attachment and invasion into the M-cells (microfold cells). Transition of the epithelial barrier requires adaptation of the entire metabolism to the nutrient supply of the new environment within the lymphatic tissue. Accordingly, the pathogen switches gene expression to defence and survival factors that facilitate evasion of the hosts immune system and extracellular proliferation (Trülzsch *et al.*, 2007).

After oral uptake *Y. pseudotuberculosis* passes through the gastrointestinal tract until it reaches the terminal part of the ileum (Hamama *et al.*, 1992; Bottone, 1997). Initially bacteria need to attach to and traverse through the mucus layer to reach the intestinal epithelium. To get access to the lymphatic tissue beneath the epithelium, bacteria specifically adhere to the β_1 integrins on the apical part of the M-cells, which are localized above the Peyer's patches (Marra and Isberg, 1997). This initial adhesion is mediated by the rod-like ~100 kDa outer-membrane protein invasin (InvA*)* that efficiently binds to the $\alpha_5\beta_1$ integrin receptors on the M-cells. Invasin exhibits a 100-fold higher binding affinity to these receptors than the natural ligand fibronectin, rendering it a potent competitor for a successful infection. Ligand binding leads to integrin clustering, which triggers cytoskeletal rearrangements to form membrane protrusions that finally internalize the bacteria by the

so-called zipper mechanism (Isberg and Leong, 1990; Dersch and Isberg, 1999; Hamburger *et al.*, 1999; Xiong *et al.*, 2001; Grassl *et al.*, 2003; Fairman *et al.*, 2012). In addition to the formation of filopodia or pseudopodia M-cells bear a natural phagocytic activity, which further facilitates bacterial entry into the lamina propria. Subsequently, bacteria penetrate the underlying Peyer's patches and disseminate to mesenteric lymph nodes and deeper organs like liver, spleen and kidney (Grützkau *et al.*, 1990; Autenrieth and Firsching, 1996; Bottone, 1997; Neutra, 1999; Barnes *et al.*, 2006) (Fig. 1.1).

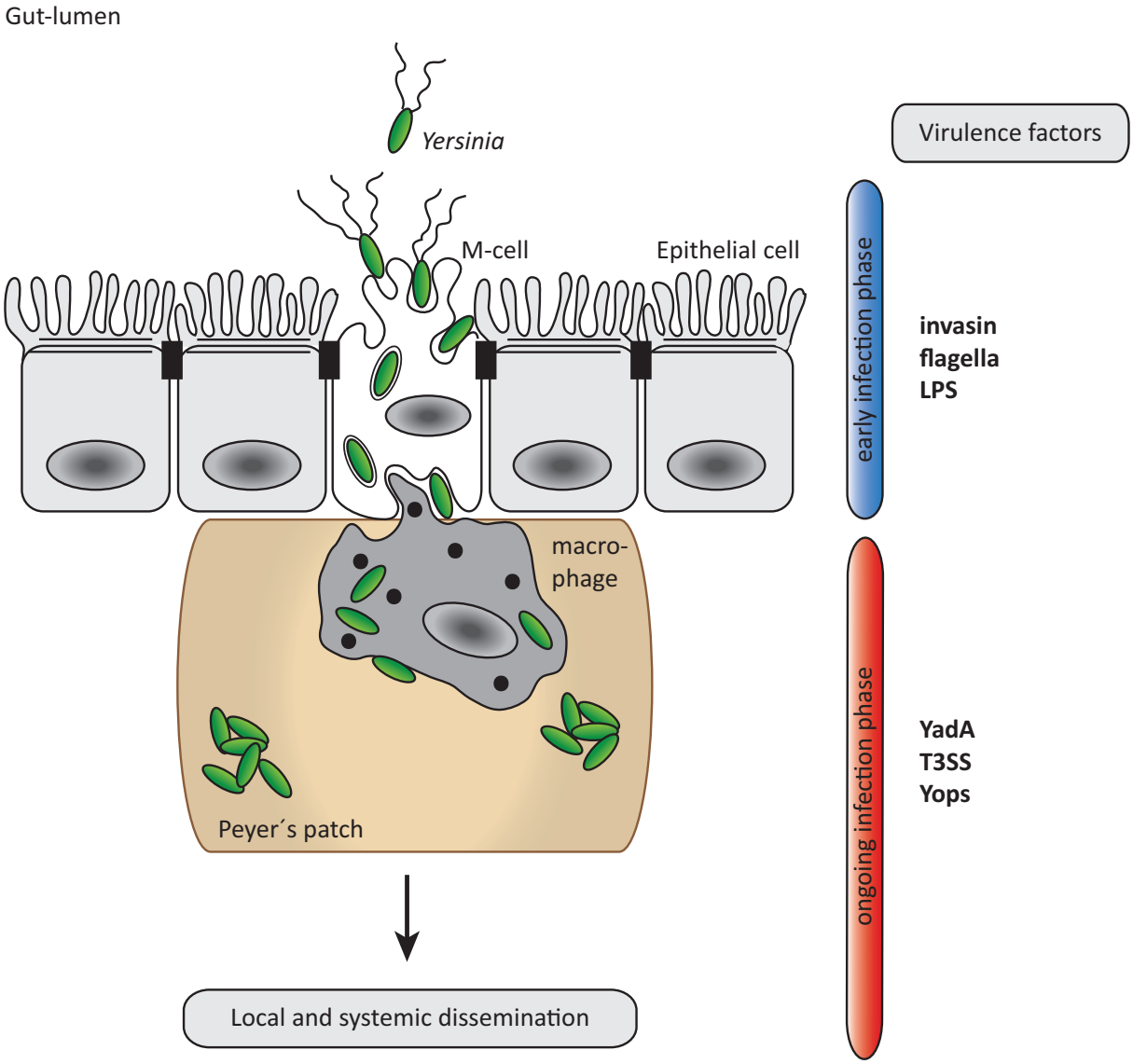

Fig. 1.1 Schematic model of *Y. pseudotuberculosis* entry into the host tissue
During the early phase of infection yersiniae are flagellated and express extracellular invasin, which mediates adherence to β_1 integrins on the M-cells. Subsequently, bacteria are phagocytosed to the underlying lymphoid tissue where they can survive and proliferate extracellularly due to the release of Yop effector proteins. Type III secretion (T3SS)-mediated injection of these proteins into host cells protects the bacteria from macrophage-induced killing and down-regulates the immune response of the host, modified from Sansonetti, (2004).

Immediately after crossing the gut-epithelium expression of invasin is down-regulated while expression of plasmid-encoded virulence factors (*yadA*, *yop*, *ysc* genes) is induced. Among these plasmid-derived factors the non-fimbrial adhesin YadA (*Yersinia* adhesion A) mediates bacterial adhesion within the host tissue. Further it induces bacterial autoaggregation to permit extracellular proliferation in microcolonies and confers resistance to the bactericidal activity of the complement system and killing by antimicrobial peptides (AMPs) (Balligand *et al.*, 1985; Kapperud *et al.*, 1985; Heise and Dersch, 2006; Trülzsch *et al.*, 2007; Kirjavainen *et al.*, 2008).

In addition to YadA virulence-plasmid encoded factors including the *ysc* type III secretion system (T3SS) and *yop* (*Yersinia* outer protein) effector genes are key determinants for bacterial survival and proliferation under hostile conditions. The T3SS forms needle-like surface appendages that mediate direct contact to eukaryotic host cells. Delivery of the Yop effectors induces cytoskeletal rearrangements of the target cells, blocks phagocytosis by macrophages and polymorphonuclear leukocytes (PMNs) and induces apoptosis. Furthermore, production of pro-inflammatory cytokines and chemokines is prevented to suppress the hosts immune response (Bliska and Black, 1995; Fallman *et al.*, 1995; Schulte *et al.*, 1996; Boland and Cornelis, 1998; Cornelis, 1998; Cornelis, 2002b; Denecker *et al.*, 2002; Fallman and Gustavsson, 2005; Peters *et al.*, 2013). Besides the T3SS, a chromosomally encoded type VI secretion system (T6SS) was identified in *Yersinia* that might be important for bacterial survival within the host tissue (Pieper *et al.*, 2009; Robinson *et al.*, 2009).

Expression of the plasmid-encoded virulence genes is controlled by the transcriptional activator LcrF (low calcium response F) in response to host temperature and host-cell contact. The 5'-UTR of *lcrF* forms a unique, *cis*-acting RNA element encompassing a secondary structure with two stem-loops. The second hairpin sequesters the *lcrF* ribosomal binding site in a so-called fourU motif and therefore blocks translation at moderate temperatures. At 37°C (host body temperature) this structure melts and permits ribosomal attachment, which finally induces translation of the late virulence genes (Böhme *et al.*, 2012). Thermoregulation of *lcrF* is modulated by YmoA, which represses transcription of *lcrF* from a single promoter at 25°C. Besides the temperature-dependent *lcrF* thermometer not much is known about the control of the late virulence genes. In contrast, the regulatory network implicated in control of the primary invasion factor invasin is well characterized and will be discussed in the following.

1.2. Regulation of invasin expression

Considering the energy efficiency, a stringent regulation of virulence gene expression is pivotal. Therefore, bacteria possess a huge subset of control elements, mechanisms and levels of regulation, facilitating rapid responses to changing conditions. Invasin expression is induced out-side the host at moderate temperatures in a nutrient-rich environment during stationary growth. However, *invA* expression is part of a complex regulatory cascade, which is briefly explained in the following and summarized in Fig. 1.2.

Invasin expression is subjected to transcriptional control by the **MarR-type regulator RovA** (Regulator of virulence A). At 25°C during growth in complex medium the global winged-helix regulator preferentially binds palindromic AT-rich sequences with $^{A}/_{T}$ ATTAT $^{A}/_{T}$ motifs within the *invA* promoter, which directly stimulates *invA* transcription.

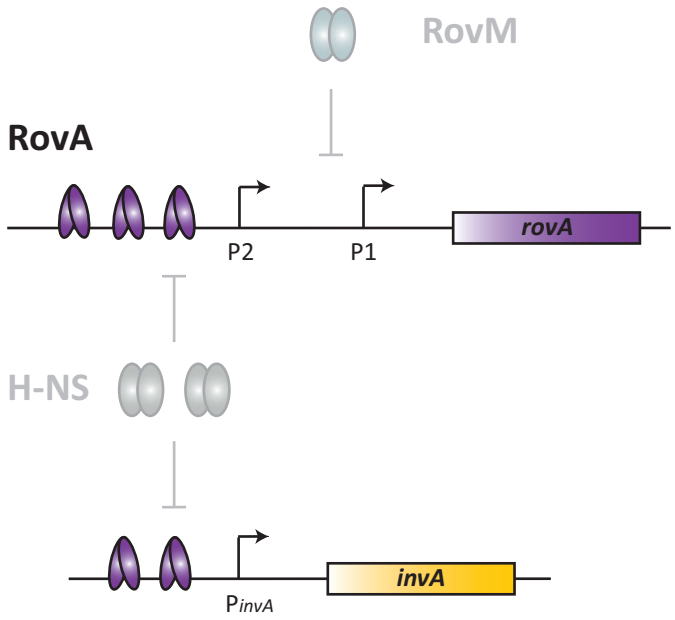

Fig. 1.2 Regulatory cascade of *Yersinia* invasin expression at 25°C
At 25°C invasin expression is activated by the global transcription factor RovA. RovA-binding to the *invA* promoter is antagonized by the histone-like protein H-NS. Furthermore, during growth in nutrient-deprived medium, the LysR-type regulator RovM is expressed and represses transcription of r*ovA* by binding upstream of promoter P1.

RovA is transcribed from two different promoters P1 and P2 located 76 bp and 343 bp upstream of the *rovA* translational start site and exhibits positive autoregulation. Herein, binding of several RovA dimers to an extended AT-rich sequence far upstream of the P2 promoter (high affinity binding-site) is required for full *rovA* expression in response to moderate temperatures, stationary growth and nutrient-rich medium. Upon temperature

shifts the thermosensor undergoes reversible conformational changes, which release the regulator from its target DNA and lead to enhanced degradation by Lon proteases (Nagel *et al.*, 2001; Heroven *et al.*, 2004; Herbst *et al.*, 2009; Quade *et al.*, 2012).

Moreover, transcription of *invA* and *rovA* is subject to H-NS-mediated silencing (Heroven *et al.*, 2004; Heroven *et al.*, 2007). The **histone-like nucleoid-structuring protein H-NS** is a highly abundant 15 kDa DNA-binding protein. It belongs to the class of nucleoid-associated proteins (NAPs). The H-NS binding sites in the upstream region of the *invA* transcriptional start site and in the upstream region of the *rovA* P2 promoter overlap with the RovA recognition sites. Under inducing conditions RovA acts as an antirepressor and relieves H-NS binding due to the higher affinity to target promoter regions (Amit *et al.*, 2003; Heroven *et al.*, 2004; Tran *et al.*, 2005; Cathelyn *et al.*, 2007; Blädel *et al.*, 2013).

Besides H-NS, the **LysR-type regulator protein RovM** (Regulator of virulence M) specifically interacts with a 30 bp stretch in-between both *rovA* promoters (close to P1) thus repressing *rovA* transcription. H-NS and RovM operate independently from each other, as they bind to distant palindromic consensus sequences, but both are required for efficient *rovA* silencing. Binding of H-NS might induce structural rearrangements of the DNA (e.g. loop formation), which might facilitate RovM-DNA complex formation. Since RovM expression is induced under nutrient-limiting conditions, which is reciprocal to the RovA expression, nutrient-dependent *rovA* transcription is mediated via RovM (Heroven *et al.*, 2004; Heroven and Dersch, 2006; Heroven *et al.*, 2007).

Recent data show that RovA is required for full *Yersinia* virulence in the mouse model of infection: *rovA* mutant strains were significantly attenuated in their invasion and colonization properties and showed a delayed progression of the infection. However, loss of *rovA* resulted in a more severe phenotype than loss of *invA*, indicating that RovA is an important regulator of virulence gene expression, which goes beyond invasin control (Heroven and Dersch, 2006). Indeed, microarray analysis revealed that RovA is a global regulator that affects expression of various metabolic, stress resistance and virulence genes, which may be required during the early phase of infection (Cathelyn *et al.*, 2007). RovA is controlled by RovM, which in turn is governed by the global post-transcriptional Csr system (Heroven *et al.*, 2008).

1.2.1. The carbon storage regulator (Csr) system

Besides the mostly well-understood transcriptional regulation mechanisms, it becomes more and more evident that post-transcriptional mechanisms provide a rapidly responding tool in gene regulation. Herein, *cis*- and *trans*-acting small RNAs and other RNA elements such as RNA thermometers and riboswitches, RNA-binding proteins and RNases are key-players, which promptly modify the existing messenger RNA instead of initiating *de novo* synthesis (Anderson *et al.*, 2002; Schiano and Lathem, 2012).

The carbon storage regulator (Csr) system is a global post-transcriptionally acting system. It has been identified in a variety of pathogenic bacteria like *Vibrio cholerae* and *Legionella pneumophila*. Homologous systems have also been found for example in *Pseudomonas aeruginosa* designated as Rsm (repressor of stationary-phase metabolites) systems (White *et al.*, 1996; Romeo, 1997; Liu *et al.*, 1997; Suzuki *et al.*, 2002; Kay *et al.*, 2005; Wang *et al.*, 2005). The overall fate of this system is to control translation of target mRNAs thus exerting regulatory roles in the central carbon flux, motility, biofilm formation, quorum sensing and pathogenesis. Csr/Rsm systems comprise an RNA-binding protein referred to as CsrA, RsmA or RsmE, which affects the stability or translation of target transcripts. Non-coding RNAs (ncRNAs), with several CsrA-binding sites sequester CsrA proteins and antagonize their function (Romeo, 1998; Heroven *et al.*, 2012a; Romeo *et al.*, 2013) (Fig. 1.3).

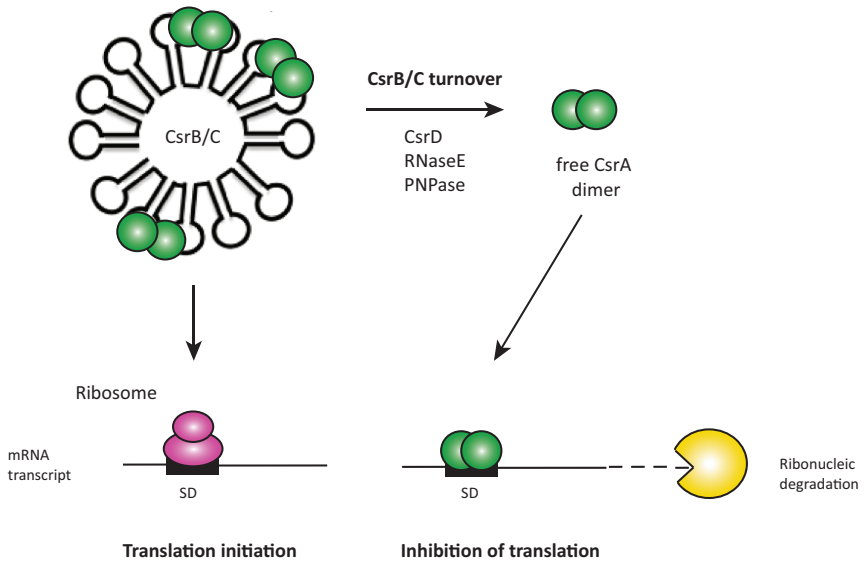

Fig. 1.3 General mechanism of the Csr regulon
Secondary structures of CsrB and CsrC non-coding RNAs harbour various CsrA-binding motifs within stem-loop structures. CsrA-binding to these consensus sequences antagonizes binding to GGA motifs within the SD site in mRNA transcripts. Therefore ribosomes can attach and initiate translation. Upon CsrB/C turnover by components of the degradosome, CsrA dimers dissociate from the sRNAs and block the SD sequences of target mRNAs. Consequently translation is inhibited and the mRNA is prone to degradation by ribonucleases, modified from Romeo *et al.* (2013).

CsrA is highly conserved among prokaryotes and forms homodimers with a size of approximately 18 kDa. Each monomer is composed of five β-strands (β1-β5) and one short α-helix (α1) followed by an unstructured, unfolded C-terminus. The monomers are connected via anti-parallel β-sheet pairing, which form the stabilizing hydrophobic core of the homodimer. The interface of those two interacting polypeptide subunits represents the RNA-binding surface. CsrA-binding to its target mRNA requires two distinct steps: initially a high-affinity 5'-$^{A}/_{U}$CANGGANG$^{U}/_{A}$-3 binding site within a stem-loop structure of the 5'-UTR is recognized by the first CsrA RNA-binding surface. Upon binding, the mRNA transcript undergoes conformational changes, increasing CsrA's affinity for the single-stranded SD sequence, which is finally bound by the second RNA-binding surface (bridging complex) (Fig. 1.4). Herein, spacing of the two recognition sites (optimal spacing ≥18 nt) determines the stability of the repression complex and leads to efficient translation inhibition (Gutiérrez *et al.*, 2005; Schubert *et al.*, 2007; Mercante *et al.*, 2009; Heroven *et al.*, 2012a).

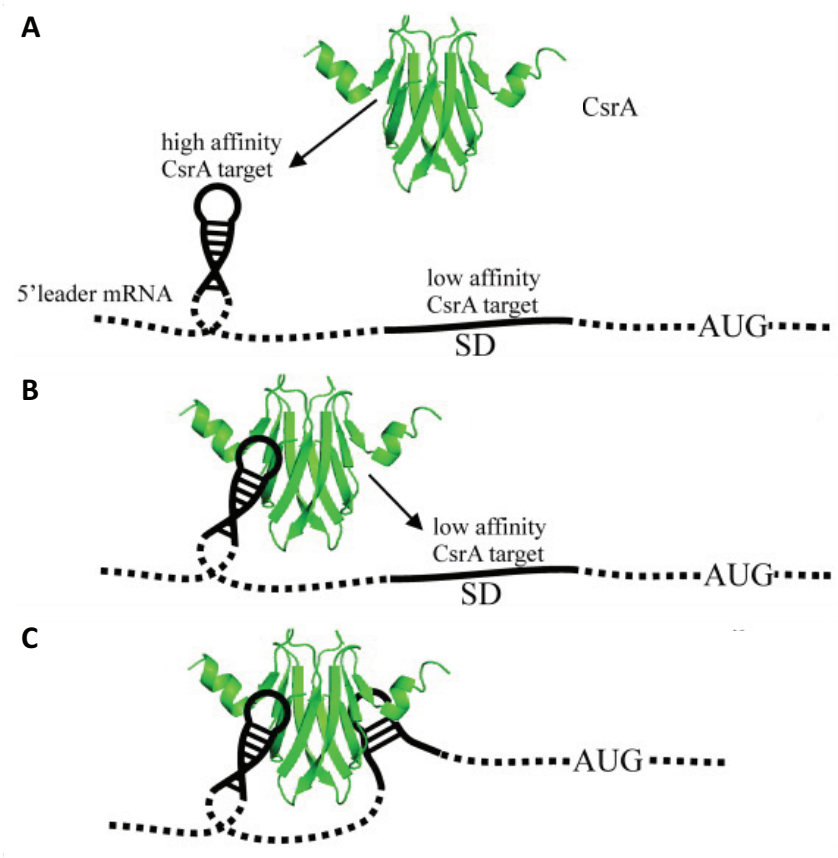

Fig. 1.4 Dual-step target recognition by CsrA
A CsrA initially binds to a high-affinity binding site, usually located within a loop-region upstream of the SD site. **B** CsrA-binding leads to conformational changes that allow binding to the low-affinity binding site within the SD sequence. **C** Binding sequesters the SD sequence for ribosomal attachment, modified from Mercante *et al.* (2009).

Exceptions to this dual-step recognition exist. For instance, CsrA inhibits Hfq mRNA translation by binding to one single site overlapping the SD sequence (Baker *et al.*, 2007). In case of *Salmonella hilD* CsrA-binding occurs at the SD sequence and further includes the initiation start codon (Martínez *et al.*, 2011). In *E. coli* CsrA blocks translation of the *cstA* gene by binding to GGA motifs even downstream of the translation initiation codon (Dubey *et al.*, 2003).

The GGA motifs for CsrA recognition are often found in the 5'-UTR of target mRNAs and overlap the SD sequence. Hence CsrA competes with the 30S ribosomal subunit for access to the SD sequence. Consequently, CsrA-binding physically blocks ribosomal attachment and facilitates RNase E-mediated cleavage of the messenger (Liu *et al.*, 1995; Dubey *et al.*, 2005; Babitzke and Romeo, 2007; Schubert *et al.*, 2007; Mercante *et al.*, 2009; Schiano and Lathem, 2012)

Non-coding RNAs antagonize CsrA function. These RNAs are highly structured and provide several stem-loop structures containing the GGA consensus sequence to which CsrA binds preferentially. Exposition of the GGA motifs within single-stranded portions of the hairpins renders them into highly affine CsrA targets. For instance, *E. coli* CsrB possesses 22 putative CsrA-binding sites while CsrC harbours 13 of these motifs. CsrA preferentially binds to these exposed motifs and is sequestered away from its target mRNA, leading to translation initiation (Babitzke and Romeo, 2007). In general, the overall amount of CsrA in the cell remains constant while its availability is controlled by its affinity to the ncRNAs. In *Yersinia* the two Csr-type RNAs CsrB and CsrC have been identified which are only 50 to 55% identical to their orthologous Csr RNAs in *E. coli* or *Salmonella spp* (Heroven *et al.*, 2012a). In *Y. pseudotuberculosis* CsrB exhibits nine putative CsrA-binding sites, whereas CsrC shows six hairpins with single-stranded GGA motifs.

Since sequestration does not alter the overall amount of CsrA in the cell but interferes with the protein activity, it is hypothesized that slight variations in the total amount of CsrA protein might have dramatic effects on the global control of target mRNAs (Liu *et al.*, 1997; Babitzke and Romeo, 2007; Romeo *et al.*, 2013; Adamson and Lim, 2013).

Despite CsrA-mediated translation inhibition, two exceptions from the rule are known so far. In these cases CsrA-binding to target mRNAs drives translation initiation. One example is the

regulation of the flagellar master regulator *flhDC* in *E. coli*. CsrA binds directly to the mRNA transcript, which results in stabilization of the messenger due to physical protection of the 5' end from RNase E-mediated cleavage (Soutourina *et al.*, 1999; Wei *et al.*, 2001; Romeo *et al.*, 2013; Yakhnin *et al.*, 2013). The other deals with the molybdenum cofactor (MOCO)-sensing riboswitch, that is formed by the 5'-UTR of the *moaA* mRNA in *E. coli*. CsrA-binding to this highly structured mRNA leader induces conformational changes of the mRNA secondary structure, activating translation of the messenger (Romeo *et al.*, 2013).

1.2.2. Regulation of the Csr system in *Yersinia* and other *Enterobacteriaceae*

Heroven *et al.* (2008) could show, that the protein effector (CsrA) of the Csr system controls the expression of invasin and RovA, by indirectly activating RovM expression. Besides invasin, CsrA of *Y. pseudotuberculosis* affects over 500 open reading frames (ORFs) as identified by microarray analyses. 3% of the differentially regulated genes are implicated in bacterial virulence and stress response. Moreover, a *csrA* mutant strain exhibits a completely avirulent phenotype in the mouse model of infection, emphasizing that CsrA-directed control mechanisms are absolutely required for successful infections (Heroven *et al.*, 2012a; Heroven, unpublished data; Kroll, unpublished data).

Autoregulation

Since free CsrA is in equilibrium with bound CsrA, which is sequestered by the ncRNAs CsrB and CsrC, only freely available CsrA dimers can bind to putative target mRNAs (in rare cases highly affine target mRNAs may sequester CsrA from its RNA antagonists). Therefore, a tight and efficient regulation is required to facilitate rapid and robust signalling in response to changing environments. Herein CsrA indirectly controls transcription of its antagonistic RNAs CsrB and CsrC and implies further autoregulatory mechanisms (Gudapaty *et al.*, 2001; Romeo *et al.*, 2013). It is known from *E. coli* that CsrA possesses five different promoters, two of which are σ^S-dependent. Promoter P3 is primarily responsible for an increase in CsrA upon entry into the stationary growth phase. However, CsrA blocks translation by binding to its own mRNA target while it indirectly activates its own transcription. Further, CsrA of *E. coli* activates σ^S expression in response to low temperatures and during exponential growth. σ^S in turn activates CsrA transcription, implicating a positive feedback-loop (Yakhnin *et al.*, 2011; Romeo *et al.*, 2013). So far, a *csrA* autoregulation phenomenon has not been observed

in *Yersinia* (Hoßmann, unpublished data). Binding of CsrA to the Csr-type RNAs positively affects their stability in *E. coli*, *Salmonella spp* and *Pseudomonas*. In *Yersinia* for instance, CsrC is highly stable (half-life of 100 min) while its stability is drastically decreased in a *csrA* deficient strain (11 min Δ*csrA*), emphasizing that CsrA is absolutely required for ncRNA integrity (Reimmann *et al.*, 2005; Böhme, 2010; Heroven *et al.*, 2012a). Moreover, both ncRNAs are mainly counter-regulated in *Yersinia* as upregulation of one RNA leads to simultaneous downregulation of the other and *vice versa*. In several other species it is known that the Csr RNAs complement one another and that loss of *csrB* or *csrC* resembles a *csrA* overexpression phenotype in *Salmonella* (Lenz *et al.*, 2005; Fortune *et al.*, 2006). However, in *Y. pseudotuberculosis* loss of *csrB* or *csrC* does not influence Csr-dependent *rovA* expression, which would resemble a *csrA* overexpression phenotype, indicating that other regulatory mechanisms might compensate for loss of both ncRNAs (Heroven *et al.*, 2008; Heroven *et al.*, 2012a).

The two-component systems BarA/UvrY and PhoP/PhoQ

Another level of regulation is the CsrA-mediated activation of CsrB and CsrC transcription (Heroven et al., 2012b). Herein, CsrA indirectly activates the two-component system (TCS) BarA/UvrY, which responds to by-products of carbon metabolism in *E. coli*, hence responding to the metabolic state of the cell (Chavez *et al.*, 2010). It is composed of the sensor kinase (SK) BarA and its cognate response regulator (RR) UvrY. The BarA/UvrY TCS of *E. coli* induces upregulation of both Csr-type RNAs on the transcriptional level. Unlike to other species that harbour homologues of the Csr/Rsm system, UvrY/BarA-mediated transcriptional activation is restricted to the ncRNA CsrB in *Yersinia*; however, the activating signal for BarA/UvrY is still unknown in this pathogen. During growth in rich medium this TCS is only poorly expressed, which results in low CsrB levels that indirectly increase CsrC levels, indicating that CsrC is the predominant CsrA antagonist in *Yersinia* (Weilbacher *et al.*, 2003; Fortune *et al.*, 2006; Heroven *et al.*, 2008; Jonas and Melefors, 2009). Recent data highlight the importance of the PhoP/PhoQ TCS, which is a global Mg^{2+}-responsive regulon. At 25°C the response regulator PhoP binds directly to PhoP box-like sequences upstream of the *Yersinia csrC* gene, leading to its transcriptional activation and finally induces *rovA* expression via the CsrABC-RovM cascade (Groisman, 2001; Nuss *et al*., 2014).

The cAMP receptor protein Crp

The cyclic adenosine monophosphate (cAMP) receptor protein Crp is a global transcription factor of *Enterobacteriaceae* and represents the key regulator of the catabolite repression. Crp is a homodimer with a size of 45 kDa. The subunits are linked via the N-terminal domain, while the C-terminus mediates DNA-binding. Binding of cAMP to the Crp N-terminus induces conformational changes that activate Crp and leads to binding to TGTGA-N_6-TCACA consensus sequences in target promoter regions (Kolb *et al.*, 1993; Busby and Ebright, 1999). Under glucose-limiting conditions increased amounts of cAMP-Crp complexes are formed that drive the catabolic utilisation of alternative sugars. In parallel, activated Crp acts on the transcription of virulence-associated genes (Gunasekera *et al.*, 1992; Saier, 1998; Zheng *et al.*, 2004). Recently, it was shown for *Yersinia* that Crp regulates expression of CsrB and CsrC in response to the media composition. Herein, Crp indirectly represses UvrY, which in turn leads to reduced CsrB levels ending up with an increase of cellular CsrC. Interestingly, CsrC is additionally influenced by Crp in a CsrB-independent manner, since Crp still exerts positive effects on CsrC in a *csrB* mutant strain (Heroven *et al.*, 2008; Heroven *et al.*, 2012b).

The RNA chaperone Hfq

The RNA chaperone Hfq (host factor for phage Qβ) has a size of 11 kDa. Subunits assemble to form a donut-shaped hexameric protein, which is primarily involved in RNA annealing and metabolism. The ring-like architecture bears two distinct RNA-binding sites, which exhibit different RNA sequence preferences. The distal face binds poly(A) sites while the proximal face binds sRNAs and mRNAs. Hfq was first identified as host factor for the replication of bacteriophage Qβ RNA and is a homologue of the eukaryotic Sm or Sm-like proteins that are involved in RNA degradation and splicing. In fact, the chaperone facilitates the interaction of sRNAs with their designated mRNA targets either leading to stabilization or destabilization of the target RNA (Muffler *et al.*, 1996; Brennan and Link, 2007; Vogel and Luisi, 2011).

For instance, Hfq assists sRNA-mRNA pairing leading either to translation inhibition by blocking the ribosomal binding site (RBS) or to translation initiation by exposing the RBS for 30S-binding. Further, Hfq-binding to sRNAs protects the transcripts from RNase E-mediated cleavage while formation of an sRNA-mRNA complex can be prone to increased RNase E-mediated cleavage. Direct interaction of Hfq with target mRNAs leads to polyadenylation

(mediated by poly(A) polymerase), which renders the transcript highly accessible to 3'-5' exoribonucleases (Vogel and Luisi, 2011).

Besides controlling a large number of sRNAs and mRNAs, Hfq is also involved in controlling the regulatory RNAs implicated in the Csr/Rsm regulatory system. In *P. aeruginosa* Hfq stabilizes the Csr-type RNA RsmY thus enhancing translation of RsmA targets. Binding sequences of Hfq and RsmA are overlapping within the ncRNA. Therefore, bound Hfq protects RsmY from RNase E-mediated cleavage while the stabilized ncRNA sequesters RsmA (Sorger-Domenigg *et al.*, 2007).

In *Y. pseudotuberculosis* the abundance of both Csr RNAs is positively affected by Hfq. Interestingly, Hfq stabilizes the CsrB RNA while it exerts a positive transcriptional effect on CsrC, which is likely to be indirect and not mediated via CsrA (Böhme, 2010).

The nucleoid-associated proteins H-NS and YmoA

Most recently, it was found that the nucleoid-associated proteins H-NS and YmoA are implicated in *Yersinia* Csr regulation. The histone-like nucleoid structuring protein H-NS serves a dual function in nucleoid structuring on the one hand and silencing of laterally acquired genes on the other hand. The N-terminal oligomerisation domain is needed for H-NS dimerization, whereas the C-terminal domain confers DNA-binding capacity. H-NS dimerization leads to the formation of exposed C-terminal regions that mediate binding to AT-rich consensus sequences (5'-TCGATATATT-3), which are especially abundant in intergenic regions throughout the bacterial chromosome. Since the AT-content in foreign DNA is often much higher than in the resident chromosome, xenogenic DNA is bound with higher affinity (Tupper *et al.*, 1994; Dorman *et al.*, 1999; Grainger *et al.*, 2006; Lucchini *et al.*, 2006; Oshima *et al.*, 2006).

H-NS-binding to AT-rich motifs, which are in close proximity to each other (nucleation site) leads to protein oligomerisation along the linear DNA duplex in a concentration-dependent manner and ends with the complete coverage of the respective DNA site (DNA coating) (Fig. 1.5 B). When the AT-rich sites are located further apart, formation of a looped DNA is initiated, which is referred to as DNA-bridging and leads to condensation of the DNA stretch (Fig. 1.5 A). Besides correct spacing of the binding sites, DNA topology is decisive for efficient H-NS-mediated silencing. The availability of narrow minor grooves and a bent trajectory of the duplex are prerequisites for H-NS attachment. Finally, DNA coating constitutes a physical

blockage of transcription initiation by RNA polymerase, while the formation of DNA-protein-DNA bridges even traps RNA polymerase and stalls transcription. Structural rearrangements of the DNA (like bending or wrapping) reverse H-NS-binding (Rimsky *et al.*, 2002; Dame *et al.*, 2005; Dillon *et al.*, 2007; Noom *et al.*, 2007).

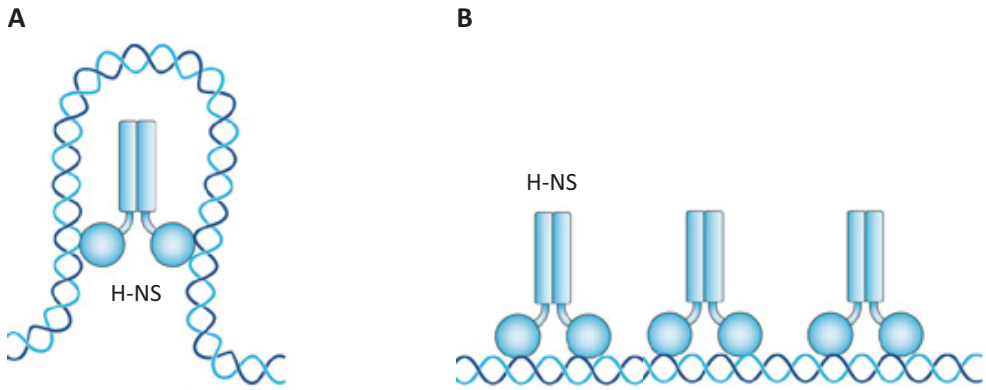

Fig. 1.5 H-NS-mediated DNA binding patterns
H-NS binds to AT-rich sequences within double-stranded DNA leading either to DNA bridging **(A)** or coating **(B)**. When H-NS-binding sites are located in close proximity on the same DNA strand, DNA is evenly coated by the dimer. In contrast, when H-NS-binding sites are further apart binding leads to DNA loop-formation, referred to as DNA bridging, modified from Dillon *et al.* (2007).

Moreover, H-NS is able to form heterodimeric complexes with YmoA/Hha-family proteins (Nieto *et al.*, 2002; McFeeters *et al.*, 2007), which function as transcriptional repression complexes of essential cell invasion genes in *Yersinia* and *Salmonella* (Ellison *et al.*, 2003; Olekhnovich and Kadner, 2007).

YmoA/Hha family members belong to a group of sequence-related low molecular-weight proteins, with a size of about 8 kDa. *Yersinia* YmoA and the *E. coli* homologue Hha (high hemolysin activating protein) exhibit extensive sequence similarity of 82% resulting in structural homology (Fig. 1.6). Both proteins are composed of a core structure that bears three helical bundles (1-3). The shortest helix (4) is positioned more distant to the 3-helical bundle and is oriented differentially in both organisms. Albeit the high sequence similarity, YmoA could not restore a Δ*hha* phenotype in *E. coli*, indicating that both proteins act in a different manner and are not completely functional homologues (de la Cruz *et al.*, 1992; McFeeters *et al.*, 2007).

Members of the YmoA/Hha-family are involved in virulence gene regulation among the *Enterobacteriaceae* in response to temperature and osmolarity. YmoA is rapidly degraded at

37°C by ClpXP and Lon proteases, while protein integrity is stable at moderate temperatures. Herein, YmoA represses virulence-plasmid encoded genes at 25°C, while these are activated at elevated temperatures due to proteolysis of YmoA. *Vice versa* virulence factors needed for the early host colonization like invasin are activated by YmoA at 25°C (Jackson *et al.*, 2004; Madrid *et al.*, 2007; Böhme, 2010; Böhme *et al.*, 2012).

Proteins of this family where shown to influence DNA supercoiling, although they have not been reported to bind DNA by themselves. Interestingly, YmoA/Hha-family proteins exert a structural mimicry to the H-NS oligomerisation domains, which enables them to form heterodimeric complexes with these histone-like proteins. In *E. coli* for instance, replacement of the H-NS N-terminal domain by Hha could restore some *hns*-mediated phenotypes (Rodríguez *et al.*, 2005). For *Y. enterocolitica* it was shown that YmoA/H-NS heterodimers form a repression complex, which competes with RovA homodimers for similar binding regions in the *inv* promoter region, resulting in transcriptional abolishment (Nieto *et al.*, 2002; Ellison *et al.*, 2003; Ellison and Miller, 2006).

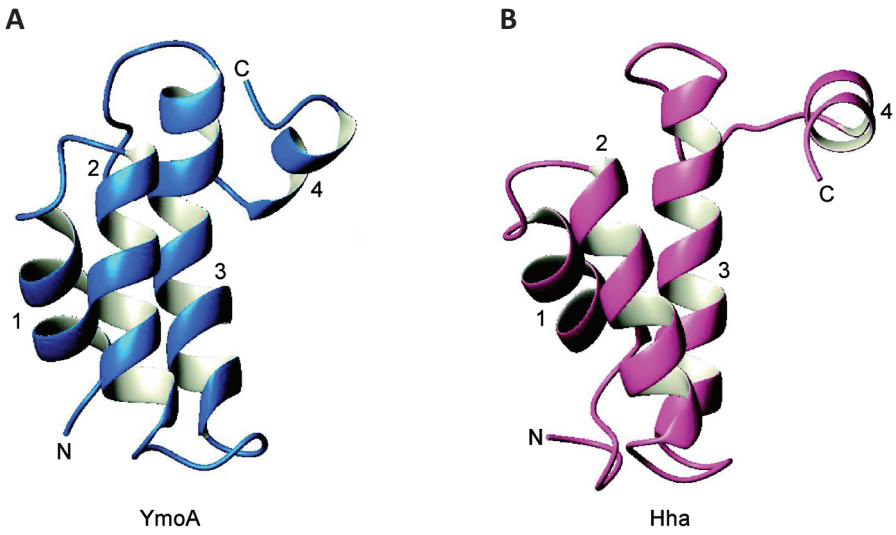

Fig. 1.6 Ribbon structure of YmoA and its homologue Hha
A YmoA is an all-helical protein with a core structure of three helical bundles (1-3). The fourth helix is the shortest and is positioned against the outer face of the C-terminal end of helix 3. **B** The overall shape, secondary structure and functional elements of YmoA and Hha are conserved between both proteins. The most decisive difference is the orientation of the fourth helix, modified from McFeeters *et al.* (2007).

In *Y. pseudotuberculosis* H-NS exhibits a positive post-transcriptional impact on the CsrC RNA, whereas CsrB is influenced in a negative fashion, most likely due the counter-regulation of both RNAs. So far, there is no evidence for a direct interaction between H-NS

and the ncRNA. Furthermore, in *Y. pseudotuberculosis* YmoA is crucial for the control of the Csr-type RNAs. It enhances the stability of CsrC while the CsrB levels are slightly downregulated, possibly due to the counter-regulation of both Csr-type RNAs. However, the underlying mechanism of the YmoA-mediated CsrC stabilization is unknown yet, but involves a stabilizing stem-loop structure within the 5'-region of the CsrC RNA (Böhme, 2010).

Nevertheless, H-NS can complement the loss of *ymoA* with regard to the CsrC RNA levels, indicating that both proteins might act in a cooperative manner to ensure RNA integrity (Böhme, 2010). Indeed, members of the H-NS protein family were shown to interact with RNAs to manipulate their stability (Brescia *et al.*, 2004; Silva *et al.*, 2008). Whether heterodimers might interact with highly structured RNA sequences like CsrC still remains unknown.

Components of the degradosome

RNA turnover is highly coordinated and involves RNase E, which is an endonuclease that preferentially attacks 5' monophosphorylated ends of mRNA transcripts. Rapid degradation of cleavage products involves polynucleotide phosphorylase (PNPase) and RNase II activity, which operate as 3'-5' exoribonucleases. Moreover in *E. coli* RNase E is one component of the multi-protein degradosome complex, which further consists of PNPase, the RNA helicase RhlB and enolase. RNase E, PNPase and RNase II as well as components of the degradosome are involved in CsrBC turnover to release bound CsrA dimers. Recently it was found that CsrA represses the specificity factor CsrD, which selectively targets CsrBC to render the ncRNAs accessible to RNase E-mediated cleavage in *E. coli*. More precisely Suzuki *et al.* (2006) showed that CsrB turnover depends on CsrD, but CsrC decay occurs independent of CsrD (Suzuki *et al.*, 2006; Carpousis, 2007; Romeo *et al.*, 2013). This is in-line with findings from *Yersinia* where CsrD negatively affects CsrB levels in the cell, while CsrC levels remain unaffected (Seekircher, unpublished data).

Taken together, the *Yersinia* Csr system underlies a tight and versatile regulation, which involves autoregulatory feedback-loops and several globally acting regulators like H-NS and Crp (Fig. 1.7). Despite similarities in the overall function of the system, differences concerning its regulation exist between *Yersinia* and other enterobacterial species. The structure and sequence of both Csr-type RNAs differs significantly among *Yersinia* species and *E. coli* or *S. typhimurium*. Further expression of both Csr-type RNAs is activated by the

BarA/UvrY TCS in *E. coli.* In contrast *csrC* expression is not induced by this TCS in *Yersinia*. Here UvrY-mediated upregulation of CsrB even leads to decreased CsrC levels. Moreover, both Csr-type RNAs are highly abundant in *E. coli* and *S. typhimurium* under standard growth conditions while CsrB of *Yersinia* is barely expressed.

Identification of possible regulators that differentially affect *csrB* and *csrC* expression would provide deeper insights into this complex regulatory system.

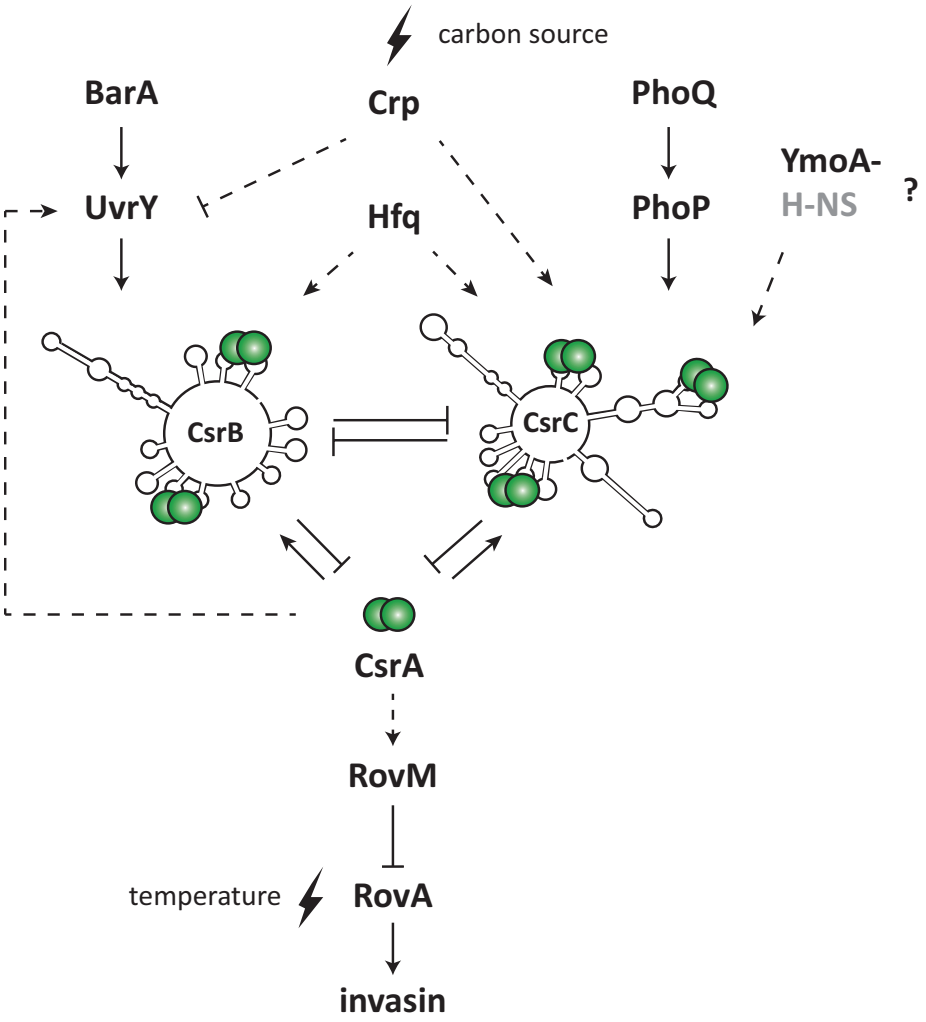

Fig. 1.7 Regulatory factors controlling the *Yersinia* Csr system
During the last decades several transcriptional and post-transcriptional regulators were identified. Recently, the Csr system was discovered as global virulence regulator system. The major players, namely the CsrBC non-coding RNAs are stabilized by CsrA-binding and counter-regulate each other. Moreover CsrB transcription is activated by response regulator UvrY of the two-component system BarA/UvrY in response to (yet unknown) environmental stimuli. The TCS is indirectly activated by CsrA, while repressed by Crp. Herein, Crp responds to the nutrient composition of the surrounding medium. In addition, Crp positively affects CsrC transcript levels in a CsrB-independent manner. Interestingly, the RNA chaperone Hfq exerts positive transcriptional effects on both ncRNAs, while the nucleoid-structuring protein YmoA and H-NS mediate post-transcriptional control. Whether both proteins act in a cooperative manner is still unknown. YmoA and H-NS predominantly affect CsrC levels, which then in turn modulate CsrB expression. Upregulation of one or both ncRNAs sequesters CsrA, whereby RovM is repressed and RovA is activated leading to *invA* expression (dashed lines = indirect effect, solid lines = direct interaction).

1.3. Aim of the study

The main purpose of this study was to investigate the regulation of the CsrC RNA, the major CsrA antagonist in *Y. pseudotuberculosis*. CsrC and CsrA are key components of the Csr system that control *Yersinia* virulence especially during the early phase of infection (Heroven *et al.*, 2008). CsrA binds to consensus sequences within target mRNAs leading to an alteration of the transcript stability. Sequestration by the Csr-type RNAs antagonizes this post-transcriptional control mechanism and is decisive for the availability of active CsrA protein. Since CsrA levels in the cell are essentially constant, the abundance of Csr-type RNAs is pivotal for the balance between bound and active CsrA protein (Gudapaty *et al.*, 2001; Romeo *et al.*, 2013).

Recently, the *Yersinia* modulator A (YmoA) was found to stabilize the CsrC sRNA. YmoA-mediated CsrC stabilization involved a stem-loop structure formed by the first +81 nt of the CsrC RNA (Böhme, unpublished data). According to this one goal was to unravel the molecular mechanism that underlies this stabilization.

Intracellular levels of CsrB and CsrC RNA are controlled by distinct regulatory factors and both Csr-type RNAs respond to different environmental stimuli and growth parameters (Heroven *et al.*, 2008; Heroven *et al.*, 2012b). Since CsrC is highly abundant during the early virulence phase (Böhme, unpublished data), the major aim of this work was to identify and characterize possible mechanisms and factors implicated in the expression of the CsrC RNA.

2. Material and methods

2.1. Material

2.1.1. Strains and plasmids

E. coli and *Yersinia* strains used in this study are listed in Tab. 2.1. Utilized plasmids are indicated in Tab. 2.2.

Tab. 2.1 Bacterial strains

Strain	Description	Reference
***E. coli* K-12**		
BL21λDE3	F⁻ *ompT gal dcm lon hsdSB*(rB - mB -) λDE3	(Studier and Moffatt, 1986)
DH10β	F⁻ *endA1 recA1 galE15 galK16 nupG rpsL* Δ*lacX74* Φ80*lacZ* Δ*M15 araD139* Δ(*ara,leu*)*7697 mcrA* Δ(*mrr⁻ hsdRMS⁻mcrBC*), λ⁻	(Casadaban and Cohen, 1980)
KB4	BL21λDE3 Δ*stpA*, Δ*hha*, Δ*hns*	K. Böhme
S17-1λ*pir*	*recA thi pro hsdR*⁻ M1⁺(RP4--2Tc::Mu--Km::Tn7), λ*pir*	(Simon *et al.*, 1983)
Y. pseudotuberculosis		
YPIII	pIB1, wildtype	(Bolin *et al.*, 1982)
YP50	YPIII, Δ*ymoA*, Kan^R	A. K. Heroven
YP53	YPIII, Δ*csrA*, Kan^R	(Heroven *et al*., 2008)
YP72	YPIII, Δ*rovM*	(Heroven *et al*., 2012b)
YP80	YPIII, Δ*hfq*	A. K. Heroven
YP89	YPIII, Δ*crp*	(Heroven *et al*., 2012b)
YP68	YPIII, Δ*clpP,* Δ*lon,* Amp^R, Kan^R	(Herbst *et al.,* 2009)
YP69	YPIII, Δ*csrB*	(Heroven *et al*., 2008)
YP107	YPIII, Δ*rovA*	(Quade *et al*., 2012)
YP126	YPIII, Δ*csrC*	(Heroven *et al*., 2012b)
YP138	YPIII, Δ*pnp*	R. Steinmann
YP148	YPIII, Δ*rovC*, Kan^R	This study
YP191	YPIII, Δ*invA*, Kan^R	R. Geyer
YPIII *ypsI*	YPIII, Δ*ypsI,* Kan^R	(Atkinson *et al.*, 1999)
YPIII *ypsR*	YPIII, Δ*ypsR,* Kan^R	(Atkinson *et al*., 1999)
YPIII *ytbI*	YPIII, Δ*ytbI,* Cm^R	(Atkinson *et al*., 1999)
YPIII *ytbR*	YPIII, Δ*ytbR,* Cm^R	(Atkinson *et al*., 1999)
YPIII *ypsI/ytbI*	YPIII, Δ*ypsI/ytbI,* Cm^R, Kan^R	(Atkinson *et al*., 1999)
YPIII *ypsR/ytbR*	YPIII, Δ*ypsR/ytbR,* Cm^R, Kan^R	(Atkinson *et al*., 1999)

^{R} resistance cassette

Tab. 2.2 Plasmids

Plasmid	Description	Reference
pACYC184	cloning vector, ori p15A, Tet^R, Cm^R	(Chang and Cohen, 1978)
pHSG575	cloning vector, ori pSC101, Cm^R	(Takeshita *et al.*, 1987)
pTS02	pGP20, ori pSC101, *lacZ*$^+$, Amp^R	(Böhme *et al*., 2012)
pTS03	pGP20, ori pSC101, RBS-*lacZ*$^+$, Amp^R	T. Stolz
pAKH3	pGP704, ori R6K, *sacB*$^+$, Cm^R	(Heroven *et al.*, 2012b)
pAKH11	pET28a(+), ori 3286 ,*hns*$^+$, Kan^R	(Heroven *et al*., 2004)
pAKH37	pACYC184, p15A, *crp*$^+$, Cm^R	(Heroven *et al*., 2012b)
pAKH47	pGP20, ori pSC101, *rovA'-'lacZ* (17)^c, Tet^R	(Heroven and Dersch, 2006)
pAKH56	pACYC184, p15A, *csrA*$^+$, Cm^R	(Heroven *et al*., 2012b)
pAKH63	pGP20, ori pSC101, *rovM'-'lacZ* (41)^c, Tet^R	(Heroven and Dersch, 2006)
pAKH71	pACYC184, p15A, *ymoA*$^+$, Cm^R	A. K. Heroven
pAKH74	pACYC184, p15A, *hns*$^+$, Cm^R	A. K. Heroven
pAKH77	pASK-IBA5plus, f1, *ymoA*$^+$, Amp^R	A. K. Heroven
pAKH85	pACYC184, p15A, Δ*tet*, Cm^R	(Heroven and Dersch, 2006)
pAKH101	pHT124, pMB1 (ColE1), *csrB-lacZ* (-431 to +4)^a, Amp^R	(Heroven and Dersch, 2006)
pAKH139	pFU67, ori 29807, *crp'-'lacZ* (1)^c, Amp^R	A. K. Heroven
pAKH172	pET28a(+), ori 3286 ,*csrA*$^+$, Kan^R	A. K. Heroven
pAKH189	pTS03, ori pSC101, *rovC-lacZ* (-618 to -39)^b, Amp^R	A. K. Heroven
pBW137	pFU67, ori 29807, *hfq'-'lacZ* (21)^c, Amp^R	B. Waldmann
pGB4	pACYC184, p15A, *hfq*$^+$, Cm^R	This study
pGB9	pACYC184, p15A, *rovC*$^+$, Cm^R	This study
pGB176	pACYC184, p15A, *crp*$^+$, Cm^R	This study
pJH8	pTS03, ori pSC101, *csrA-lacZ* (-121 to -14)^b, Amp^R	J. Hoßmann
pJH11	pKB14, ori pMB1, *csrA'-'lacZ* (6)^c, Amp^R	J. Hoßmann
pJH17	pKB14, ori pMB1, *csrA'-'lacZ* (12)^c, Amp^R	J. Hoßmann
pJH18	pKB14, ori pMB1, *csrA'-'lacZ* (61)^c, Amp^R	J. Hoßmann
pKB4	pHSG575, ori pSC101, *ymoA*$^+$, Cm^R	K. Böhme
pKB7	pGP20, ori pSC101, *uvrY'-'lacZ* (3)^c, Tet^R	K. Böhme
pKB45	pTS03, ori pSC101, *csrC-lacZ* (-355 to +4)^a, Amp^R	K. Böhme
pKB46	pTS03, ori pSC101, *csrC-lacZ* (-355 to +81)^a, Amp^R	K. Böhme
pKB60	pHSG575, ori pSC101, *csrA*$^+$, Cm^R	K. Böhme
pKB63	pGP20, ori pSC101, *csrA'-'lacZ* (5)^c, Amp^R	K. Böhme
pMK07	pFU53, ori pSC101*, *rovC'-'luxCDABE* (8)^c, Amp^R	M. Kroll
pRS40	pBAD33, ori M13, *rne*$^-$, Cm^R	R. Steinmann
pRS68	pBAD33, ori M13, *csrA*$^+$, Cm^R	R. Steinmann
pSSE11	pACYC184, p15A, *rovC*$^+$, Cm^R	This study
pSSE16	pTS02, ori pSC101, *tdcF*'-'*lacZ* (3)^c, Amp^R	This study
pSSE20	pTS02, ori pSC101, *rnpA*'-'*lacZ* (3)^c, Amp^R	This study
pSSE21	pTS02, ori pSC101, YPK_0604'-'*lacZ* (3)^c, Amp^R	This study
pSSE27	pTS02, ori pSC101, *groEL*'-'*lacZ* (3)^c, Amp^R	This study
pSSE28	pTS02, ori pSC101, *dnaK*'-'*lacZ* (3)^c, Amp^R	This study
pSSE29	pTS02, ori pSC101, *grpE*'-'*lacZ* (7)^c, Amp^R	This study

Plasmid	Description	Reference
pSSE32	pTS02, ori pSC101, *rovC*'-'*lacZ* (3)[c], Amp^R	This study
pSSE35	pAKH3, Δ*rovC*, Amp^R	This study
pSSE51	pTS02, ori pSC101, *pnp*'-'*lacZ* (3)[c], Amp^R	This study
pSSE52	pTS02, ori pSC101, *rne*'-'*lacZ* (3)[c], Amp^R	This study
pSSE64	pTS02, ori pSC101, YPK_3566'-'*lacZ* (3)[c], Amp^R	This study
pSSE67	pTS03, ori pSC101, *rovC-lacZ* (-618 to -14)[b], Amp^R	This study
pSSE68	pACYC184, p15A, *rovC-his*$^+$, Cm^R	This study

[a] relative to transcriptional start

[b] relative to translational start

[c] amino acids

2.1.2. Media and supplements

Liquid media were prepared as indicated below. Solid media were prepared by adding 15 g agar per 1 l medium (except for *Yersinia* selective agar).

LB medium (Luria-Bertani) (Sambrook, 2001)

Bacto yeast extract	5 g
Bacto tryptone	10 g
NaCl	5 g
dem. water	ad 1 l

BHI medium (Brain-Heart infusion)

BHI (BD Biosciences, USA)	37 g
dem. water	ad 1 l

DMEM:F12

Equal volumes of Dulbeccos Modified Eagle Medium (DMEM) and F12 medium (Gibco) were mixed under sterile conditions. The DMEM was prepared as indicated in Tab. S 1.

RPMI-1640 + GlutaMax-I

RPMI medium was ordered from Gibco and supplemented with 7.5% newborn calf serum (NCS) (Sigma-Aldrich).

***Yersinia* selective agar** (Schiemann, 1979)

Yersinia selective agar base (Oxoid, UK)	29 g
dem. water	ad 500 ml

After autoclaving *Yersinia* selective supplements (Oxoid, UK) were added according to the manufacturers instructions.

Media (except for DMEM:F12 and RPMI) were autoclaved prior to use. For the preparation of agar plates, antibiotics were added to the cooled solutions under sterile conditions as indicated in Tab. 2.3.

Tab. 2.3 Antibiotics

Antibiotic	Stock solution	Final concentration
Carbenicillin	100 mg/ml in dem. H_2O	100 µg/ml
Chloramphenicol	30 mg/ml in ethanol	30 µg/ml
Kanamycin	50 mg/ml in dem. H_2O	50 µg/ml
Tetracycline	5 mg/ml in ethanol	5 µg/ml

2.1.3. Oligonucleotides

Tab. 2.4 lists all oligonucleotide primers used for molecular cloning. Oligonucleotides that were applied for probe generation (DIG-labelled northern blot probes) are depicted in **Tab. 2.5** while primers used for RT-PCR are indicated in Tab. 2.6. Primers were purchased from metabion GmbH, Germany.

Tab. 2.4 Oligonucleotides for DNA amplification in molecular cloning

Oligonucleotide	Sequence (5'>3')	Restriction site
Oligonucleotides for plasmid generation		
III108	GCG GCG GGA TCC GAG GAT ATA TCA TGA AGT CAG	*Bam*HI
III286	CGC GCG GTC GAC CAT ATT CAA CGC CGA ATA ATG C	*Sal*I
III287	CGC GCG GGA TCC CTA GAG GAA GTT CAG GTA GCC	*Bam*HI
III585	GCG CGG ATC CAA ACG TAA CTC CCT AGG AAA T	*Bam*HI
III654	GCG CGG ATC CGG TAG AGT TTA TCG CTC GC	*Bam*HI
III655	GCG CGG ATC CAC TGA CTT CAT GAT ATA TCC TC	*Bam*HI
III656	GCG CGG ATC CCG TCT ATT CAT GAT AAC TCT CC	*Bam*HI
III662	GCG CGG ATC CGG AGT TAA CAA ACG TAA CTC C	*Bam*HI
III773	GCG CGG ATC CTA GTC GTT CTA ACG ATG ATA GT	*Bam*HI
III774	GCG CGG ATC CTT AGC TGC CAT TGG TAT TTC C	*Bam*HI

Oligonucleotide	Sequence (5'>3')	Restriction site
III775	GCG CGG ATC CGG CCG ACT AAG CTT AAC CA	*Bam*HI
III776	GCG CGG ATC CAT TTT ACC CAT CTA AAA CGC CT	*Bam*HI
III777	GCG CGG ATC CGG CGA AGC GGT CAT CAA TA	*Bam*HI
III778	GCG CGG ATC CTT ACT ACT CAT GGA TAT CTC C	*Bam*HI
III779	GCG CGG ATC CGC ATA AAG CCA TCA TAG AG	*Bam*HI
III780	GCG CGG ATC CTT CTT TCT CAT ATC TAT GTC C	*Bam*HI
IV455	GCG CGT CGA CGG AGT CAG CAA AAT TGT ACC	*Sal*I
IV458	GCG CGT CGA CAT TCT TTT CAT CTT TAA CTT ACT C	*Sal*I
IV459	GCG CGG ATC CGC ACT ACT GGA TTA TTC GTT	*Bam*HI
IV464	GCG CGG ATC CCA CGG CCT GCC TTG CGA TC	*Bam*HI
IV735	GCG CGG ATC CCA GCT CTG ATT GGA TTA ATT CAG	*Bam*HI
IV736	GCG CGT CGA CAT GTC ACT CAT ATT ATT GTC CAT C	*Sal*I
IV923	GCG CGT CGA CAT TTT GGC TAT TCA TCC ACG TC	*Bam*HI
V655	CGC GCG GGA TCC CTA *GTG ATG ATG ATG ATG ATG* GAG GAA GTT CAG GTA GCC	*Sal*I
Oligonucleotides for mutagenesis		
III844	**CAT ATG AAT ATC CTC CTT AGT** TGT CCT ATC TGA CAT GC	
III845	GCG CGA GCT CGG CAG AGT TAA TGT AAT GTT CC	*Sac*I
III920	GCG CGA GCT CGG CTT GCT CAC TGA TAT G	*Sac*I
III921	**GAA GCA GCT CCA GCC TAC AC**A TCT ATG TCC TCT TAT TTT GGC	

underlined restriction site, **bold** sequence homologous to kan resistance cassette, *italic* His-tag

Tab. 2.5 Oligonucleotides used to generate DIG-labelled northern blot probes

Transcript	Oligonucleotide	Sequence (5'>3')
csrA	V4	TGA TTG GCG ATG AGG TTA CGG
	V5	TTC TGC TTG GAT GCG CTG GT
csrB	555	CGG CGC GGA TCC CTC TCA CAC CAG CTG TG
	556	GGG GGC GTC GAC GGC AAA CTC AAT ATC CTG
csrC	582	GCG GCG GTC GAC CCT TCA TCC CGT GGT AGG
	583	GGG CGC GGA TCC GAT TGG GCC GGA ATC TAG C
csrC (+1 to +151)[a]	I521	GGG CGC GTA ATA CGA CTC ACT ATA GGA GCG AAT TTT GTA AAG TGG C
	I522	CCA GTG TCC TAA CAT CCC T
rovC	III286	CGC GCG GTC GAC CAT ATT CAA CGC CGA ATA ATG C
	IV91	GCG CGA GCT CGC TCC TCT TTG CAT TCC AC
rovC (+1 to +77)[a]	V773	GTA ATA CGA CTC ACT ATA GGA TGA CGT GGA TGA ATA GCC
	V777	CAT TCC CAC GCG AAG TCA TTA T
rovM (-81 to +67)[b]	I523	GGG CGC GTA ATA CGA CTC ACT ATA GGC GTT GTC CTT TAT TGA TAA C
	I524	GCA ACA GCT ACA AAG GTT C
pnp	IV527	TTG CTG ACT CCG ATT ATT CG
	IV528	GAA GAC GAC CGC GCC CAA C
rne	IV529	CGC GAC TCA GCA AGA AGA G
	IV530	GCC GAT GTC TGG GCG CAG

[a] nucleotides relative to transcriptional start
[b] nucleotides relative to translational start
underlined T7promoter

Tab. 2.6 Oligonucleotides for cDNA amplification in RT-PCR analysis

Transcript	Oligonucleotide	Sequence (5'>3')
csrA	V4	TGA TTG GCG ATG AGG TTA CGG
	V5	TTC TGC TTG GAT GCG CTG GT
dnaJ	III763	GCA GCG TGC ATC CCG TGG TTC
	III764	GGT TTA GCA CCG CTA CCG TGG
dnaK	III72	GCT GGT TTG TCT GTT TCC GAC
	III73	GCA CAG CGG CAC CAA TGG C
groEL	III962	GAT GGC GTA GGC GAT GAA GCG
	III963	CGG CAA CGC CGC CAG CCA G
groES	III960	CTG GCA CTG CAG CGG GTA AAT C
	III961	GCC TTC ACG CCG TAA CCA TCG
grpE	III765	GCG CGA AAG CCT GTT ACG CGC
	III766	CGC TCC AGA TTG TCA ATC ACT GG
rnpA	III80	TGA ACG TAA TCG GAT AAA GCG C
	III81	GTC AAC GCA CGG TTA TCG AGG
sopB	III393	CCG ACG TAA AGC CGC GAT AC
	III394	CCT CGT TCA TAA GCA CTC GTC
tdcF	III68	GGA TTC TGT ATG CTT CAG GGC
	III69	CCA GCC TGT AGA AGA ACA GC
YPK_0604	III923	GTG GCA TGG AAT GCC AAT GGC
	III924	GAC GTA CAA CAT CAG CAG GCG
YPK_3548	V647	ATG TAT TTA CGG CGT CTT TAC GAT C
	V648	TTA GAT GCT ATC CGG CTG GTG G
YPK_3552	V649	GCT CAC CTT ACG TGC CAG CGT
	V650	CCG CAT TAT CGA TCC ACC CTA TG
YPK_3559	V651	CGG CCC AAC TGG ATG TGC TC
	V652	CAT GCA GAT GGC GGC TTT GC
YPK_3566	V653	CAT CTT CGA CAT TAT TTT TAA CTG TC
	V654	GTT CAC AAT GCA GTT GGT AAC TC

2.1.4. Enzymes, antibodies and kits

All enzymes, antibodies and kits are listed in Tab. 2.7**,** Tab. 2.8 and Tab. 2.9.

Tab. 2.7 Enzymes

Enzyme	Manufacturer
Antarctic phosphatase	NEB
Benzonase	Merck
DNaseI	Roche
Lysozyme	Sigma
Mango *Taq* polymerase	Bioline
Phusion polymerase	Finnzymes
Pronase	Roche
Restriction enzymes	NEB
RiboLock RNase inhibitor	Thermo Scientific
RNase A	Qiagen
T4 DNA ligase	Promega
Taq polymerase	NEB

The anti-invasin and anti-His antibodies were monoclonally generated from mice, while the majority of antibodies was polyclonally genearted in rabbits.

Tab. 2.8 Antibodies

Antibody	Manufacturer	Dilution
Primary antibody		
Anti-YmoA	Davids Biotechnology	1:6000
Anti-RovM	Davids Biotechnology	1:6000
Anti-RovA	Davids Biotechnology	1:6000
Anti-InvA	Dersch and Isberg, 1999	1:10000
Anti-His	Qiagen	1:2000
Anti-H-NS	Davids Biotechnology	1:100000
Anti-CsrA	Davids Biotechnology	1:8000
Secondary antibody		
anti-digoxygenin alkaline phosphatase	Roche	1:8000
anti-rabbit immunoglobulin horseradish peroxidase	Cell signalling	1:8000
anti-mouse immunoglobulin horseradish peroxidase	Cell signalling	1:5000

Tab. 2.9 Commercial kits

Kit	Manufacturer
Dig-luminescent detection	Roche
Gene Expression Hybridization kit	Agilent
KREA*pure* purification kit	Kreatech
MangoMix	Bioline
Microarray Hybridization Chamber Kit	Agilent
QIAquick™ Gel extraction	Qiagen
QIAquick™ PCR Purification	Qiagen
QIAquick™ Plasmid Midiprep	Qiagen
QIAquick™ Plasmid Miniprep	Qiagen
RNA Nano6000	Agilent
SensiFAST™ SYBR No-ROX One-Step Kit	Bioline
SV Total RNA Isolation	Promega
Transcript Aid™ T7 High Yield Transcription kit	Fermentas
ULS™ Fluorescent Labelling Kit for Agilent Arrays	Kreatech

2.1.5. Size standards

Applied size standards are indicated in Tab. 2.10.

Tab. 2.10 Molecular size standards

Size standard	Manufacturer
GeneRuler DNA Ladder mix	Thermo Scientific
RNA Molecular Weight Marker I, Dig-labelled	Roche
PageRuler Prestained Protein Ladder	Thermo Scientific

2.1.6. Chemicals

Chemicals and the corresponding manufacturers are indicated in Tab. 2.11.

Tab. 2.11 Chemicals

Chemical	Manufacturer
Acetic acid	Roth
Acrylamide/bisacrylamide (30%)	Roth
Acrylamide/bisacrylamide (40%)	Roth
Adenosine 5' Triphosphate (ATP)	NEB
Agar (*E. coli*)	Roth
Agar noble (*Yersinia*)	BD Biosciences
Agarose	PEQLAB
Ammonium persulfate (APS)	Sigma-Aldrich
Anhydrotetracycline (AHT)	Biozol Diagnostics
Arabinose	Roth
Bactor Brain Heart Infusion	BD Biosciences
Bactor tryptone	BD Biosciences
Bacto yeast extract	BD Biosciences
Beta-mercaptoethanole	Sigma-Aldrich
Blocking reagent	Roche
Boric acid	Roth
5-bromo-4-chloro-3-indolyl-beta-D-galactopyranoside (X-gal)	Roth
Bromophenole blue	Roth
Carbenicillin	Roth
CDP-*Star*	Roth
Chloramphenicol	Roth
Chlororform	J.T. Baker
Chlororform-isoamylalcohol 24:1	Applichem
Coomassie brilliant blue G250	Roth
Complete-mini EDTA-free protease inhibitor	Roche
Dimethylformamide (DMF)	Roth
Disodium phosphate	Roth

Chemical	Manufacturer
dNTP-mix	NEB
Dithiothreitol (DTT)	Roth
Ethanol absolute	Sigma-Aldrich
Ethidiumbromide	Applichem
Ethylenediaminetetraacetic acid (EDTA)	Roth
Formaldehyde	Roth
Formamide	Applichem
Glycerole	Applichem
Glycine	Roth
Hydrochloric acid	Roth
Imidazole	Roth
IPTG	VWR International
Isopropanole	J.T. Baker
Kanamycine	Roth
LB medium (*E. coli*)	Roth
Magnesium chloride	Roth
Magnesium sulfate	Merck
Milk powder	Applichem
Maleic acid	Merck
Methanole	J.T. Baker
MOPS	Applichem
n-lauroylsarcosine	Sigma-Aldrich
Ni-NTA	Macherey und Nagel
2-Nitrophenyl-beta-D-galactopyranosid	Omnilab
PCR DIG Labelling Mix	NEB
Phenole/Chloroform/Isoamylalcohol	Roth
Phosphate buffered saline (PBS)	Biochrom
Potassium acetate	Roth
Potassium chloride	Roth
Potassium dihydrogen phosphate	Roth
Restore Plus Western Blot Stripping Buffer	Thermo Scientific
Rifampicin	Serva
Rubidiumchloride	Applichem
Sodium acetate	Roth
Sodium carbonate	Roth
Sodium chloride	Roth
Sodium citrate	Merck
Sodium-dodecylsulfate (SDS)	Applichem
Sodium hydrogencarbonate	Applichem
Strep-Tactin® Superflow	IBA
Streptavidin-Hrp	NEB
Sucrose	Roth
Tetramethylethylenediamine	Roth
TRICINE	Roth
Trizma	Sigma-Aldrich
Trypan blue	Biochrom

Chemical	Manufacturer
Trypsin-EDTA	Sigma-Aldrich
Tween R-20	Roth
Western Lightning Plus-ECL	Perkin Elmer
Yersinia agar	Oxoid
Yersinia selective supplement	Oxoid

2.1.7. Technical equipment and material

The technical equipment and used material are given in Tab. 2.12.

Tab. 2.12 Technical equipment and material

Equipment	Manufacturer
Agilent 2100 Bioanalyzer	Agilent
Breathe-Easy® sealing membrane	Sigma-Aldrich
Bunsen Burner Fireboy	IBS Integra
Cell incubator HERA cell 150	Thermo Scientifc
Centrifuge 3-18 K	Sigma
ChemiDoc XRS$^+$	BioRad
Clean bench Maxisafe 20202	Thermo Scientifc
Electroporation cuvettes	PEQLAB
Electroporator GenePulser II	BioRad
ELISA Reader iMarK Microplate	BioRad
Falcon tubes (15 ml, 50 ml)	Greiner
Filter filtropur S plus (0.22 µm)	Sarstedt
Filter membranes (0.2 µm GSWP)	Millipore
FrenchPress Digi	G. Heinemann
GelDoc XRS$^+$	BioRad
Glass bottles, beakers and flasks	Schott
Glass pipettes	Hirschmann
Hemocytometer (Neubauer improved)	Marienfeld
Hybridization oven OV-2	Biometra
Immobilon-P membrane (PVDF)	Millipore
Incubator	Hereaus
NanoDrop ND-1000	PEQLAB
Nitrocellulose membrane	Roche
Nylon membrane	Whatman
Magnetic stirrer MR3001	Heidolph
Microcentrifuge 5415 R	Eppendorf
Microcentrifuge Mini-Spin plus	Eppendorf
Microcentrifuge tubes (0.2 ml, 1.5 ml, 2 ml)	Sarstedt
Microtiter plates	Greiner
Microwave Panasonic ProII	Panasonic
Mini-protean II Tetra cell	BioRad

Equipment	Manufacturer
PerfectBlue Gel systems	PEQLAB
Petri dishes	Greiner
pH meter 827 pH lab	Metrohm
Pipette tips	Sarstedt
Pipettes	Eppendorf
Pipettor Accu-Jet	Brand
Power Pack PS9009	Biometra
Power Supply Power Pac Universal	BioRad
Precision balance	Sartorius
Protein blotting system Mini Trans-blot cell	BioRad
Shaker Multitron 2	Infors HT
Spectrophotometer UV/VIS Ultrospec 2100 pro	Amersham biosciences
Sterile 96-well plates (for luminescence detection)	Corning
Sterile cell culture flasks (75 cm^3)	Greiner
Sterile filters Stericup (0.22 µm)	Millipore
Sterile plastic pipettes	Greiner
Thermocycler T3000	Biometra
Thermocycler Mastercycler personal	Eppendorf
Thermomixer comfort (1.5 ml, 2 ml)	Eppendorf
TransBlot SD Semi-Dry Transfer Cell	BioRad
UV-crosslinker	Stratagene
UV-cuvettes	Sarstedt
Vacuum blotter Model 785	BioRad
Vaccum pump	BioRad
Varioskan Flash	Thermo Scientifc
Vortexer	Scientific industries
Water bath	GFL
Whatman paper	GE Healthcare

2.1.8. Software

For the analysis of sequence data the programs and databases of NCBI (National Centre for Biotechnology Information) as well as the Kegg (Kyoto Encyclopedia of Genes and Genomes) database resource were used. For data processing the program ApE (A plasmid Editor), Excel:Mac (Microsoft Office 2011) and GraphPad Prism were used. Graphic editing was performed by means of Adobe Photoshop CS5 extended (Version 12.1 Adobe Systems inc.) and Adobe Illustrator CS5 (Version 15.1.0 Adobe Systems inc.). Further, Word:Mac and PowerPoint:Mac (Microsoft Office 2011) were used.

2.2. Cell biological methods

2.2.1. Culture of eukaryotic cells

Cell culture work was performed under laminar flows. Culture media and supplements were prewarmed to 37°C in a water bath. Adherent HEp-2 cells were cultured in 75 cm^3 cell culture flasks in RPMI-1640 medium at 37°C, 95% humidity and 5% CO_2-atmosphere. The HEp-2 cells were passaged when the cells reached confluency (dish coverage of 90 to 95%, every second day). Therefore, cells were washed with 1x PBS (10 ml) and incubated with trypsin (appr. 2 ml) at 37°C until cells started rounding up (appr. 10 min). Detachment was promoted by tapping the culture flask. Trypsinization was stopped by the addition of growth medium (appr. 8 ml) to the cells. Afterwards, cells were gently resuspended.

2.2.2. Determination of the cell density

the cell density was determined by means of a hemocytometer (Neubauer improved). 90 µl trypan blue were mixed with 10 µl resuspended cells and loaded onto the counting chamber. Cells were counted in each of the four large squares. The cell number per ml was calculated by multiplying the average of the four squares by factor 10^4. Finally, the cells were resuspended in the appropriate volume of culture medium to adjust the desired cell density and seeded into the respective cell culture dish.

2.2.3. Cell contact assay

Cell contact assays were used to monitor bacterial gene expression in response to physical contact to host cell. Here, epithelial HEp-2 cells (human epidermoid carcinoma cells, larynx) were used as they express β1-integrins on their surface and are well established in *Yersinia* infection model systems (Isberg *et al.*, 1987; Eitel and Dersch, 2002).

5.9 x 10^4 HEp-2 cells were seeded in 200 µl RPMI medium in 95-well flat bottom plates and incubated overnight in a cell incubator. *Y. pseudotuberculosis* strains harbouring luciferase promoter fusions were grown at 25°C to the stationary phase (16 h). The eukaryotic cells were washed three-times with 1x PBS and finally overlaid with 200 µl 1x PBS. Wells containing solely 200 µl PBS served as negative controls. The bacteria were diluted to an OD_{600} of 0.1 and 10 µl of this suspension was centrifuged onto the Hep-2 cells (3 min, 170 x

g). The plate was covered with Breathe-Easy® foil and incubated for 2.5 hours at 25°C in a Varioskan plate reader. Bioluminescent emission was measured every ten minutes to monitor the kinetics of host cell contact-dependent expression of the reporter fusion.

2.3. Microbiological methods

2.3.1. Cultivation and stock keeping of microorganisms

Bacterial overnight cultures were inoculated from a single colony picked from an agar plate under sterile conditions. For incubation a shaker was used at 200 rpm either at 25°C (*Y. pseudotuberculosis*) or 37°C (*E. coli*).

For subculturing in liquid medium, a defined volume of the overnight culture was used to inoculate the main culture, which was incubated in a shake incubator at the appropriate temperature.

To culture the bacteria on solid medium the bacteria were stroke on agar plates under sterile conditions and grown for one to two days. Grown agar plates were stored at 4°C for up to four weeks.

Bacterial glycerol stock cultures were prepared to store the bacteria for a longer period of time. Therefore, 1.25 ml bacterial suspension from an over night culture were mixed with 0.75 ml 80% glycerol and stored at -80°C.

2.3.2. Sterilization techniques

Culture media and buffers were heat-sterilized in an autoclave for 20 min at 121°C at 1-2 bar. Heat-sensitive solutions were filter-sterilized by means of Stericup® filter units (Millipore). Glassware was sterilized in heat in a dry-heat sterilizer at 180°C. Working places and other material were disinfected by ethanol (70%) or 1 to 7% Pursept®.

2.3.3. Determination of the bacterial cell number

To quantify the bacterial cell number the optical density (OD) was measured at 600 nm in a spectrophotometer. 1 ml of the bacterial suspension was filled into single-use UV-microcuvettes (path length 1 cm) and measured against sterile LB-medium as a blank. When

dealing with high-density cultures (over night cultures), bacterial cultures were diluted 1:10 in LB before the measurement. An OD_{600} of 1 resembles $1*10^9$ cells/ml containing 150 µg total protein (Miller, 1992; Sambrook, 2001).

2.4. Molecular biological methods for DNA analysis

2.4.1. Isolation of total bacterial DNA from Gram-negative bacteria

The following method describes the isolation of chromosomal and plasmid DNA from Gram-negative bacteria.

For isolation of chromosomal DNA 3 ml of an overnight culture were centrifuged for 4 min at 12000 rpm and resuspended in 350 µl resuspension buffer. To dissolve lipids and proteins of the bacterial cell wall 20 µl of 10% SDS and 100 µl of the enzyme pronase (10 mg/ml) were added and incubated for 1 h at 45°C, as the pronase exhibits its maximum activity at this temperature.

In order to remove the proteins and lipids a phenol/ chloroform extraction was performed. 150 µl of phenol (pH 8) were added to the mixture and incubated for 1 h at 37°C with occasional inversion of the microcentrifuge tubes until the solution became clear. Afterwards, 600 µl of chloroform were added, mixed for 5 seconds and centrifuged at 12000 rpm for 15 min at RT. The centrifugation enables a stable separation of the watery and the organic phase. The organic phase in the lower compartment contained the proteins, which denatured and precipitated by adding the detergents. In contrast, the DNA remained in the watery phase. Lipids and amphiphilc proteins were found at the interphase between polar and non-polar solution. The upper phase containing the DNA was transferred to a new sterile reaction vessel. For further purification the DNA was precipitated by adding 60 µl of 3 M sodium acetate (1/10 of the volume) and 1 ml ice-cold 100% ethanol, which removes the hydration shell from the DNA. The precipitated DNA had a viscous structure and could be pooled off the solution by means of a sterile glass stick. To remove remaining salts the DNA was washed twice with ice-cold ethanol and incubated for 1 h at 37°C after addition of 400 µl TE buffer and 20 µl RNase A (10 mg/ml). This step will remove all residual RNA from the reaction mixture. Afterwards, the DNA was precipitated once again with 40 µl 3 M sodium acetate and washed twice with 100% ice-cold ethanol. Residual ethanol was

removed by heat evaporation at 55°C and the remaining DNA was resuspended in an appropriate volume of dem. H_2O and stored until use at -20 °C.

Resuspension buffer: 50 mM Tris-HCl, pH 8.0, 50 mM EDTA, pH 8.0
TE buffer: 10 mM Tris/HCl, pH 8.0, 1 mM EDTA, pH 8.0
Pronase: 10 mg/ml in dem. water, pre-incubate at 42°C for 1 h

2.4.2. Isolation of plasmid DNA

The plasmid DNA isolation is based on the principle of alkaline lysis (Birnboim and Doly, 1979). The basic principle is the conformational difference between the chromosomal and the plasmid DNA. In contrast to the supercoiled plasmid DNA the chromosomal DNA (not supercoiled) will be denatured irreversibly by treating it with alkaline solutions. Following neutralization the chromosomal DNA is precipitated and can be removed in accordance with the proteins and remaining cell debris by centrifugation whereas the plasmid DNA will renature and remain in the supernatant.

Plasmid mini preparation

For the isolation of plasmid DNA (high- and low-copy number) from *E. coli* with high purity in small scale the "QIAprep® Spin Miniprep Kit" (Qiagen, Hilden) was used. This system is based on the principle of alkaline lysis, neutralization and separation of the precipitate, which consists of chromosomal DNA and protein debris from the plasmid DNA in the supernatant. The high purity is achieved by making use of the anion-exchange column as the plasmid DNA binds to the column matrix whereas the impurities are removed by several washing steps. The purified plasmid DNA is then eluted from the column by the addition of water.
20 ml of an overnight culture were harvested by centrifugation for 6 min at 6000 rpm in a centrifuge and the plasmid DNA was isolated as described by the manufacturer. The plasmid DNA was stored at -20°C until use.

Plasmid midi preparation

For the isolation of plasmid DNA (high- and low-copy number) from *E. coli* with high purity in medium scale the "QIAGEN Plasmid Midi Kit" (Qiagen, Hilden) was used. Like the QIAprep® Spin Miniprep Kit this system is based on the principle of alkaline lysis.

100 ml of an overnight culture were harvested by centrifugation at 6000 rpm and plasmids were isolated as described by the manufacturer. Finally the DNA was resuspended in 50 µl of nuclease-free water and stored at -20°C until use.

2.4.3. Photometric determination of nucleic acid concentration

The principle of the photometric measurement of DNA-concentrations relies on the fact that the aromatic ring systems of the purine- and pyrimidine-bases show an absorption maximum at λ = 260 nm. An absorption of 1.0 equals a DNA-concentration of 50 µg/ml double-stranded DNA or a RNA-concentration of 40 µg/ml (single stranded), respectively (Sambrook, 2001). The DNA-concentration is proportional to the UV-irradiation that it absorbs. Thus, the UV-spectrum can be used as a measure for the DNA-concentration.
To determine the amount and purity of the nucleic acid a NanoDrop (PEQLAB, Germany) was used. In case of pure nucleic acids the ratio lies in between 1.8 and 2.0 whereas pure DNA has a value of 1.8 and pure RNA has 2.0. A quotient smaller than 1.8 indicates protein impurities and a quotient larger than 2.0 indicates impurities.

2.4.4. Separation of DNA by agarose gel electrophoresis

Electrophoresis describes a biochemical separation process that makes use of charged molecules that migrate in an electric field for separation purposes. Due to their sugar-phosphate backbone nucleic acids are negatively charged and migrate to the anode when an electric field is applied. Generally, agarose gels in form of horizontal gel-plates were used as inert matrix for gel electrophoresis. The polysaccharide meshwork of the red algae serves as a molecular sieve with a distinct pore size that enables the separation of charged (linear) DNA molecules by size. The smaller a DNA fragment is, the faster is its velocity of migration.
By varying the agarose concentration (0.8-2.0%) the pore size of the agarose-meshwork can be modified so that smaller or larger fragments can be separated more efficiently. 0.8-2.0% agarose gels allow a separation from 0.1 kb to 20 kb (Sambrook, 2001).
In general 0.8-2.0% agarose gels were used in 1x TAE. Samples were mixed 1:6 with 6x loading dye and loaded onto the gel. The separation of the nucleic acid fragments was carried out in an electric field by applying 100-120 volt for 45 min. Afterwards the gel was incubated in ethidiumbromide for 15-20 min. Ethidiumbromide is a planar intercalating

agent that incorporates sequence-unspecifically in between the bases of neighboring DNA molecules and fluoresces (λ = 590 nm) under UV-light (λ = 312nm). The fluorescent intensity is proportional to the amount of bound DNA. Fragments having the same size can be detected as distinct bands, which can be documented photographically. Characterization of the fragment-sizes was done by comparing the bands with size-standards (see 2.1.5). For detection the GelDoc XRS$^+$ (BioRad) imaging system was used.

TAE buffer (50x): 2 M Tris/HCl pH 8.3, 1M acetic acid, 0.1 M EDTA
Loading dye (6x): 10 mM Tris/HCl, pH 7.5, 50 mM EDTA, 50% (v/v) glycerol, 1 spatula bromophenol blue
Ethidium bromide staining solution: 2 g/ml ethidium bromide in 1x TAE

2.4.5. Purification and isolation of DNA from agarose gels

To isolate and purify DNA-fragments (size range from 70 bp to 10 kb) from agarose gels after electrophoretic separation the "QIAquick Gel Extraction Kit" (Qiagen, Hilden) was used. The kit contains a silica-membrane assembly that allows DNA-binding under high-salt conditions, while elution is performed under low-salt buffer conditions.

After gel electrophoretic separation and staining of the DNA-fragments with ethidium bromide the desired fragments were excised from the gel by means of a scalpel on a UV-transilluminator. Subsequently the DNA was isolated as described by the manufacturer. The DNA was eluted by the addition of nuclease-free water and stored at -20°C until use.

2.4.6. *In vitro* amplification of DNA (PCR)

The polymerase chain reaction (PCR) provides an extremely sensitive approach to selectively amplify small amounts of defined DNA from a mixture of DNA-molecules.

The flanking regions upstream and downstream of the DNA-region of interest enable hybridization with two chemically synthesized oligonucleotides (primers), which will bind strand-specific and in an antiparallel fashion to these flanking regions.

Besides the magnesium concentration, the stringency of the primer binding depends on the hybridization (annealing) temperature, which is determined by the base composition of the primer itself. For oligonucleotides with a length of 18-22 bp it can be determined according to the following formula (Itakura *et al.*, 1984):

T_m [°C]= [(Number of bases A + T) x 2 °C + (Number of bases G + C) x 4 °C] – 5 °C

After hybridization of the primers to the template DNA, the free 3'-OH groups form the starting point for the DNA polymerase that elongates the single strand complementary to the template DNA resulting in a double stranded molecule.

The whole PCR is base on three repetitive steps, which are repeated 20 to 40 times. First the double-stranded molecules are denatured by heat (95°C) in order to provide single-stranded DNA. For primer annealing the mixture is cooled down to the respective temperature and in the final step the DNA synthesis (elongation) takes place at the optimum temperature of the polymerase.

For this study the *Taq*-polymerase and the *Phusion*®-polymerase (Finnzymes) were used. The *Phusion*®-polymerase is a synthetic polymerase that possesses an additional DNA-binding domain and a *Pfu*-like polymerase domain. To prevent unspecific primer-annealing the PCR setups were pipetted on ice and started after pre-heating of the thermocycler.

Example of a PCR-reaction

Template DNA	1 ng-200 ng
Polymerase buffer (10x)	10 µl
Polymerase	2.5 Units
dNTP mixture (10 mM each)	2 µl (200 µM each)
Oligonucleotide	100 ng/µl per Primer
dem. H_2O	ad 100 µl

Chromosomal DNA of the respective clones or the *Y. pseudotuberculosis* wild type was used as template DNA. In case of a colony-PCR, bacterial colony material was directly resuspended in the PCR reaction mixture. A typical PCR cycle used in this study is described below. Steps 2 to 4 were repeated up to 35 times:

1. **Initial Denaturation** - 95°C for 5 min

2. Denaturation - 95°C for 1 min

3. Hybridization (Annealing) - usually 56°C for 1 min

4. DNA-synthesis (Elongation) - 1 to 3 min at 72°C (dep. on Polymerase, product length)

5. Terminal Elongation - 10 min at 72°C

6. Cooling of the probes until use at 15°C

2.4.7. Purification and isolation of DNA from solution

To purify DNA-fragments from solutions like PCR setups or restriction digests, the “QIAquick PCR Purification Kit” (Qiagen, Hilden) was used as described by the manufacturer. DNA-binding and clean-up relies on the same high- and low-salt conditions as the gel extraction procedure (2.4.5) and removes impurities like primers, polymerases, dNTPs and salts. To prevent DNA degradation, samples were stored at -20°C until use.

2.5. Molecular cloning

Cloning was used for the replication or expression of foreign genes or DNA-fragments in a high amount to monitor phenotypic changes or genetic alterations of the recipient organism. The gene of interest was amplified by PCR (2.4.6), cloned into a suitable vector (2.5) and transformed into a recipient strain (2.5.7). In principle the desired fragment was amplified by PCR (2.4.6), purified (2.4.7) and digested with the respective restriction enzymes. After a second PCR clean-up fragments were ligated into the target vector according to the molecular cloning techniques as described in the following. The vector itself was digested and dephosphorylated as described below, and was re-isolated from an agarose gel after electrophoretic separation.

2.5.1. Cloning of PCR products via restriction sites

Molecular cloning of PCR-fragments into a suitable vector system involves primers that possess recognition sequences for restriction endonucleases at their 5’-ends. These recognition sequences account only for a small portion of the homologous sequence so that the insertion of the restriction site does not alter the specificity of the primer.
The purified PCR products (2.4.7) were digested by restriction endonucleases (2.5.2) and ligated (2.5.4) into a vector that was digested with the same endonucleases.

2.5.2. Restriction of DNA

To characterize and identify double-stranded DNA-molecules the application of restriction endonucleases is a common method. For this study class-II restriction endonucleases by New England Biolabs (Ipswich, USA) and the corresponding buffers were used. The applied

buffers provided the optimal working conditions for the respective enzyme. For double-digestion setups the buffer, which enabled the highest activity for both enzymes was chosen as described by the manufacturer.

The setup was incubated for 3 hours at 37°C. Restriction was stopped either by heat-denaturation of the enzyme or by adding 6 x loading dye. Subsequent gel electrophoresis allowed the identification and evaluation of the resulting banding pattern.

Example of a restriction digest

DNA	0.1-1.0 µg
Reaction Buffer (10 x)	6 µl
Restriction Enzyme (1 U/ µl)	1 µl
dem. H_2O	ad 60 µl

2.5.3. Dephosphorylation of 5'-ends of DNA

To prevent the self-ligation of restricted vector fragments, the fragments were dephosphorylated after the restriction digest. Therefore, 1 µl antarctic phosphatase (NEB, Ipswich, USA) and 6 µl antarctic phosphatase buffer were added to the inactivated restriction setups to hydrolyse the 5'-phophate groups. Incubation was carried out for 1 h at 37°C. Since phosphatase treated fragments lack the 5'-phopsphoryl ends needed by the ligase, self-ligation is prevented and the vector background is decreased. Subsequent addition of 6x loading dye and electrophoretic separation inactivated the enzyme.

2.5.4. Ligation of DNA fragments

DNA-ligases catalyse the formation of phosphodiester-bonds between neighbouring 3'-hydroxy and 5'-phosphate ends of double-stranded DNA-molecules. Thus, DNA-fragments that exhibit sticky- or blunt-ends can be covalently fixed. In genetic engineering the T_4-DNA-ligase from bacteriophage T_4 is commonly used to connect either sticky- or blunt-ends. For efficient ligation the molar ratio of vector- to insert-DNA was set from 1:3 to 1:6. The ligation setup was incubated for 2 to 3 h at RT. The T_4-DNA-ligase and the corresponding buffer were purchased from Promega (Madison, USA).

Example of a ligation setup

Plasmid DNA	100 ng
Insert DNA	400 ng
T_4-DNA-ligase Buffer (10 x)	1 µl
T_4-DNA-ligase (60 U)	1 µl
ATP	1 µl
dem. H_2O	ad 10 µl

2.5.5. Plasmid construction

Plasmids generated during this study and the corersponding oligonucleotides are listed in Tab. 2.13.

Tab. 2.13 Plasmid construction

Plasmid	Description	Primer pair
pSSE11	pACYC184, p15A, *rovC*$^+$, Cm^R	III286-III287
pSSE16	pTS02, ori pSC101, *tdcF*'-'*lacZ* (3)^c, Amp^R	III654-III655
pSSE20	pTS02, ori pSC101, *rnpA*'-'*lacZ* (3)^c, Amp^R	III585-III662
pSSE21	pTS02, ori pSC101, YPK_0604'-'*lacZ* (3)^c, Amp^R	III108-III656
pSSE27	pTS02, ori pSC101, *groEL*'-'*lacZ* (3)^c, Amp^R	III773-III774
pSSE28	pTS02, ori pSC101, *dnaK*'-'*lacZ* (3)^c, Amp^R	III775-III776
pSSE29	pTS02, ori pSC101, *grpE*'-'*lacZ* (7)^c, Amp^R	III777-III778
pSSE32	pTS02, ori pSC101, *rovC*'-'*lacZ* (3)^c, Amp^R	III779-III780
pSSE35	pAKH3, Δ*rovC*, Amp^R	III920-III921 (upstream) III844-III845 (downstream) III920-III845 (3-step)
pSSE51	pTS02, ori pSC101, *pnp*'-'*lacZ* (3)^c, Amp^R	IV464-IV455
pSSE52	pTS02, ori pSC101, *rne*'-'*lacZ* (3)^c, Amp^R	IV459-IV458
pSSE64	pTS02, ori pSC101, YPK_3566'-'*lacZ* (3)^c, Amp^R	IV735-IV736
pSSE67	pTS03, ori pSC101, *rovC-lacZ* (-618 to -14)^b, Amp^R	IV923-III779
pSSE68	pACYC184, p15A, *rovC-his*$^+$, Cm^R	III286-V655

2.5.6. DNA sequencing

Sequencing of plasmids was performed at the Department of Genome Analysis (GMAK, in-house facility) at the Helmholtz Centre for Infection Research, Germany.

2.5.7. Bacterial transformation

In genetic engineering transformation describes the uptake of free DNA into a cell (Winnacker, 1990). Many organisms possess a natural competence that enables the up-take of free DNA into the cell with low efficiency. To increase the transformation efficiency the cells can be treated either physically and/or chemically. Gold standards in genetic engineering are either the calcium chloride technique (Mandel and Higa, 1970; Rodriguez, 1983) or electroporation (Calvin and Hanawalt, 1988; Dower *et al.*, 1988).

Generally transformation procedures are used to clone a distinct gene. Therefore a plasmid bearing the gene of interest is introduced to a bacterial strain. The plasmid is replicated in the bacteria which amplifies the introduced gene was well. Selection of transformed bacteria is done via antibiotic resistance screening.

For some *E. coli* and all *Y. pseudotuberculosis* strains used in this study the electroporation technique was applied. The majority of *E. coli* strains was transformed by means of chemically competent cells.

Preparation of electrocompetent bacteria

To prepare electrocompetent bacteria 20 to 50 ml BHI medium were inoculated 1:50 (*Y. pseudotuberculosis*) or 1:100 (*E. coli*) with an overnight culture of the respective bacteria and grown for about 3 h at 25°C (*Y. pseudotuberculosis*) or 37°C (*E. coli*), 200 rpm, to an OD_{600} between 0.5-0.8. Following a 10 min incubation on ice the cells were harvested by centrifugation at 6000 rpm for 6 min at 4°C. The bacterial pellet was washed twice with 10 ml dem. ice-cold water and centrifuged as described before. Subsequently, the *E. coli* pellet was resuspended in the appropriate amount of ice-cold 10% glycerol. Competent *E. coli* cells were stored in 40 µl aliquots at -80°C.

The *Yersinia* pellet was resuspended in the appropriate volume of transformation buffer. The competent cells were directly used for transformation as 40 µl aliquots.

Transformation buffer *Yersinia*: 272 mM sucrose, 15% glycerole
Transformation buffer *E. coli:* 10% glycerole

Transformation via electroporation

The uptake of foreign DNA by electrocompetent bacteria is enabled by a voltage pulse that modifies the membrane potential for a short period of time, which increases the permeability of the cell membrane.

An aliquot of electrocompetent cells was thawed on ice and plasmid DNA was added to the bacterial suspension and mixed thoroughly. Ligation reactions were dialyzed prior to electroporation for 20 min by means of a filter membrane that allowed salt exchange.

The bacteria with the DNA to be transformed were pipetted into pre-chilled electroporation cuvettes (2 ml). The cuvette was inserted into the electroporation unit and exposed to the voltage pulse. The following parameters were applied:

Capacity	25 µF
Voltage Pulse	2500 V
Resistance	200 Ω
Time constant	5 msec

After electroporation the bacteria were directly mixed with 1 ml BHI medium without antibiotics and incubated for 2 h at 25 °C (*Y. pseudotuberculosis*) or for 1h at 37°C (*E. coli*) at 200 rpm. During this time the bacteria were allowed to regenerate and to express the antibiotic resistance mediated by the transformed plasmid. After phenotypic expression bacteria were pelleted by centrifugation at 6000 rpm for 2 min, RT. The pellet was resuspended in 100 µl LB and plated onto agar plates. Incubation was performed for one to two days at 25 °C (*Y. pseudotuberculosis*) or 37°C (*E. coli*). Selection was done by antibiotic resistance screening on agar plates, containing the respective antibiotic agent.

Preparation of chemically competent bacteria

Chemically competent *E. coli* cells were mainly used to transform ligation setups or plasmid DNA. Therefore, bacteria were inoculated 1:100 in 100 ml LB medium supplemented with 20 mM $MgSO_4$ and grown at 37°C. After 3 to 5 hours the bacterial cells were harvested at 6000 rpm for 5 min at 4°C and washed with 0.4 volumes of ice-cold TFB-I. Afterwards, cells were centrifuged again at 6000 rpm for 5 min at 4°C. Subsequently, the pellet was

resuspended in 1/25 (of the initial volume) ice-cold TFB-II. 100 µl aliquots were prepared and stored at -40°C.

TFB-I: 30 mM KAc, 10 mM $CaCl_2$, 50 mM $MnCl_2$, 100 mM RbCl, 15% glycerole, adjust pH 5.8 with acetic acid
TFB-II: 10 mM PIPES, pH 6.5, 75 mM $CaCl_2$, 10 mM RbCl, 15% glycerole, adjust pH 6.5 with KOH

Transformation via heat shock

Introduction of foreign DNA into chemically competent cells was performed by heat-shock treatment. Therefore, 10 to 100 ng (max 30 µl) DNA were mixed with 100 µl of the chemically competent bacteria and chilled on ice for 5 min. Then, bacteria were exposed to 42°C for 1 min and immediately cooled in ice for another minute. Subsequently, 1 ml BHI medium was added and phenotypic expression was allowed at 37°C for 1 h at 800 rpm using a thermomixer (Eppendorf, Germany). Afterwards, bacteria were streaked on agar plates containing the respective antibiotic agent and were incubated over night at 37°C.

2.6. Mutagenesis of *Y. pseudotuberculosis*

For the construction of gene deletion mutants in *Y. pseudotuberculosis* suicide plasmids derived from the pAKH3 plasmid were introduced into the respective strain and integrated via homologous recombination. Plasmid construction, introduction into *Yersinia* and subsequent mutant verification were carried out as described in the following.

2.6.1. Construction of mutagenesis plasmids

For construction of mutagenesis plasmids a PCR fragment harboring a kanamycin resistance cassette flanked by the upstream and downstream regions of the respective gene was generated. Therefore, the kanamycin (*kan*) gene (appr. 1.6 kb) was amplified using primers I661 and I662 with plasmid pKD4 as template. Next, upstream and downstream regions of the target gene each encompassing 500-bp in length were amplified with chromosomal *Yersinia* DNA as template. Herein, the reverse primer of the upstream fragment harboured a 20 nt 5'-end overhang that was homologous to the start of the *kan* gene, while the forward primer of the downstream fragment encompassed a 20 nt homologous region to the kanamycin end at its 3'-region. Each of the two fragments was separated on 2% agarose gels

to remove any residual primers, which would otherwise interfere with subsequent PCR amplification.

Finally, a three-step PCR was performed using the *kan* fragment as well as the upstream and downstream fragments of the respective gene as templates. The forward primer of the upstream fragment and the reverse primer of the downstream fragment were used as primer pair for this setup. The resulting fragment usually had a size of approx. 2.6 kb and was digested with *Sac*I and ligated into the *Sac*I site of pAKH3.

2.6.2. Bacterial conjugation

Conjugation describes the transfer of genetic material from one prokaryotic cell to another prokaryotic cell, mediated by direct cytosolic contact (Madigan and Martinko, 2000).

For this study plasmids with a suicide R6K-ori were used. For independent replication of this plasmid the chromosomally encoded π-protein (*pir*) is needed which is harbored by the *E. coli* strain S17-1λ*pir.* In contrast to the *E. coli* strain *Y. pseudotuberculosis* can take up the plasmids via conjugation but they cannot replicate the plasmids as they are lacking the π-protein. Only those bacteria that integrated the plasmid into their chromosome will be able to express the antibiotic resistance encoded on the suicide-plasmid. The pAKH3 plasmid served as suicide plasmid. This plasmid was used to delete genes of interest in the bacterial chromosome.

Conjugation was carried out by inoculating 5 ml BHI medium 1:50 with an over night culture of *Y. pseudotuberculosis*, or 3 ml LB 1:100 with *E. coli* S17-1λ*pir* carrying the suicide-plasmid. Both cultures were incubated at the appropriate temperature for 3 h at 200 rpm until cells reached the exponential growth phase. In case of *E. coli* the cells were allowed to form the sexpili by removing them from the shaking process after 2.5 h and incubating them in a non-shaking incubator at 37°C for the remaining 30 min.

Collecting the bacteria on filter paper in close proximity started conjugation. Therefore the filter paper was placed into a sterile funnel, connected to a vacuum pump. First, 1 ml of the donor strain culture (*E. coli* S17-*1λpir)* was harvested on the filter paper and washed with 3 ml LB medium to remove contaminating antibiotics. Then 3 ml of the *Y. pseudotuberculosis* culture (recipient strain) were added on top of the filter. The filter was removed from the funnel and placed onto an LB plate without any antibiotics and conjugation was allowed to take place for 4 h or over night. Finally, bacterial cells were removed from the filter paper by

adding 2 ml LB and scraping carefully over the filter by means of a pipet tip. 100 µl of this suspension were directly plated on *Yersinia* selective agar containing the respective antibiotic(s). The remaining portion was pelleted in a 2 ml collection tube at 6000 rpm for 2 min. and plated on the same selective medium and incubated for 48 h at 25°C.

2.6.3. Mutant verification

Homologous recombination of the mutagenesis plasmid into the *Yersinia* genome results in a merodiploid strain that harbours both, the wildtype and mutant copy of the target locus. Accordingly, a second recombination event is required to remove the plasmid resulting in loss of the target gene, which is replaced by the *kan* cassette. Integration of the plasmid at the desired genomic locus was checked by PCR. Subsequent plating of the merodiploid strain on LB plates supplemented with 10% sucrose and kanamycin provokes plasmid excision. The plasmid harbours the *sacB* gene that is induced upon growth on sucrose but favours the production of a toxic substance that inhibits bacterial growth (Gay *et al.*, 1985). Consequently, only those bacteria that got rid of the plasmid backbone by a second recombinatorial event can survive. After sucrose exposure bacteria are selectively screened on LB plates either containing kanamycin or carbenicillin. Bacteria growing on carbenicillin still harbour the plasmid backbone, while those only growing on kanamycin went through a second recombination event and lost the plasmid. Loss of the plasmid was verified by PCR and integrity of the upstream and downstream regions was checked by DNA sequencing.

Finally, the *kan* resistance gene was removed by the Flp/FRT-system as described by Datsenko and Wanner (2000). Therefore, the thermo-sensitive pCP20 plasmid encoding the constitutively expressed recombinase flippase (Flp) was introduced into the respective mutant strain. Flippase-binding to the two distant FRT-sites (Flp recognition target) at the 5'- and 3'-end of the *kan* gene leads to recombination of both regions deleting the *kan* gene in-between. To remove the plasmid, an overnight culture of the mutant carrying the pCP20 plasmid was diluted 1:50 in BHI medium and incubated at 42°C for 2 h at 800 rpm in a thermomixer (Eppendorf, Germany).

2.7. Molecular biological methods for RNA analysis

2.7.1. Isolation of total RNA from Gram-negative bacteria

To analyse the impact of distinct virulence factors on the transcriptional level, total RNA was isolated from *Y. pseudotuberculosis* cells.

Bacterial cultures were grown under the desired conditions and 2 ml were harvested by centrifugation for 1 min at 12000 rpm. The pellets were resuspended in 0.4 volume parts of stop solution and immediately snap-frozen in liquid nitrogen. This step is crucial to inactivate any exogenous ribonuclease activity. After a second centrifugation step for 1 min at 12000 rpm, the supernatant was decanted and the pellet was resuspended in 200 µl lysozyme solution and incubated for 5 min at room temperature to lyse the cells. RNA isolation was then performed with the "SV Total RNA Isolation System" (Promega, USA) according to the manufacturer's instructions.

Stop solution: 5% (v/v) aqua phenol, 100% ethanol (v/v)
Lysozyme solution: 50 mg/ml lysozyme in TE buffer (pH 7.5)
TE buffer (pH 7.5): 100 mM Tris-HCl pH7.5, 1 mM EDTA pH 8.0

2.7.2. Determination of RNA purity

The principle of the photometric measurement of RNA-concentrations relies on the fact that the aromatic ring systems of the purine- and pyrimidine-bases show an absorption maximum at λ = 260 nm. An absorption of 1.0 equals an RNA-concentration of 40 µg/ml (single stranded) respectively (Sambrook, 2001). To determine RNA concentration the absorbance was measured at 260 nm by a NanoDrop (PEQLAB, Germany). The purity was assessed by measuring the ratio of 260 nm and 280nm. Pure RNA has a A_{260}/A_{280} ratio of 2.0.

2.7.3. Separation of RNA by agarose gel electrophoresis and northern blotting

To investigate specific RNA transcript levels, the isolated total RNA was separated on agarose gels. The principle is the same as explained for the DNA agarose gel electrophoresis (2.4.4). Negatively charged RNA molecules migrate to the anode, when an electric field is applied. According to the pore size of the gel (adjusted to the size of the transcript of interest), smaller fragments migrate faster than the larger ones and thus they are separated

by size. Prior to loading, the RNA was mixed with loading dye, denatured at 70°C for 10 min and subsequently cooled to reduce formation of secondary structures. Usually 5 to 10 µg/µl RNA were prepared in a total volume of 20 µl and mixed with 5 µl loading dye. For size discrimination total RNA of the respective mutant strain was loaded.
As loading control and proof of RNA integrity the 23S and 16S ribosomal RNA were visualized on an UV-transilluminator. Gel run was performed at 120 V for 60 min in 1x MOPS buffer. For each northern blot RNA was isolated from three independent cultures (biological triplicates).

5x RNA loading dye: 0.03% (w/v) bromophenol blue, 4 mM EDTA pH 7.5, 0.1 mg/ml ethidium bromide, 2.7% (v/v) formaldehyde, 31% (v/v) formamide, 20% (v/v) glycerol in 4x MOPS buffer.
20x MOPS buffer: 200 mM MOPS, 50 mM sodium acetate, 10 mM EDTA.

Subsequently, the electrophoretically separated RNA was transferred to a positively charged nylon membrane by vacuum blotting for 1.5 hours at a pressure of 5 cm Hg in 10x SSC buffer. RNA transcripts were linked to the membrane by UV-exposure in a UV-cross-linker (Stratagene, USA) at 120,000 microjoules for two times. The next steps of pre-hybridization, probe hybridization, membrane washing and immunological detection were performed according to the manufacturer's instructions of the "DIG-luminescent Detection Kit" (Roche, Germany). DIG-labeled DNA probes were synthesized by PCR using *Taq*-polymerase (NEB) and digoxigenin-labeled dNTPs.

Example of a labelling-PCR mixture

dem. H_2O	69 µl
ThermoPol buffer (10x, NEB)	10 µl
DigPCR-nucleotide mix (10x, Roche)	10 µl
25 mM $MgSO_4$	5 µl
Primer a (10 µM)	1 µl
Primer b (10 µM)	1 µl
Chromosomal DNA	3 µl
Taq-polymerase	1 µl

Probes and the corresponding transcripts and the primer pairs used are listed in Tab. 2.5.

The hybridized DNA probes were detected by means of CDP-star (Roche, Germany). Here, the membrane was incubated with the chemiluminescent solution and developed with the ChemiDoc XRS$^+$ (BioRad, USA) imaging system.

20x SSC: 3 M NaCl, 0.3 M Sodiumcitrate, pH 7.0.

2.7.4. RNA stability assay

To study the decay of distinct RNA transcripts in various *Y. pseudotuberculosis* mutant strains, mRNA transcript levels were monitored after stopping transcription.
For this purpose bacterial cultures were grown to the desired growth phase, rifampicin in a final concentration of 1 mg/ml was added to block transcription, and 2 ml samples were taken in intervals of 0, 10, 20, 30, 40, 50, 60 min after addition of rifampicin. Sampling was done as described in section 2.7.1.
To finally assess the decay rate of each RNA transcript the relative amount of RNA in each sample was determined. Therefore, northern blots were analysed by means of the ChemiDoc XRS$^+$ (BioRad, USA) imaging system. The Biorad Image Lab^{TM} software provides a densiometric analysis tool to quantify the amounts of RNA. Relative mRNA concentrations were plotted on a half-logarithmic scale and an exponential regression line was applied, to calculate the half-life of a specific transcript. Each stability assay was performed at least from three independent cultures (biological triplicates).

Rifampicin solution: 20 mg/ml in methanol (absolute)

2.7.5. RT-PCR analysis and data evaluation

Another approach to investigate the impact of distinct factors on RNA transcript levels is the semi-quantitative detection of target transcripts by means of quantitative real-time reverse-transcription PCR (qRT-PCR). The whole mRNA population is reverse transcribed into complementary DNA (cDNA). Subsequent PCR analysis of target genes is accompanied by the accumulation of a fluorescent dye (SYBR® Green) that is monitored during each PCR cycle and allows relative quantification (Bustin *et al.*, 2005). Total RNA was isolated using the SV total RNA isolation kit (Promega) (2.7.1). To ensure that the prepared RNA is free of contaminating DNA, an additional DNaseI digestion step was applied.

Example of a DNaseI digestion setup

RNA (app. 1000-2000 ng/µl)	20 µl
RNase-free H_2O	30.7 µl
Incubation buffer (10x, Roche)	6.0 µl
Ribolock	0.3 µl
DNaseI (Roche)	3.0 µl

The mixture was incubated at 37°C for 1 h. Afterwards, the RNA was purified and precipitated. The digestion mixture was filled up to 240 µl with RNase-free water and mixed with 200 µl phenol-chloroform-isoamylalcohol (PCI). The homogenate was separated into aqueous and organic phase by centrifugation at 12000 rpm for 10 min at room temperature. The upper aqueous phase was transferred into a new microcentrifuge tube and mixed with 200 µl chloroform-isoamylalcohol (24:1) and centrifuged again at 12000 rpm for 3 min at room temperature. Subsequently, the aqueous phase was transferred into a new microcentrifuge tube and precipitation was carried out by adding 20 µl 3M NaAc per 200 µl solution. After addition of 500 µl 100% ethanol, the mixture was inverted three-times and RNA was allowed to precipitate for 1 h at -20°C. Finally, RNA was pelleted by centrifugation at 12000 rpm for 20 min at 4°C and washed once with 80% ethanol. Pellets were dried by means of a vacuum-centrifuge at 65°C and resuspended in 50 µl RNase-free water and the concentration was adjusted to 25 ng/µl and stored at -20°C.

Samples were checked for chromosomal DNA contamination by PCR using primers for the highly abundant H-NS gene (primer-pair 166-182).

RT-PCR analysis was performed with the "SensiFast SYBR no-ROX One-step" kit (Bioline). A master mix was prepared for each primer-pair based on a standard 12.5 µl final reaction volume. The *sopB* gene was used as reference gene, since it exhibited identical expression levels in the wildtype strain and the tested mutant strains.

Each reaction tube was equipped with 10 µl of the master mix, and then 2.5 µl RNA sample were added. For each primer-pair a non-template control containing RNase-free water instead of an RNA template was used.

Example of a single RT-PCR mix

SensiFast SYBR no-ROX One-step mix (2x)	6.25 µl
Forward primer (10 µM)	0.5 µl
Reverse primer (10 µM)	0.5 µl
Reverse transcriptase	0.125 µl
RiboSafe RNase inhibitor	0.25 µl
RNase-free water	1.75 µl
RNA (25 ng/µl)	2.5 µl

Reverse transcription and subsequent detection of the fluorescently-labelled cDNA was carried out in a Rotor-Gene Q real-time PCR cycler (Qiagen, Germany) using the following three-step cycling programme:

1. cDNA generation (1 cycle):	Reverse transcription	45°C, 20 min
	polymerase activation	95°C, 5 min

2. target gene amplification with specific primer-pairs (40 cycles):

95°C, 10 sec (denaturation)
58°C, 20 sec (primer annealing)
72°C, 10 sec (extension)

Gene specific primers are listed in

Tab. 2.6. Each RT-PCR reaction was performed in triplicates with RNA isolated from at least biological duplicates.

Data analysis was performed according to (Pfaffl, 2001). The cycle thresholds (Ct) of each gene were determined after setting the threshold to 0.005. This value is defined as the number of cycles required for the fluorescent signal to cross the background fluorescence and is indicative for the expression of a gene (e.g. low Ct values represent highly abundant transcripts and *vice versa*) (Bustin *et al.*, 2005). Relative transcription levels were calculated according to the following formula, assuming an optimal primer efficiency of 2 (one

duplication per cycle). In case of the YmoA-dependent genes, primer efficiencies were determined by means of serial dilutions of chromosomal DNA and the generation of a standard curve.

$$\text{relative expression} = \frac{2^{\text{mean Ct}\mathbf{wildtype}_{geneX} - \text{mean Ct}\mathbf{mutant}_{geneX}}}{2^{\text{mean Ct}\mathbf{wildtype}_{sopB} - \text{mean Ct}\mathbf{mutant}_{sopB}}}$$

2.7.6. Microarray analysis and data evaluation

Microarray analysis is an application that monitors the genome-wide gene expression and is often used to compare gene expression patterns between different strain backgrounds or different growth conditions. Therefore, Custom Microarray 8x15K slides from Agilent Technologies were designed by the webdesign application eArray available at (http://www.genomics.agilent.com).

Sequences of the oligonucleotide probes were designed according to the NCBI Genome Genbank (NC_010465 and NC_006153) and encompassed 60 nt in length. The array covered three different probes for the 4172 chromosomal open reading frames (ORFs > 30 codons) from *Y. pseudotuberculosis* YPIII and six different probes for the 92 virulence plasmid (pYV) encoded ORFs from *Y. pseudotuberculosis* IP32953 (Heroven et al., 2012).

RNA was prepared using the SV total RNA isolation kit (Promega) as described above (2.7.1). Therefore, 16 independent cultures of *Y. pseudotuberculosis* YPIII and the *rovC* mutant (YP148) were grown in DMEM-F12 medium at 25°C for 16h. Contaminating chromosomal DNA was removed by an additional DNaseI-step (2.7.5) and checked for remaining DNA by analytical PCR (as described 2.4.6). RNA concentration and quality was assessed by means of an Agilent 2100 Bioanalyzer using the RNA 6000 Nano kit according to the manufacturer's instructions. A RIN (RNA integrity number) between 9 to 10 was indicative for high quality RNA without degradation. Subsequently, total RNA from four independent cultures was pooled and approx. 1 µg of pooled RNA was used for Cy5-labelling (red, wildtype RNA) or Cy3-labelling (green, *rovC* mutant RNA) using the ULS^{TM} Fluorescent labelling kit for Agilent Arrays (Kreatech). Non-incorporated dyes were removed by KREA*pure* purification columns as described by the manufacturer. RNA concentration and the degree of labelling (DoI) were determined using a Nanodrop (PEQLAB) and the DoI calculation sheet (www.kreatech.com).

300 ng of each labelled-RNA were mixed, fragmented and hybridized to the customized microarray slides (Agilent 8x15K) using the Agilent Gene expression hybridization kit (Agilent) and a Microarray Hybridization Chamber kit (Agilent) as indicated by the manufacturer. Hybridization was carried out for 17 h at 65°C in a hybridization oven at 10 rpm. Afterwards, the microarray slide was washed and dried and data were scanned using the Axon GenePix Personal 4100A scanner. Array images were captured using the software package GenePix Pro 6.015. Dr. Johannes Klein performed data processing, bioinformatical evaluation, normalization and statistical analysis as described by Heroven et al. (2012b).

2.8. Protein Biochemical methods

2.8.1. Preparation of whole cell extracts

To monitor the amount of proteins in various strain backgrounds or under various conditions, whole cell extracts were analysed. Extracts were prepared from liquid cultures. Therefore, the OD_{600} was denoted and 1 ml of the bacterial culture was pelleted at 12000 rpm for 5 min at RT. The supernatant was removed and the pellet was resuspended in the appropriate volume of SDS loading buffer, yielding a final OD_{600} equivalent of 1. Subsequently, protein samples were denatured at 95°C for 5 min in a thermomixer (Eppendorf, Germany) and cooled on ice. Samples were stored at -20°C until use. Depending on the protein 5 to 20 µl whole cell extract were applied on analytical PAA-gels.
Whole cell extracts for western blotting were prepared from three independent cultures.

SDS loading buffer (6x): 20% (v/v) glycerole, 3% (w/v) SDS, 8% (w/v) β-mercaptoethanol, 62.5 mM Tris/HCl, pH 6.8, 1 spatula bromophenol blue

2.8.2. Heterologous expression of proteins

Heterologous protein expression is used to express recombinant proteins by bacteria to ensure a rapid and efficient isolation. The corresponding gene is introduced into an expression vector and modified either at the *C*- or *N*- terminal end with a hexa-histidin- or *Strep*-tag. The His-tag, made of six histidin residues, enables protein purification via Nickel-NTA-affinity chromatography while the expression vector possesses an inducible promoter. In this study the expression vector pET28(a)+ was used. It harbours the inducible T_7

promotor, which is recognized by the T_7-polymerase encoded in the chromosome of *E. coli* BL21λDE3. Transcription from this promoter was induced by the addition of 1 mM IPTG (Isopropyl-β-D-thiogalactopyranosid). The *Strep*-tag is a short peptide (WSHPQFEK), which binds to the sepharose-based *Strep*-Tactin® matrix. Since it is a small and chemically balanced tag, it ensures proper protein folding and full bioactivity. In this study the pAKS-IBA5plus plasmid was used, which generates *N*-terminally tagged fusion proteins. Proteins are expressed from the *tet*-promoter, which functions independently from the genetic background of the bacterial strain and is induced by 2 µg/ml AHT (anhydrotetracycline). The used vector-systems are indicated in Tab. 2.14.

Tab. 2.14 Overexpression plasmids

Plasmid	Description	Reference
pAKH11	pET28a(+), ori 3286 ,*hns*$^+$, Kan^R	(Heroven *et al.*, 2004)
pAKH74	pACYC184, p15A, *hns*$^+$, Cm^R	A. K. Heroven
pAKH77	pASK-IBA5plus, *ymoA*$^+$, Amp^R	A. K. Heroven
pAKH172	pET28a(+), ori 3286 ,*csrA*$^+$, Kan^R	A. K. Heroven

To express recombinant protein 500 ml LB medium supplemented with the corresponding antibiotic were inoculated 1:100 from an overnight culture and incubated at 37°C, 180 rpm. When the logarithmic growth phase was reached (OD_{600} 0.6-0.8) protein expression was induced upon addition of 1 mM IPTG or 2 µg/ml AHT for 5 h at 26°C, 180 rpm. Bacterial cells were harvested by centrifugation at 6000 x g for 15 min at 4°C. Afterwards the supernatant was discarded and the pellet was either stored at -20°C until use or directly used for protein isolation. The bacterial pellet (from 500 ml culture) was resuspended in 10 ml ice-cold lysis buffer (supplemented with 1 protease tablet (Roche)) and lysed with a French pressure cell (G. Heinemann, Germany). Bacterial lysates were cleared by centrifugation at 12000 x g for 20 min at 4°C. The supernatant containing the protein crude extract was transferred to a falcon tube and purified via Ni-NTA affinity chromatography (2.8.3) or *Strep*-Tactin® chromatography (2.8.4).

Lysis Buffer (His-tag): 50 mM Tris/HCl pH 8.0, 250 mM NaCl, 20 mM imidazol
Lysis buffer/wash buffer (*Strep*-Tag): 100 mM Tris/HCl pH 8.0, 150 mM NaCl, 1 mM EDTA

2.8.3. Protein purification via Ni-NTA affinity chromatography

Immobilized metal chelate affinity chromatography (Porath *et al.*, 1975; Janknecht *et al.*, 1991) is used for protein purification. Separation of the protein mixture depends on the binding properties of the target protein towards the applied ligand (nickel), which is immobilized to a matrix (nitrilo-triacetate). The target protein is coupled to a 6x His-tag which binds to this ligand. After removing unbound proteins by several washing steps the target protein is eluted by displacement through an additional binding partner (imidazol).

Gravity flow columns were loaded with 500 µl Ni-NTA-Superflow (Qiagen, Hilden) and equilibrated with one column volume (CV) lysis buffer. Afterwards the crude extract was applied to allow binding of the fusion protein to the Ni-NTA column matrix. Ni-NTA-Superflow consists of a highly cross-linked agarose meshwork coupled to nitrilotriacetate (NTA), which can complex four out of six binding sites of a nickel ion. The remaining binding sites are available for the deprotonated histidin-residues of the hexahistidin-tag. The ε-nitrogen atom of the hexahistidin side-chains interacts with the d-orbitals of the nickel ion. This bond is either released by protonation or by excess of another ligand.

Unbound proteins were removed by washing the Ni-NTA matrix with two CV wash buffer I and two subsequent washing steps with wash buffer II. The target protein was eluted by adding 2.5 ml elution buffer. Fractions of 500 µl were collected in 1.5 ml microcentrifuge tubes. Afterwards, the protein concentration was determined as described in section 2.8.5 and the purification was checked by SDS-PAGE (2.8.6).

Wash buffer I: 50 mM Tris/HCl pH 8.0, 250 mM NaCl, 20 mM imidazol
Wash buffer II: 50 mM Tris/HCl pH 8.0, 250 mM NaCl, 40 mM imidazol
Elution buffer: 50 mM Tris/HCl pH 8.0, 250 mM NaCl, 250 mM imidazol

2.8.4. Protein purification via *Strep*-Tactin superflow affinity chromatography

Purification of *Strep*-tagged fusion proteins is based on a similar principle as the Ni-NTA affinity chromatography. The underlying mechanism is derived from the strong interaction of biotin with streptavidin. The *Strep*-tag is capable to bind to the same binding pocket as the biotin molecule hence ensuring a strong interaction with streptavidin. Streptavidin was further optimized to *Strep*-Tactin®, which allows even better interaction of both protein partners.

Gravity flow columns were loaded with 500 µl *Strep*-Tactin® Superflow (IBA, Germany) and equilibrated with one column volume (CV) buffer W. The crude extract was applied and allowed to bind to the column matrix. Unbound protein was removed by washing with four CV of buffer W. Bound *Strep*-tag fusion protein was eluted by 2.5 ml elution buffer, which was collected in fractions of 500 µl in microcentrifuge tubes. Desthiobiotin specifically competes for the biotin-binding pocket. Finally, the protein concentration was determined as described in section 2.8.5 and the purity was analysed by SDS-PAGE (2.8.6).

Buffer W: 100 mM Tris/HCl pH 8.0, 150 mM NaCl, 1 mM EDTA
Buffer E: 100 mM Tris/HCl pH 8.0, 150 mM NaCl, 1 mM EDTA, 2.5 mM desthiobiotin

2.8.5. Determination of protein concentration

To determine the protein concentration the Bradford assay was applied (Bradford, 1976). The principle of this method is the formation of colored dye-protein complexes. Here, the dye Coomassie-Brilliant-Blue G250 was used. It binds unspecifically to cationic and unpolar, hydrophobic side chains of amino acids in an acidic environment. The interaction with arginine is of highest importance. By forming the complex the absorption maximum of this dye is shifted from λ = 465 nm to λ = 595 nm. By determining the extinction of bovine serum albumin (BSA) of known concentration (20 – 1000 µg/ml in dem. water) a calibration curve was determined, which was used to calculate the protein concentration of the samples.
250 µl Bradford reagent were mixed with 5 µl of the respective protein or water (blank). The OD was measured at λ = 595 nm and the protein concentration was calculated by means of the calibration curve.

2.8.6. Discontinuous SDS-polyacrylamide gel electrophoresis

Discontinuous SDS-polyacrylamide gel electrophoresis (SDS-PAGE) was used to separate proteins according to their molecular mass (Laemmli, 1970). The gel consists of long polyacrylamide chains that are cross-linked by N', N'-methylene-bisacrylamide thus forming a dense three-dimensional network.
To achieve a sharp separation of the proteins in the gel a discontinuous gel was casted which implies that the stacking and the separation gel exhibit a pH gradient (pH 6.4 and pH 8.8). For this study either SDS-polyacrylamide (PAA) gels or Tris-TRICINE-PAA gels were prepared.

Tris-TRICINE-PAGE is optimal for the separation and resolution of small proteins (< 30 kDa) like YmoA or CsrA (Schägger, 2006).

Receipt for four SDS-PAA gels (15%)

Reagent	**Separation gel**	**Stacking gel**
Acrylamide (30%)	5.0 ml	1.1 ml
Buffer A	2.5 ml	-
Buffer B	-	2.5 ml
dem. water	2.5 ml	6.5 ml
APS (10%)	50 µl	80 µl
TEMED	50 µl	40 µl

Buffer A: 1.5 M Tris/HCl pH 8.8, 4% SDS
Buffer B: 0.5 M Tris/HCl pH 6.8, 4% SDS

Receipt for one Tris-TRICINE gel (15%, 1.5 mm spacer)

Reagent	**Separation gel**	**Stacking gel**
Acrylamide (30%)	7.5 ml	1.1 ml
3x gel buffer	5.0 ml	3.1 ml
Glycerole	1.5 ml	-
dem. water	1.5 ml	7.6 ml
APS (10%)	150 µl	150 µl
TEMED	15 µl	15 µl

3x gel buffer: 3 M Tris/HCl pH 8.45, 0.3% (v/v) SDS

After polymerization the gels were transferred to a mini-protean II electrophoresis chamber (BioRad, USA). SDS-PAGE was carried out in 1x running buffer, while for TRICINE-PAGE 1x anode and 1x cathode buffer were applied. Protein samples were loaded into the gel pockets (max. volume 20 µl) and electrophoresis was carried out at 25 mA per gel (SDS-PAGE) or 100 mA per gel (TRICINE-PAGE) until the bromophenol blue frontier reached the lower rim of the gel. For size discrimination of the proteins one lane was loaded with the molecular-weight marker "Page-Ruler^{TM} Prestained Protein Ladder". Subsequently, the gels were either stained with Coomassie brilliant blue or further subjected to western blotting.

SDS-PAGE
Running buffer (10x): 33 mM Tris/Hcl pH 8.3, 192 mM glycine, 0.1% SDS

TRICINE-PAGE
Anode buffer (10x): 0.1 M Tris base, 0.0225 M HCl
Cathode buffer (10x): 0.1 M Tris base, 0.1 M TRICINE, 0.1% SDS

2.8.7. Coomassie brilliant blue staining

Gels were stained for 30 min in Coomassie brilliant blue solution with gentle agitation. The Coomassie staining is a standard method (Towbin *et al.*, 1992) to stain proteins in a polyacrylamide gel. The dye Coomassie-Brilliant-Blue G250 binds to cationic and unpolar side chains of amino acids and thus stains the proteins unspecifically. The gel washed in hot water for 5 minutes under gentle agitation and incubated in hot Coomassie reagent the protein bands were visible against the non-coloured background.

Coomassie reagent: 60 mg/l Coomassie Brilliant Blue G250, 35 mM HCl

2.8.8. Western blot analysis and immunological detection

Western blot analysis was used to transfer proteins from a gel matrix onto a hydrophobic PVDF membrane by means of electro-blotting (Towbin *et al.*, 1992). Subsequently, immunological detection with protein-specific antibodies was performed, which in turn were recognised by secondary antibodies coupled to horseradish peroxidase (HRP). This enzyme converts a chemical compound into a luminescent signal that is detected by an imaging system.

Whole cell extracts were prepared as described in section 2.8.1and separated by SDS- or TRICINE-PAGE as defined in 2.8.6. Protein transfer was performed by wet-blotting. Blotting was performed at 100 V for 1 h.

For immunological detection the membrane was blocked in TBST-M for 16 h and vigorously rinsed in TBST. The primary antibody (directed against the protein of interest) was diluted in TBST-M and the membrane was incubated for 1 h under gentle agitation. Applied antibodies are indicated in Tab. 2.8. The membrane was washed twice with TBST to remove residual antibody and incubated with a secondary antibody (directed against the primary antibody) diluted in TBST-M for another hour. Finally, the membrane was washed twice with TBST,

developed by using the Western Lightning ECL II kit (Perkin Elmer), and documented with the ChemiDoc XRS$^+$ (BioRad, USA) imaging system.

Transblot buffer: 25 mM Tris, 192 mM glycine, 20% MetOH

TBST: 20 mM Tris/HCl pH 7.5, 150 mM NaCl, 0.05% TWEEN-20

TBST-M: 20 mM Tris/Hcl pH 7.5, 150 mM NaCl, 0.05% TWEEN-20, 5% non-fat dry milk

2.8.9. Promoter activity assay

Promotor activity assays were used to determine the transcription or translation rate of genes. Therefore, the promoter region of interest was cloned upstream of the β-galactosidase reporter gene (*lacZ*). Fusions harbouring the ribosomal binding site of the gene of interest are termed translational fusions, whereas those fusions relying on the ribosomal binding site of the β-galactosidase gene are designated as transcriptional fusions. Upon activation of the respective promoter the *lacZ* gene will be transcribed and the β-galactosidase activity can be used as a measure for the promoter activity (Miller, 1972).

3 ml LB-medium were supplemented with the respective antibiotics, inoculated with the respective strains, and cultured over night at the conditions needed. For this work, the majority of the assays was conducted after growth at 25°C to the stationary growth phase. After incubation the optical density (OD_{600}) of the bacterial culture was determined at λ = 600 nm in 1:10 dilutions.

200 µl cell suspension were lysed with 50 µl of 0.1% SDS solution and 50 µl chloroform. After a 10 min incubation time 1.8 ml 1x Z-buffer was added and the reaction was started by adding 0.4 ml of ONPG (ortho-nitrophenyl-β-D-galactopyranosid). ONPG was used as the artificial chromogenic substrate for the enzyme β-galactosidase, which converts the colourless ONPG to the yellow colored product ortho-nitrophenol (ONP, λ_{max} = 420 nm). As soon as a visual yellow coloration of the sample occured the reaction was by adding 1 ml of 1 M sodium carbonate. The reaction time was denoted and the OD_{420} as a measure for the β-galactosidase activity and the OD_{550} as a measure for the bacterial background were determined by an ELISA reader.

The β-galactosidase activity was determined according to the following formula:

$$\beta\text{-galactosidase activity} = \frac{OD_{420nm} * 6.75}{OD_{600nm} * V * t}$$

t = Reaction time in minutes V = used bacterial volume in ml

6.75 = Extinction coefficient of cleaved ONPG in µmol/min/mg protein

Z-buffer (5x): 61 mM Na_2HPO_4 x 2 H_2O, 39 mM NaH_2PO_4 x 1 H_2O, 10 mM KCl, 10 mM Mg_2SO_4 x 7 H_2O
ONPG: 4 mg/ml in dem. water (store at 4°C, protected from light)
Sodiumcarbonate: 1M Na_2CO_3

2.8.10. Electrophoretic mobility shift assay (EMSA) with RNA

Electrophoretic mobility shift assays are valuable tools to monitor the interaction between DNA or RNA molecules and proteins. The migration of free DNA/RNA in a native gel matrix differs to the migration of DNA-protein or RNA-protein complexes and can be visualized.
The respective protein was heterologously expressed as described under section 2.8.2 and dialyzed against 1x band shift buffer. RNA was *in vitro* transcribed according to the TranscriptAid™ T7 High Yield Transcription kit (Fermentas). First, a DNA template was generated by PCR using specific primer pairs to amplify the genomic region of interest (see Tab. 2.5). *In vitro* transcription was carried out at 37°C for 2 h (transcripts >100 nt) or over night (transcripts <100 nt) according to the following protocol:

Example of an *in vitro* transcription (*iv*t) setup:

TranscriptAid™ reaction buffer	4.0 µl
ATP/CTP/GTP/UTP mix	8.0 µl
Template DNA	6.0 µl
TranscriptAid™ enzyme mix	2.0 µl

Subsequently, template DNA was removed by DNaseI digestion. Therefore, 2 µl DNaseI were added to the *iv*t mix and incubated for 15 min at 37°C. DNaseI was inactivated by adding 2 µl EDTA (0.5 M) and incubation at 65°C for 10 min. Finally, the RNA transcripts were purified by phenol:chloroform and precipitated with ethanol (section 2.7.5). Aliquots containing 1000 ng/µl RNA were stored at -20°C until use.
The protein concentration was assessed prior to each band shift experiment as described in section 2.8.5. Each binding reaction was carried out with proteins isolated from two

independent purification procedures. Protein dilutions were prepared in 1x band shift buffer yielding a final concentration of 5 to 37 pmol protein (YmoA, H-NS, YmoA-H-NS) or 7.5 to 75 pmol protein (CsrA) in the binding reaction. The RNA concentration was adjusted to 10 pmol in RNase-free water and was denatured at 70°C for 10 min and cooled down at room temperature to allow refolding of the RNA. Then RNA samples were mixed with band shift buffer to a final concentration of 1x in 10 µl. For each binding reaction 10 µl RNA were carefully mixed with 5 µl protein dilution and incubated at 25°C for 20 min. Subsequently, the binding mixtures were loaded on 4% TBE gels and separated at 80 V for 50 min in 1x TBE running buffer by using a mini-protean II electrophoresis chamber (BioRad, USA).

Receipt for a native TBE gel (1.5 mm spacer)

RNase-free water	8.0 ml
TBE buffer (10x)	1.0 ml
Acrylamide (40%)	1.0 ml
TEMED	10 µl
APS (10%)	100 µl

Afterwards, RNA-protein complexes were transferred onto positively-charged nitrocellulose membranes by semi-dry blotting using the TransBlot SD Semi-Dry Transfer Cell (BioRad) in 1x TBE buffer at 20 V for 30 min. RNA cross-linking and immunological detection (DIG-labelling principle) was carried out as described in section 2.7.3. Primer-pairs used for the DNA template amplification were also used for the generation of DIG-labelled probes.

Band shift buffer (10x): 0.1 M Tris/HCl pH 7.5, 0.1 M $MgCl_2$, 1 M KCl, 75% glycerol, 0.03 M DTT
TBE buffer (10x): 900 mM Tris/HCl, 900 mM boric acid, 25 mM EDTA pH 8.0

3. Results

Initial colonization of the intestinal tract is mediated via the outer-membrane protein invasin, which promotes tight binding to the M-cells and therefore allows efficient uptake of the bacteria (Isberg *et al.*, 1987; Marra and Isberg, 1997). Although invasin is a crucial virulence factor, a constant expression of this protein would be energetically unfavourable and would represent a good target for the host's immune system. Consequently, expression is tightly regulated by the MarR-type regulator RovA that is part of a complex regulatory network comprising H-NS, RovM, the Csr system, Crp and the two-component system BarA/UvrY, in response to environmental cues (Heroven and Dersch, 2006; Heroven *et al.*, 2007; Heroven *et al.*, 2008; Heroven *et al.*, 2012b). Most recently, YmoA, a member of the YmoA/Hha-family was found to control synthesis of invasin via the Csr-RovM-RovA regulatory cascade (Böhme, unpublished data).

3.1. Molecular characterization of YmoA-dependent CsrC regulation

YmoA is the *Yersinia* homologue of the *E.coli* Hha protein. Both proteins comprise nucleoid-structuring proteins that modulate expression of horizontally acquired genes (Madrid *et al.*, 2002; Madrid *et al.*, 2007). In *Y. pseudotuberculosis* YPIII, YmoA was found to control the amount of the ncRNA CsrC, thereby affecting the Csr-RovM-RovA-InvA early virulence regulatory cascade. Previous data demonstrated that YmoA post-transcriptionally affects CsrC RNA stability. In the absence of YmoA, CsrC RNA is rapidly degraded (half-life$_{CsrC}$ (wildtype) ≈ 100 min versus half-life$_{CsrC}$ (Δ*ymoA*) ≈ 46 min). Furthermore, a stabilizing stem-loop structure within the first 81 nucleotides of the ncRNA was shown to be crucial for YmoA-dependent CsrC regulation (Heroven *et al.*, 2008; Böhme, unpublished data). However, the underlying mechanism how YmoA affects CsrC ncRNA stability still remains unknown.

3.1.1. No direct interaction between YmoA and the CsrC RNA

YmoA does not bear any known DNA- or RNA-binding domain. However, YmoA/Hha protein family members form heterodimeric complexes with the prokaryotic transcription factor H-NS, thereby regulating gene expression (Nieto *et al.*, 2002; Ellison and Miller, 2006; McFeeters *et al.*, 2007). Recently, Brescia *et al.* (2004) demonstrated that H-NS is able to bind both, double-stranded DNA as well as mRNA and ncRNA transcripts. Most interestingly, H-NS was found to be required for post-transcriptional regulation of CsrC synthesis. This indicated that YmoA might either act alone or in association with H-NS to bind to the CsrC RNA to affect its stability. The YmoA-dependent +81 stem-loop structure could be involved in this interaction (Böhme, unpublished data).

To monitor whether YmoA alone or YmoA/H-NS complexes affect CsrC RNA integrity, gel mobility shift assays were performed. The YmoA protein was either applied as homodimer or as a heterodimer co-purified with H-NS. For this purpose *Yersinia* YmoA and H-NS proteins were heterologously overexpressed in an *E. coli* BL21λDE3 background deficient of all *Yersinia* YmoA and H-NS homologues (Δ*stpA*, Δ*hha* and Δ*hns*). The CsrC RNA was transcribed *in vitro*, incubated with increasing amounts of affinity-purified protein and separated on 4% native TBE gels.

Data demonstrate, that neither YmoA or H-NS alone nor the YmoA-H-NS heterodimer was able to bind to the CsrC transcripts, even when high amounts of protein were applied (Fig. 3.1). This strongly indicates that YmoA-mediated CsrC stabilization relies on an indirect mechanism and occurs through other YmoA/H-NS-dependent regulators.

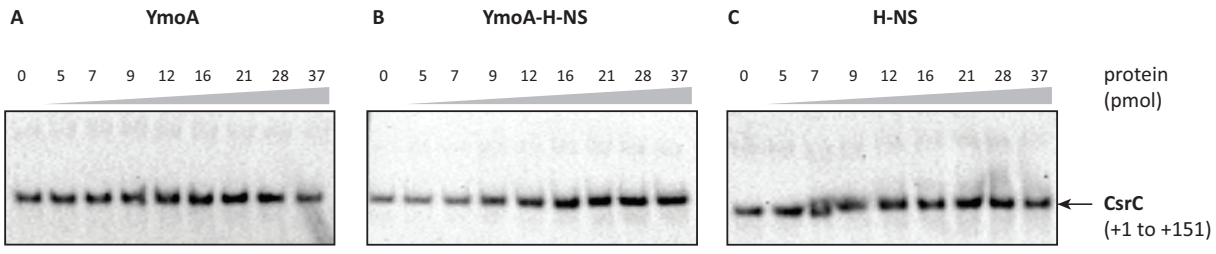

Fig. 3.1 YmoA and H-NS cannot bind to the CsrC RNA
To monitor if YmoA can bind directly to CsrC RNA transcripts, electrophoretic mobility shift assays (EMSAs) were performed. CsrC ncRNA was transcribed *in vitro* (CsrC ncRNA +1 to +151 nt from transcriptional start). 3 pmol RNA were denatured, cooled down at RT to refold the RNA and incubated with increasing amounts (5 pmol to 37 pmol protein) of YmoA protein (**A**), YmoA-H-NS heterodimer (**B**) or H-NS protein (**C**) at 25°C. Binding reactions were separated on 4% TBE gels, transferred onto nitrocellulose membranes and probed with digoxigenin (DIG)-labelled PCR fragments encoding the *csrC* gene.

3.1.2. YmoA affects RNA chaperones and RNAses

In order to identify other YmoA-dependent regulators that might affect CsrC stability, microarray analysis was performed (Heroven and Böhme, unpublished). Comparison of total RNA from *Y. pseudotuberculosis* YPIII (wildtype) and YP50 (Δ*ymoA*) revealed more than 400 differentially regulated genes in the mutant strain (Tab. S 2). Among these genes, expression of RNA degrading and folding genes (YPK_0604*, tdcF* and *rnpA*) was significantly induced in YP50. Furthermore, genes encoding for proteins involved in the heat shock response such as chaperones (*dnaJ, dnaK, grpE, groEL, groES*) were shown to be significantly upregulated in the *ymoA* mutant. YmoA-dependency of these candidate genes was validated by RT-PCR, using total RNA isolated from YPIII and YP50 grown at 25°C to early stationary phase (Fig. 3.2 A). Expression of all candidate genes was repressed by YmoA. The *grpE, dnaJ, groES, tdcF,* YPK_0604 and *rnpA* gene expression differed significantly. To further confirm these findings, expression of translational *lacZ*-reporter fusions was compared in the YPIII wildtype and the *ymoA* mutant strain YP50. Expression of the *dnaJ/dnaK* operon, the *groEL/groES* operon and *tdcF* was significantly upregulated in the YP50 strain (Fig. 3.2 B), confirming the results of the RT-PCR. This demonstrated that the expression of several genes, which are involved in RNA degradation and folding, is influenced by the YmoA protein.

To test whether one or more of the newly identified chaperone molecules is/are involved in stabilizing the CsrC RNA, mutant strains of the respective candidate genes were supposed to be generated. Unfortunately, multiple different attempts to construct either mutant strains or overexpression plasmids of *tdcF/*YPK_0604, *dnaJ/dnaK* or *rnpA* failed. Since these ribonucleases or ribozymes are involved in global mRNA cleavage (Guerrier-Takada *et al.*, 1983; Morishita *et al.*, 1999; Altman *et al.*, 2005), changes in their expression level might be deleterious to the cell. In fact, deletion of the *rne* gene encoding for RNase E is lethal for *E. coli* (Ono and Kuwano, 1979).

RNase E and PNPase, both components of the degradosome, are involved in CsrBC turnover in *E. coli* and *Salmonella spp* respectively (Suzuki *et al.*, 2006; Viegas *et al.*, 2007). Therefore, the YmoA-dependent expression of RNase E and PNPase was tested. However, no YmoA-mediated effect on the expression of both genes was observed (Fig. S 1). In contrast to *E. coli* a dominant negative *rne* mutant did not affect CsrBC abundance at all while a *pnp* mutation lead to decreased CsrC and increased CsrB levels (Fig. S 2).

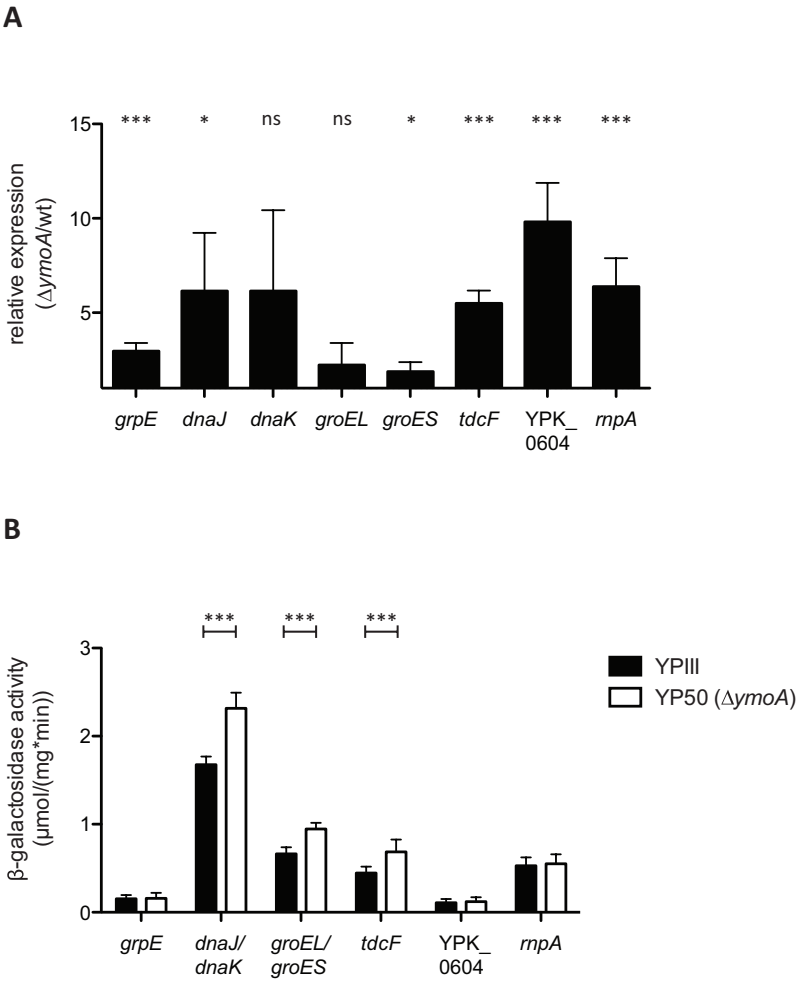

Fig. 3.2 Expression of RNA chaperones and RNases is repressed by YmoA

A To verify the results obtained from the microarray analysis, one-step real-time RT-PCR analysis was performed with specific primer pairs for selected genes involved in RNA folding and stabilization. RNA was isolated from eight independent cultures of the *Y. pseudotuberculosis* wildtype (YPIII) reference strain and of three independent cultures of the Δ*ymoA* (YP50) candidate strain. Gene expression levels were normalized to the *sopB* reference transcript for YPIII and YP50, respectively (according to (Pfaffl, 2001) relative expression > 1 = YmoA-repressed, relative expression < 1 = YmoA-induced) and are given as relative expression of each gene in relation to *sopB*. Data are given as means and standard deviation. Data were analysed by Student's t test. Stars indicate the results that differed significantly between wildtype and *ymoA* mutant (*** P<0.001, * P<0.05, ns = not significant).

B To prove that the promoter activity of the selected genes involved in RNA folding and stabilization is YmoA-dependent, β-galactosidase activity (µmol/(mg*min)) of the respective translational fusion was monitored in *Y. pseudotuberculosis* YPIII and YP50 (Δ*ymoA*). Strains were transformed with plasmids pSSE29 (*grpE'-'lacZ*), pSSE28 (*dnaJ'-'lacZ*), pSSE27 (*groEL'-'lacZ*), pSSE16 (*tdcF'-'lacZ*), pSSE21 (YPK_0604*'-'lacZ*) and pSSE20 (*rnpA'-'lacZ*), grown at 25°C in LB medium to stationary phase. Data are means and standard deviations of three independent experiments, each performed with biological triplicates. Data were analysed by Student's t test. Stars indicate the results that differed significantly from the control (*** P<0.001).

3.1.3. Loss of *csrA* cannot be overcome by YmoA

CsrA is the best described RNA-binding protein, which directly interacts with CsrC ncRNA transcripts. Nonetheless, previous studies reported that CsrA induces transcription of *csrC* in *E. coli* but does not alter CsrC RNA stability (Weilbacher *et al.*, 2003).

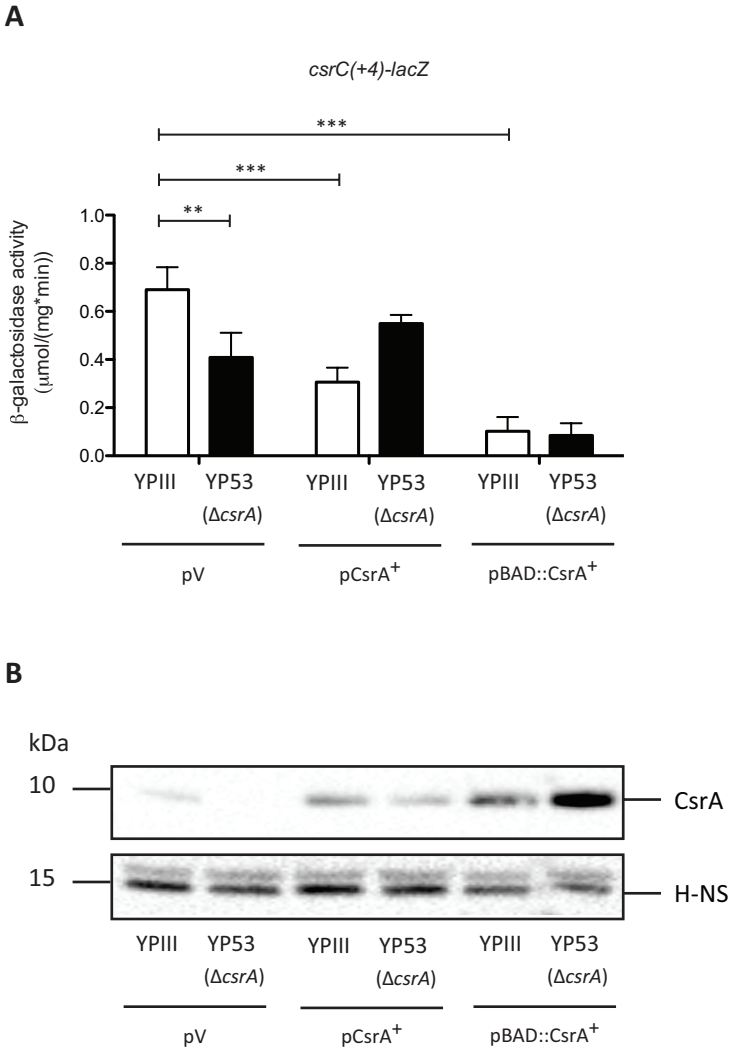

Fig. 3.3 Moderate CsrA levels control *csrC* transcription
A Expression of a transcriptional *csrC-lacZ* reporter fusion (pKB45) was analysed in *Y. pseudotuberculosis* wildtype YPIII and YP50 (ΔymoA). β-galactosidase activity (µmol/(mg*min)) was monitored in strains either harbouring the empty vector pAKH85 (pV, midi copy) or its derivative pAKH56 (pCsrA$^+$). In addition, CsrA was overproduced from an arabinose-inducible plasmid (pRS68) upon induction with 0.05% arabinose. Cultures were grown at 25°C in LB medium for 16h. Data represent means and standard deviations of two independent experiments, each performed with biological duplicates. Data were analysed by Student's t test. Stars indicate the results that differed significantly (*** P<0.001, ** P<0.01).
B The same samples were used to compare the protein concentration of CsrA in YPIII and YP50 by western blot analysis. Whole cell extracts were prepared, separated on 12% Tris-TRICINE gels and transferred onto an Immobilon-P membrane. Proteins were detected by immunoblotting with a polyclonal antibody directed against CsrA. YP53 (Δ*csrA*) served as negative control. Immunoblotting with a polyclonal antibody against H-NS was used as loading control.

As shown in Fig. 3.3 expression of *csrC-lacZ* reporter fusions was reduced in the abscence of CsrA compared to the wildtype. The reporter fusion was designed to only harbour the first four nucleotides of the *csrC* coding region and therefore lacked CsrA-binding elements, demonstrating that transcription of *csrC* is affected. Phenotypes were reconstituted either with a midi-copy *csrA*$^+$ plasmid (pCsrA$^+$) or when transcribed from a strong arabinose-inducible promoter (p_{BAD}::CsrA$^+$). Loss of *csrA* could be fully compensated by *in trans* complementation with both CsrA$^+$ plasmids and, CsrA overexpression seemed to reduce *csrC* transcription in the wildtype (Fig. 3.3). This was particularly evident for both strains when very high endogenous CsrA levels were generated by expression from the arabinose-inducible promoter.

Contrary to previous data that showed no CsrA-mediated effect on CsrC transcript stability in *E. coli* (Weilbacher *et al.*, 2003), CsrA of *Y. pseudotuberculosis* positively affects CsrC stability (Böhme, unpublished data). Herein, CsrC was rapidly degraded in abscence of CsrA (half-life$_{CsrC}$ (wildtype) ≈ 100 min, half-life Δ*csrA* ≈ 11 min). As CsrC stability was also reduced in the *ymoA* mutant strain, it was hypothesized that YmoA might act via CsrA on CsrC. Epistasis studies were performed to determine whether CsrA-mediated stabilization of CsrC depends on YmoA. Ectopic expression of CsrA could not re-store CsrC RNA levels in a *ymoA* mutant but fully re-stored a *csrA* deletion. In contrast, ectopic expression of YmoA only restored the lack of CsrC RNA caused by a *ymoA* deletion but not by a *csrA* deletion (Fig. 3.4). These data clearly show that CsrA is essential for proper CsrC expression/stabilization but presence of YmoA is indispensable, since a *ymoA* deletion cannot be fully overcome by ectopic CsrA expression. Moreover, a *csrA* deletion cannot be overcome by introducing a *ymoA*$^+$ plasmid, which leads to the assumption that YmoA might not or only to a small extent act via CsrA on CsrC integrity. We wanted to confirm these results by complementation studies in a *csrA/ymoA* double mutant strain, but multiple independent attempts to construct the double mutant failed. As both single mutants exhibit a severe growth defect (data not shown), it is likely that loss of both regulatory proteins might be deleterious to the cell.

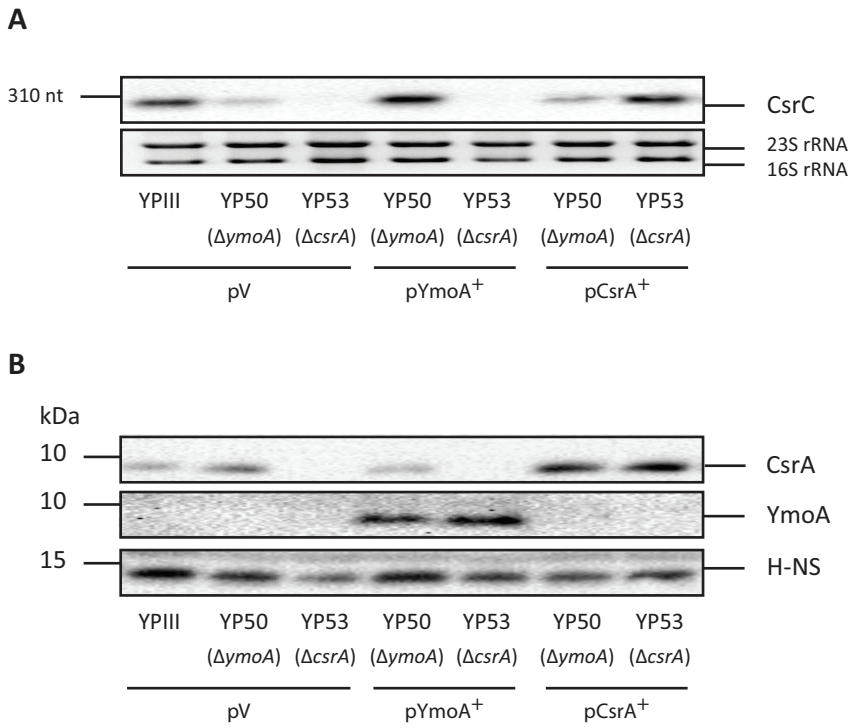

Fig. 3.4 Loss of *csrA* cannot be complemented by YmoA
A Reciprocal complementation of CsrA and YmoA was analysed by monitoring CsrC RNA levels. *Y. pseudotuberculosis* YPIII, YP50 (Δ*ymoA*) and YP53 (Δ*csrA*) were transformed with the empty vector pHSG576 (pV) and reciprocally complemented with pKB4 (pYmoA$^+$) and pKB60 (pCsrA$^+$). Overnight cultures were grown at 25°C in LB medium. Total RNA was prepared, separated on 0.7% MOPS agarose gels, transferred onto a nylon-membrane and probed with a digoxigenin (DIG)-labelled PCR fragment encoding the *csrC* gene. 16S and 23S rRNAs were used as loading controls. **B** In parallel, whole cell extracts of the same cultures were prepared for western blotting to monitor the concentration of YmoA and CsrA protein. Samples were separated on 12% Tris-TRICINE gels and transferred onto an Immobilon-P membrane. Proteins were detected by immunoblotting with polyclonal antibodies directed against YmoA and CsrA. Immunoblotting with a polyclonal antibody against H-NS was used as loading control.

3.1.4. YmoA affects CsrA levels in the cell

CsrA protein levels were decreased in a *ymoA* mutant strain during exponential growth at 37°C (Steinmann, 2013). According to these data it might be possible that the RNA-binding protein CsrA itself is controlled by YmoA and therefore mediates CsrC RNA stabilization. To test the hypothesis whether YmoA-mediated transcriptional effects lead to decreased *csrA* expression, a transcriptional *csrA-lacZ* fusion was analysed in YPIII and YP50 grown at 25°C to stationary phase. In *E. coli* CsrA encompasses five different promoters (Yakhnin *et al.*, 2011), which are also present in *Y. pseudotuberculosis* (Hoßmann, unpublished data). The reporter fusion harboured promoters P4 and P5, as both promoters exhibit the same expression level like P3 in *Y. pseudotuberculosis*, which is the strongest promoter in *E. coli* (Yakhnin *et al.*, 2011; Hoßmann, unpublished data). However, no difference in *csrA* transcription was monitored between the wildtype and a *ymoA* mutant strain (Fig. 3.5 A).

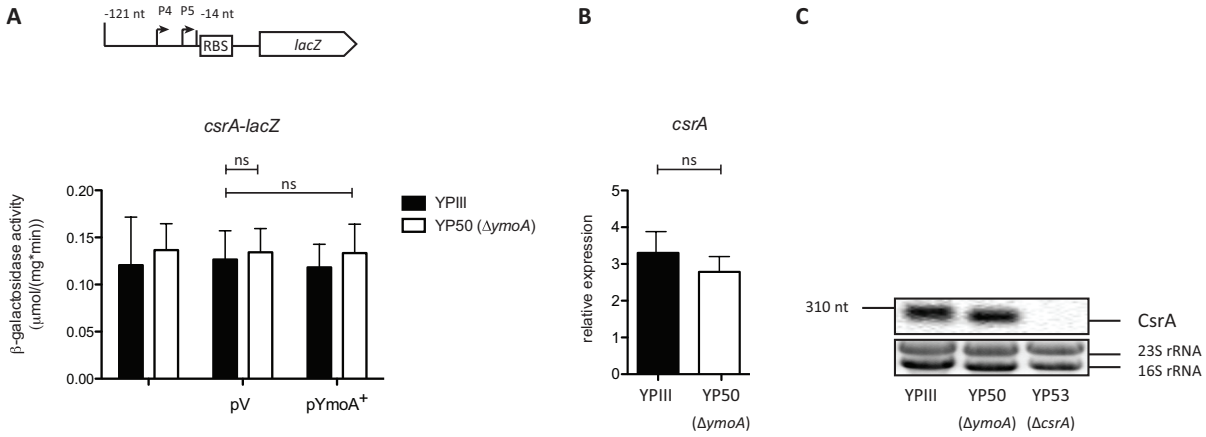

Fig. 3.5 Transcription of *csrA* and cognate mRNA levels remain unaffected by YmoA
A Expression of a transcriptional *csrA-lacZ* reporter fusion (pJH8) was analysed in *Y. pseudotuberculosis* wildtype YPIII and YP50 (Δ*ymoA*). β-galactosidase activity (µmol/(mg*min)) was monitored in strains either harbouring the empty vector pAKH85 (pV) or its derivative pAKH71 (pYmoA$^+$). Cultures were grown at 25°C in LB medium for 16 h. Data are means and standard deviations of three independent experiments, each performed with biological duplicates. Data were analysed by Student's t test (ns = not significant).
B CsrA transcript levels in *Y. pseudotuberculosis* wildtype YPIII and YP50 (Δ*ymoA*) were monitored by one-step real-time RT-PCR analysis with specific primer pairs for the *csrA* gene. RNA was isolated from four independent cultures of YPIII and YP50 (Δ*ymoA*) grown as indicated above. Gene expression levels were normalized to the *sopB* reference transcript for YPIII and YP50 (according to Pfaffl (2001)) and are given as relative expression of the respective gene in relation to *sopB*. Data are given as means ± standard deviation. Data were analysed by Student's t test (ns = not significant).
C Transcript levels of CsrA were analysed by northern blotting. Overnight cultures of *Y. pseudotuberculosis* YPIII (wildtype) and YP50 (Δ*ymoA*) were grown at 25°C in LB medium. Total RNA was prepared, separated on 0.7% MOPS agarose gels, transferred onto a nylon-membrane and probed with a digoxigenin (DIG)-labelled PCR fragment encoding the *csrA* gene. YP53 (Δ*csrA*) served as negative control. 16S and 23S rRNAs were used as loading controls.

To further confirm these findings, total RNA was isolated from YPIII and YP50 stationary cells grown at 25°C and used for comparative RT-PCR analysis and northern blotting (Fig. 3.5 B+C). Clearly no difference in CsrA transcript abundance was reported, excluding further stabilizing or destabilizing effects on the mRNA transcript.

As no obvious effect of YmoA on CsrA transcription or mRNA stability was observed, the impact of YmoA on CsrA translation was investigated. Therefore YPIII and YP50 cells were grown to stationary phase at 25°C, samples for promoter activity assays and western blotting were prepared in parallel. As shown in Fig. 3.6 A endogenous CsrA levels were reduced in the *ymoA* mutant strain, which could be partially complemented with a *ymoA*$^+$ plasmid. Expression of a translational *csrA'-'lacZ* fusion remained unaltered in the *ymoA* mutant strain (Fig. 3.6 B). Although the impact of YmoA on endogenous CsrA was seen in majority of the time, it was occasionally absent, leading to the assumption that YmoA exerts a (minor) positive effect on the CsrA protein level.

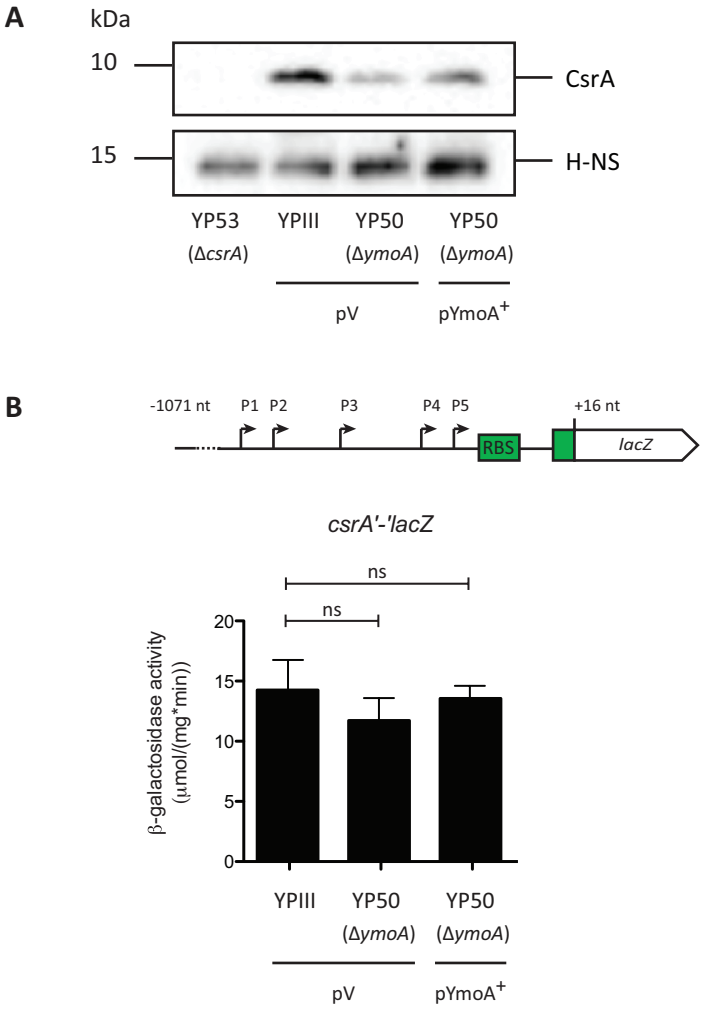

Fig. 3.6 YmoA affects CsrA protein level but not translation
A Protein concentration of CsrA in YPIII and YP50 was compared by western blot analysis. Strains were transformed with the empty vector pAKH85 (pV) and complemented with its derivative pAKH71 (pYmoA$^+$). Whole cell extracts were prepared from cultures grown at 25°C in LB medium for 16 h, separated on 12% Tris-TRICINE gels and transferred to an Immobilon-P membrane. Proteins were detected by immunoblotting with a polyclonal antibody directed against CsrA. YP53 (Δ*csrA*) served as negative control. Immunoblotting with a polyclonal antibody against H-NS was used as loading control.
B Expression of a translational *csrA*'-'*lacZ* reporter fusion (pKB63) was analysed in *Y. pseudotuberculosis* wildtype YPIII and YP50 (Δ*ymoA*). β-galactosidase activity (µmol/(mg*min)) was monitored in strains either harbouring the empty vector pAKH85 (pV) or its derivative pAKH71 (pYmoA$^+$). Cultures were grown like described above. Data are means and standard deviations of three independent experiments, each performed with biological triplicates. Data were analysed by Student's t test (ns = not significant). Graphic representation of *lacZ* fusions: white = *lacZ*, green = *csrA,* RBS = ribosomal binding site, nt = nucleotides, numbers indicate distance relative to transcriptional start site, P1 to P5 = promoters.

Since wildtype and *ymoA* mutant strain did not exhibit any significant difference on the translational *csrA'-'lacZ* fusion, further reporter constructs with varying coding region lengths were implied. Comparison of all three fusions should monitor whether the coding region of *csrA* is important for YmoA-dependent expression. Moreover, these constructs were transcribed from arabinose-inducible promoters (P_{BAD}::*csrA-lacZ*) to exclude additional transcriptional effects. The fusions started directly downstream of the last promoter ($P5_{csrA}$)

and harboured +18 nt, +36 nt or 138 nt of the *csrA* coding region (Fig. 3.7). Expression of *csrA* did not differ between wildtype and *ymoA* mutant strain, indicating that the overall translation was not affected by loss of *ymoA* in any of the three different fusions. Surprisingly, *in trans* complementation with a *ymoA*$^{+}$ plasmid lead to a slight decrease of *csrA* expression when the first 18 nt or 36 nt of the *csrA* coding region were fused to *lacZ*. However, this effect was not seen with the fusion harbouring the complete *csrA* coding sequence (+ 183 nt) (Fig. 3.7).

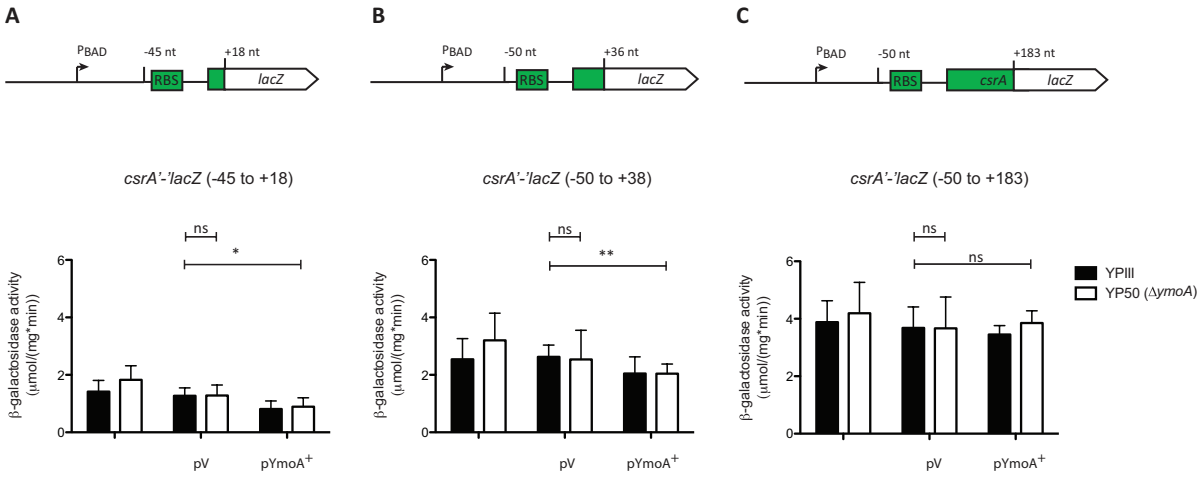

Fig. 3.7 YmoA does not affect *csrA* translation
Expression of translational *csrA*'-'*lacZ* reporter fusions was analysed in *Y. pseudotuberculosis* wildtype YPIII and YP50 (Δ*ymoA*). *csrA'-'lacZ* activity was monitored for fusions harbouring the first 18 nt of the *csrA* coding region (pJH11) (**A**), the first 36 nt of the *csrA* coding region (pJH17) (**B**) or the whole coding region (+183 nt, except the stop codon, pJH18) (**C**). β-galactosidase activity (µmol/(mg*min)) was monitored in strains either harbouring the empty vector pAKH85 (pV) or its derivative pAKH71 (pYmoA^{+}). Cultures were grown at 25°C in LB medium supplemented with 0.05% arabinose (to induce *csrA* transcription from the P_{BAD} promoter) for 16 h. Data are means and standard deviations of three independent experiments, each performed with biological triplicates. Data were analysed by Student's t test. Stars indicate data that differed significantly from each other (**P<0.01, * P<0.05, ns = not significant). Graphic representation of *lacZ* fusions: white = *lacZ*, green = *csrA,* RBS = ribosomal binding site, nt = nucleotides, numbers indicate distance relative to transcriptional start site.

In summary, YmoA has a positive effect on CsrA protein levels in the cell, but this effect does not result from transcriptional or translation regulation. Therefore CsrA protein stability was assessed. To do so, protein synthesis of *Y. pseudotuberculosis* YPIII (wildtype) or YP50 (Δ*ymoA*) overnight cultures was stopped by adding chloramphenicol to a final concentration of 200 µg/ml. Whole cell extracts were prepared from samples taken 60 min, 120 min, 180 min and 240 min after addition of chloramphenicol and CsrA protein levels were visualized by western blotting. Consistent with the data from the western blot (Fig. 3.6 A) diminished CsrA protein levels were found in the *ymoA* mutant strain (Fig. 3.8). However, CsrA protein

stability was not affected by loss of *ymoA* and remained identical after blockage of protein synthesis. Although it is still unclear how YmoA controls the CsrA levels, it is assumed that YmoA modulates the endogenous CsrA levels to control the stability of CsrC.

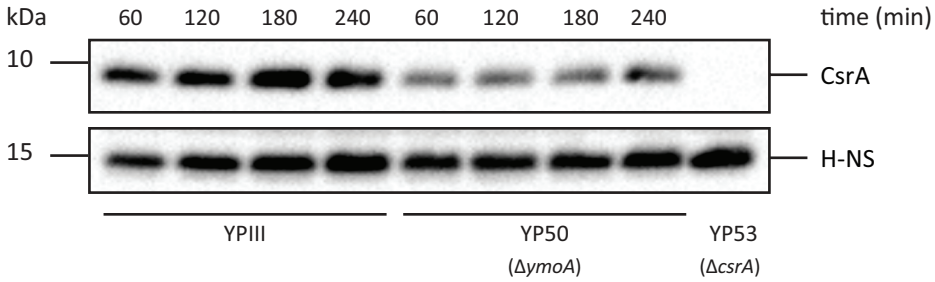

Fig. 3.8 YmoA does not alter CsrA protein stability
CsrA protein stability was assessed in *Y. pseudotuberculosis* YPIII und YP50 (Δ*ymoA*) by western blot analysis. Cultures were grown overnight at 25°C in LB medium. Protein synthesis was stopped by the addition of chloramphenicol to a final concentration of 200 µg/ml. Whole cell extracts were taken 60 min, 120 min, 180 min and 240 min after addition of chloramphenicol. Samples were separated on 12 % Tris-TRICINE gels and transferred onto an Immobilon-P membrane. Proteins were detected by immunoblotting with a polyclonal antibody directed against CsrA. YP53 (Δ*csrA*) served as negative control. Immunoblotting with a polyclonal antibody against H-NS was used as loading control.

To prove that minor changes in the endogenous CsrA level elicit major effects on CsrC levels, a titration experiment was performed. The CsrA protein concentration was assessed in YP53 (Δ*csrA*) by means of an arabinose-inducible promoter that was fused to the *csrA* gene and compared to the wildtype. Afterwards, CsrA and CsrC levels were compared. Levels of CsrC RNA increase with increasing CsrA protein levels, but when a certain threshold in endogenous CsrA is reached, CsrC RNA levels remain constant (Fig. 3.9, 0.0035 to 0.004% arabinose). Moreover, results indicate that minimal amounts of CsrA are enough to re-store CsrC levels in the cell.

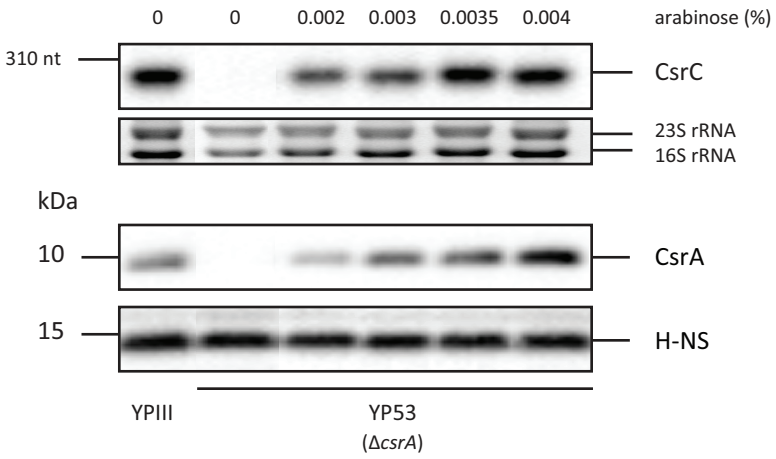

Fig. 3.9 Low abundance of CsrA is enough to assess CsrC integrity
To evaluate CsrC transcript levels in relation to endogenous CsrA protein, northern and western blot samples were prepared simultaneously. *Y. pseudotuberculosis* YPIII and YP53 (Δ*csrA*) harbouring the pP_{BAD}::*csrA* plasmid (pRS68), were grown at 25°C in LB medium supplemented with different concentrations of arabinose. Transcript levels of CsrC were analysed by northern blotting. Total RNA was prepared, separated on 0.7% MOPS agarose gels, transferred onto a nylon-membrane and probed with a digoxigenin (DIG)-labelled PCR fragment encoding the *csrA* gene. 16S and 23S rRNAs were used as loading controls. CsrA protein concentration was analysed by western blotting. Samples were separated on 12% Tris-TRICINE gels and transferred onto an Immobilon-P membrane. Proteins were detected by immunoblotting with a polyclonal antibody directed against CsrA. Immunoblotting with a polyclonal antibody against H-NS was used as loading control.

Concluding, no direct binding between YmoA and the CsrC RNA was reported. Nonetheless, YmoA seems to control proteins involved in CsrC turnover like indicated by the microarray results, which revealed a small set of RNA chaperones that were upregulated in absence of YmoA. Furthermore, it is likely that YmoA acts via CsrA on CsrC stability, as slightly reduced CsrA levels were observed in the *ymoA* mutant.

Differential regulation of a huge number of genes in the *ymoA* mutant strongly suggests the involvement of multiple regulatory components as players in a complex regulatory network controlling CsrC integrity.

3.2. Identification of novel transcriptional regulators affecting CsrC

For *Y. pseudotuberculosis* it was shown that the regulatory RNA CsrB is controlled by the BarA/UvrY two-component system (TCS) in response to environmental signals. Furthermore, the cAMP receptor protein Crp indirectly controls this TCS leading to repression of *csrB* expression. However, Crp exerts a positive effect on CsrC levels by a so far unknown mechanism (Heroven *et al.*, 2008; Heroven *et al.*, 2012b). As shown in this work the nucleoid-associated protein YmoA affects CsrC stability most likely via control of the CsrA levels. Furthermore, previous results imply the involvement of multiple different factors such as RNA chaperones and RNA destabilizing elements. The second part of this work focuses on the identification and characterization of novel regulators implicated in CsrC synthesis or turnover.

3.2.1. Genetic screening in *Y. pseudotuberculosis* YPIII identifies a novel CsrC regulator

In order to identify regulatory factors that control *csrC* expression in response to the early virulence conditions, a plasmid-borne gene library (pACYC184 backbone) from *Y. pseudotuberculosis* YPIII was introduced into the wildtype strain carrying a *csrC-lacZ* reporter plasmid (pKB46). The reporter fusion encompassed the stem-loop structure formed by the first +81 nt of the CsrC RNA, which is required for YmoA-dependent CsrC regulation. By using this reporter construct, transcriptional and post-transcriptional regulators should be found. Approximately $2x10^3$ clones were screened on X-Gal agar plates at 25°C. Three candidates were isolated. Two formed darker blue colonies and exhibited significantly increased *csrC-lacZ* activity (>150%), while one candidate formed pale blue colonies and exhibited significantly reduced *csrC-lacZ* expression levels (< 60%) at 25°C (Fig. 3.10). The first two candidates harboured gene bank plasmids encoding either the Crp or the Hfq protein of *Y. pseudotuberculosis,* which were previously shown to positively affect CsrC levels in the cell (Böhme, unpublished data; Heroven *et al.*, 2012b), demonstrating that the selection procedure was successful and is reliable.

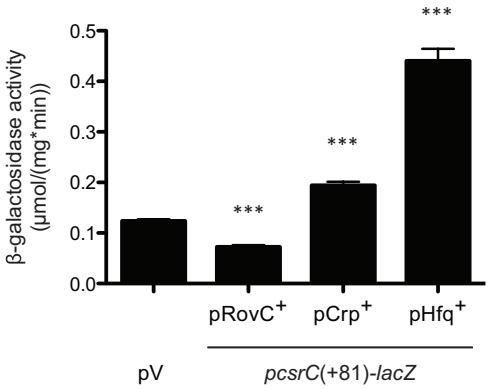

Fig. 3.10 Gene bank screening reveals three putative regulators of CsrC
Expression of a transcriptional *csrC-lacZ* reporter fusion (pKB46) was analysed in *Y. pseudotuberculosis* wildtype strain YPIII. β-galactosidase activity (µmol/(mg*min)) was monitored in strains either harbouring different gene bank plasmids (pRovC$^+$, pCrp$^+$, pHfq$^+$) or the empty vector pACYC184 (pV). Data are means and standard deviations of one experiment, performed with technical duplicates. Data were analysed by Student's t test. Stars indicate the results that differed significantly from the control (*** P<0.001).

The latter clone, which beared a negative effect on *csrC-lacZ* expression, carried a single, common open reading frame (ORF), encoding a hypothetical protein of 247 amino acids (YPK_3567). *In silico* analyses using the BLAST algorithm showed that this gene is highly conserved in two pathogenic members of the genus - *Y. pestis* and *Y. pseudotuberculosis,* but cannot be found in *Y. enterocolitica* or other *Yersinia* species. It does not exhibit homology to any known and characterized protein domain. This new protein was named RovC for regulator of virulence associated with CsrC. Its monocistronic coding sequence was located directly downstream of a type VI secretion system and upstream of the YPK_3568 gene encoding for a pseudouridine synthase. To ensure that the RovC protein is solely responsible for *csrC* repression, the gene was subcloned and the resulting plasmid pSSE11 was transformed into *Y. pseudotuberculosis* YPIII harbouring the respective *csrC-lacZ* reporter plasmid (pKB46) (data not shown).

In order to evaluate the impact of RovC on the expression of *csrC*, a *rovC* mutant strain was generated. First, *csrC-lacZ* expression in *Y. pseudotuberculosis* YPIII (wildtype) and a *rovC* deletion mutant (YP148) was assessed. Furthermore, CsrC and CsrB transcript levels were monitored to see if RovC affects both Csr-type RNAs (Fig. 3.11).

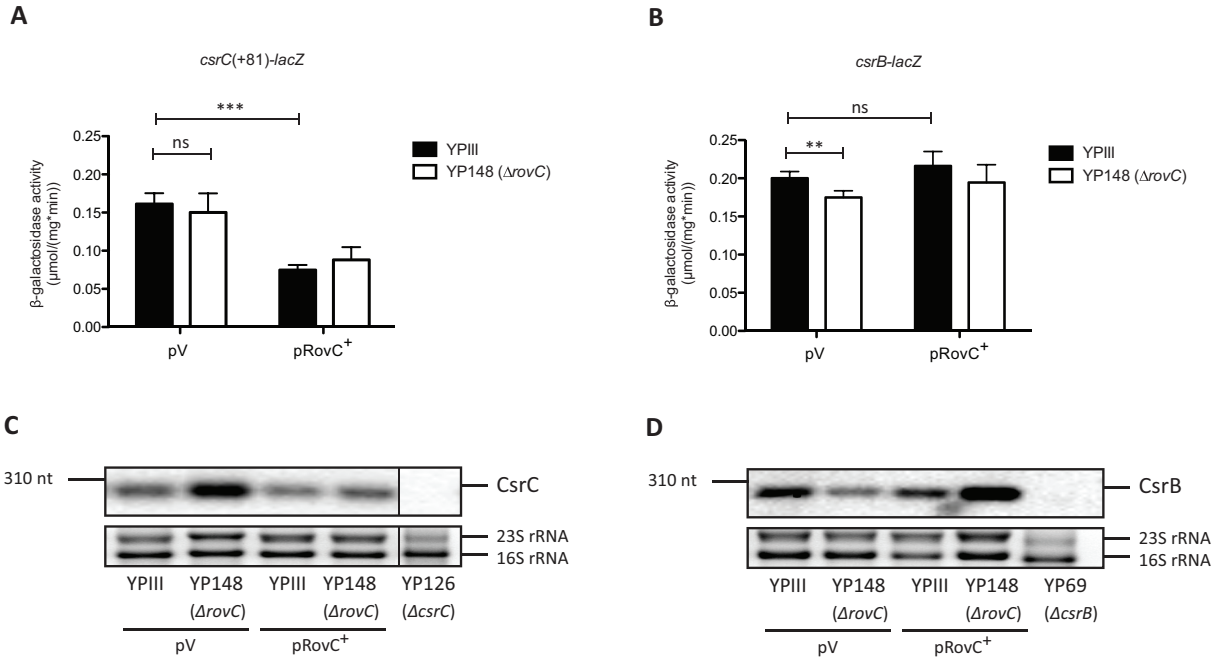

Fig. 3.11 Loss of *rovC* leads to increased CsrC and decreased CsrB levels at 25°C
Expression of transcriptional *csrC-lacZ* (pKB46) (**A**) and *csrB-lacZ* (pAKH101) (**B**) fusions was measured in *Y. pseudotuberculosis* YPIII (wildtype) and YP148 (Δ*rovC*). Strains were transformed with the empty vector pAKH85 (pV) and complemented or overexpressed with pSSE11 (pRovC$^+$). β-galactosidase activity (µmol/(mg*min)) was measured after cells were grown at 25°C in LB medium for 16 h. Data are means and standard deviations of two independent experiments, each performed at least in triplicates. Data were analysed by Student's t test. Stars indicate the results that differed significantly from each other (*** P<0.001, ** P<0.05, ns = not significant). Transcript levels of CsrC (**C**) and CsrB (**D**) were analysed by northern blotting. *Y. pseudotuberculosis* YPIII (wildtype) and YP148 (Δ*rovC*) were used without any plasmid or they were transformed with the empty vector pAKH85 (pV) or the complementation plasmid pSSE11 (pRovC$^+$). YP69 (Δ*csrB*) or YP126 (Δ*csrC)* were used as control strains. Overnight cultures were grown at 25°C in LB medium. Total RNA was prepared, separated on 0.7% MOPS agarose gels, transferred onto a nylon-membrane and probed with a digoxigenin (DIG)-labelled PCR fragment encoding either the *csrC* or *csrB* gene. 16S and 23S rRNAs were used as loading controls.

Interestingly, deletion of the *rovC* gene did lead to a small, but not significant induction of *csrC* expression and significantly reduced *csrB* transcription (Fig. 3.11 A+B). In contrast, RovC overproduction significantly repressed *csrC* transcription while *csrB* expression remained unaffected. Northern blot analyses clearly demonstrate that a *rovC* deletion leads to decreased CsrB and increased CsrC levels (Fig. 3.11 C+D), which can be explained by the counter-regulation of both RNAs. Notably, the effect of a *rovC* deletion on CsrC levels was not always as drastic as shown in Fig. 3.11, which could be explained by the very low transcript abundance of RovC in the cell at 25°C during stationary growth (compare to Fig. 3.31).

Since RovC mainly affects expression of the CsrC transcript, further analyses were focussed on the RovC-mediated regulation of this non-coding RNA. To investigate if the stem-loop structure, which seems to be involved in YmoA-mediated CsrC transcript stabilization, is

important for RovC-dependent CsrC regulation, reporter fusions either with (p*csrC*(+81)-*lacZ*) or without (p*csrC*(+4)-*lacZ)* the stem-loop region were compared in *Y. pseudotuberculosis* wildtype (YPIII) harbouring a *rovC*$^{+}$ plasmid (Fig. 3.12). However, presence or absence of this loop structure did not affect RovC-mediated *csrC* expression, indicating that RovC acts independently of the loop region and likeley exerts transcriptional effects on CsrC.

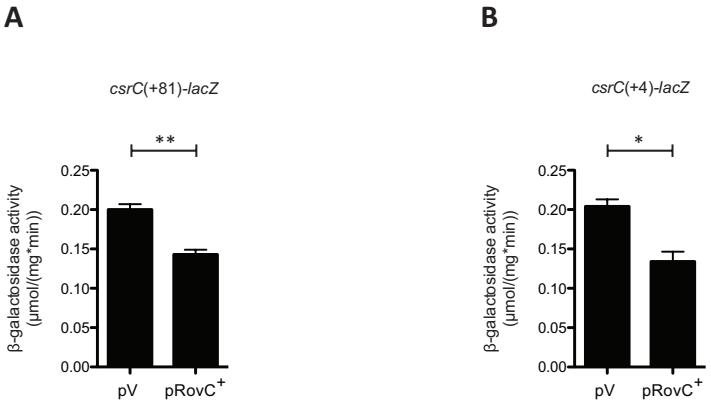

Fig. 3.12 RovC represses CsrC-transcription independent of the stem-loop structure
To see, whether RovC-mediated *csrC* regulation depends on the stem-loop structure, *csrC-lacZ* transcriptional fusions, harbouring either the loop structure (+81 nt of the ncRNA, pKB46) (**A**) or not (+4 nt of the ncRNA, pKB45) (**B**), were monitored in *Y. pseudotuberculosis* wildtype (YPIII). β-galactosidase activity (µmol/(mg*min)) was monitored with bacteria grown at 25°C in LB medium for 16 h. Data are given as means and standard deviations of three independent experiments, each performed with one replicate. Stars indicate the results that differed significantly from each other (** P<0.01, * P<0.05).

3.2.2. RovC does not affect CsrC mRNA transcript stability

First analyses indicated that RovC affects transcription of CsrC. As a next step, post-transcriptional effects of RovC on the CsrC RNA were analysed by comparing the CsrC RNA stability in *Y. pseudotuberculosis* YPIII (wildtype) and YP148 (Δ*rovC*). Transcription was stopped by adding rifampicin and samples were taken directly after addition of rifampicin (0 min) and after 80 min. RNA was prepared and analysed by northern blotting and CsrC RNA concentration was quantified in YPIII and YP148. The fold change of transcription levels was similar in the presence and abscence of RovC, which indicated that neither RovC deletion nor overproduction lead to altered CsrC stability. This strongly suggests that RovC acts as transcriptional repressor of CsrC (Fig. 3.13).

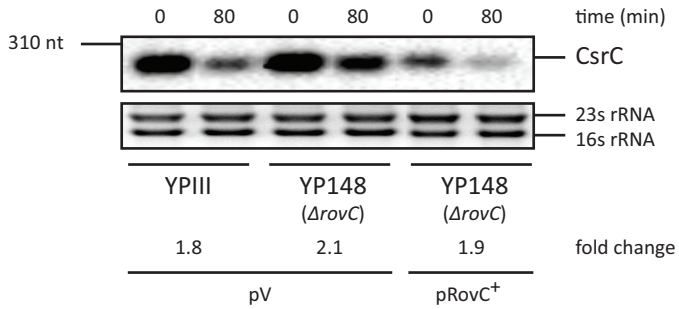

Fig. 3.13 CsrC transcript stability is unaffected in a *rovC* deletion mutant
Transcript stability of CsrC was monitored by northern blot analysis in *Y. pseudotuberculosis* YPIII (wildtype) and YP148 (Δ*rovC*). Strains were transformed with the empty vector pAKH85 (pV) and complemented with its derivative pSSE11 (pRovC$^+$). Overnight cultures were grown at 25°C in LB medium. To stop transcription, rifampicin was added to stationary phase cells in a final concentration of 1 mg/ml. Samples were taken directly after rifampicin addition (0 min) or after 80 min. Total RNA was prepared, separated on 0.7% MOPS agarose gels, transferred onto a nylon-membrane and probed with a digoxigenin (DIG)-labelled PCR fragment encoding the *csrC* gene. 16S and 23S rRNAs were used as loading controls. The relative band intensity was documented and the relative mRNA concentrations were normalized to the 23S and 16S rRNAs. The fold change is given as rel. intensity t_0/rel. intensity t_{80} for each strain.

3.2.3. RovC does not affect known factors involved in CsrC expression

So far different factors have been identified that positively affect CsrC transcription or stability. These factors comprise I) the two-component system BarA/UvrY, which induces CsrB expression and represses CsrC levels, II) the Crp and Hfq proteins, which indirectly stimulate CsrC transcription and III) the RNA-binding protein CsrA that stabilizes CsrC transcripts (Heroven *et al.*, 2008; Böhme, unpublished data; Heroven *et al.*, 2012b).

To monitor whether RovC might act via any of these factors, expression of these factors was compared in *Y. pseudotuberculosis* YPIII (wildtype) and a *rovC* deletion mutant (YP148) (Fig. 3.14). Herein, only *csrB* transcription was altered (repressed) in YP148, which could be explained by the compensatory effect of the two Csr-type RNAs, indicating that RovC might act independent of already known CsrC regulators.

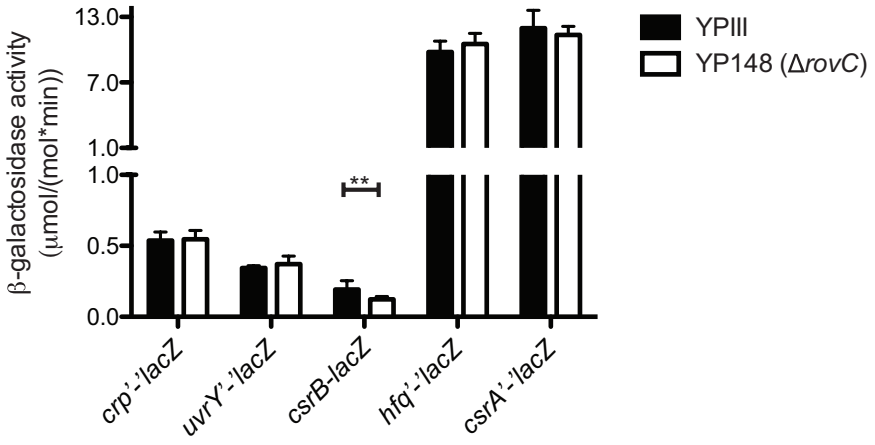

Fig. 3.14 RovC does not affect known regulatory factors upstream of CsrC
Expression of different *lacZ*-reporter fusions (pAKH139 = *crp'-'lacZ*, pKB7 = *uvrY'-'lacZ*, pAKH101 = *csrB-lacZ*, pBW137 = *hfq'-'lacZ* and pKB63 = *csrA'-'lacZ*) was measured in *Y. pseudotuberculosis* YPIII (wildtype) and YP148 (Δ*rovC*). β-galactosidase activity (µmol/(mg*min)) was monitored after cells were grown at 25°C in LB medium for 16 h. Data are means and standard deviations of three independent experiments, each performed at least in duplicates. Data were analysed by Student's t test. Stars indicate the results that differed significantly from each other (** P<0.01).

3.2.4. RovC overexpression affects the whole Csr cascade

Recently it was shown, that the *Y. pseudotuberculosis* Csr system controls a subset of genes (*rovM*, *rovA*), which in turn modulates the expression of the primary internalization factor invasin (Heroven *et al.*, 2008). To test, whether RovC acts via CsrC on the whole Csr-cascade, *rovM, rovA* and *invA* expression was analysed in *Y. pseudotuberculosis* YPIII (wildtype) and YP148 (Δ*rovC*). As shown in Fig. 3.15 (A+B+C) loss of *rovC* does not significantly change expression levels of *rovM* or *rovA*. In contrast, expression of a *rovM'-'lacZ* fusion and endogenous RovM levels were strongly induced upon RovC overproduction. Accordingly, *rovA'-'lacZ* fusions and endogenous RovA and InvA levels were significantly repressed, demonstrating that RovC modulates the whole Csr cascade.

In conclusion, the hypothetical protein RovC was identified as novel transcriptional regulator of CsrC. Furthermore, RovC-dependent invasin synthesis was shown to occur via the Csr-RovM-RovA cascade, when RovC was overexpressed.

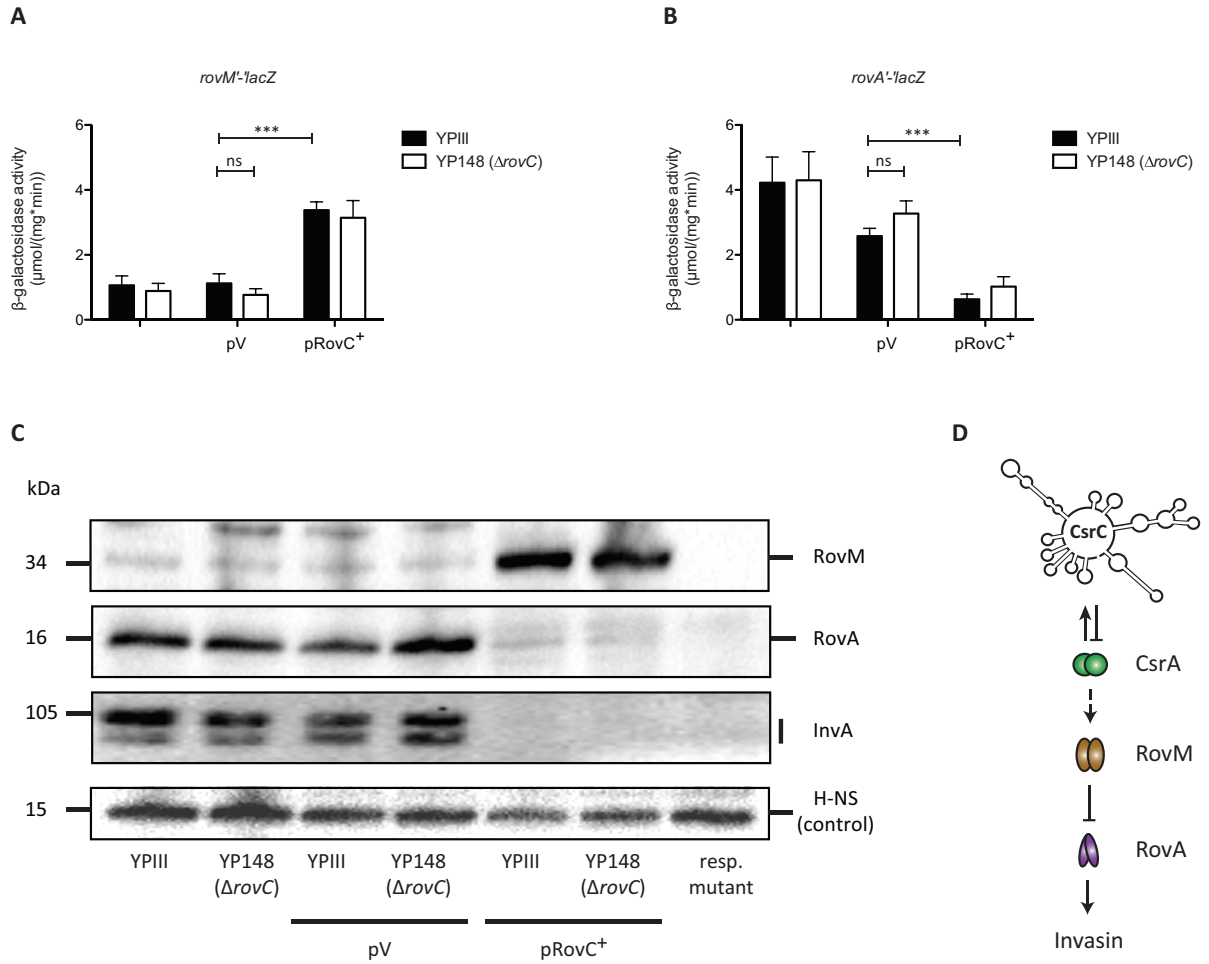

Fig. 3.15 RovC controls invasin synthesis via the CsrBC-RovM-RovA cascade

Expression of translational *rovM'-'lacZ* (pAKH63) (**A**) and *rovA'-'lacZ* (pAKH47) (**B**) fusions was monitored in *Y. pseudotuberculosis* YPIII (wildtype) and YP148 (Δ*rovC*). Strains were transformed with the empty vector pAKH85 (pV) and complemented or overexpressed with its derivative pSSE11 (pRovC$^+$). β-galactosidase activity (µmol/(mg*min)) was measured after cells were grown at 25°C in LB medium for 16 h. Data are means and standard deviations of three independent experiments, each performed at least in duplicates. Data were analysed by Student's t test. Stars indicate the results that differed significantly from each other (*** P<0.001, ns = not significant).

C Protein concentrations of RovM, RovA and invasin (InvA) in YPIII und YP148 were compared by western blot analysis. Strains were transformed with the empty vector pAKH85 (pV) and complemented or overexpressed with its derivative pSSE11 (pRovC$^+$). Whole cell extracts were prepared from cultures grown at 25°C in LB medium for 16 h, separated on 12% Tris-TRICINE gels (RovM, RovA) or 10% SDS-PAA gels (InvA) and transferred onto an Immobilon-P membrane. Proteins were detected by immunoblotting with polyclonal antibodies directed against RovM, RovA and InvA. The respective mutant (Δ*rovM* = YP72, Δ*rovA* = YP107, Δ*invA* = YP191) served as negative control. Immunoblotting with a polyclonal antibody against H-NS served as loading control. **D** Schematic representation of the Csr cascade that regulates invasin expression.

3.3. Impact of RovC: a global approach (microarray analysis)

To identify additional genes under control of RovC, a microarray was performed using total RNA from *Y. pseudotuberculosis* YPIII (wildtype) and YP148 (Δ*rovC*) grown at 25°C to stationary phase in DMEM-F12 medium. The impact of RovC on CsrB and CsrC levels was most pronounced under these conditions (data not shown). Mixed Cy3- (Δ*rovC*) and Cy5- (wildtype) labelled RNA was hybridized to an Agilent customized microarray carrying 4172 chromosomally-encoded and 92 plasmid-encoded genes of *Y. pseudotuberculosis*.

Tab. 3.1 Classification of RovC-dependent genes

Gene ID	Gene locus	Fold change	Description	Category - class
Virulence genes				
Downregulated loci (YPK_3567 activated)				
YPK_1268	*ail*	-1,9	virulence-related outer membrane protein	virulence factor
YPK_3552		-1,8	type VI secretion protein, VC_A0114 family	virulence factor
YPK_3553		-2,2	putative lipoprotein	virulence factor
YPK_3554		-2,2	conserved hypothetical protein	virulence factor
YPK_3555		-1,8	conserved hypothetical protein	virulence factor
YPK_3561	*impG*	-1,9	type VI secretion protein, VC_A0110 family	virulence factor
YPK_3562	*impF*	-3,7	type VI secretion system lysozyme-related protein	virulence factor
YPK_3563	*hcp*	-19,9	protein of unknown function DUF796	virulence factor
YPK_3564	*impC*	-3,3	type VI secretion protein, EvpB/VC_A0108 family	virulence factor
YPK_3565		-3,6	type VI secretion protein, VC_A0107 family	virulence factor
Genetic information storage and processing				
Downregulated loci (YPK_3567 activated)				
YPK_0282	*rpsJ*	-1,8	ribosomal protein S10	Translation
YPK_0284	*rplD*	-2,1	ribosomal protein L4/L1e	Translation
YPK_0285	*rplW*	-1,9	Ribosomal protein L25/L23	Translation
YPK_0288	*rplV*	-1,8	ribosomal protein L22	Translation
YPK_0337	*rplJ*	-1,8	ribosomal protein L10	Translation
YPK_0338	*rplL*	-2,0	ribosomal protein L7/L12	Translation
YPK_0354	*hupA*	-1,8	histone family protein DNA-binding protein	Replication
YPK_3231	*hupB*	-1,8	histone family protein DNA-binding protein	Replication
YPK_3757	*rplU*	-1,8	ribosomal protein L21	Translation
YPK_4249		-1,7	ribosomal protein L34	Translation
Metabolism				
Downregulated loci (YPK_3567 activated)				
YPK_0025	*yiaF*	-2,1	putative lipoprotein	Amino acid transport
YPK_0076	*hutU*	-2,3	urocanate hydratase	Amino acid transport
YPK_0077	*hutH*	-3,5	histidine ammonia-lyase	Amino acid transport
YPK_0078	*hutT*	-2,6	amino acid permease-associated region	Energy production and conversion
YPK_0364	*aceB*	-2,2	malate synthase A	Energy production and conversion

YPK_0365	*aceA*	-1,7	isocitrate lyase	Energy production and conversion
YPK_1375		-3,1	extracellular solute-binding protein family 1	Inorganic ion transport and metabolism
YPK_1377		-1,8	ABC transporter related	Amino acid transport
YPK_1463	*sfuA*	-1,8	extracellular solute-binding protein family 1	Inorganic ion transport and metabolism
YPK_1520	*fabB*	-1,8	beta-ketoacyl synthase	Lipid transport and metabolism
YPK_2070	*oppA*	-1,8	extracellular solute-binding protein family 5	Amino acid transport
YPK_3445	*sodC*	-1,9	superoxide dismutase	Inorganic ion transport and metabolism
YPK_4225	*atpG*	-1,8	ATP synthase F1, gamma subunit	Energy production and conversion
Upregulated loci (YPK_3567 repressed)				
YPK_0906		1,8	holin family 2	Amino acid transport Inorganic ion transport and metabolism
Cellular processes and signaling				
Downregulated loci (YPK_3567 activated)				
YPK_1760		-2,1	N-acetylmuramyl-L-alanine amidase, negative regulator of AmpC, AmpD	Defense mechanisms
YPK_1917	*hslJ*	-1,8	protein of unknown function DUF306 Meta and HslJ	Posttranslational modification
YPK_2017	*cstA*	-1,8	carbon starvation protein CstA	Signal transduction mechanisms
YPK_2630	*ompA*	-2,0	OmpA domain protein transmembrane region-containing protein	Cell wall/membrane/envelope biogenesis
YPK_2649			porin Gram-negative type	Cell wall/membrane/envelope biogenesis
YPK_2784	*spr*		NLP/P60 protein	Cell wall/membrane/envelope biogenesis
YPK_0270	*fkpA*	-1,7	peptidylprolyl isomerase	Posttranslational modification
YPK_3452	*htrA*	-1,8	protease Do	Posttranslational modification
Transport and secretion, structural proteins				
Upregulated loci (YPK_3567 repressed)				
YPK_0702	*flhA*	1,8	type III secretion FHIPEP protein	Cell motility; Intracellular trafficking, secretion, and vesicular transport
Others (no described function)				
Downregulated loci (YPK_3567 activated)				
YPK_0547		-1,8	protein of unknown function DUF883 ElaB	
YPK_1772		-1,8	protein of unknown function DUF1480	
YPK_2643		-1,8	protein of unknown function DUF1379	
YPK_4187		-1,9	HAD-superfamily hydrolase, subfamily IA, variant 3	General function prediction only
Upregulated loci (YPK_3567 repressed)				
YPK_0102		1,9	4-oxalocrotonate tautomerase family enzyme	General function prediction only
Hypothetical Proteins				
Downregulated loci (YPK_3567 activated)				
YPK_0497		-3,7	conserved hypothetical protein	
YPK_2025		-1,8	conserved hypothetical protein	
YPK_2200		-2,9	hypothetical protein YPK_2200	
YPK_3549		-6,2	conserved hypothetical protein	
YPK_3567		-6,2	conserved hypothetical protein	
YPK_4107		-2,0	conserved hypothetical protein	
YPK_4108		-2,4	conserved hypothetical protein	

In total, 56 genes showed a 1.7-fold or greater difference in transcript abundance between the wildtype and the *rovC* mutant strain (Tab. 3.1). The majority of these genes was activated by RovC, whereas only two genes were repressed.

About fourteen of all RovC-dependent transcripts were related to metabolic adaptation processes and another twelve encoded for hypothetical proteins and other genes with unknown function. The remaining transcripts were related to virulence (ten genes), genetic information processing (ten genes), cellular processes and transport and secretion (ten genes) (Fig. 3.16). Accordingly, RovC seems to play a role in virulence but also in metabolic responses and is involved in information processing with regard to genetic and cellular relevance.

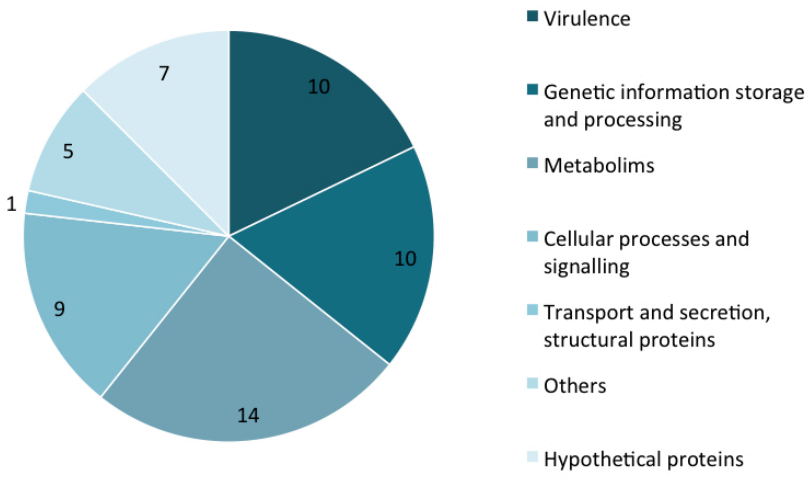

Fig. 3.16 Overall impact of RovC on *Y. pseudotuberculosis* gene expression
Differentially regulated genes between the *Y. pseudotuberculosis* wildtype strain (YPIII) and the *rovC* mutant (YP148). 16 independent cultures of YPIII and YP148 were grown in minimal medium (DMEM:F12, 1:1 mixture) at 25°C to stationary phase (16 h). For RNA preparation always two cultures were pooled. Total RNA was isolated and eight cultures of YPIII were pooled for labelling with Cy5. Four cultures (each pooled from two separate cultures) of YP148 were used for Cy3 labelling. RNA probes were hybridized to a customized Agilent microarray slide, carrying 4172 chromosomal and 92 plasmid-encoded genes of *Yersinia*. Data were normalized and genes with an overall fold-change of ≥ 1.7 were clustered into different categories according to the KEGG database or identified by BLAST searches. Differentially regulated genes are given in absolute numbers. Gene categories are indicated on the right hand side.

3.3.1. RovC induces a virulence-associated type VI secretion system

Remarkably nine genes, belonging to one operon, were activated by RovC. BLAST analyses revealed that the whole cluster belongs to the type VI secretion operon-4 of *Y. pseudotuberculosis* YPIII (T6SS4, gene IDs from YPK_3550 to YPK_3566) (Fig. 3.17). This operon encompasses 16 genes with a total size of 23.6 kb. Especially the *hcp* gene (YPK_3563), coding for the hemolysin coregulated protein, is strongly down-regulated (19-

fold) in a *rovC* mutant. Hcp from *P. aeruginosa* forms hexameric nanotubules that resemble the bacteriophage T4 tail and is a major component of the bacteriophage-like subassembly of the T6SS, which contacts the target cells (Mougous *et al.*, 2006; Ballister *et al.*, 2008). These tubules emerge at the cell surface but can also be secreted into the surrounding medium (Osipiuk *et al.*, 2011; Jones *et al.*, 2014).

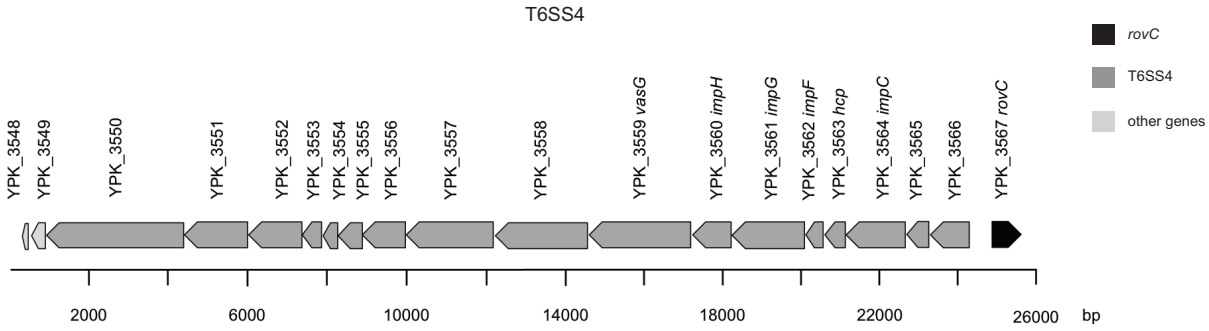

Fig. 3.17 Schematic representation of the type VI secretion system 4 (T6SS4) of *Y. pseudotuberculosis*
The T6SS4 cluster is composed of 16 genes (YPK_3550 to YPK_3566), encompassing a size of 23.6 kb. The *rovC* gene is found directly downstream of this cluster oriented in the opposite direction.

To validate the results obtained from the microarray analysis, RT-PCR of four identified RovC targets (T6SS genes) and one unrelated gene was performed. As shown in Fig. 3.18 the unrelated gene YPK_3548 directly upstream of the T6SS cluster was not affected, while the other candidates that belonged to the T6SS4 were significantly downregulated when *rovC* was abscent. Strikingly, the *rovC* gene is located directly downstream of this operon (Fig. 3.17), encoded in the opposite direction. According to this characteristic organization, RovC might be a perfect candidate for a transcription factor assigned to this T6S system.

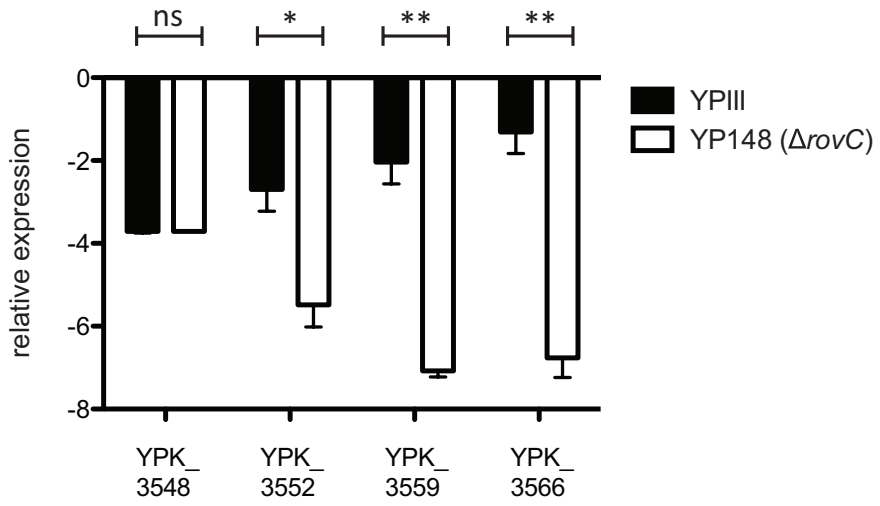

Fig. 3.18 RT-PCR of selected T6SS genes, identified as RovC dependent in the microarray
To verify the results from the microarray, one-step real-time RT-PCR analysis was performed with specific primer pairs for selected genes of the T6SS4. RNA was isolated from eight independent cultures for the *Y. pseudotuberculosis* wildtype (YPIII) reference strain and from three independent cultures of the Δ*rovC* candidate strain. Gene expression levels were normalized to the *sopB* reference transcript for YPIII and YP148 respectively (according to (Pfaffl. 2001)) and are given as relative expression of the respective gene in relation to *sopB*. Data are given as means ± standard deviation. Data were analysed by Student's t test. Stars indicate the results that differed significantly from each other (** P<0.01. * P<0.05. ns = not significant).

3.3.2. The type VI secretion system is activated by RovC and temperature

To verify that the identified T6SS4 is indeed activated by RovC, expression of a translational fusion of the first gene within this operon (gene ID YPK_3566) was compared in YPIII and YP148 (Δ*rovC*). Results clearly demonstrate that RovC is crucial for the activation of this T6SS4 (Fig. 3.19 A+B). In *Y. pestis* and *Y. pseudotuberculosis* YPIII and IP31758 expression of the T6SS4 operon was found to be temperature-regulated. Accordingly, it is preferentially expressed at moderate temperatures, while it is inactive at elevated temperatures like 37°C (Pieper *et al.*, 2009; Zhang *et al.*, 2011; Gueguen *et al.*, 2013). To prove these findings, reporter fusions of the T6SS were compared at 25°C and 37°C in presence or absence of the *rovC* gene.

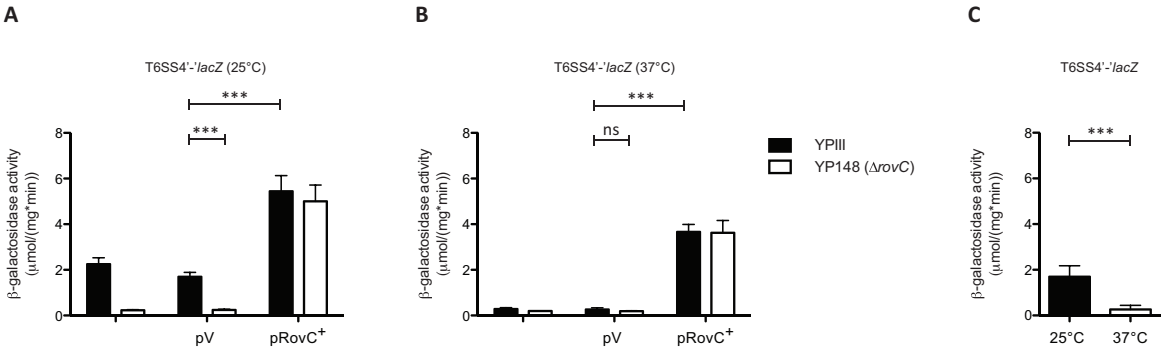

Fig. 3.19 T6SS4 is induced at 25°C and shows RovC-dependency
RovC-dependent expression of a translational T6SS4*'-'lacZ* (pSSE64) fusion was monitored in *Y. pseudotuberculosis* YPIII wildtype and YP148 (Δ*rovC*). Strains were transformed with the empty vector pAKH85 (pV) and complemented or overexpressed with its derivative pSSE11 (RovC^{+}). β-galactosidase activity (µmol/(mg*min)) was measured after strains were grown in LB medium at 25°C (**A**) or 37°C (**B**) for 16 h. Data are means and standard deviations of two independent experiments, each performed at least in triplicates. Data were analysed by Student's t test. Stars indicate the results that differed significantly from each other (*** P<0.001, ns = not significant). **C** Temperature-dependent expression of a translational T6SS4*'-'lacZ* (pSSE64) fusion in *Y. pseudotuberculosis* YPIII wildtype was monitored and analysed as described above.

Expression of the T6SS was switched on at 25°C, whereas no activity was found at 37°C (Fig. 3.19 C). Herein, presence of RovC was absolutely required to activate T6SS4 expression. Furthermore, overexpression of RovC could activate T6SS4 expression under non-inducing conditions at 37°C (Fig. 3.19 B). Moreover, recent findings in *Y. pseudotuberculosis* YPIII suggest that this particular type VI secretion system (T6SS4) is induced by exposure to low pH and by quorum-sensing (Zhang *et al.*, 2011; Zhang *et al.*, 2013). In contrast to these previous studies no induction of T6SS4 was found upon exposure to low pH or when investigating the impact of different quorum-sensing mutant strains in *Y. pseudotuberculosis* YPIII (Fig. S 3).

3.4. Environmental control of the novel regulator RovC

During host-colonization bacteria face a rapidly changing environment regarding temperature, nutrient and oxygen supply, ion availability and the surrounding pH. Especially the temperature shift from a moderate tempered environment (15°C - 25°C) to the warm-blooded host (37°C) is a major factor that regulates virulence gene expression in *Yersinia.* In addition to temperature the growth phase and nutrient availability are crucial parameters in controlling gene regulation. In order to gain more information about RovC and its expression pattern, this part of the work focuses on the environmental parameters that affect expression of this novel transcriptional regulator.

3.4.1. Transcription of *rovC* depends on temperature and growth conditions

The recent work identified RovC as essential activator of the T6SS4, which was reported to respond to acid stress and quorum-sensing (Zhang *et al.*, 2011; Zhang *et al.*, 2013). Therefore, *rovC* expression was monitored in media with different pH values and in different quorum-sensing mutant strains. Results clearly demonstrated that *rovC* was maximally expressed in a neutral or slightly basic mileu, while acidity leads to slightly decreased (but not significant) *rovC* expression. Furthermore, *rovC* expression was not affected by single and double mutants eliminating the two quorum-sensing systems of *Y. pseudotuberculosis* (Fig. 3.20).

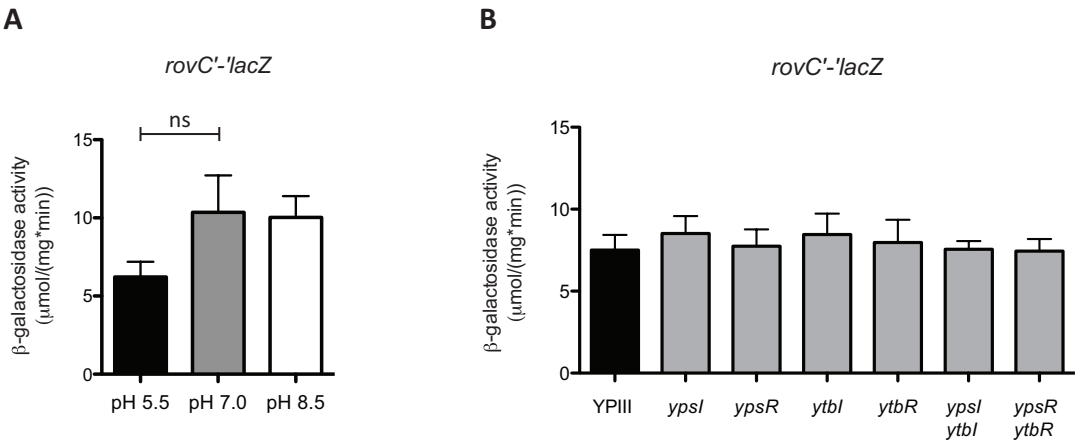

Fig. 3.20 Expression of *rovC* in response to pH and quorum-sensing mutant strains
A pH-dependent expression of a translational *rovC-'lacZ* (pSSE32) fusion was monitored in *Y. pseudotuberculosis* YPIII wildtype. β-galactosidase activity (µmol/(mg*min)) was measured from overnight cultures grown at 25°C in LB medium with different pH values (pH 5.5. pH 7.0. pH 8.5). Data are means and standard deviations of two independent experiments, each performed at least in triplicates. Data were analysed by Student's t test. Data did not differ significantly from each other (ns = not significant).
B Expression of translational *rovC'-'lacZ* (pSSE32) fusions was monitored in different quorum-sensing YPIII mutant strains (YPIII *ypsI. ypsR. ytbI. ytbR. ypsI/ytbI. ypsR/ytbR*). β-galactosidase activity (µmol/(mg*min)) was measured after strains were grown in LB medium at 25°C for 16 h. Data are means and standard deviations of two independent experiments, each performed at least in triplicates. Data were analysed by Student's t test. Data did not differ significantly from each other.

Next, *rovC* transcriptional and translational fusions were analysed in *Y. pseudotuberculosis* YPIII (wildtype) at 25°C and 37°C during exponential and stationary growth phase. The translational fusion harboured the first eleven nucleotides of the *rovC* coding region, while the transcriptional fusion ended directly upstream of the Shine-Dalgarno sequence. Expression of *rovC'-'lacZ* translational reporter fusions was slightly induced at 25°C during stationary growth (Fig. 3.21 B). This was confirmed by comparing RovC transcript levels (Fig. 3.21 C). RovC transcript seems to be absent at 37°C in the stationary phase. *In vitro* transcriptome data could confirm the finding, that RovC mRNA is maximally expressed at 25°C during stationary growth (Nuss, unpublished data), suggesting a maximal *rovC* expression under conditions mimicking environmental growth. Notably, RovC transcript levels were consistent with the translational fusions but not with the transcriptional fusion, indicating that post-transcriptional regulation might be involved in RovC control. Although high *rovC* expression levels were detected with the translation fusion, the transcriptional fusion exhibited only basal expression and the RovC mRNA was barely detectable.

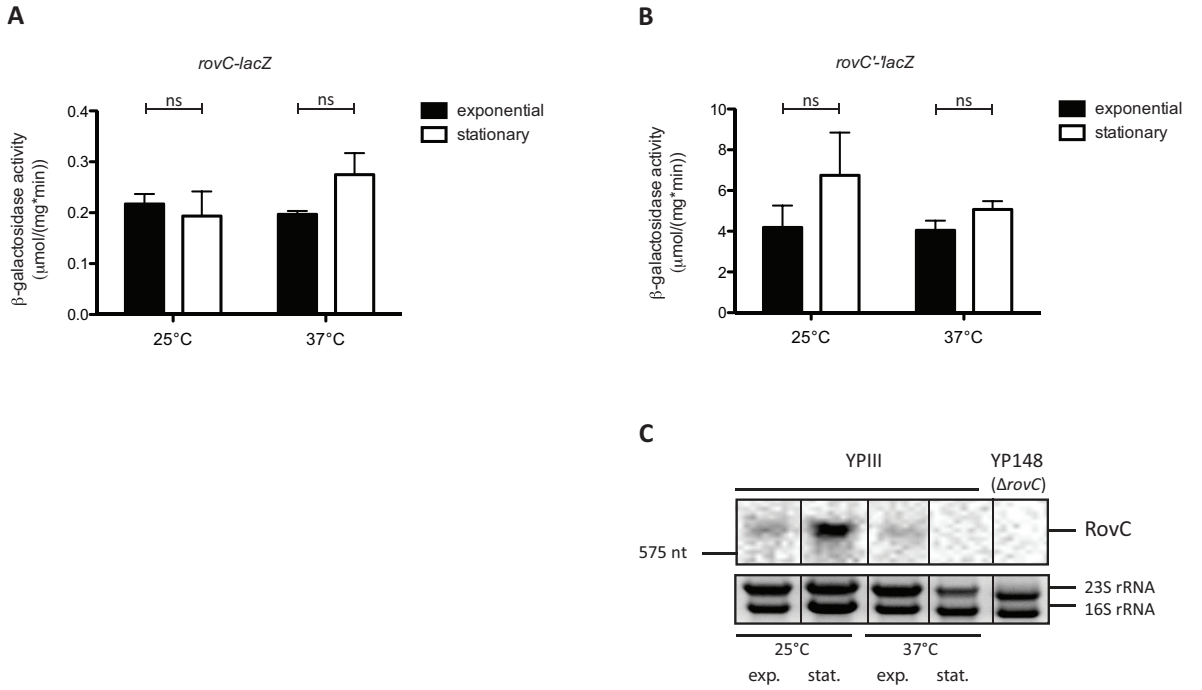

Fig. 3.21 Expression of *rovC* is favoured at 25°C during stationary growth
Expression of transcriptional *rovC-lacZ* (pSSE67) (**A**) and translational *rovC'-'lacZ* (pSSE32) (**B**) fusions was monitored in *Y. pseudotuberculosis* YPIII (wildtype). β-galactosidase activity (µmol/(mg*min)) was measured after strains were grown in LB medium at 25°C or 37°C for 4 h (exponential) or 16 h (stationary). Data are means and standard deviations of two independent experiments, each performed at least in triplicates. Data were analysed by Student's t test. Stars indicate the results that differed significantly from each other (ns = not significant). **C** RovC transcript levels were analysed by northern blotting. Strains were grown in LB medium at 25°C or 37°C for 4 h (exp) or 16 h (stat). Total RNA was prepared, separated on 0.7% MOPS agarose gels, transferred onto a nylon-membrane and probed with a digoxigenin (DIG)-labelled PCR fragment encoding the *rovC* gene. 16S and 23S rRNAs were used as loading controls. The *rovC* mutant strain YP148 served as negative control; exp = exponential, stat = stationary growth.

In *Y. pseudotuberculosis* synthesis of the Csr RNAs is strongly affected by changes in the nutrient availability. The Crp protein, whose activity is governed by the glucose availability, controls both RNAs. Under glucose-limiting conditions Crp is activated upon binding to the cAMP second messenger and controls gene regulation (Busby and Ebright, 1999; Heroven *et al.*, 2012b). Consequently, *rovC* expression was compared for bacterial growth in complex LB medium and a minimal medium (DMEM:F12, mixture 1:1) that contained glucose as major carbon source. Expression of *rovC'-'lacZ* fusions was slightly induced during growth in minimal medium, while RovC transcript levels were identical at both conditions (Fig. 3.22), indicating that *rovC* expression is not primarily influenced by the nutrient availability.

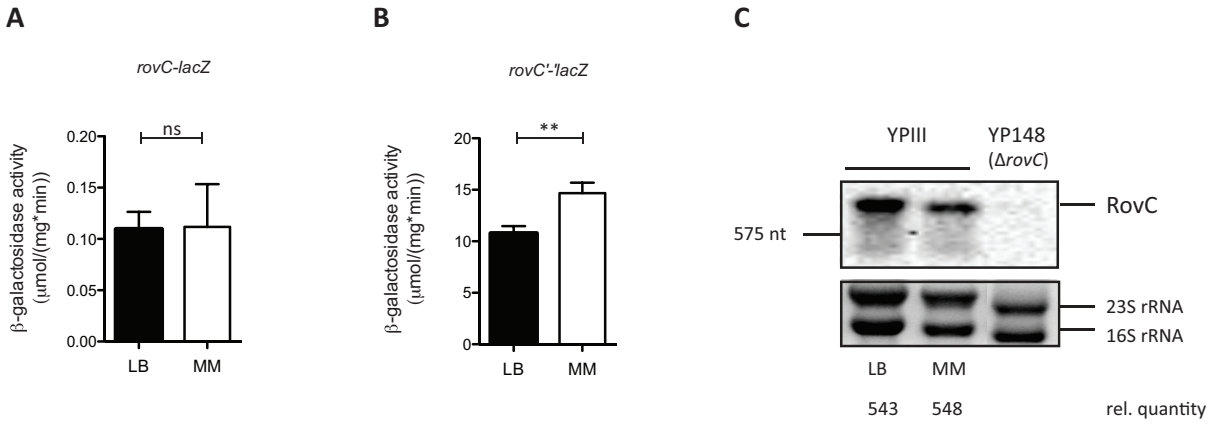

Fig. 3.22 Nutrient supply does not alter *rovC* expression
Expression of transcriptional *rovC-lacZ* (pSSE67) (**A**) and translational *rovC'-'lacZ* (pSSE32) (**B**) fusions was monitored in *Y. pseudotuberculosis* YPIII (wildtype). β-galactosidase activity (µmol/(mg*min)) was measured after strains were grown in LB medium (LB) or minimal medium (MM = DMEM:F12, 1:1 mixture) at 25°C for 16 h. Data are means and standard deviations of two independent experiments, each performed at least in triplicates. Data were analysed by Student's t test. Stars indicate the results that differed significantly from each other (** P<0.01, ns = not significant). **C** RovC transcript levels were analysed by northern blotting. Strains were grown in LB medium or minimal medium (MM = DMEM:F12, 1:1 mixture) at 25°C for 16 h. Total RNA was prepared, separated on 0.7% MOPS agarose gels, transferred onto a nylon-membrane and probed with a digoxigenin (DIG)-labelled PCR fragment encoding the *rovC* gene. 16S and 23S rRNAs were used as loading controls. The *rovC* mutant strain YP148 served as negative control.

3.4.2. Expression of *rovC* is not induced by cell contact

Host cell-contact is another signal that can trigger virulence gene expression, e.g. in *Yersinia* plasmid-encoded virulence genes were induced upon bacterial-binding to eukaryotic cells (Opitz, 2013). In order to investigate if *rovC* expression exhibits cell-contact dependency, an *in vitro* model was applied. To do so, bacteria harbouring a *rovC-luxCDABE* reporter plasmid were incubated with or without eukaryotic cells and *rovC* expression was monitored. As shown in Fig. 3.23, *rovC* expression was not induced upon bacterial contact to human epithelial cells (HEp-2), indicating that other factors or environmental parameters are required for RovC activation.

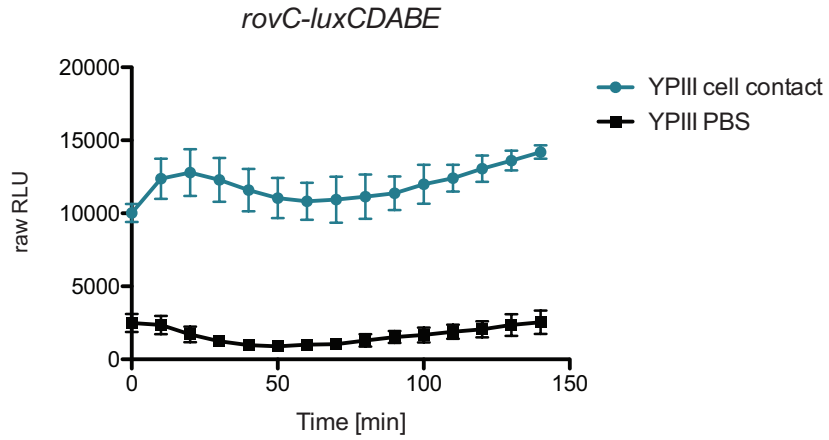

Fig. 3.23 Expression of *rovC* is not induced by contact to eukaryotic cells
Expression of *rovC-luxCDABE* (pMK07) was monitored in *Y. pseudotuberculosis* YPIII (wildtype) in presence (cell contact) or absence (PBS) of HEp-2 cells. Strains were grown at 25°C for 16 h and used to infect the HEp-2 cells. The bioluminescent emission was measured every 10 min to monitor the kinetics of host cell dependent *rovC-luxCDABE* induction. The experiment was performed twice with essentially identical results.

3.4.3. RovC is not autoregulated

Feedback-loops are the simplest control elements of transcriptional regulatory networks. In the Csr regulatory cascade for instance, CsrA is required for CsrBC stability on the one hand while CsrB and CsrC control CsrA activity on the other hand. Furthermore, also RovA and RovM are autoregulated (Heroven and Dersch, 2006; Heroven *et al.*, 2008).

To monitor whether RovC can regulate its own expression, a *rovC'-'lacZ* fusion was assessed in *Y. pseudotuberculosis* YPIII (wildtype) and a *rovC* deletion mutant (YP148). As shown in Fig. 3.24 RovC is not autoregulated.

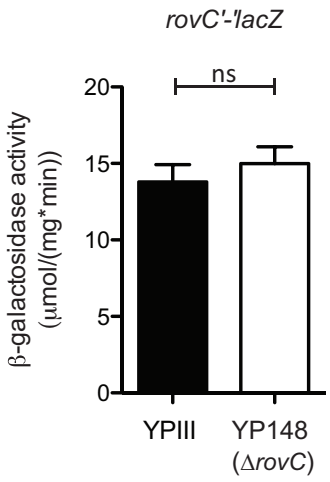

Fig. 3.24 RovC is not autoregulated
Expression of a translational *rovC'-'lacZ* (pSSE32) fusion was monitored in *Y. pseudotuberculosis* YPIII (wildtype) and YP148 (Δ*rovC*). β-galactosidase activity (µmol/(mg*min)) was measured after strains were grown in LB medium at 25°C for 16 h. Data are means and standard deviations of two independent experiments, each performed at least in triplicate. Data were analysed by Student's t test. Stars indicate the results that differed significantly from each other (ns = not significant).

3.4.4. Synthesis of *rovC* requires *Yersinia*-specific activators

BLAST analyses revealed that RovC is unique in *Y. pestis* and *Y. pseudotuberculosis*. Nevertheless, it might be possible that factors, which are present in other bacterial strains, can modulate *rovC* expression. To test this hypothesis, *rovC'-'lacZ* expression was monitored in *E. coli*. While *rovC* expression was basal in *E. coli*, it was significantly induced in *Y. pseudotuberculosis*, but was still elevated in comparison to the empty vector control (pV) Fig. 3.25). This strongly suggests that *Yersini*a-specific factors are required for full RovC activation.

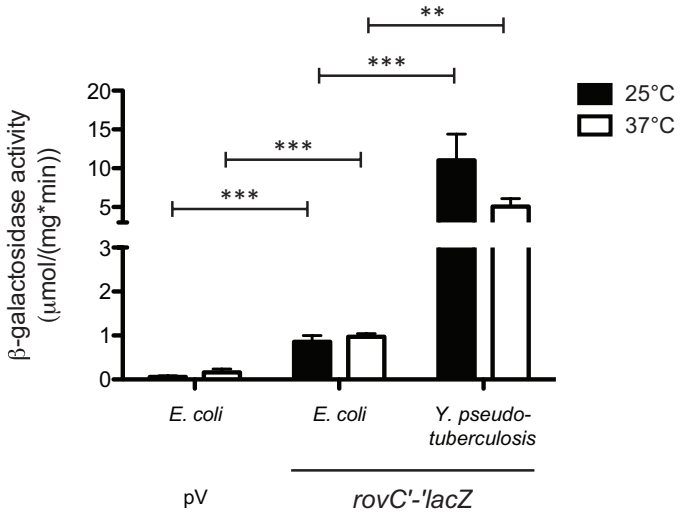

Fig. 3.25 Synthesis of *rovC* requires *Yersinia*-specific activators
Expression of a translational *rovC'-'lacZ* (pSSE32) fusion was monitored in *Y. pseudotuberculosis* YPIII (wildtype) and *E. coli* DH10β. The empty vector pTS02 in *E. coli* served as control (pV). β-galactosidase activity (µmol/(mg*min)) was measured after strains were grown in LB medium at 25°C and 37°C for 16 h. Data are means and standard deviations of two independent experiments, each performed at least in triplicates. Data were analysed by Student's t test. Stars indicate the results that differed significantly from each other (*** P<0.001. ** P<0.01).

3.5. Identification of regulatory elements that control RovC expression

The hypothetical protein RovC was found to be a *Yersinia*-specific factor, which is maximally expressed at 25°C during stationary growth, unaffected by the nutrient supply. Moreover, cell contact-dependent induction and autoregulation were not implicated in *rovC* expression control. Further, it was shown that RovC is associated with the Csr system, namely that it regulates *csrC* transcription and therefore has an impact on the downstream genes *rovM*, *rovA* and *invA*.

In this context several regulators that were shown to control the Csr regulatory network, were analysed regarding their impact on *rovC* expression.

3.5.1. The regulators Crp, YmoA and CsrA control *rovC* expression

So far Hfq, RovM, YmoA, CsrA and Crp encompass regulators that control the Csr system in *Yersinia* (Böhme, unpublished data Heroven *et al.*, 2012a; Heroven *et al.*, 2012b). To monitor whether these factors might influence *rovC* expression, *rovC* reporter fusions (pSSE32) were monitored in the different mutant strains. As shown in Fig. 3.26 *rovC* expression was not affected by loss of *hfq* or *rovM*, while deletion of *ymoA*, *csrA* and *crp* significantly increased *rovC'-'lacZ* expression. Consequently, the latter three regulators were chosen for further *rovC* expression analyses.

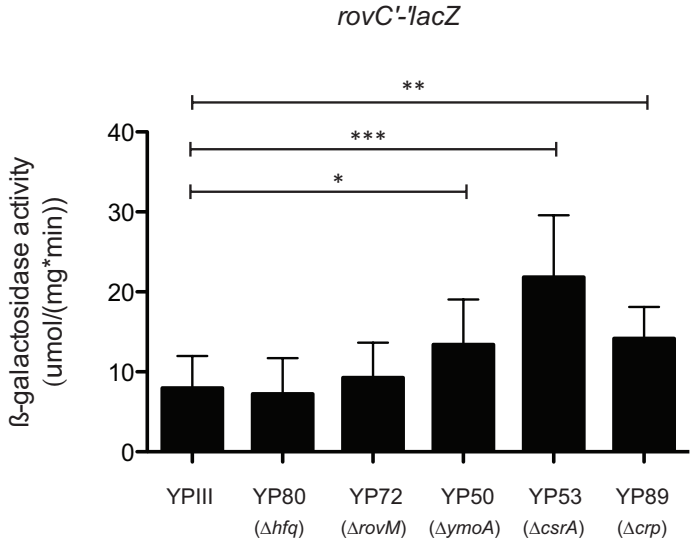

Fig. 3.26 YmoA, CsrA and Crp repress *rovC* synthesis at 25°C
Expression of a translational *rovC'-'lacZ* (pSSE32) fusion was monitored in *Y. pseudotuberculosis* YPIII (wildtype), YP80 (Δ*hfq*), YP72 (Δ*rovM*), YP50 (Δ*ymoA*), YP53 (Δ*csrA*) and YP89 (Δ*crp*). β-galactosidase activity (µmol/(mg*min)) was measured after strains were grown in LB medium at 25°C for 16 h. Data are means and standard deviations of three independent experiments, each performed at least in triplicate. Data were analysed by Student's t test. Stars indicate the results that differed significantly from each other (*** P<0.001. ** P<0.01. * P<0.05).

Therefore, three different reporter fusions were generated as depicted in Fig. 3.27. The translational fusion harboured the first eleven nucleotides of the *rovC*-coding region (+50 nt relative to the transcriptional start site (TSS)). The transcriptional fusions differ in their upstream region; the pSSE67 fusion ends directly upstream of the Shine-Dalgarno sequence (+25 nt relative to TSS) while the pAKH189 fusion stops at the TSS (+1).

When the complete *rovC* 5'-UTR is missing (Fig. 3.27 A), *rovC* does not exhibit YmoA dependency. However, fusions harbouring additional 25 nt of the 5'-UTR or even the complete 5'-UTR plus additional eleven nucleotides of the *rovC*-coding region, they show YmoA dependent expression (Fig. 3.27 B+C). Interestingly, *in trans* complementation with pYmoA$^+$ leads to increased *rovC* expression with all of the three reporter constructs.

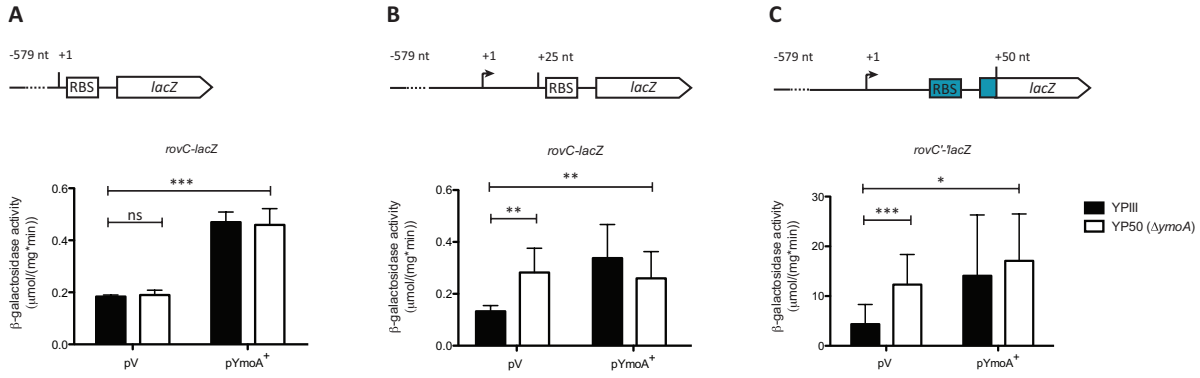

Fig. 3.27 YmoA represses *rovC* transcription and translation
Expression of two different transcriptional *rovC-lacZ* (pAKH189) (**A**), (pSSE67) (**B**) and one translational *rovC'-'lacZ* (pSSE32) (**C**) fusions was monitored in *Y. pseudotuberculosis* YPIII (wildtype) and YP50 (Δ*ymoA*). Strains were transformed with the empty vector pAKH85 (pV) and complemented or overexpressed with the midi-copy plasmid pAKH71 (pYmoA$^+$). β-galactosidase activity (µmol/(mg*min)) was measured after strains were grown in LB medium at 25°C for 16 h. Data are means and standard deviations of two independent experiments, each performed at least in triplicate. Data were analysed by Student's t test. Stars indicate the results that differed significantly from each other (*** P<0.001, ** P<0.01, * P<0.05), graphic representation of *lacZ* fusions: white = *lacZ*, blue = *rovC,* RBS = ribosomal binding site, nt = nucleotides, numbers indicate distance relative to transcriptional start site.

CsrA exhibits the most pronounced effect on *rovC* expression. Loss of *csrA* leads to highly increased *rovC* transcription (Fig. 3.28 A+B), which can be complemented with a *csrA*$^+$ plasmid. The translational fusion also indicates CsrA-dependent *rovC* expression (Fig. 3.28 C). Herein, CsrA overexpression even further repressed *rovC* translation. In summary, CsrA represents a repressor of *rovC* transcription. In consideration of the enhanced repressional impact on the translational fusion, repression might include additional sequences in the first nucleotides of the *rovC*-coding region.

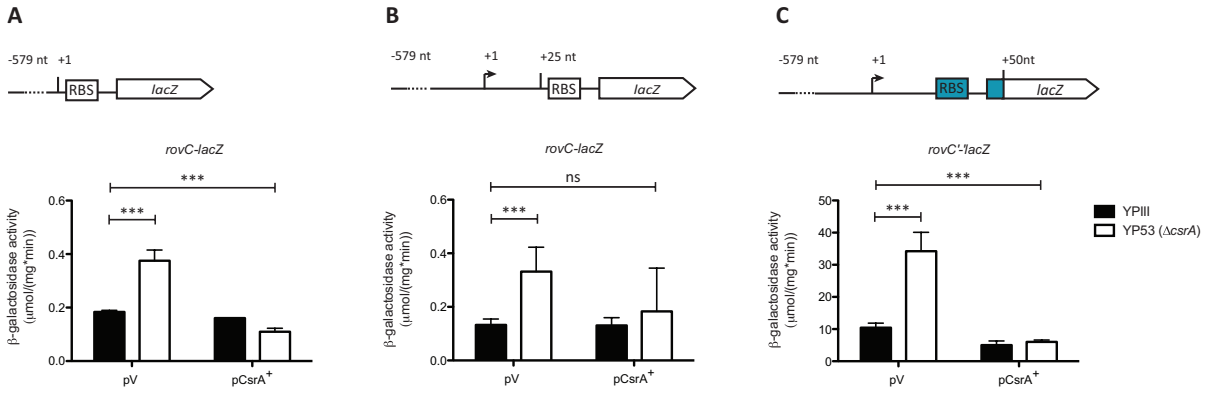

Fig. 3.28 CsrA represses *rovC* transcription and translation
Expression of two different transcriptional *rovC-lacZ* (pAKH189) (**A**), (pSSE67) (**B**) and one translational *rovC'-'lacZ* (pSSE32) (**C**) was monitored in *Y. pseudotuberculosis* YPIII (wildtype) and YP53 (Δ*csrA*). Strains were transformed with the empty vector pAKH85 (pV) and complemented or overexpressed with the midi-copy plasmid pAKH56 (pCsrA$^+$). β-galactosidase activity (µmol/(mg*min)) was measured after strains were grown in LB medium at 25°C for 16 h. Data are means and standard deviations of two independent experiments, each performed at least in triplicates. Data were analysed by Student's t test. Stars indicate the results that differed significantly from each other (*** P<0.001. ns = not significant), graphic representation of *lacZ* fusions: white = *lacZ*, blue = *rovC,* RBS = ribosomal binding site, nt = nucleotides, numbers indicate distance relative to transcriptional start site.

Like shown in Fig. 3.29 *rovC* expression is increased in a *crp* mutant background for all three *rovC-lacZ* fusions. However, *in trans* complementation with a Crp$^+$ plasmid can only restore the phenotype for the transcriptional reporter fusions (Fig. 3.29 A), while complementation is limited for the translational fusion (Fig. 3.29 B+C). Concluding, these data show that Crp functions as transcriptional repressor of RovC.

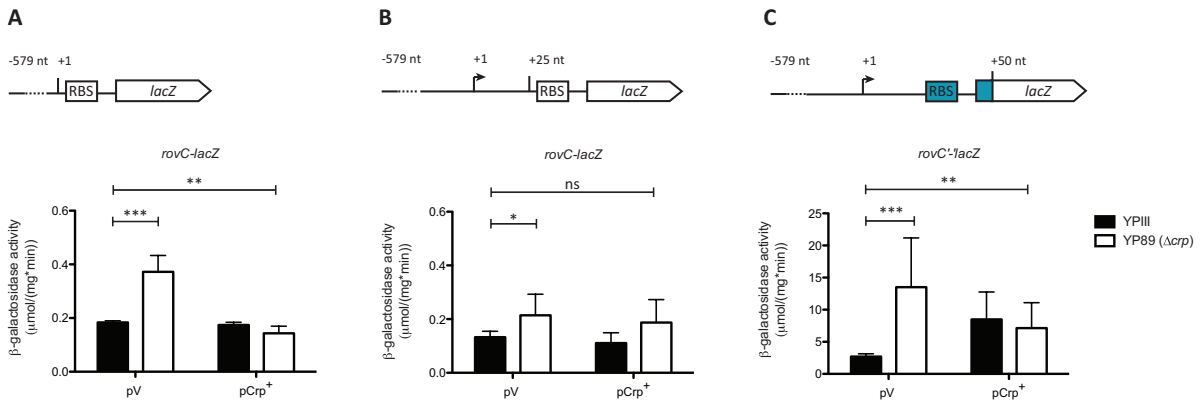

Fig. 3.29 Crp represses *rovC* transcription and translation
Expression of two different transcriptional *rovC-lacZ* (pAKH189) (**A**) (pSSE67) (**B**) and one translational *rovC'-'lacZ* (pSSE32) (**C**) as monitored in *Y. pseudotuberculosis* YPIII (wildtype) and YP89 (Δ*crp*). Strains were transformed with the empty vector pAKH85 (pV) and complemented or overexpressed with the midi-copy plasmid pAKH37 (pCrp$^+$). β-galactosidase activity (µmol/(mg*min)) was measured after strains were grown in LB medium at 25°C for 16 h. Data are means and standard deviations of two independent experiments, each performed at least in triplicates. Data were analysed by Student's t test. Stars indicate the results that differed significantly from each other (*** P<0.001, * P<0.05, ns = not significant), graphic representation of *lacZ* fusions: white = *lacZ*, blue = *rovC,* RBS = ribosomal binding site, nt = nucleotides, numbers indicate distance relative to transcriptional start site.

Next, the impact of Crp, YmoA and CsrA on the RovC transcript levels and on endogenous RovC protein concentration was monitored. Northern blot analyses in YPIII, YP50 (Δ*ymoA*), YP53 (Δ*csrA*) and YP89 (Δ*crp*) indicate elevated RovC transcript levels in all three mutant strains compared to the wildtype, whereby the repressional impact of CsrA is most pronounced (Fig. 3.30 A). Northern blot results confirm the promoter-fusion experiments (Fig. 3.27-Fig. 3.29) and demonstrate a negative impact of YmoA, Crp and CsrA on *rovC* expression. Moreover, it became evident that there is nearly no RovC transcript detectable in the *Yersinia* wildtype strain. In order to analyse if the elevated RovC mRNA levels lead to increased amounts of endogenous RovC protein, an anti-RovC antibody should be generated. So far, different independent attempts to generate this antibody failed. Purification was not successful since it was not possible to obtain soluble protein. In all attempts the protein seemed to colocalize with the membrane fraction or was entrapped in inclusion bodies. Therefore, a plasmid-based His-tagged version of RovC (C-terminal His-tag), under control of its own promoter, was introduced into the cells. Immunoblotting with an anti-His antibody revealed increased amounts of endogenous RovC protein in the *ymoA*, *csrA* and *crp* mutant strain compared to the wildtype (Fig. 3.30 B). Herein, loss of *csrA* exerts the strongest derepression on endogenous RovC, confirming the results obtained from the northern blot analysis.

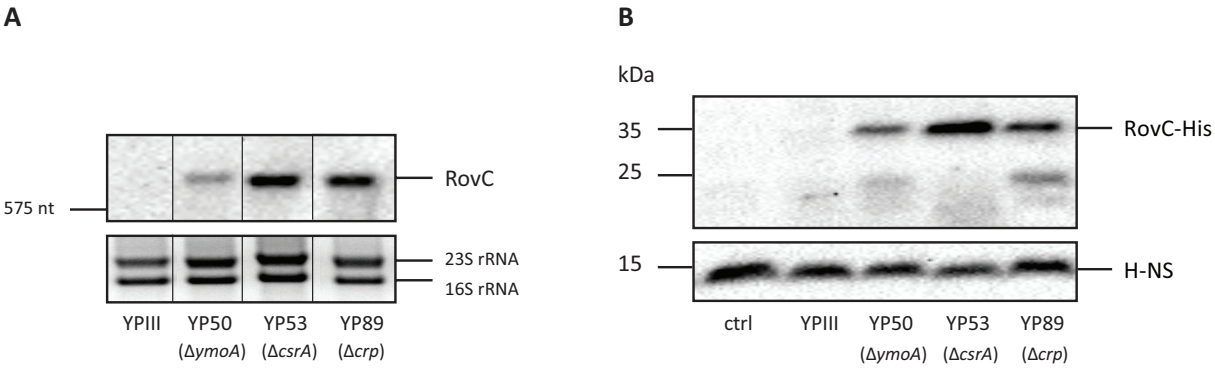

Fig. 3.30 RovC mRNA and protein are repressed by YmoA, CsrA and Crp
A RovC transcript levels were analysed by northern blotting. Strains were grown in LB medium at 25°C to stationary growth phase (16 h). Total RNA was prepared from YPIII, YP50 (Δ*ymoA*), YP53 (Δ*csrA*) and YP89 (Δ*crp*), separated on 0.7% MOPS agarose gels, transferred onto a nylon-membrane and probed with a digoxigenin (DIG)-labelled PCR fragment encoding the *rovC* gene. 16S and 23S rRNAs were used as loading controls.
B Protein concentrations of RovC-His in YPIII, YP50 (Δ*ymoA*), YP53 (Δ*csrA*) and YP89 (Δ*crp*) were compared by western blot analysis. Strains were transformed with pSSE68, harbouring a C-terminal RovC-His-tag under control of its own promoter. Whole cell extracts were prepared from cultures grown at 25°C in LB medium for 16 h, separated on 8% Tris-TRICINE gels and transferred onto an Immobilon-P membrane. Proteins were detected by immunoblotting with a monoclonal antibody directed against the His-tag. YPIII served as negative control (ctrl). Immunoblotting with a polyclonal antibody against H-NS served as loading control.

3.5.2. CsrA has a dual function: control of transcription and transcript stability

Expression analysis of transcriptional and translation *rovC-lacZ* reporter constructs indicated that CsrA might act as transcriptional repressor of *rovC*. However, CsrA is well known as post-transcriptional regulator that controls the stability of its target mRNAs and usually induces rapid degradation (Romeo *et al.*, 2013). According to this, the role of CsrA on *rovC* synthesis was examined more closely.

First, RovC transcript levels were compared in the *Y. pseudotuberculosis* wildtype strain (YPIII) and the *csrA* mutant strain (YP53). As shown by the northern blot (Fig. 3.31) RovC transcript levels were highly increased in a *csrA* mutant in comparison to the wildtype and could be complemented with a *csrA*$^+$ plasmid.

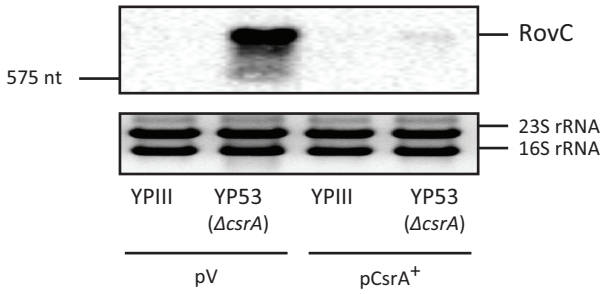

Fig. 3.31 CsrA represses RovC mRNA synthesis
RovC transcript levels were analysed by northern blotting. YPIII and YP53 (Δ*csrA*) were transformed with the empty vector pAKH85 (pV) or with its derivative pAKH56 (pCsrA$^+$). Strains were grown in LB medium at 25°C to stationary growth phase. Total RNA was prepared, separated on 0.7% MOPS agarose gels, transferred to a nylon-membrane and probed with a digoxigenin (DIG)-labelled PCR fragment encoding the *rovC* gene. 16S and 23S rRNAs were used as loading controls.

To analyse whether CsrA influences RovC mRNA degradation, the RovC mRNA stability was compared in *Y. pseudotuberculosis* wildtype (YPIII) and the *csrA* mutant strain (YP53). Therefore, both strains were transformed with a midi-copy plasmid harbouring RovC under control of its own promoter (pSSE11), as in the normal wildtype background RovC mRNA is barely detectable. RNA degradation was assessed by the addition of rifampicin, which blocks transcription and the remaining transcript levels were monitored over time. Results indicate that two different phenomena can be observed. Like previously shown in the northern blot (Fig. 3.30 A), overall RovC mRNA levels were drastically increased in the *csrA* mutant strain in comparison to the wildtype (Fig. 3.33). Surprisingly, a reciprocal impact of CsrA on RovC mRNA stability was observed. When CsrA was absent, the transcript stability of RovC was reduced by more than 50%. In the wildtype background RovC had a half-life of about 41

minutes, while this was reduced to 13 minutes in absence of CsrA, indicating that CsrA exerts a stabilizing effect on this mRNA target.

Taken together, CsrA exerts a negative transcriptional effect on *rovC* expression, while it bears both, positive and negative post-transcriptional effects on the RovC mRNA.

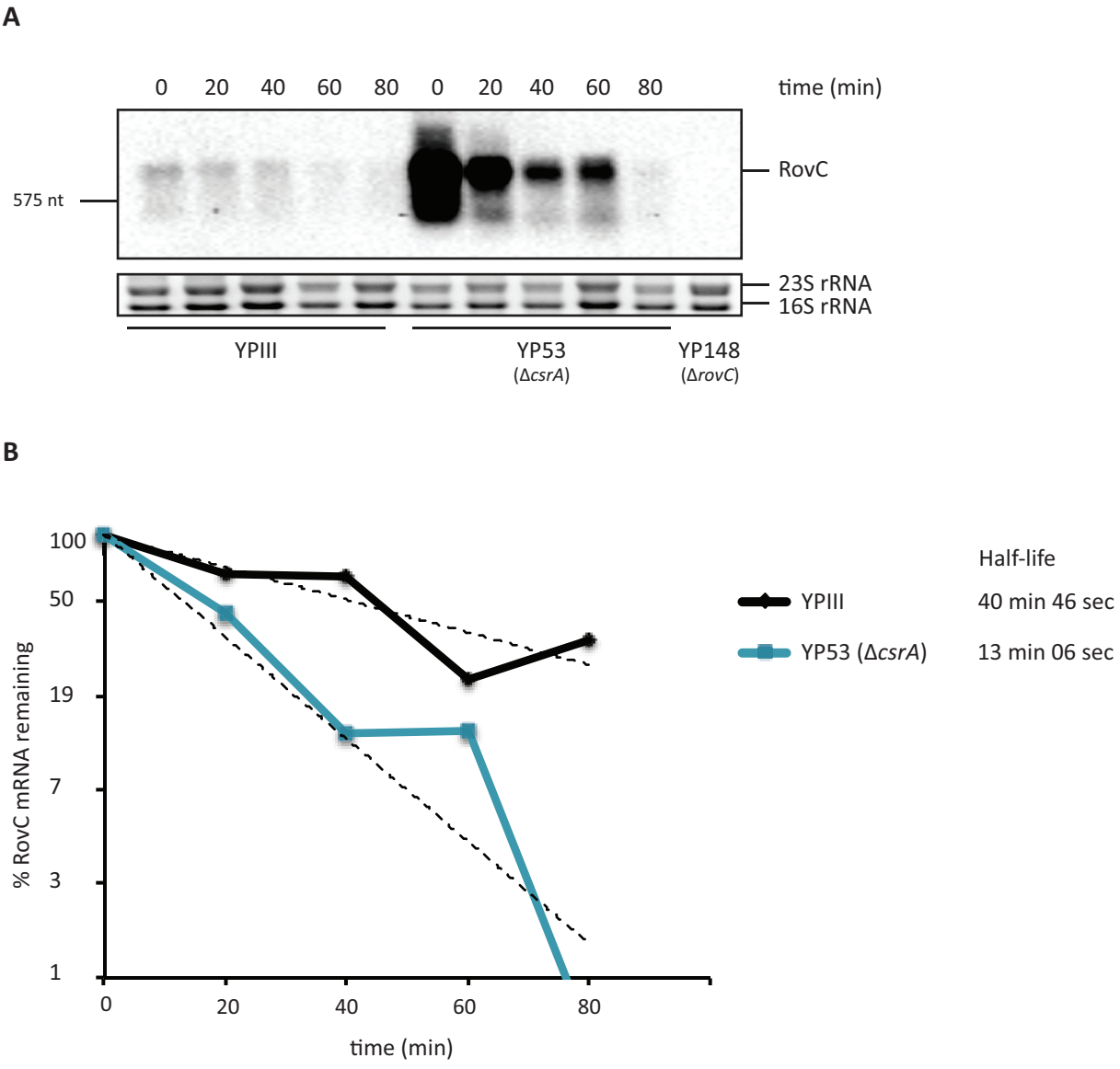

Fig. 3.32 CsrA stabilizes RovC transcript

A To compare RovC transcript stability in *Y. pseudotuberculosis* wildtype (YPIII) and YP53 (Δ*csrA*) a stability assay was performed. Strains were transformed with pSSE11, increasing the copy number of RovC transcript especially in the wildtype. Cultures were grown in LB medium at 25°C for 16 h. Transcription was stopped by adding rifampicin to a final concentration of 1 mg/ml. Samples were taken directly after rifampicin addition (0 min) and after 20 min, 40 min, 60 min and 80 minutes. Total RNA was isolated, separated on 0.7% MOPS agarose gels, transferred onto a nylon-membrane and probed with a digoxigenin (DIG)-labelled PCR fragment encoding the *rovC* gene. 16S and 23S rRNAs were used as loading controls and YP148 (Δ*rovC*) was used as negative control.

B The northern blots were documented and the relative band intensity was calculated in relation to the 23S and 16S rRNAs. The graph represents the remaining percentage of RNA (y-axis) over time (x-axis) on a half-logarithmic scale. The half-life of the RovC mRNA transcript was calculated via the exponential regression (dashed lines).

3.5.3. CsrA directly binds to the RovC mRNA

CsrA homodimers preferentially bind RNA consensus sequences like 5'-$^{A}/_{U}$CANGGANG$^{U}/_{A}$-3' (N = any nucleotide) (Schubert *et al.*, 2007). With regard to recently performed *in vitro* transcriptome analyses (Nuss, unpublished data) the transcriptional start site (TSS) of the *rovC* leader transcript was mapped 39 nucleotides upstream of the RovC translational start codon ($RovC_{AUG}$) (Fig. 3.33 A (+1)). Within this region, in addition to the GGA motif of the Shinde-Dalgarno sequence, a second GGA motif was localized in close proximity to the TSS (+1). Further 32 nucleotides downstream of the $RovC_{AUG}$ a third GGA motif was present (Fig. 3.33 A).

In order to see, whether CsrA interacts directly with the RovC 5'-UTR, electrophoretic mobility shift assays (EMSAs) were performed. RNA was *in vitro* transcribed from a PCR template, harbouring the T7 promoter for the bacteriophage T7 RNA polymerase. The *in vitro* transcribed RovC RNA fragment (overall length = 77 nt) harboured all three putative CsrA-binding sites. The CsrA protein was heterologously expressed in *E. coli* BL21λDE3 and affinity purified via a C-terminal His-tag. 10 pmol RNA were incubated with increasing amounts of protein. EMSA analysis clearly demonstrates a direct interaction of CsrA with the RovC RNA (Fig. 3.33 B). Initial interactions of the RovC transcript and the CsrA protein occurred, when a 2.4-fold excess of CsrA protein was applied (24 pmol CsrA protein). This corresponds to the model that CsrA binds to RNA as a homodimer (Schubert *et al.*, 2007). RovC mRNA is fully shifted in presence of 56 pmol to 75 pmol CsrA protein, indicating that at least two binding sites may exist. In comparison to the RovM negative control, which shows a slight, unspecific CsrA-binding, the CsrA-RovC interaction is clearly more specific, even at lower protein concentrations.

In conclusion, CsrA acts as repressor most presumably by indirectly repressing *rovC* transcription. Surprisingly, CsrA is required for RovC stabilization, while it also effieciently inhibits its translation, which seems to be mediated by direct CsrA-binding to the upstream region of the RovC RNA.

The whole analysis indicates that RovC expression is tightly controlled on different levels of regulation and is subject to a complex and multifacted regulatory network.

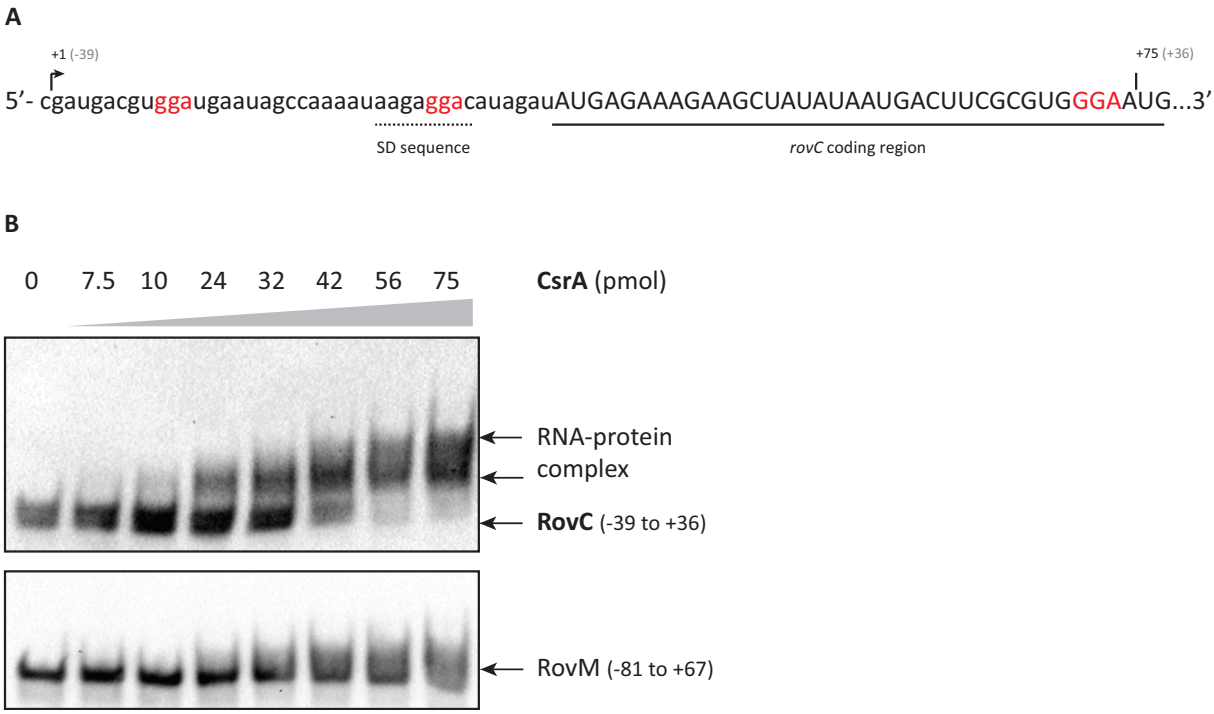

Fig. 3.33 CsrA directly binds to the RovC mRNA
A Schematic representation of the *in vitro* transcribed RovC RNA (+1 to +75 nt), black numbers = nucleotides relative to transcriptional start site (TSS), grey numbers = nucleotides relative to translational start site. The TSS is marked as +1, the Shine-Dalgarno (SD) sequence is denoted by a dashed line, GGA motifs are highlighted in red, capital letters indicate the *rovC*-coding region.
B To show that CsrA can directly bind RovC mRNA transcripts, electrophoretic mobility shift assays (EMSAs) were performed. RovC and RovM mRNA was *in vitro* transcribed (RovC mRNA starts at +1 and harbours 36 nt of the coding region). 10 pmol of each RNA were denatured, cooled down at RT to refold the RNA and incubated with increasing amounts of CsrA protein (7.5 pmol to 75 pmol protein) at 25°C. Complexes were separated on a 4% TBE gel, transferred onto nitrocellulose membranes and probed with digoxigenin (DIG)-labelled PCR fragments encoding the *rovC* or *rovM* gene. RovM *in vitro* transcribed RNA served as negative control (numbers indicate nucleotides relative to the translational start site).

3.5.4. ClpP and Lon proteases control RovC protein level

Besides transcriptional, post-transcriptional and translational control, protein stability and folding carried out by ATP-dependent chaperones and proteases, represents another level of regulation (Timmermans and Van Melderen, 2010). The proteases ClpXP and Lon have been implicated in the virulence gene regulation of *Yersinia* species (Pederson *et al.*, 1997; Jackson *et al.*, 2004) and were shown to control RovA and YmoA protein integrity. At elevated temperatures both proteins are prone to degradation by those proteases (Herbst *et al.*, 2009; Böhme, unpublished data). To test, whether the RovC protein may be targeted by these serine proteases, endogenous RovC levels were compared in the *Y. pseudotuberculosis* wildtype and a *clpP/lon* double-mutant strain at 25°C during exponential and stationary

growth. Like shown in Fig. 3.34 endogenous RovC was upregulated when both proteases were absent, irrespective of the growth phase. This analysis indicated that RovC is subjected to ClpP/Lon-dependent proteolysis at lower temperatures.

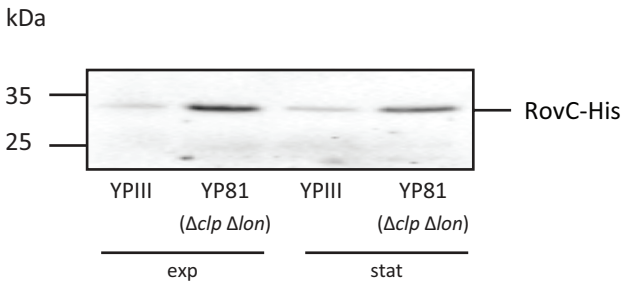

Fig. 3.34 RovC protein is degraded by ClpP/ Lon protease
Protein concentrations of RovC-His in YPIII and YP81 (Δ*clpP* Δ*lon*) were compared by western blot analysis. Strains were transformed with pSSE68, harbouring a C-terminal RovC-His-tag. Whole cell extracts were prepared from cultures grown at 25°C in LB medium for 4 h (exp) or 16 h, (stat) separated on 8% Tris-TRICINE gels and transferred onto an Immobilon-P membrane. Proteins were detected by immunoblotting with a monoclonal antibody directed against the His-tag; exp = exponential, stat = stationary growth.

4. Discussion

Adaptation to rapidly changing environments is pivotal for pathogens to persist under hostile conditions and to establish a successful infection. Such adaptation processes often involve the adjustment of the overall metabolic and stress response pathways, go along with dramatic changes in the bacterial gene expression pattern and are often governed by global regulatory systems. The Csr (carbon storage regulator) system plays a central role in the adaptation of bacterial pathogens during the infectious process and mediates switching towards different physiological stages (Lucchetti-Miganeh *et al.*, 2008; Heroven *et al.*, 2012a). The Csr system is composed of the RNA-binding protein CsrA whose activity is antagonized by non-coding RNAs, e.g. CsrB and CsrC in *Yersinia*. Regulation of the Csr-type RNAs is crucial for the control of CsrA activity (Gudapaty *et al.*, 2001). Accordingly, the investigation of regulatory factors that modulate *csrC* expression in *Y. pseudotuberculosis* was subject of this work.

4.1. YmoA-mediated control of CsrC levels

YmoA/Hha family members are low-molecular weight proteins that modulate virulence gene expression in response to temperature (Madrid *et al.*, 2007). Recent data indicate that YmoA activates the expression of the early virulence regulator gene *rovA* and the RovA-dependent *invA* gene. This induction is mediated through YmoA-controlled changes in the composition of the Csr system (Böhme, unpublished data).

4.1.1. YmoA does not bind directly to CsrC RNA

YmoA positively affects *csrC* expression, which results in CsrC RNA stabilization. Stabilization involves a predicted hairpin structure in the 5'-region of CsrC. Herein, the first stem loop seems to enhance CsrC synthesis most likely by promoting a stable RNA structure. In addition, H-NS, another member of the nucleoid-associated protein family, was found to activate CsrC post-transcriptionally, as decreased CsrC levels due to loss of YmoA can be complemented by H-NS overexpression (Böhme, unpublished data). Besides interference with transcriptional control, H-NS was shown to modulate the stability of the DsrA and RpoS mRNA by directly interacting with these messengers (Brescia *et al.*, 2004; Silva *et al.*, 2008).

Although YmoA lacks a DNA- or RNA-binding domain, it bears structural homology to the H-NS oligomerisation domain and is able to form heterodimeric complexes with H-NS. Accordingly, dimer formation with YmoA alters the biological activity of H-NS, leading to a reduced or increased DNA-binding potential (McFeeters *et al.*, 2007; Banos *et al.*, 2008). For instance, YmoA/H-NS heterodimers form a repression complex in *Y. enterocolitica,* which competes with RovA homodimers for similar binding regions in the *invA* promoter region, resulting in transcriptional abolishment (Ellison and Miller, 2006). Moreover, complex formation of YmoA with H-NS antagonized binding of the TcaR2 inducer complex to promoter regions of multiple insecticidal genes (*tc* genes = toxin complex) in *Y. enterocolitica,* triggering transcriptional repression (Starke and Fuchs, 2014). Therefore, it was hypothesized that YmoA, H-NS or the YmoA/H-NS heterodimeric complexes might be able to interact with the CsrC RNA. However, neither YmoA or H-NS nor YmoA/H-NS heterodimers were able to bind to the CsrC RNA *in vitro* (Fig. 3.1). The H-NS analogue StpA from *E. coli* is an RNA chaperone that appears to bind to unstructured RNA by weak and transient binding only, which is drawn back to weak electrostatic interactions (Zhang *et al.*, 1996; Schreiber and Fersht, 1996; Mayer *et al.*, 2007; Doetsch *et al.*, 2011). Although similar electrostatic interactions might contribute to the YmoA-mediated CsrC stabilization, it is more likely that the influence of YmoA or YmoA/H-NS heterodimers is indirect and occurs through the regulation of other components that in turn affect CsrC stability.

4.1.2. YmoA represses RNA control elements

To further identify genes under control of YmoA, microarray analysis (Heroven and Böhme, unpublished data) was performed. This analysis and RT-PCR experiments in this work demonstrated that multiple genes encoding RNA folding and degrading enzymes were affected by YmoA. RNA turnover is a highly coordinated process that involves several distinct factors and mechanisms like endo- and exoribonucleases, RNA-binding proteins (e.g. Hfq) and non-coding anti-sense sRNAs (Romeo *et al.*, 2013). In *E. coli* the specificity factor CsrD controls the decay of CsrB and CsrC RNA in an RNase E-dependent manner (Suzuki *et al.*, 2006). RNase E is a 5'-3' endoribonuclease, which recognizes single-stranded 5'-monophosphorylated ends. Moreover, RNase E represents a major component of the bacterial degradosome, a multiprotein complex that facilitates turnover of highly structured RNAs such as CsrB and CsrC due to the cooperative activity of different enzymes

encompassing polynucleotide phosphorylase (PNPase), the ATP-dependent RNA helicase RhlB and enolase (glycolytic enzyme) (Viegas and Arraiano, 2008). In *Salmonella spp* loss of *rne* resulted in vast stabilization of CsrB and CsrC transcripts. In contrast, loss of *pnp* leads to considerable accumulation of decay intermediates. Especially in case of CsrC high amounts of shortened transcript were detected (Viegas *et al.*, 2007). Similarly, CsrB and CsrC RNAs were strongly stabilized in an *E. coli* strain lacking RNase E activity. Furthermore, the stability of the CsrB RNA was highly increased in a *pnp* mutant strain, while the stability of CsrC was only slightly elevated compared to the wildtype (Suzuki *et al.*, 2006). As both RNases are involved in processing of CsrB and CsrC RNAs in *E. coli* and *Salmonella*, YmoA-mediated control of these major degradosome components was investigated in *Y. pseudotuberculosis.* However, neither of the two RNases was YmoA-dependent. Accordingly, CsrB and CsrC levels remained constant in an *rne* dominant-negative strain. Loss of *pnp* resulted in decreased CsrC RNA levels, which is contradictory to present studies. Viegas *et al*., (2007) reported highly elevated levels of CsrC decay intermediates in absence of *pnp.* Possibly loss of *pnp* leads to the same accumulation of decay intermediates in *Y. pseudotuberculosis*. However, at least in a *ymoA* mutant strain, such processed CsrC transcripts were not detectable (Heroven, unpublished data). As the *Y. pseudotuberculosis* CsrC RNA bears only 50-54% structural identity to the *E. coli* and *Salmonella* homologues, and transcript levels were not affected by loss of *rne*, it is likely that different RNA degrading enzymes are involved in CsrC turnover than in *E. coli* and *Salmonella*. Furthermore, also the involvement of the specificity factor CsrD seems unlikely, as CsrC levels remained unaffected in the absence of this factor (Seekircher, unpublished data). Nevertheless, implication of a homologous system that operates via distinct RNases cannot be excluded.

Indeed, the major components of the *E. coli* heat shock response, like the ATP-dependent DnaK-DnaJ-GrpE complex or the GroE chaperone that consists of the chaperonin GroEL and its co-chaperonin GroES (Cimdins *et al.*, 2013) were upregulated in a *ymoA* mutant. Despite their usual function in retaining protein integrity in response to heat-stress, co-expression of *dnaK-dnaJ-grpE* or *groEL-groES* leads to mRNA stabilization and increases gene expression levels in *E. coli* (Georgellis *et al.*, 1995; Yoon *et al.*, 2008). Furthermore, an operon encoding for a unique ribonuclease that is homologous to the rat liver perchloric acid-soluble protein (L-PSP) showed higher transcript levels in the absence of functional YmoA. Members of this protein family represent translational inhibitors, which directly affect target mRNAs by

endonucleolytic cleavage and lead to disaggregation of the ribosomes (Morishita *et al.*, 1999). Although family members share a high sequence homology among bacteria and eukaryotes, the cellular function of these proteins in prokaryotes remains unknown.

The most interesting candidate among the differentially regulated RNA control elements was *rnpA* - the gene encoding for the ribozyme RNase P (ribonuclease P), which is conserved in almost all organisms. Expression of *rnpA* was upregulated in a *ymoA* mutant. It processes 5'-ends of pre-tRNAs and other RNA molecules in *E. coli,* including the riboswitch within the 5'-UTR of *btuB* and the mRNA of the *lac* operon. Cleavage is assigned to single-stranded regions in-between neighbouring hairpin structures or within the single-stranded portions of the loop regions themselves (Altman *et al.*, 2005; Altman, 2011; Mondragón, 2013).

Notably, mRNA half-lives depend on the secondary structure of the messengers 5'-end. Herein, the structural motif (loop or bulge), the nucleotide sequence, and the size of the hairpin and folding energies determine the mRNA stability (Carrier and Keasling, 1999; Yoon *et al.*, 2008). For instance, the presence of a simple stem-loop structure of approximately 60 nt in close proximity to the 5'-UTR of the *E. coli ompA* gene can provide protection from RNase E-dependent cleavage (Emory *et al.*, 1992; Arnold *et al.*, 1998). Based on these findings the stem-loop structure found in the CsrC 5'-end could serve two distinct functions: on the one hand it might act as stabilizing element that protects the RNA from degradation or it may constitute the target structure for RNase-dependent cleavage. In presence of YmoA RNase P levels might be low and the highly structured 5'-end of the CsrC RNA could protect the transcript from ribonucleolytic cleavage. Additionally, YmoA could control RNA-binding proteins that are involved in proper stem-loop formation to protect CsrC from degradation. Upon loss of YmoA, RNase P levels could increase and the hairpin structures at the 5'-end might be recognised as cleavage sites, leading to CsrC degradation. In this context the YmoA-mediated derepression of mRNA chaperone molecules might promote stabilization of mRNAs encoding for further RNA-degrading enzymes.

Unfortunately, involvement of these RNA degrading enzymes in CsrC turnover could not be analysed, as mutant construction and overexpression of the respective candidates failed. Possibly, changes in the expression level of these global mRNA cleavage factors (Guerrier-Takada *et al.*, 1983; Morishita *et al.*, 1999; Altman *et al.*, 2005) might be deleterious to the cell. In fact, deletion of the *rne* gene is lethal for *E. coli* (Ono and Kuwano, 1979) and *Y. pseudotuberculosis* (only *rne* dominant-negative mutant is viable).

4.1.3. Interplay of YmoA and CsrA determines CsrC levels

Decreased CsrC levels in the *Y. pseudotuberculosis ymoA* mutant could be partially overcome by CsrA overexpression, but not *vice versa*, indicating that CsrA is located downstream of YmoA and is required for full CsrC integrity. The RNA-binding protein CsrA is crucial for CsrC (and CsrB) synthesis and stability in *Y. pseudotuberculosis* (Böhme, unpublished data; Heroven *et al*., 2012a). This is also true for other species like *Erwinia* (Chatterjee and Cui, 2002)*, Pseudomonas* (Sorger-Domenigg *et al.*, 2007) and *Salmonella* (Fortune *et al.*, 2006). In contrast, the CsrA proteins from *E. coli*, *Vibrio* or *Legionella* do not exert a stabilizing effect on the cognate Csr-type RNA (Gudapaty *et al.*, 2001; Weilbacher *et al.*, 2003; Lenz *et al.*, 2005; Heroven *et al.*, 2012a). Instead, CsrA activates transcription of *csrB* and *csrC* in *E. coli* (Gudapaty *et al.*, 2001; Weilbacher *et al.*, 2003). Interestingly, CsrA was also found to be involved in transcriptional regulation of *csrC* in *Y. pseudotuberculosis.* This control takes place in a concentration-dependent manner, since a certain amount of CsrA is required for activation of *csrC* transcription. However, CsrA overexpression leads to transcriptional repression of *csrC*. Similarly, CsrA from *E. coli* stimulates *csrC* transcription, most probably by controlling the response regulator UvrY, rather than by stabilizing the transcript (Weilbacher *et al.*, 2003).

The hypothesis that YmoA might act via CsrA on the CsrC level was supported by the observation that YmoA modulates the intracellular CsrA level. Regulation of the Csr system is part of a complex autoregulatory circuit. Herein, the amount of free CsrA molecules is decisive for the precise regulation of the target mRNAs (Gudapaty *et al.*, 2001; Romeo *et al.*, 2013; Adamson and Lim, 2013). For instance, one third of cellular CsrA is bound by CsrB in *E. coli* but the total intracellular CsrA concentration exceeds the CsrA-binding capacity of CsrB. Therefore, the CsrB and CsrC levels determine the quantity of active CsrA (Gudapaty *et al.*, 2001). Accordingly, changes in the intracellular CsrA level require prompt compensation. Slight variations of endogenous CsrA concentration, as provoked by loss of *ymoA*, might in turn have dramatic effects on the whole autoregulatory circuit and may contribute to the YmoA-mediated CsrC control. A balanced CsrA level in the cell seems to be very important to maintain cellular processes, as either *csrA* deletion or overexpression causes pleiotropic effects (e.g. growth defect, attenuated virulence) in *Y. pseudotuberculosis.* Moreover, as depicted by microarray analysis, a huge number of genes is differentially regulated in a *csrA*

mutant strain (Heroven, unpublished data). In *E. coli* and *V. cholerae* loss of *csrA* is lethal for the bacteria due to excessive glycogen levels (Romeo *et al.*, 1993; Timmermans and Van Melderen, 2009). Further, analysis to unravel the YmoA-mediated control of CsrA synthesis indicated that YmoA is not involved in transcriptional regulation of *csrA*. Moreover, CsrA mRNA levels remained unaffected by loss of *ymoA.*

As seen from previous microarray data (Tab. S 2), YmoA affects the expression of several chaperone molecules that are involved in proper protein folding (Heroven, unpublished data). In the *ymoA* mutant strain these molecules are deregulated, which may result in improper folding of a certain amount of CsrA proteins. However, protein stability assays revealed that the stability of CsrA protein remained unaffected in a *ymoA* mutant.

Concluding, YmoA does not seem to control CsrA synthesis on the transcriptional, post-transcriptional (via modulation of mRNA stability) or post-translational level. Consequently, a putative involvement of YmoA in *csrA* translation initiation or translation efficiency was assumed. Manifold mechanisms and structures have been identified that alter bacterial translation. Mainly the 5'-UTR that harbours the SD sequence is to be mentioned within this context (Nakamoto, 2009). 5'-UTRs form secondary structures, that provide binding sites for small regulatory RNAs or RNA-binding proteins, which alter stability or translation of the mRNA (Chen *et al.*, 1991; Agaisse and Lereclus, 1996; Geissmann *et al.*, 2009; Babitzke *et al.*, 2009). Moreover, riboswitches or thermosensors that undergo conformational changes upon ligand-binding or temperature-shifts are important control elements with regard to protein translation (Winkler, 2005; Kortmann and Narberhaus, 2012; Serganov and Nudler, 2013). However, no strong differences in *csrA* translation became apparent using CsrA translational reporter fusions in a *ymoA* mutant in comparison to the wildtype control (Fig. 3.7).

Most recently the 3'-UTRs, which make up intrinsic transcriptional terminator sequences, were assigned as translational control elements (Kawano *et al.*, 2005; Chao *et al.*, 2012). Particularly the 3'-UTR of the *Staphylococcus aureus* IcaR mRNA harbours an anti-SD sequence, which base-pairs to the SD sequence of its own 5'-UTR and consequently inhibits ribosome loading (Ruiz de los Mozos *et al.*, 2013). Since the present CsrA translation studies were conducted by means of different *csrA'-'lacZ* promoter fusions, regulatory events implicating base pairing of 5'- and 3'-UTR cannot be reflected by this analytical method.

Thus, it might be possible that formation of such a terminator complex is favoured in absence of *ymoA* due to indirect stabilizing effects.

Moreover, many of the small and large ribosomal subunits are deregulated in a *ymoA* mutant (Heroven and Böhme, unpublished data), probably evoking an imbalance of the translation machinery. The YmoA homologue Hha from *E. coli* was shown to repress transcription of rare codon tRNAs (García-Contreras *et al.*, 2008). However, type I fimbrial expression and hence biofilm formation are biased towards rare codon usage and Hha-mediated depletion of rare codon tRNAs represses fimbrial expression and biofilm formation. Whether YmoA influences processes that are associated with rare codon usage in *Y. pseudotuberculosis,* remains to be shown.

The impact of YmoA on endogenous CsrA levels seems to be a minor effect, since CsrA levels are only slightly reduced. In contrast, loss of *ymoA* elicits a considerable effect on the intracellular CsrC levels. However, as seen from microarray analysis, YmoA is a global regulator that affects more than 400 genes (Heroven and Böhme, unpublished data). For instance, loss of *ymoA* leads to dramatic growth defects and bears an avirulent phenotype in the mouse model of infection (Böhme, unpublished data). Considering these observations, it seems feasible that unspecific effects provoked by loss of *ymoA* might lead to decreased CsrA levels.

Most recently, it has been reported that in addition to the Csr-type RNAs other RNAs and also proteins are able to counteract CsrA function. In *E. coli* the McaS RNA depicts another CsrA antagonist, which bears two distinct CsrA-binding sites in exposed stem-loop regions. It acts independently from CsrB or CsrC and efficiently controls biofilm formation when CsrB is absent (Jørgensen *et al.*, 2013). In this context it might be possible that a small RNA is upregulated in the *ymoA* mutant strain, which might sequester CsrA proteins. Another mechanism implies a highly abundant mRNA transcript, which competes for CsrA-binding. The FimAICDHF mRNA from *S. typhimurium,* encoding for type I fimbriae, possesses several CsrA-binding sites in its 5'-UTR that sequester intracellular CsrA proteins. This is a very uncommon mechanism since mRNA expression levels are usually considerably lower than ncRNA levels. Strikingly, levels of the FimAICDHF 5'-UTR even exceed intracellular CsrB and CsrC levels. Therefore, the main function of this mRNA is to control CsrA activity rather than controlling expression of the plasmid-encoded type I fimbrial proteins (Sterzenbach *et al.*, 2013). Recently, the first protein opponent of CsrA was described: the flagellar assembly

factor FliW from *Bacillus subtilis.* FliW associates with flagellin (Hag) in response to high cytoplasmic flagellin levels, while Hag mRNA translation is repressed by CsrA-binding to the SD sequence. Upon export of flagellin, CsrA is sequestered by FliW (partner-switching of FliW), thereby releasing the Hag mRNA for translation (Yakhnin *et al.*, 2007; Mukherjee *et al.*, 2011). Upregulation of such RNA elements or other regulatory factors that are present in a *ymoA* deficient strain and are able to sequester CsrA protein, could be responsible for the reduced stability of CsrC. This might also explain why the CsrC RNA is highly unstable in a *csrA* mutant background (half-life ~11 min), while its stability is reduced to a lesser extent in a *ymoA* mutant (half-life ~46 min) (Böhme, 2010).

Concluding, YmoA-mediated CsrC stabilization is an indirect process, in which even YmoA-H-NS heterodimers do not exhibit CsrC-binding capacity. Data propose that YmoA might repress RNA-degrading enzymes, like ribonuclease P, which in turn govern CsrC turnover. Alternatively, YmoA could activate RNA chaperone molecules that protect CsrC RNA from degradation. In consideration of slightly decreased CsrA levels in a *ymoA* deficient strain, an imbalance of the total CsrA amount might have pleiotropic effects on various cellular processes, finally leading to reduced CsrC stability. Herein, YmoA could mediate proper folding of the CsrC RNA, which allows CsrA-binding to the Csr-type RNA, thereby stabilizing the transcript. Another scenario could describe the up-regulation of a CsrA antagonist (e.g. protein or RNA) in a *ymoA* mutant strain that sequesters CsrA from the Csr-type RNAs, rendering them more accessible to RNA-degrading enzymes.

4.2. Identification and characterization of RovC - a new virulence-associated factor of *Y. pseudotuberculosis*

Genomic studies and experimental approaches revealed that almost all Csr/Rsm systems encompass more than one Csr/Rsm RNA (Lenz *et al.*, 2005; Kulkarni *et al.*, 2006; Lapouge *et al.*, 2008). Especially *Vibrio cholerae* and *Pseudomonas fluorescence* possess three different Csr-type RNAs (Lenz *et al.*, 2005; Kay *et al.*, 2005). For several species it was shown that these ncRNAs can complement for one another (Cui *et al.*, 1996; Weilbacher *et al.*, 2003; Lenz *et al.*, 2005), whereas this was not the case in *Y. pseudotuberculosis.* This pathogen harbours at least two Csr-type RNAs, CsrB and CsrC, that seem to be differentially regulated and might serve diverse functions accordingly. For instance, Crp controls CsrB expression via repression of the UvrY response regulator of the BarA/UvrY TCS (Heroven *et al.*, 2012b), while not much is known about CsrC control. Previous analysis in our group indicate that Crp, Hfq and YmoA indirectly activate CsrC. Herein, Crp exerts indirect positive effects on CsrC via CsrB, which most presumably arises due to the counter-regulation of both RNAs and a second CsrB-indepentend activation (Heroven *et al.*, 2012b). The RNA chaperone Hfq indirectly stimulates *csrC* expression on the transcriptional level, while YmoA indirectly mediates CsrC stabilization (Böhme, unpublished data). This study describes the identification and characterization of an additional CsrC regulator.

4.2.1. RovC - a new regulator of *Y. pseudotuberculosis* CsrC RNA

Screening of a genomic library of *Y. pseudotuberculosis* for additional CsrC regulators revealed a hypothetical protein (YPK_3567) that was found to control *csrC* expression and was designated as regulator of virulence associated with CsrC (RovC). Within this work, the novel factor was confirmed to be a protein that encompasses 247 amino acids and is highly conserved among *Y. pestis* and *Y. pseudotuberculosis*. However, it does not exhibit homology to any known protein or even contains a conserved DNA-binding domain. Furthermore, RovC overexpression lead to significant repression of *csrC* transcription, while deletion of this factor promoted increased expression of a transcriptional *csrC-lacZ* reporter fusion and elevated CsrC levels in the cell. So far, it is unclear whether RovC exerts a direct effect on CsrC, as attempts to overproduce and purify RovC protein for DNA-binding studies failed. RovC-dependent expression of known Csr-type RNA regulators such as Crp, UvrY, Hfq and

CsrA did not show any effect. Herein, the only exception was CsrB, whose transcription was repressed upon loss of *rovC*. This effect can be caused by the counter-regulation of both RNAs as described by Heroven *et al*. (2008). Deletion of *rovC* exerts minor effects on the Csr downstream genes *rovM, rovA* and *invA,* whereas RovC overexpression leads to dramatic changes in the endogenous RoM, RovA and invasin levels, as RovA and hence invasin are only barely detectable in a *rovC*$^{+}$ strain. Interestingly, RovC overexpression exhibited a much more pronounced effect on endonenous RovM, RovA and InvA as on the CsrC levels, which suggests that RovC might affect RovM, RovA and InvA also independently from the Csr-cascade.

Concluding, these results indicate that RovC might constitute an important additional regulator that controls the abundance of the CsrC RNA and therefore might affect the level of free CsrA molecules in response to certain environmental conditions, which in turn affect the early virulence genes.

4.2.2. Expression control of *rovC*

The overall amount of RovC seems to be very low under laboratory growth conditions, as the RovC mRNA and the endogenous RovC protein were barely detectable via northern and western blotting. RovC is maximally synthesized at 25°C during stationary growth, while it is basally expressed at 25°C and 37°C in the exponential phase. Moreover, no effect on *rovC* expression was seen upon host cell contact or during growth at different pH values. RovC is not autoregulated and growth under nutrient limitation does not alter its expression pattern. *csrC* is maximally expressed during the late stationary phase at 25°C and is mainly affected by the composition of the growth medium. This Csr-type RNA exerts low levels in minimal medium while it is highly activated in complex medium such as LB (Heroven *et al.*, 2008). Recently, Crp and UvrY were shown to be indirectly involved in *csrC* expression control (Heroven *et al.*, 2012b). However, neither Crp nor UvrY contribute to CsrC regulation in response to the nutrient-availability. As shown in this study, even RovC does also not participate in this nutrient-dependent control of CsrC, but it might be involved in the temperature- and growth phase-dependent regulation.

Interestingly, only basal expression of *rovC* was reported in an *E. coli* background, implicating that RovC is not only a *Yersinia*-specific factor, but might also require a *Yersinia*-specific activator. Nevertheless, negative regulators that were found to control *rovC* synthesis are

also present in *E. coli:* the nucleoid-associated protein YmoA, the cAMP receptor protein Crp and the global regulator CsrA (reviewed in Fig. 4.1).

Loss of *ymoA* leads to increased *rovC* expression and elevated RovC protein levels. However, YmoA overexpression revealed a positive effect on *rovC* transcription and translation. During stationary growth at 25°C endogenous YmoA levels are very low (compare Fig. 3.4). Introduction of a midi-copy *ymoA*$^{+}$ plasmid leads to highly increased YmoA synthesis in comparison to the wildtype, challenging the cell with a dramatic imbalance of this particular protein. Since YmoA represents a global regulator, it might exhibit unspecific effects e.g. it could titrate the transcriptional regulator H-NS, hence manipulating its target recognition pattern. So far, the impact of H-NS on *rovC* expression remains elusive and will be subject of future analysis. Regarding the YmoA-dependent *rovC* expression, data highlight the importance of the *rovC* 5'-UTR (nucleotides +1 to +25 rel. to TSS): loss of 25 nt within the *rovC* upstream region abolished YmoA-mediated repression of the reporter fusion and suggests a transcriptional effect. Herein, YmoA (possibly in association with H-NS) might block RNA-polymerase-binding by occupying the DNA-duplex downstream of the transcriptional start site, like it was proposed for the *yscW-lcrF* transcript in *Y. pseudotuberculosis* (Böhme *et al.*, 2012). Moreover, YmoA-mediated post-transcriptional effects, like discussed previously for CsrC, might be reasonable to be implicated in *rovC* expression.

Under glucose-limiting conditions cAMP-Crp complexes bind their target DNA an thus control gene expression in response to the nutrient availability (Gunasekera *et al.*, 1992; Saier, 1998; Zheng *et al.*, 2004). Recently, a tight connection of the cAMP-Crp regulatory system and the Csr system was shown to link carbon metabolism and *Yersinia* virulence (Heroven *et al.*, 2012b). Accordingly, Crp activates *csrB* transcription via repression of the response regulator UvrY. Resulting from the counter-regulation of both Csr-type RNAs, *csrC* expression is abolished in a *crp* mutant strain. As shown in the present study, loss of *crp* leads to highly increased *rovC* expression, which is reflected by elevated levels of RovC mRNA and endogenous protein. Most interestingly, only the transcriptional fusions could be fully complemented by Crp overexpression. Contrary, the translational fusion was only partially complemented. Furthermore, loss of *crp* also leads to highly increased CsrB levels (Heroven *et al.*, 2012b). The highly abundant CsrB RNA might sequester the bulk CsrA molecules, which in turn derepresses *rovC* transcription and translation and might also

explain why Crp overexpression only partially complements the phenotype. To test whether the Crp-mediated impact on *rovC* expression depends on CsrA, epistasis studies should be performed. In the case that Crp operates independently of CsrA, Crp overexpression in a *csrA* mutant background should repress *rovC* transcription.

In general, Crp could function as transcriptional repressor of *rovC*. The Crp consensus sequence is described as TGTGA-N_6-TCACA (Kolb *et al.*, 1993; Busby and Ebright, 1999). The first consensus (TGTGA) of this region is found 141 nt upstream of the transcriptional start site of *rovC*, while the second half comprises CAACC instead of TCACA and hence differs from the proposed binding site. Nevertheless, it was shown for *Y. pestis* that Crp directly interacts with the promoter region of the *sycO-ypkA-ypoJ* operon and represses its transcription. Herein, two binding sites were determined: one binding region was located immediately downstream of the -10 region and did not exhibit any similarity to the proposed consensus region (AATGATAGATATCACCGT), while at least the sequence of the 5'-end of the second site is in agreement with the Crp consensus sequence (TGTGATTAACTCAACC) (Zhan *et al.*, 2009). This region overlapped with the translational start site of the operon. According to these data, it might be plausible that Crp directly represses *rovC* transcription but prospective experimental evidence is indispensable.

Both proteins, YmoA and Crp exert an effect on the *rovC* 5'-UTR. Most interestingly, the environmental control (e.g. temperature) of RovC synthesis was only reflected by the translational fusion (Fig. 3.21), which stresses the implication of post-transcriptional RovC control processes. Indeed, loss of *clpP* and *lon* proteases resulted in decreased RovC protein levels. In *Y. pseudotuberculosis* ClpP and Lon proteases control the temperature-dependent degradation of YmoA at 37°C (Böhme *et al.*, 2012), and could thereby contribute to the YmoA-mediated influence on RovC levels.

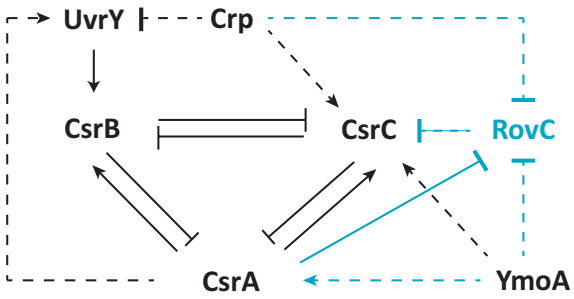

Fig. 4.1 Putative connection of CsrC regulatory factors in *Y. pseudotuberculosis*
Dashed lines = indirect regulation, solid lines = direct interactions, bars = repression, arrows = activation, blue colour represents connections indentified in this work.

4.2.3. CsrA exerts dual level control on *rovC*

Besides YmoA and Crp, CsrA seems to be the most important regulator of RovC. Interestingly, CsrA bears both, transcriptional and post-transcriptional effects on *rovC* expression in *Y. pseudotuberculosis*. Upon loss of *csrA,* highly increased RovC mRNA levels and protein concentrations were denoted. CsrA is known to act via binding to its target mRNA thus influencing translation and/or stability of the mRNA (Romeo, 1998). Target recognition involves CsrA-binding to unpaired nucleotides (Schubert *et al.*, 2007). Since unpaired regions are typical features of RNA secondary structures and are not found in DNA duplexes, it is unlikely that CsrA directly affects *rovC* transcription. Nonetheless, CsrA-mediated transcriptional effects on other components of the Csr system have been reported previously. Weilbacher *et al.* (2003) revealed a positive transcriptional effect of CsrA on *csrC* in *E. coli,* which did not involve CsrA-mediated RNA stabilization. So far, the underlying mechanism is unknown but is likely to occur indirectly.

In addition to transcriptional repression, CsrA prevents *rovC* translation as the translational *rovC'-'lacZ* fusion was strongly repressed upon CsrA overexpression. *In vitro* gel shift assays indicate a direct interaction between CsrA and the RovC upstream region (5'-UTR plus 36 nt of *rovC* coding region). Fig. 4.2 represents two distinct secondary structure predictions of the used *in vitro* transcribed RovC RNA (+1 to +75 nt rel. to the transcriptional start site). *In silico* analysis predict a *rovC* secondary structure, which possesses a base-paired ribosomal binding site. This would indicate that CsrA-binding to the GGA motif within the Shine-Dalgarno (SD) sequence is not possible. However, both predicted structures bear one accessible GGA motif, either in close proximity to the upstream or downstream site of the SD sequence. With regard to this structure, one would assume that CsrA binds first to the exposed GGA motifs and has no access to the GGA motif within the SD sequence.

Recent studies in *P. aeruginosa,* which harbours the CsrA homologue RsmE, could show that RsmE protein dimers bind to their RsmZ sRNA target (homologue to CsrB) in a sequential, specific and cooperative manner (Duss, 2012; Duss *et al*., 2013). The model shows that initial RsmE-binding leads to conformational changes in the RNA secondary structure, which then provides the structural basis for additional RsmE-binding. A related mechanism is proposed for RsmE-binding to the *hcnA* 5'-UTR in *P. fluorescence* (Schubert *et al.*, 2007) and CsrA-binding to the *glgC* 5'-upstream region in *E. coli* (Mercante *et al.*, 2009).

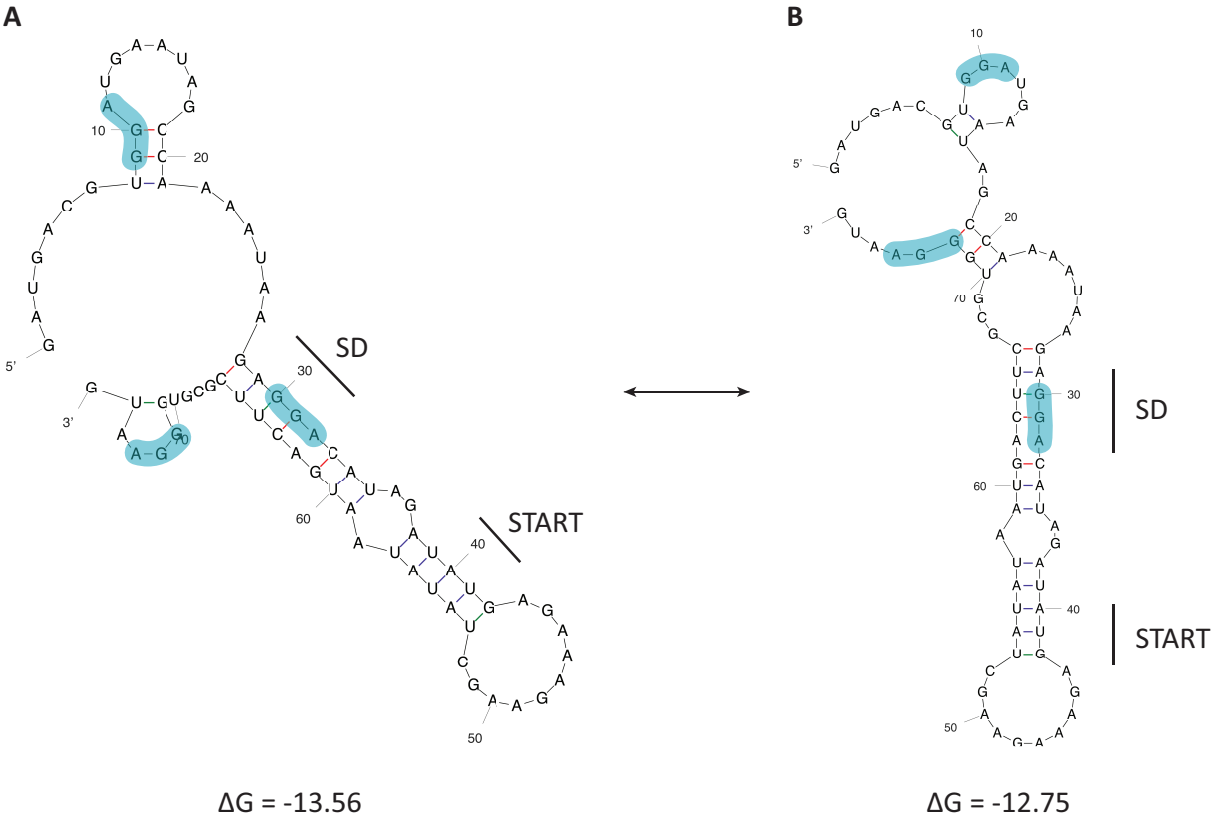

Fig. 4.2 Schematic representation of the RovC mRNA upstream region
The Mfold program (Zuker, 2003) was used to predict the secondary structure of the RovC upstream region. The two most probable predictions with the lowest free energy (ΔG) are shown. The Shine-Dalgarno sequence (SD) and the AUG start codon (START) are marked. GGA motifs are highlighted in blue. Numbers indicate the nucleotides relative to the *rovC* transcriptional start site.

RsmE-binding to HcnA implies additional GGA motifs in the SD upstream region. When these GGA sequences are tightly gripped by RsmE, they fold into a loop structure that is fixed by a 3 base-pair stem (Schubert *et al.*, 2007). GGA motifs upstream the *glgC* SD sequence represent a high affinity CsrA-binding site that mediates CsrA-binding to the low-affinity binding site within the SD (Mercante *et al.*, 2009). Both experiments demonstrate initial CsrA-binding events at the terminal GGA motif, that provoke conformational changes in the RNA secondary structure to render the SD sequence accessible for the second RsmE/CsrA-binding surface. Sequential CsrA-binding, leading to changes in the RNA secondary structure, might also be involved in RovC-CsrA interactions. Initial RsmE/CsrA-binding usually requires a high-affinity binding-site (see Fig. 1.4) with a sequence motif of 5'-$^{A}/_{U}$CANGGANG$^{U}/_{A}$-3', that is located upstream of the SD sequence (Schubert *et al.*, 2007). Strikingly, the 5'-terminal GGA motif of RovC exhibits a nearly perfect high-affinity RsmE/CsrA-binding site (as proposed by Schubert *et al.*, 2007), emphasizing the discussed hypothesis of CsrA-RovC

interaction. The importance of the 5'-GGA motif is further stressed by the translational *rovC'-'lacZ* fusion, which exhibits strong CsrA dependency, but lacks the downstream GGA motif. Accordingly, the GGA motif located downstream of the SD is supposed to play a minor role during CsrA-RovC interaction. Besides the sequential binding that goes along with structural rearrangements of the RNA, CsrA dimers preferentially bind to recognition sites that are interspersed by ≥18 nt (Mercante *et al.*, 2009). Notably, the GGA motif in close proximity to the 5'-end of the RovC upstream region provides optimal spacing of exactly 18 nt to the SD site and further supports the involvement of conformational changes upon initial CsrA-binding to the first recognition site.

CsrA-binding to the SD sequence of target transcripts usually destabilizes the messenger, e.g. *pgaABCD* and *glgC* mRNA in *E. coli* (Baker *et al.*, 2002; Pannuri *et al.*, 2011). In contrast, RovC mRNA stability assays indicate destabilization of the RovC mRNA when CsrA is absent. In exceptional cases CsrA-binding promotes protection of the 5'-end from RNase E-mediated cleavage and stabilizes the transcript (Yakhnin *et al.*, 2013). In particular, CsrA-binding to the extreme 5'-end of the *flhDC* leader RNA occupies RNase E cleavage sites (AU-rich sequence) and confers protection from this ribonuclease. *In silico* modelling of the RovC upstream region reveals a single stranded AU-rich sequence (+20 to +30 nt) that might constitute a putative RNase E target site (Fig. 4.2) CsrA-binding could render this target site inaccessible for RNase E-mediated cleavage, leading to transcript stabilization. Translation of the *rovC* transcript is highly increased in absence of CsrA. Despite of representing RNase E cleavage sites, AU-rich sequences in the 5'-UTRs of mRNAs also represent target sites for the ribosomal protein S1 (Arnold *et al.*, 1998). In this context a high degree of mRNA occupancy by ribosomes in the 5'-UTR represents a physical hindrance of RNase E-binding and protects the messenger from degradation (Arnold *et al.*, 1998; Komarova *et al.*, 2002; Komarova *et al.*, 2005). In the presence of CsrA, ribosomes could be replaced by the homodimer leading to translational blockage (as seen with the translational reporter fusion). Whether CsrA-binding to RovC mRNA really leads to degradation or is protective still needs to be elucidated. However, with regard to the binding model presented above and the strong CsrA-mediated repressional impact on the translational *rovC'-'lacZ* fusion, it seems likely that CsrA-binding to the RovC mRNA blocks translation.

Taken together, the *rovC* expression analysis with regard to the three regulators YmoA, Crp and CsrA represents an interconnected network that is involved in fine-tuning the *csrC*

expression level (Fig. 4.1). As shown in this study, YmoA exerts a slightly negative effect on CsrA. CsrA in turn is highly important for CsrC integrity and strongly represses *rovC* transcription and translation. Also, Crp might directly interact with the *rovC* promoter region, leading to transcriptional repression. Moreover, Crp might act indirectly on *rovC* expression by modulating the cellular CsrB levels (via UvrY). Loss of *crp* leads to dramatic increases in CsrB concentration, which might in turn sequester CsrA proteins from RovC RNA, relieving the repressional effect. All these connections might resemble an interdependency of the four regulators that are all involved in maintaining CsrC levels in the cell and hence tightly control the global Csr system.

4.2.4. RovC is required for T6SS activation

Expression analysis of RovC revealed a very limited transcript and protein abundance in the *Y. pseudotuberculosis* YPIII wildtype strain under standard growth conditions (complex medium, 25°C, stationary growth). The strongest influence of RovC was observed upon overproduction e.g. on the Csr-RovM-RovA cascade. Nevertheless, microarray analysis, comparing the transcriptome of the *Yersinia* wildtype and its isogenic *rovC* mutant, identified a relatively small regulon of 54 RovC-activated genes, indicating that even a low *rovC* expression suffices to induce target gene expression. Among the 56 differentially regulated genes only two were repressed by RovC (a holin-family protein and one 4-oxalocrotonate tautomerase family enzyme). No impact was denoted for proteins belonging to the flagella, motility or chemotaxis apparatus of the cell or the stress adaptation machineries. Differential expression of some ribosomal proteins was denoted in a *rovC* mutant strain, which was accompanied by upregulation of distinct genes that are involved in amino acid metabolism and energy production. Also, RovC regulates proteins involved in cell wall biogenesis. For instance, RovC activates the *ompA* gene that encodes for a porin, which is required for diffusion of small solutes, plays a role as phage receptor molecule, maintains the structural integrity of the bacterial cell and mediates host cell attachment of *E. coli* (Wang, 2002; Shin *et al.*, 2005; Sandrini *et al.*, 2013).

Most remarkably, the present data show that RovC is not only a repressor of CsrC but is further an activator of the type VI secretion system T6SS4 in *Y. pseudotuberculosis*. Recently, type VI secretion systems have been discovered as versatile nanomachines, which structurally resemble the puncturing device of bacteriophages. Bacterial T6SS comprise five

major building blocks: I) a contractile tail sheath, which is anchored to the inner membrane by II) a base plate and III) a TssJLM complex, IV) a tail tube and V) a spike - the puncturing device at the tail tube tip (Ho *et al.*, 2014) (Fig. 4.3).

Hcp (haemolysin coregulated protein) and VgrG (valine-glycine repeat G) are well-characterized structureal and functional components of the secretion apparatus. As this sophisticated nanomachine guides protein export and delivery into target cells, a rapid conformational change of the sheath structure propels the T6SS spike and tube components (Hcp/VgrG) out of the cell to target both, pro- and eukaryotes. Effector translocation leads to cytoskeletal rearrangements and cell death in eukaryotes (e.g. macrophages, HeLa cells), while it kills other Gram-negative bacteria, highlighting the importance of this organelle in competition with the host microbiota and the host cells themselves (Filloux *et al.*, 2008; Ma *et al.*, 2009; Hood *et al.*, 2010; Ma and Mekalanos, 2010; Russell *et al.*, 2011; Filloux, 2013; Ho *et al.*, 2014).

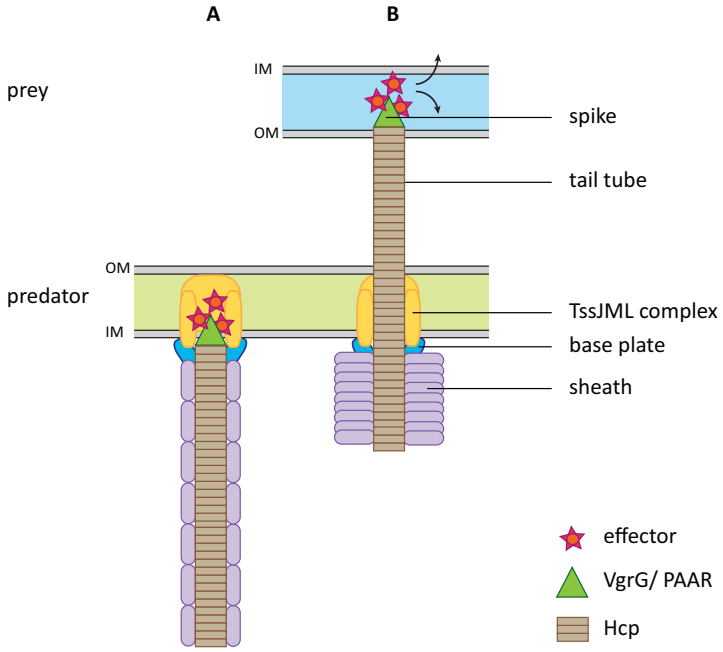

Fig. 4.3 Structural components of the T6SS
Similarly to the architecture of bacteriophage T4, bacterial type VI secretion systems (T6SSs) are composed of a contractile sheath, which is anchored to the bacterial inner (IM) and outer membrane (OM) by the base-plate and the TSSJLM complex. Initially the tail sheath is extended (**A**) but upon structural rearrangement the contractile sheath propels the tail tube across the two membranes, injecting the spike along with antibacterial and antieukaryotic effector molecules into the target cell (prey) (**B**). In comparison to the T4 machinery the bacterial T6SS is mechanistically inverted since it punctures the cell (predator) from the inside to deliver effector proteins, modified from Ho *et al.* (2014).

T6SS are found throughout the genomes of most Gram-negative organisms such as plant, animal and human pathogens as well as soil and environmental isolates (Bernard *et al.*,

2010). Comparative genome analysis in *Yersinia* revealed the presence of four complete and two incomplete T6SS loci (T6SS1-T6SS6) in *Y. pseudotuberculosis* YPIII (Zhang *et al.*, 2011). The four complete clusters are composed of 13 core components as defined by Boyer *et al.* (2009), and are organized in huge operons and possibly serve different functions in dependence on the surrounding conditions (Bingle *et al.*, 2008; Pukatzki *et al.*, 2009). The T6SS4 belongs to a special cluster that is unique in *Y. pestis* (YPO0499-YPO0516 or y3658-y3677) and *Burkholderia spp* in concern of sequence and organization homologies (Zhang *et al.*, 2011). In contrast to the other T6SS clusters found in *Yersinia*, it appears to be controlled from a single promoter and is strongly influenced by the surrounding temperature (Han *et al.*, 2004; Cathelyn *et al.*, 2006; Pieper *et al.*, 2009).

Interestingly, RovC is genetically linked to the T6SS4 of *Y. pseudotuberculosis* as it is located immediately downstream of the T6SS4 operon in the opposite direction (see Fig.3.17). Expression analyses of the T6SS4 indicated a temperature-dependent regulation. T6SS4 is expressed at 25°C but not at elevated temperatures like 37°C. This is in-line with the findings that RovC is maximally induced at moderate temperatures and hence can activate expression of its associated T6SS4 operon. This thermally controlled synthesis has also been observed by other groups (Zhang *et al.*, 2011; Zhang *et al.*, 2013). Additionally, they could demonstrate that the effector protein Hcp is released, indicating that T6SS4 is not only expressed but also functional at 25°C.

As previously mentioned, Hcp is the hallmark of a functional T6SS. Hcp orthologs are found throughout the organisms that carry T6SS gene clusters and seem to be crucial structural components on the one hand and vital effectors with regard to bacterial virulence (Pukatzki *et al.*, 2009). For instance, the human pathogen *Burkholderia pseudomallei,* defective for *hcp,* reveals an attenuated phenotype in the mouse model of infection (Hopf *et al.*, 2014). Most strikingly, *hcp* expression is 20-fold reduced in a Δ*rovC* background (see Tab. 3.1), whereas the remaining T6SS genes are affected to a lesser extent. This might point towards post-transcriptional modifications (e.g. separation of distinct mRNAs by RNases), as all genes of this operon are transcribed as one polycistronic RNA. With regard to bacterial virulence the precise role of the Hcp protein has not been described yet and will be subject of future analysis. However, deletion of the T6SS4 locus reduced the uptake of *Y. pestis* by macrophages proposing a phagocytosis promoting function (Robinson *et al.*, 2009). Nonetheless, as suggested by Gueguen and co-workers, expression of T6SS4 might be

beneficial to *Y. pseudotuberculosis* YPIII in the environmental reservoir or during competition with the gut-microbiota rather than in the mammalian host.

Previous studies reported that the T6SS4 of YPIII can be activated by AHL-dependent quorum-sensing and exposure to an acidic environment (Zhang *et al.*, 2011; Zhang *et al.*, 2013). This is in contrast to the data presented here, as no inducing effect was seen on T6SS4 expression in different quorum-sensing mutant strains or upon exposure to an acidic environment. Discrepancies to these studies may arise from the used reporter fusions: Zhang *et al*. made use of long reporter fusions, that harboured 674 nt of the T6SS4 (YPK_3566) upstream region (instead of 503 nt as used in this study). Probably, regulatory elements implicated in the AHL-dependent quorum-sensing and pH control are situated in these additional 171 nt.

Although the overall architecture and structural components of T6SSs are well conserved among the different species, their functionality and regulation is multifaceted and adopted to the specialised needs of the particular organism and its biological niche. To reduce the energetic costs that go along with assembly, contraction and disassembly of the organelle in response to the diverse stimuli, T6S is tightly controlled on the transcriptional and post-transcriptional level (Mougous *et al.*, 2007; Kitaoka *et al.*, 2011). Since many T6SS represent horizontally acquired genetic elements, repression by histone-like proteins (e.g. H-NS) is not surprising as members of this family control the expression of foreign DNA elements (Lucchini *et al.*, 2006). For instance, the T6SS of *P. putida* is regulated by the H-NS analogue TurA (Renzi *et al.*, 2010). Moreover, regulation by quorum-sensing, involvement of transcription factors and two-component systems, alternative sigma factors and small non-coding RNAs as well as phosphorylation processes that switch between an active and inactive state of these multiprotein complexes contribute to T6SS regulation (Bernard *et al.*, 2010; Gueguen *et al.*, 2013). The latter post-transcriptional control mechanism was found in *P. aeruginosa*. Here, the whole secretion system switches between a resting and an activate state. The core scaffolding protein Fha is activated upon phosphorylation and drives effector release, while dephosphorylation events shut the system down (Mougous *et al.*, 2007).

Most recently, Gueguen *et al.* (2013) showed that the *Y. pseudotuberculosis* YPIII T6SS4 is directly activated by OmpR in response to envelope stress. OmpR is the response regulator of the two-component system OmpR/EnvZ that responds to a variety of stresses including osmotic and envelope stress (Mizuno and Mizushima, 1990). Strikingly, three different

OmpR-binding sites within the upstream region of the first gene encoded in the T6SS4 operon were predicted by *in silico* analysis (Gueguen *et al.*, 2013). Binding of purified OmpR protein to all three sites was confirmed by gel mobility shift assays, highlighting OmpR as a direct transcriptional regulator of this T6SS cluster (Gueguen *et al.*, 2013; Zhang *et al.*, 2013). Strikingly, two of the three OmpR-binding sites overlap either with the *rovC*-coding region or with its cognate promoter region (see Fig. 4.4 O1+O2).

Presence of OmpR-binding sites within the 5'-UTR and coding region of *rovC* might participate in control of RovC gene expression or in RovC-dependent T6SS4 regulation. Deletion of the *rovC* gene included deletion of the first OmpR-binding site in the coding region and resulted into loss of T6SS4 expression. However, RovC overproduction from a plasmid that harbours *rovC* under control of its own promoter could activate T6SS4 expression. Interestingly, two of the OmpR-binding sites (O1 and O3) act as activating elements, while OmpR-binding to the O2 region repressed T6SS4 activity. Accordingly, a connection between OmpR and RovC might be possible.

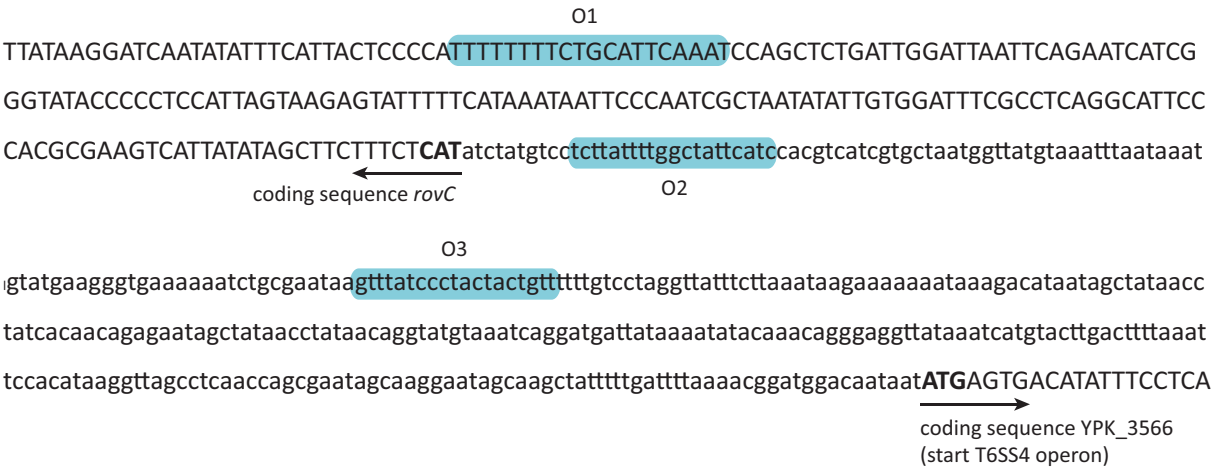

Fig. 4.4 Upstream region of the T6SS4 harbours three OmpR-binding sites
The upstream region of the first T6SS4 gene (YPK_3566) encompasses three different OmpR-binding sites (O1-O3), highlighted in blue. Bold CAT indicates the start codon of the *rovC* gene that is transcribed in opposite direction to the T6SS. Bold ATG highlights the translational start site of the first gene within the T6SS4 cluster. Capital letters represent coding regions; small letters reflect the intergenic region.

Both, OmpR and RovC, confer thermoregulation that activates T6SS at moderate temperatures. So far, nothing is known about the interplay of the two factors. Most interestingly, the T6SS4-*lacZ* reporter fusions harbour a shorter upstream region than those implemented by Zhang *et al*. (2011; 2013). The additional 171 nt that are present in the T6SS4-*lacZ* fusion from Zhang and co-workers harbour the first OmpR-binding site (O1) and were responsive to an acidic environment and AHL-dependent quorum-sending, indicating

that this OmpR-binding site might be important for integration of these environmental stimuli. This shows that multiple transcription factors are likely to be involved in T6SS control. In *V. cholerae* for instance, *hcp* transcription is modulated by the TetR-like protein HpaR in association with quorum-sensing regulators and by the HlyU transcription factor (Williams *et al.*, 1996; Ishikawa *et al.*, 2009).

In a nutshell, RovC was discovered as transcriptional repressor of CsrC, that affects the downstream genes *rovM*, *rovA* and *invA* via the Csr cascade. Furthermore, RovC activates expression of the type VI secretion system T6SS4, which might be beneficial during environmental survival of the bacteria or during competition with the host microbiota.

RovC itself is expressed at moderate temperatures and tightly controlled by Crp, YmoA and CsrA - all factors that govern the Csr system. The RNA-binding protein CsrA directly interacts with the RovC 5'-UTR to administer its turnover and indirectly controls its transcription. Further, ClpP and Lon proteases direct RovC protein homeostasis. The explicit RovC working-model is summarized in Fig. 4.5.

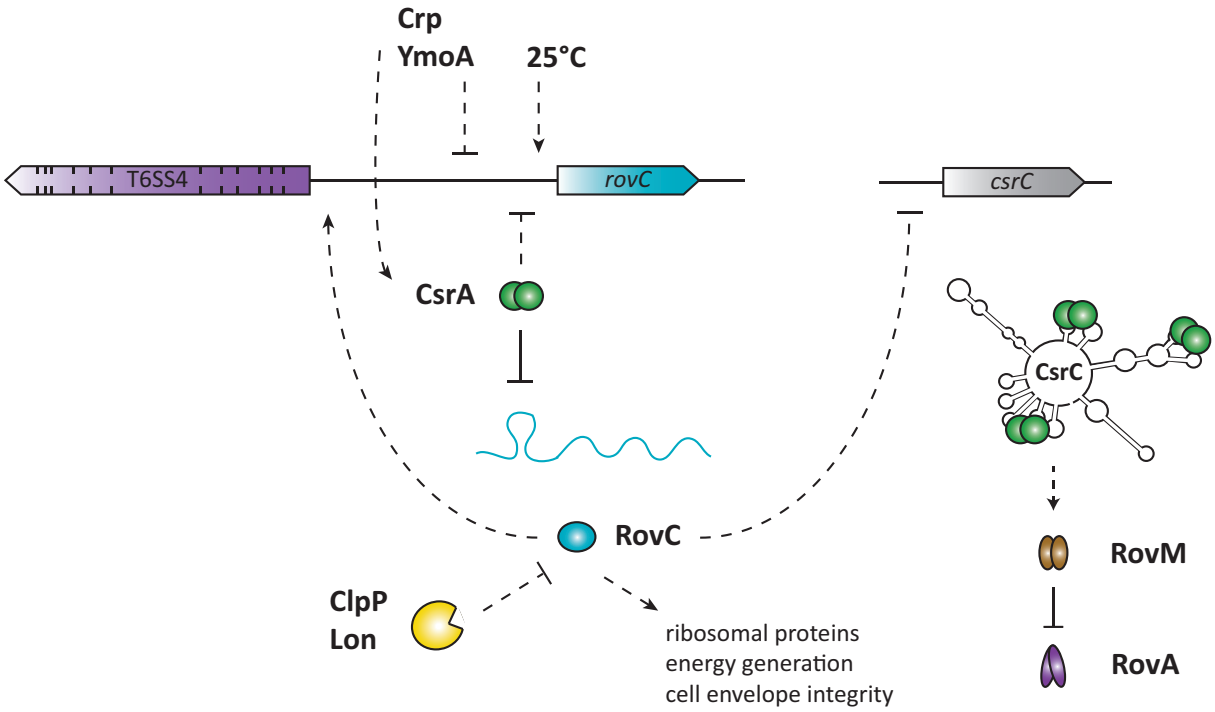

Fig. 4.5 Working-model of *rovC* regulation
At 25°C *rovC* expression is governed by the concerted action of the regulators YmoA, Crp and CsrA. YmoA most presumably acts via indirect mechanisms on *rovC* transcription, while Crp could directly interact with the *rovC* promoter region. CsrA exhibits a dual-level control: it indirectly represses transcription and most likely directly interferes with translation. Elevated RovC levels lead to transcriptional repression of *csrC* and finally abolish RovA synthesis. Moreover, RovC activates expression of the T6SS4 and controls synthesis of ribosomal proteins, energy generation processes and cell envelope integrity. Finally ClpP and Lon proteases maintain cellular RovC levels.

5. Outlook

As shown in the present work, YmoA-mediated stabilization of the Csr-type RNA CsrC involves several different regulatory factors. Herein, YmoA represses chaperone molecules that could stabilize the mRNA of RNA-degrading enzymes as well as ribonucleases like RNase P that control RNA turnover. Therefore, clean deletion mutants of these factors should be generated to perform CsrC stability assays. Further, double mutants lacking *ymoA* and the respective RNA degrading factor could be supportive to understand the connection between YmoA and these factors. In addition to RNA degrading factors, YmoA slightly diminishes the level of endogenous CsrA protein that is instantly required for CsrC stabilization. The explicit underlying mechanism of YmoA-mediated CsrA repression is not yet fully understood and will be subject to future analysis. For example, highly sensitive experimental procedures, like radioactive pulse-chase experiments to determine the translation rate and protein degradation of CsrA in the *ymoA* mutant will help to unravel the fundamental molecular basics. Moreover, YmoA-dependent modifications of the CsrA 5'-UTR or 3'-UTR should be investigated.

Furthermore, this work identified the protein RovC as transcriptional repressor of *csrC* and activator of the *Y. pseudotuberculosis* type VI secretion system T6SS4. Since RovC does not show any homology to known proteins neither in its sequence nor in its protein domains, structure resolution by means of crystallization attempts will help to gain more information about the potential function of this protein. In this context, RovC protein expression and purification needs to be optimized. This is also necessary to perform DNA EMSA experiments to unravel whether RovC binds directly to the promoter regions of *csrC* or the T6SS4.

Crp was found to repress *rovC* transcription. To elucidate, if Crp directly interacts with the *rovC* promoter region, DNA EMSA studies should be performed. In case of an indirect mechanism, epistasis studies with *csrA crp* double mutants will be conducted to monitor a putative hierarchy or interdependency of the two regulators.

YmoA seems to exert a transcriptional effect on *rovC*, which might be associated with H-NS. As discussed previously, both proteins might form a repression complex that interferes with *rovC* expression. Therefore, the impact of H-NS on *rovC* transcription and translation should be evaluated by gene expression analysis, and further completed by YmoA-H-NS DNA EMSA studies.

Moreover, RovC RNA stability assays should be performed in a *csrA* mutant to elucidate the underlying mechanism of CsrA-mediated RovC mRNA stabilization. Herein, deletion or mutation of the GGA motifs in the *rovC* upstream region or within the SD sequence will be valuable. To monitor if and how the three factors are connected, epistasis studies are required.

Expression analyses indicate that both, RovC and the T6SS4 are thermoregulated and are maximally expressed at 25°C. With regard to various environmental parameters that were shown to activate T6SS4, expression of this system seems to be beneficial outside the host rather than in the inside. Therefore, the implication of conditions that resemble the natural reservoir of yersiniae could be investigated with regard to lower temperatures like 17°C or 4°C. Functional analysis of the T6SS4 including clean knock-out mutants of the ATPase components of the secretion apparatus or deletion of functional and structural components like Hcp, will monitor their role during environmental survival. Moreover, the T6SS4 homologue from *Y. pestis* exhibited a phagocytosis promoting effect, which could be relevant for proliferation and survival strategies within the host tissue. Functional analysis in macrophage cell lines should help to clarify this hypothesis in *Y. pseudotuberculosis*.

To see whether the functional linkage of RovC and the T6SS4 is specific, the impact of RovC on the remaining three type VI secretion systems needs to be addressed by gene expression analysis and DNA EMSA studies.

OmpR was previously shown to activate transcription of T6SS4. Interestingly, OmpR-binding sites are located in the upstream and coding region of *rovC*, giving rise to the assumption that both factors might either be connected or differentially regulate each other. Gene expression analysis and epistasis studies will shed light into this observation.

Microarray analysis were performed with a *rovC* mutant strain and revealed a straightforward set of differentially regulated genes. As the present work clearly shows, RovC overproduction leads to profound phenotypes. Therefore, it is reasonable to perform an additional microarray that makes use of RovC overproduction to identify novel targets that are repressed by RovC.

BLAST analysis revealed unique conservation of RovC in *Yersinia spp.* Since expression of *rovC* was repressed in *E. coli*, introduction of a *Y. pseudotuberculosis* YPIII gene library into *E. coli* harbouring a *rovC'-'lacZ* fusion is valuable to identify *Yersinia*-specific activators of *rovC* expression.

The most promising project, which was launched recently in this group, screens for inhibitory compounds that target CsrA expression. CsrA is an excellent drug-target, since its homologues are conserved among the *Enterobacteriaceae,* implementing a broad target spectrum. Moreover, *csrA* mutant strains bear a significant growth defect and exhibit an avirulent phenotype in the mouse model of infection. In this context, RovC represents a valuable read-out system, as CsrA exerts a strong and direct repression on this factor. Consequently, CsrA inhibitory compounds induce *rovC* expression, which is easily detectable by optical *rovC*-reporter fusions (e.g. *lacZ* or *luxCDABE*).

6. Summary

The carbon storage regulator (Csr) system plays a central role during the host adaptation of *Yersinia pseudotuberculosis* and coordinates virulence gene expression in response to the metabolic state of the cell. It is composed of the RNA-binding protein CsrA whose activity is antagonized by non-coding RNAs CsrB and CsrC. Levels of the Csr-type RNAs are pivotal for the availability of active CsrA, as they sequester the RNA-binding protein from its target mRNA rendering it inactive. *Y. pseudotuberculosis* mutants lacking *csrA* exhibit an avirulent phenotype in the mouse model of infection, rendering the Csr system a valid target for drug development.

The *Yersinia* modulator A (YmoA) changes the composition of the whole system, as it controls the stability of the CsrC RNA. The present work clearly demonstrates that the stabilizing effect is not mediated via direct YmoA-CsrC interaction. In fact, YmoA represses several factors that are involved in RNA turnover, e.g. RNA chaperones DnaK-DnaJ-GrpE and GroEL-GroES as well as ribonucleases like RNase P. Moreover, YmoA-mediated repression of CsrA levels might also contribute to the CsrC stability control.

Identification of further factors that are implicated in CsrC control was accomplished by means of a genetic screening approach. Herein, the regulator of virulence associated with CsrC (RovC) was identified as transcriptional repressor of CsrC. Additionally, RovC activates the expression of the virulence-associated type VI secretion system T6SS4 in response to moderate temperatures.

Expression of *rovC* is thermoregulated and tightly controlled by Crp, YmoA and CsrA, which also regulate the Csr system. Crp and YmoA repress *rovC* transcription, whereas Crp might directly interact with the *rovC* promoter region. CsrA interacts directly with the RovC upstream region to inhibit translation and indirectly represses its transcription.

In conclusion, YmoA-mediated CsrC stabilization is an indirect process that involves downregulation of RNA degrading enzymes and partial repression of endogenous CsrA levels. Moreover, CsrC is controlled by RovC, which represses *csrC* transcription. Expression of *rovC* is in turn modulated by Crp, YmoA and CsrA, stressing the complex and multi-layered regulation of the Csr system.

7. References

Achtman, M., Zurth, K., Morelli, G., Torrea, G., Guiyoule, A., and Carniel, E. (1999) Yersinia pestis, the cause of plague, is a recently emerged clone of Yersinia pseudotuberculosis. *Proc Natl Acad Sci U S A* **96**: 14043–14048.

Adamson, D.N., and Lim, H.N. (2013) Rapid and robust signaling in the CsrA cascade via RNA-protein interactions and feedback regulation. *Proc Natl Acad Sci U S A* **110**: 13120–5.

Agaisse, H., and Lereclus, D. (1996) STAB-SD: a Shine-Dalgarno sequence in the 5' untranslated region is a determinant of mRNA stability. *Mol Microbiol* **20**: 633–43.

Altman, S. (2011) Ribonuclease P. *Philos Trans R Soc Lond B Biol Sci* **366**: 2936–41.

Altman, S., Wesolowski, D., Guerrier-Takada, C., and Li, Y. (2005) RNase P cleaves transient structures in some riboswitches. *Proc Natl Acad Sci U S A* **102**: 11284–11289.

Amit, R., Oppenheim, A.B., and Stavans, J. (2003) Increased bending rigidity of single DNA molecules by H-NS, a temperature and osmolarity sensor. *Biophys J* **84**: 2467–2473.

Anderson, D.M., Ramamurthi, K.S., Tam, C., and Schneewind, O. (2002) YopD and LcrH regulate expression of Yersinia enterocolitica YopQ by a posttranscriptional mechanism and bind to yopQ RNA. *J Bacteriol* **184**: 1287–95.

Arnold, T.E., Yu, J., and Belasco, J.G. (1998) mRNA stabilization by the ompA 5' untranslated region: two protective elements hinder distinct pathways for mRNA degradation. *RNA* **4**: 319–30.

Atkinson, S., Throup, J.P., Stewart, G.S., and Williams, P. (1999) A hierarchical quorum-sensing system in Yersinia pseudotuberculosis is involved in the regulation of motility and clumping. *Mol Microbiol* **33**: 1267–1277.

Autenrieth, I.B., and Firsching, R. (1996) Penetration of M cells and destruction of Peyer's patches by Yersinia enterocolitica: an ultrastructural and histological study. *J Med Microbiol* **44**: 285–294.

Babitzke, P., Baker, C.S., and Romeo, T. (2009) Regulation of translation initiation by RNA binding proteins. *Annu Rev Microbiol* **63**: 27–44.

Babitzke, P., and Romeo, T. (2007) CsrB sRNA family: sequestration of RNA-binding regulatory proteins. *Curr Opin Microbiol* **10**: 156–63.

Baker, C.S., Eöry, L. a, Yakhnin, H., Mercante, J., Romeo, T., and Babitzke, P. (2007) CsrA inhibits translation initiation of Escherichia coli hfq by binding to a single site overlapping the Shine-Dalgarno sequence. *J Bacteriol* **189**: 5472–81.

Baker, C.S., Morozov, I., Suzuki, K., Romeo, T., and Babitzke, P. (2002) CsrA regulates glycogen biosynthesis by preventing translation of glgC in Escherichia coli. *Mol Microbiol* **44**: 1599–1610.

Balligand, G., Laroche, Y., and Cornelis, G. (1985) Genetic analysis of virulence plasmid from a serogroup 9 Yersinia enterocolitica strain: role of outer membrane protein P1 in resistance to human serum and autoagglutination. *Infect Immun* **48**: 782–786.

Ballister, E.R., Lai, A.H., Zuckermann, R.N., Cheng, Y., and Mougous, J.D. (2008) In vitro self-assembly of tailorable nanotubes from a simple protein building block. *Proc Natl Acad Sci U S A* **105**: 3733–8.

Banos, R.C., Pons, J.I., Madrid, C., Juarez, A., Baños, R.C., and Juárez, A. (2008) A global modulatory role for the Yersinia enterocolitica H-NS protein. *Microbiology* **154**: 1281–1289.

Barnes, P.D., Bergman, M.A., Mecsas, J., and Isberg, R.R. (2006) Yersinia pseudotuberculosis disseminates directly from a replicating bacterial pool in the intestine. *J Exp Med* **203**: 1591–1601.

Bernard, C.S., Brunet, Y.R., Gueguen, E., and Cascales, E. (2010) Nooks and crannies in type VI secretion regulation. *J Bacteriol* **192**: 3850–60.

Bingle, L.E., Bailey, C.M., and Pallen, M.J. (2008) Type VI secretion: a beginner's guide. *Curr Opin Microbiol* **11**: 3–8.

Birnboim, H.C., and Doly, J. (1979) Rapid alkaline extraction procedure for screening recombinant plasmid DNA. *Nucleic Acids Res* **7**: 15–23.

Blädel, I., Wagner, K., Beck, A., Schilling, J., Alexander Schmidt, M., and Heusipp, G. (2013) The H-NS protein silences the pyp regulatory network of Yersinia enterocolitica and is involved in controlling biofilm formation. *FEMS Microbiol Lett* **340**: 41–48.

Bliska, J.B., and Black, D.S. (1995) Inhibition of the Fc receptor-mediated oxidative burst in macrophages by the Yersinia pseudotuberculosis tyrosine phosphatase. *Infect Immun* **63**: 681–685.

Bockemuhl, J., and Roggentin, P. (2004) [Intestinal yersiniosis. Clinical importance, epidemiology, diagnosis, and prevention]. *Bundesgesundheitsblatt Gesundheitsforsch Gesundheitsschutz* **47**: 685–691.

Boer, E. de, Zwartkruis-Nahuis, J.T., and Lesuis, R. (2008) [Prevalence of human pathogenic Yersinia enterocolitica in pigs]. *Tijdschr Diergeneeskd* **133**: 938–941.

Böhme, K. (2010) Identification and characterization of regulatory factors and regulatory RNA elements controlling the expression of the primary invasion factors invasin and YadA in Yersinia pseudotuberculosis. .

Böhme, K., Steinmann, R., Kortmann, J., Seekircher, S., Heroven, A.K., Berger, E., *et al.* (2012) Concerted actions of a thermo-labile regulator and a unique intergenic RNA thermosensor control Yersinia virulence. *PLoS Pathog* **8**: e1002518.

Boland, A., and Cornelis, G.R. (1998) Role of YopP in suppression of tumor necrosis factor alpha release by macrophages during Yersinia infection. *Infect Immun* **66**: 1878–1884.

Bolin, I., Norlander, I., Wolf-Watz, H., and I Bölin, L.N. (1982) Temperature-inducible outer membrane protein of Yersinia pseudotuberculosis and Yersinia enterocolitica is associated with the virulence plasmid. *Infect Immun* **37**: 506–512.

Bottone, E.J. (1997) Yersinia enterocolitica: the charisma continues. *Clin Microbiol Rev* **10**: 257–276.

Boyer, F., Fichant, G., Berthod, J., Vandenbrouck, Y., and Attree, I. (2009) Dissecting the bacterial type VI secretion system by a genome wide in silico analysis: what can be learned from available microbial genomic resources? *BMC Genomics* **10**: 104.

Bradford, M.M. (1976) A rapid and sensitive method for the quantitation of microgramm quantities of protein utilizing the prinziple of protein-dye binding. *Anal Biochem* **72**: 248–254.

Brennan, R.G., and Link, T.M. (2007) Hfq structure, function and ligand binding. *Curr Opin Microbiol* **10**: 125–33.

Brescia, C.C., Kaw, M.K., and Sledjeski, D.D. (2004) The DNA binding protein H-NS binds to and alters the stability of RNA in vitro and in vivo. *J Mol Biol* **339**: 505–514.

Brubaker, R.R. (1991) Factors promoting acute and chronic diseases caused by yersiniae. *Clin Microbiol Rev* **4**: 309–324.

Busby, S., and Ebright, R.H. (1999) Transcription activation by catabolite activator protein (CAP). *J Mol Biol* **293**: 199–213.

Bustin, S.A., Benes, V., Nolan, T., and Pfaffl, M.W. (2005) Quantitative real-time RT-PCR--a perspective. *J Mol Endocrinol* **34**: 597–601.

Butler, T. (2013) Plague gives surprises in the first decade of the 21st century in the United States and worldwide. *Am J Trop Med Hyg* **89**: 788–93.

Calvin, N.M., and Hanawalt, P.C. (1988) High-efficiency transformation of bacterial cells by electroporation. *J Bacteriol* **170**: 2796–801.

Carniel, E., Autenrieth, I., Cornelis, G., Fukushima, H., Guinet, F., Isberg, R., Pham, J., Prentice, M., Simonet, M., Skurnik, M. and Wauters, G. (2006) Y. enterocolitica and Y. pseudotuberculosis. In *Prokaryotes*. pp. 270–398.

Carpousis, A.J. (2007) The RNA degradosome of Escherichia coli: an mRNA-degrading machine assembled on RNase E. *Annu Rev Microbiol* **61**: 71–87.

Carrier, T.A., and Keasling, J.D. (1999) Library of synthetic 5' secondary structures to manipulate mRNA stability in Escherichia coli. *Biotechnol Prog* **15**: 58–64.

Casadaban, M.J., and Cohen, S.N. (1980) Analysis of gene control signals by DNA fusion and cloning in Escherichia coli. *J Mol Biol* **138**: 179–207.

Cathelyn, J.S., Crosby, S.D., Lathem, W.W., Goldman, W.E., and Miller, V.L. (2006) RovA, a global regulator of Yersinia pestis, specifically required for bubonic plague. *Proc Natl Acad Sci U S A* **103**: 13514–13519.

Cathelyn, J.S., Ellison, D.W., Hinchliffe, S.J., Wren, B.W., and Miller, V.L. (2007) The RovA regulons of Yersinia enterocolitica and Yersinia pestis are distinct: evidence that many RovA-regulated genes were acquired more recently than the core genome. *Mol Microbiol* **66**: 189–205.

Chain, P.S.G., Carniel, E., Larimer, F.W., Lamerdin, J., Stoutland, P.O., Regala, W.M., *et al.* (2004) Insights into the evolution of Yersinia pestis through whole-genome comparison with Yersinia pseudotuberculosis. *Proc Natl Acad Sci U S A* **101**: 13826–13831.

Chang, A.C., and Cohen, S.N. (1978) Construction and characterization of amplifiable multicopy DNA cloning vehicles derived from the P15A cryptic miniplasmid. *J Bacteriol* **134**: 1141–1156.

Chao, Y., Papenfort, K., Reinhardt, R., Sharma, C.M., and Vogel, J. (2012) An atlas of Hfq-bound transcripts reveals 3' UTRs as a genomic reservoir of regulatory small RNAs. *EMBO J* **31**: 4005–19.

Chatterjee, A.K., and Cui, Y. (2002) RsmA and the quorum-sensing signal, N-[3-oxohexanoyl]-L-homoserine lactone, control the levels of rsmB RNA in Erwinia carotovora subsp. carotovora by affecting its stability. *J Bacteriol* **184**: 4089–4095.

Chavez, R.G., Alvarez, A.F., Romeo, T., and Georgellis, D. (2010) The physiological stimulus for the BarA sensor kinase. *J Bacteriol* **192**: 2009–2012.

Chen, L.H., Emory, S.A., Bricker, A.L., Bouvet, P., and Belasco, J.G. (1991) Structure and function of a bacterial mRNA stabilizer: analysis of the 5' untranslated region of ompA mRNA. *J Bacteriol* **173**: 4578–4586.

Cimdins, A., Roßmanith, J., Langklotz, S., Bandow, J.E., and Narberhaus, F. (2013) Differential control of Salmonella heat shock operons by structured mRNAs. *Mol Microbiol* **89**: 715–731.

Cornelis, G.R. (1998) The Yersinia Yop virulon, a bacterial system to subvert cells of the primary host defense. *Folia Microbiol (Praha)* **43**: 253–261.

Cornelis, G.R. (2002a) The Yersinia Ysc-Yop virulence apparatus. *Int J Med Microbiol* **291**: 455–462.

Cornelis, G.R. (2002b) The Yersinia Ysc-Yop "type III" weaponry. *Nat Rev Mol Cell Biol* **3**: 742–752.

Cui, Y., Madi, L., Mukherjee, A., Dumenyo, C.K., and Chatterjee, A.K. (1996) The RsmA- mutants of Erwinia carotovora subsp. carotovora strain Ecc71 overexpress hrpNEcc and elicit a hypersensitive reaction-like response in tobacco leaves. *Mol Plant Microbe Interact* **9**: 565–573.

Dame, R.T., Luijsterburg, M.S., Krin, E., Bertin, P.N., Wagner, R., and Wuite, G.J.L. (2005) DNA bridging: a property shared among H-NS-like proteins. *J Bacteriol* **187**: 1845–1848.

Datsenko, K.A., and Wanner, B.L. (2000) One-step inactivation of chromosomal genes in Escherichia coli K-12 using PCR products. *Proc Natl Acad Sci U S A* **97**: 6640–6645.

Denecker, G., Tötemeyer, S., Mota, L.J., Troisfontaines, P., Lambermont, I., Youta, C., *et al.* (2002) Effect of low- and high-virulence Yersinia enterocolitica strains on the inflammatory response of human umbilical vein endothelial cells. *Infect Immun* **70**: 3510–3520.

Dersch, P., and Isberg, R.R. (1999) A region of the Yersinia pseudotuberculosis invasin protein enhances integrin-mediated uptake into mammalian cells and promotes self-association. *EMBO J* **18**: 1199–1213.

Dillon, S., Sasagawa, T., Crawford, A., Prestidge, J., Inder, M.K., Jerram, J., *et al.* (2007) Resolution of cervical dysplasia is associated with T-cell proliferative responses to human papillomavirus type 16 E2. *J Gen Virol* **88**: 803–813.

Doetsch, M., Schroeder, R., and Fürtig, B. (2011) Transient RNA-protein interactions in RNA folding. *FEBS J* **278**: 1634–42.

Dorman, C.J., Hinton, J.C., and Free, A. (1999) Domain organization and oligomerization among H-NS-like nucleoid-associated proteins in bacteria. *Trends Microbiol* **7**: 124–128.

Dower, W.J., Miller, J.F., and Ragsdale, C.W. (1988) High efficiency transformation of E. coli by high voltage electroporation. *Nucleic Acids Res* **16**: 6127–45.

Drummond, N., Murphy, B.P., Ringwood, T., Prentice, M.B., Buckley, J.F., and Fanning, S. (2012) Yersinia enterocolitica: a brief review of the issues relating to the zoonotic pathogen, public health challenges, and the pork production chain. *Foodborne Pathog Dis* **9**: 179–89.

Dubey, A.K., Baker, C.S., Romeo, T., and Babitzke, P. (2005) RNA sequence and secondary structure participate in high-affinity CsrA-RNA interaction. *RNA* **11**: 1579–1587.

Dubey, A.K., Baker, C.S., Suzuki, K., Jones, A.D., Pandit, P., Romeo, T., and Babitzke, P. (2003) CsrA regulates translation of the Escherichia coli carbon starvation gene, cstA, by blocking ribosome access to the cstA transcript. *J Bacteriol* **185**: 4450–4460.

Duss, O.P. (2012) Assembly, 70 kDa solution structure and mechanism of action of the bacterial non-coding RNA RsmZ in complex with the global regulatory protein RsmE. .

Eitel, J., and Dersch, P. (2002) The YadA protein of Yersinia pseudotuberculosis mediates high-efficiency uptake into human cells under environmental conditions in which invasin is repressed. *Infect Immun* **70**: 4880–4891.

Ellison, D.W., and Miller, V.L. (2006) H-NS represses inv transcription in Yersinia enterocolitica through competition with RovA and interaction with YmoA. *J Bacteriol* **188**: 5101–5112.

Ellison, D.W., Young, B., Nelson, K., and Miller, V.L. (2003) YmoA negatively regulates expression of invasin from Yersinia enterocolitica. *J Bacteriol* **185**: 7153–7159.

Emory, S.A., Bouvet, P., and Belasco, J.G. (1992) A 5'-terminal stem-loop structure can stabilize mRNA in Escherichia coli. *Genes Dev* **6**: 135–148.

Fairman, J.W., Dautin, N., Wojtowicz, D., Liu, W., Noinaj, N., Barnard, T.J., *et al.* (2012) Crystal structures of the outer membrane domain of intimin and invasin from enterohemorrhagic E. coli and enteropathogenic Y. pseudotuberculosis. *Structure* **20**: 1233–43.

Fallman, M., Andersson, K., Hakansson, S., Magnusson, K.E., Stendahl, O., Wolf-Watz, H., *et al.* (1995) Yersinia pseudotuberculosis inhibits Fc receptor-mediated phagocytosis in J774 cells. *Infect Immun* **63**: 3117–3124.

Fallman, M., and Gustavsson, A. (2005) Cellular mechanisms of bacterial internalization counteracted by Yersinia. *Int Rev Cytol* **246**: 135–188.

Filloux, A. (2013) The rise of the Type VI secretion system. *F1000Prime Rep* **5**.

Filloux, A., Hachani, A., and Bleves, S. (2008) The bacterial type VI secretion machine: yet another player for protein transport across membranes. *Microbiology* **154**: 1570–83.

Fortune, D.R., Suyemoto, M., and Altier, C. (2006) Identification of CsrC and characterization of its role in epithelial cell invasion in Salmonella enterica serovar Typhimurium. *Infect Immun* **74**: 331–9.

Fredriksson-Ahomaa, M., Stolle, A., and Stephan, R. (2007) Prevalence of pathogenic Yersinia enterocolitica in pigs slaughtered at a Swiss abattoir. *Int J Food Microbiol* **119**: 207–212.

García-Contreras, R., Zhang, X.-S., Kim, Y., and Wood, T.K. (2008) Protein translation and cell death: the role of rare tRNAs in biofilm formation and in activating dormant phage killer genes. *PLoS One* **3**: e2394.

Gay, P., Coq, D. Le, Steinmetz, M., Berkelman, T., and Kado, C.I. (1985) Positive selection procedure for entrapment of insertion sequence elements in gram-negative bacteria. *J Bacteriol* **164**: 918–921.

Geissmann, T., Marzi, S., and Romby, P. (2009) The role of mRNA structure in translational control in bacteria. *RNA Biol* **6**: 153–60.

Georgellis, D., Sohlberg, B., Hartl, F.U., and Gabain, A. von (1995) Identification of GroEL as a constituent of an mRNA-protection complex in Escherichia coli. *Mol Microbiol* **16**: 1259–1268.

Grainger, D.C., Hurd, D., Goldberg, M.D., and Busby, S.J.W. (2006) Association of nucleoid proteins with coding and non-coding segments of the Escherichia coli genome. *Nucleic Acids Res* **34**: 4642–52.

Grassl, G.A., Bohn, E., Müller, Y., Bühler, O.T., Autenrieth, I.B., Muller, Y., and Buhler, O.T. (2003) Interaction of Yersinia enterocolitica with epithelial cells: invasin beyond invasion. *Int J Med Microbiol* **293**: 41–54.

Groisman, E.A. (2001) The pleiotropic two-component regulatory system PhoP-PhoQ. *J Bacteriol* **183**: 1835–42.

Grützkau, A., Hanski, C., Hahn, H., Riecken, E.O., and Grutzkau, A. (1990) Involvement of M cells in the bacterial invasion of Peyer's patches: a common mechanism shared by Yersinia enterocolitica and other enteroinvasive bacteria. *Gut* **31**: 1011–1015.

Gudapaty, S., Suzuki, K., Wang, X., Babitzke, P., and Romeo, T. (2001) Regulatory interactions of Csr components: the RNA binding protein CsrA activates csrB transcription in Escherichia coli. *J Bacteriol* **183**: 6017–6027.

Gueguen, E., Durand, E., Zhang, X.Y., d'Amalric, Q., Journet, L., and Cascales, E. (2013) Expression of a Yersinia pseudotuberculosis Type VI Secretion System Is Responsive to Envelope Stresses through the OmpR Transcriptional Activator. *PLoS One* **8**: e66615.

Guerrier-Takada, C., Gardiner, K., Marsh, T., Pace, N., and Altman, S. (1983) The RNA moiety of ribonuclease P is the catalytic subunit of the enzyme. *Cell* **35**: 849–857.

Gunasekera, A., Ebright, Y.W., and Ebright, R.H. (1992) DNA sequence determinants for binding of the Escherichia coli catabolite gene activator protein. *J Biol Chem* **267**: 14713–14720.

Gutiérrez, P., Li, Y., Osborne, M.J., Pomerantseva, E., Liu, Q., and Gehring, K. (2005) Solution structure of the carbon storage regulator protein CsrA from Escherichia coli. *J Bacteriol* **187**: 3496–501.

Hamama, A., Marrakchi, A. el, and Othmani, F. el (1992) Occurrence of Yersinia enterocolitica in milk and dairy products in Morocco. *Int J Food Microbiol* **16**: 69–77.

Hamburger, Z.A., Brown, M.S., Isberg, R.R., and Bjorkman, P.J. (1999) Crystal structure of invasin: a bacterial integrin-binding protein. *Science (80-)* **286**: 291–295.

Han, Y., Zhou, D., Pang, X., Song, Y., Zhang, L., Bao, J., *et al.* (2004) Microarray analysis of temperature-induced transcriptome of Yersinia pestis. *Microbiol Immunol* **48**: 791–805.

Heise, T., and Dersch, P. (2006) Identification of a domain in Yersinia virulence factor YadA that is crucial for extracellular matrix-specific cell adhesion and uptake. *Proc Natl Acad Sci U S A* **103**: 3375–3380.

Herbst, K., Bujara, M., Heroven, A.K., Opitz, W., Weichert, M., Zimmermann, A., and Dersch, P. (2009) Intrinsic thermal sensing controls proteolysis of Yersinia virulence regulator RovA. *PLoS Pathog* **5**: e1000435.

Heroven, A.K., Bohme, K., and Dersch, P. (2012) The Csr/Rsm system of Yersinia and related pathogens: A post-transcriptional strategy for managing virulence. *RNA Biol* **9**.

Heroven, A.K., Bohme, K., Rohde, M., and Dersch, P. (2008) A Csr-type regulatory system, including small non-coding RNAs, regulates the global virulence regulator RovA of Yersinia pseudotuberculosis through RovM. *Mol Microbiol* **68**: 1179–1195.

Heroven, A.K., Bohme, K., Tran-Winkler, H., and Dersch, P. (2007) Regulatory elements implicated in the environmental control of invasin expression in enteropathogenic Yersinia. *Adv Exp Med Biol* **603**: 156–166.

Heroven, A.K., and Dersch, P. (2006) RovM, a novel LysR-type regulator of the virulence activator gene rovA, controls cell invasion, virulence and motility of Yersinia pseudotuberculosis. *Mol Microbiol* **62**: 1469–1483.

Heroven, A.K., Nagel, G., Tran, H.J., Parr, S., and Dersch, P. (2004) RovA is autoregulated and antagonizes H-NS-mediated silencing of invasin and rovA expression in Yersinia pseudotuberculosis. *Mol Microbiol* **53**: 871–888.

Heroven, A.K., Sest, M., Pisano, F., Scheb-Wetzel, M., Steinmann, R., Böhme, K., *et al.* (2012) Crp induces switching of the CsrB and CsrC RNAs in Yersinia pseudotuberculosis and links nutritional status to virulence. *Front Cell Infect Microbiol* **2**: 158.

Ho, B.T., Dong, T.G., and Mekalanos, J.J. (2014) A View to a Kill: The Bacterial Type VI Secretion System. *Cell Host Microbe* **15**: 9–21.

Hood, R.D., Singh, P., Hsu, F., Güvener, T., Carl, M.A., Trinidad, R.R.S., *et al.* (2010) A type VI secretion system of Pseudomonas aeruginosa targets a toxin to bacteria. *Cell Host Microbe* **7**: 25–37.

Hopf, V., Göhler, A., Eske-Pogodda, K., Bast, A., Steinmetz, I., and Breitbach, K. (2014) BPSS1504, a cluster 1 type VI secretion gene, is involved in intracellular survival and virulence of Burkholderia pseudomallei. *Infect Immun* .

Hughes, J.M. (2001) Emerging infectious diseases: a CDC perspective. *Emerg Infect Dis* **7**: 494–6.

Isberg, R.R., and Leong, J.M. (1990) Multiple β1 chain integrins are receptors for invasin, a protein that promotes bacterial penetration into mammalian cells. *Cell* **60**: 861–871.

Isberg, R.R., Voorhis, D.L., and Falkow, S. (1987) Identification of invasin: a protein that allows enteric bacteria to penetrate cultured mammalian cells. *Cell* **50**: 769–78.

Ishikawa, T., Rompikuntal, P.K., Lindmark, B., Milton, D.L., and Wai, S.N. (2009) Quorum sensing regulation of the two hcp alleles in Vibrio cholerae O1 strains. *PLoS One* **4**: e6734.

Itakura, K., Rossi, J.J., and Wallace, R.B. (1984) Synthesis and use of synthetic oligonucleotides. *Annu Rev Biochem* **53**: 323–56.

Jackson, M.W., Silva-Herzog, E., and Plano, G. V (2004) The ATP-dependent ClpXP and Lon proteases regulate expression of the Yersinia pestis type III secretion system via regulated proteolysis of YmoA, a small histone-like protein. *Mol Microbiol* **54**: 1364–78.

Janknecht, R., Martynoff, G. de, Lou, J., Hipskind, R.A., Nordheim, A., and Stunnenberg, H.G. (1991) Rapid and efficient purification of native histidine-tagged protein expressed by recombinant vaccinia virus. *Proc Natl Acad Sci U S A* **88**: 8972–6.

Jonas, K., and Melefors, O. (2009) The Escherichia coli CsrB and CsrC small RNAs are strongly induced during growth in nutrient-poor medium. *FEMS Microbiol Lett* **297**: 80–6.

Jones, C., Hachani, A., Manoli, E., and Filloux, A. (2014) An rhs Gene Linked to the Second Type VI Secretion Cluster Is a Feature of the Pseudomonas aeruginosa Strain PA14. *J Bacteriol* **196**: 800–10.

Jørgensen, M.G., Thomason, M.K., Havelund, J., Valentin-Hansen, P., and Storz, G. (2013) Dual function of the McaS small RNA in controlling biofilm formation. *Genes Dev* **27**: 1132–45.

Kapperud, G., Namork, E., and Skarpeid, H.J. (1985) Temperature-inducible surface fibrillae associated with the virulence plasmid of Yersinia enterocolitica and Yersinia pseudotuberculosis. *Infect Immun* **47**: 561–566.

Kawano, M., Reynolds, A.A., Miranda-Rios, J., and Storz, G. (2005) Detection of 5'- and 3'-UTR-derived small RNAs and cis-encoded antisense RNAs in Escherichia coli. *Nucleic Acids Res* **33**: 1040–50.

Kay, E., Dubuis, C., and Haas, D. (2005) Three small RNAs jointly ensure secondary metabolism and biocontrol in Pseudomonas fluorescens CHA0. *Proc Natl Acad Sci U S A* **102**: 17136–41.

Kirjavainen, V., Jarva, H., Biedzka-Sarek, M., Blom, A.M., Skurnik, M., and Meri, S. (2008) Yersinia enterocolitica serum resistance proteins YadA and ail bind the complement regulator C4b-binding protein. *PLoS Pathog* **4**: e1000140.

Kitaoka, M., Miyata, S.T., Brooks, T.M., Unterweger, D., and Pukatzki, S. (2011) VasH is a transcriptional regulator of the type VI secretion system functional in endemic and pandemic Vibrio cholerae. *J Bacteriol* **193**: 6471–82.

Kolb, A., Busby, S., Buc, H., Garges, S., and Adhya, S. (1993) Transcriptional regulation by cAMP and its receptor protein. *Annu Rev Biochem* **62**: 749–95.

Komarova, A. V., Tchufistova, L.S., Dreyfus, M., and Boni, I. V. (2005) AU-Rich Sequences within 5' Untranslated Leaders Enhance Translation and Stabilize mRNA in Escherichia coli. *J Bacteriol* **187**: 1344–1349.

Komarova, A. V., Tchufistova, L.S., Supina, E. V., and Boni, I. V. (2002) Protein S1 counteracts the inhibitory effect of the extended Shine-Dalgarno sequence on translation. *RNA* **8**: 1137–1147.

Kortmann, J., and Narberhaus, F. (2012) Bacterial RNA thermometers: molecular zippers and switches. *Nat Rev Microbiol* **10**: 255–65.

Kulkarni, P.R., Cui, X., Williams, J.W., Stevens, A.M., and Kulkarni, R. V (2006) Prediction of CsrA-regulating small RNAs in bacteria and their experimental verification in Vibrio fischeri. *Nucleic Acids Res* **34**: 3361–9.

la Cruz, F. de, Carmona, M., and Juaréz, A. (1992) The Hha protein from Escherichia coli is highly homologous to the YmoA protein from Yersinia enterocolitica. *Mol Microbiol* **6**: 3451–2.

Laemmli, U.K. (1970) Cleavage of structural proteins during the assembly of the head of bacteriophage T4. *Nature* **227**: 680–5.

Lapouge, K., Schubert, M., Allain, F.H.-T., and Haas, D. (2008) Gac/Rsm signal transduction pathway of gamma-proteobacteria: from RNA recognition to regulation of social behaviour. *Mol Microbiol* **67**: 241–53.

Lenz, D.H., Miller, M.B., Zhu, J., Kulkarni, R. V, and Bassler, B.L. (2005) CsrA and three redundant small RNAs regulate quorum sensing in Vibrio cholerae. *Mol Microbiol* **58**: 1186–202.

Liu, M.Y., Gui, G., Wei, B., Preston, J.F., Oakford, L., Yüksel, U., *et al.* (1997) The RNA molecule CsrB binds to the global regulatory protein CsrA and antagonizes its activity in Escherichia coli. *J Biol Chem* **272**: 17502–10.

Liu, M.Y., Yang, H., and Romeo, T. (1995) The product of the pleiotropic Escherichia coli gene csrA modulates glycogen biosynthesis via effects on mRNA stability. *J Bacteriol* **177**: 2663–72.

Lucchetti-Miganeh, C., Burrowes, E., Baysse, C., and Ermel, G. (2008) The post-transcriptional regulator CsrA plays a central role in the adaptation of bacterial pathogens to different stages of infection in animal hosts. *Microbiology* **154**: 16–29.

Lucchini, S., Rowley, G., Goldberg, M.D., Hurd, D., Harrison, M., and Hinton, J.C.D. (2006) H-NS mediates the silencing of laterally acquired genes in bacteria. *PLoS Pathog* **2**: e81.

Ma, A.T., McAuley, S., Pukatzki, S., and Mekalanos, J.J. (2009) Translocation of a Vibrio cholerae type VI secretion effector requires bacterial endocytosis by host cells. *Cell Host Microbe* **5**: 234–43.

Ma, A.T., and Mekalanos, J.J. (2010) In vivo actin cross-linking induced by Vibrio cholerae type VI secretion system is associated with intestinal inflammation. *Proc Natl Acad Sci U S A* **107**: 4365–70.

Madigan, M.T. and Martinko, J.M. (2006)**.** *Brock Biology of Microorganisms*, Eleventh E. Pearson Prentice Hall.

Madrid, C., Balsalobre, C., García, J., and Juárez, A. (2007) The novel Hha/YmoA family of nucleoid-associated proteins: use of structural mimicry to modulate the activity of the H-NS family of proteins. *Mol Microbiol* **63**: 7–14.

Madrid, C., Nieto, J.M., and Juárez, A. (2002) Role of the Hha/YmoA family of proteins in the thermoregulation of the expression of virulence factors. *Int J Med Microbiol* **291**: 425–32.

Mandel, M., and Higa, A. (1970) Calcium-dependent bacteriophage DNA infection. *J Mol Biol* **53**: 159–162.

Marra, A., and Isberg, R. (1997) Invasin-dependent and invasin-independent pathways for translocation of Yersinia pseudotuberculosis across the Peyer's patch intestinal epithelium. *Infect Immun* **65**: 3412–3421.

Martínez, L.C., Yakhnin, H., Camacho, M.I., Georgellis, D., Babitzke, P., Puente, J.L., and Bustamante, V.H. (2011) Integration of a complex regulatory cascade involving the SirA/BarA and Csr global regulatory systems that controls expression of the Salmonella SPI-1 and SPI-2 virulence regulons through HilD. *Mol Microbiol* **80**: 1637–56.

Mayer, O., Rajkowitsch, L., Lorenz, C., Konrat, R., and Schroeder, R. (2007) RNA chaperone activity and RNA-binding properties of the E. coli protein StpA. *Nucleic Acids Res* **35**: 1257–69.

McFeeters, R.L., Altieri, A.S., Cherry, S., Tropea, J.E., Waugh, D.S., and Byrd, R.A. (2007) The high-precision solution structure of Yersinia modulating protein YmoA provides insight into interaction with H-NS. *Biochemistry* **46**: 13975–82.

Mercante, J., Edwards, A.N., Dubey, A.K., Babitzke, P., and Romeo, T. (2009) Molecular geometry of CsrA (RsmA) binding to RNA and its implications for regulated expression. *J Mol Biol* **392**: 511–28.

Mercante, J., Suzuki, K., Cheng, X., Babitzke, P., and Romeo, T. (2006) Comprehensive alanine-scanning mutagenesis of Escherichia coli CsrA defines two subdomains of critical functional importance. *J Biol Chem* **281**: 31832–42.

Miller, J.H. (1972) *Experiments in molecular genetics, Cold Spring Harbor, NY: Cold Spring Harbour Laboratory Press.*

Miller, J.H. (1992) *A Short Course in Bacterial Genetics. Cold Spring Harbor, NY: Cold Spring Harbour Laboratory Press.*

Mizuno, T., and Mizushima, S. (1990) Signal transduction and gene regulation through the phosphorylation of two regulatory components: the molecular basis for the osmotic regulation of the porin genes. *Mol Microbiol* **4**: 1077–82.

Mondragón, A. (2013) Structural studies of RNase P. *Annu Rev Biophys* **42**: 537–57.

Morelli, G., Song, Y., Mazzoni, C.J., Eppinger, M., Roumagnac, P., Wagner, D.M., *et al.* (2010) Yersinia pestis genome sequencing identifies patterns of global phylogenetic diversity. *Nat Genet* **42**: 1140–3.

Morishita, R., Kawagoshi, A., Sawasaki, T., Madin, K., Ogasawara, T., Oka, T., and Endo, Y. (1999) Ribonuclease activity of rat liver perchloric acid-soluble protein, a potent inhibitor of protein synthesis. *J Biol Chem* **274**: 20688–92.

Mougous, J.D., Cuff, M.E., Raunser, S., Shen, A., Zhou, M., Gifford, C.A., *et al.* (2006) A virulence locus of Pseudomonas aeruginosa encodes a protein secretion apparatus. *Science* **312**: 1526–30.

Mougous, J.D., Gifford, C.A., Ramsdell, T.L., and Mekalanos, J.J. (2007) Threonine phosphorylation post-translationally regulates protein secretion in Pseudomonas aeruginosa. *Nat Cell Biol* **9**: 797–803.

Muffler, A., Fischer, D., and Hengge-Aronis, R. (1996) The RNA-binding protein HF-I, known as a host factor for phage Qbeta RNA replication, is essential for rpoS translation in Escherichia coli. *Genes Dev* **10**: 1143–1151.

Mukherjee, S., Yakhnin, H., Kysela, D., Sokoloski, J., Babitzke, P., and Kearns, D.B. (2011) CsrA-FliW interaction governs flagellin homeostasis and a checkpoint on flagellar morphogenesis in Bacillus subtilis. *Mol Microbiol* **82**: 447–61.

Nagel, G., Lahrz, a, and Dersch, P. (2001) Environmental control of invasin expression in Yersinia pseudotuberculosis is mediated by regulation of RovA, a transcriptional activator of the SlyA/Hor family. *Mol Microbiol* **41**: 1249–69.

Nakamoto, T. (2009) Evolution and the universality of the mechanism of initiation of protein synthesis. *Gene* **432**: 1–6.

Naktin, J., and Beavis, K.G. (1999) Yersinia enterocolitica and Yersinia pseudotuberculosis. *Clin Lab Med* **19**: 523–36, vi.

Neutra, M.R. (1999) M cells in antigen sampling in mucosal tissues. *Curr Top Microbiol Immunol* **236**: 17–32.

Nieto, J.M., Madrid, C., Miquelay, E., Parra, J.L., Rodríguez, S., Juárez, A., and Rodrı, S. (2002) Evidence for Direct Protein-Protein Interaction between Members of the Enterobacterial Hha / YmoA and H-NS Families of Proteins . *J Bacteriol* **184**:629-635.

Noom, M.C., Navarre, W.W., Oshima, T., Wuite, G.J.L., and Dame, R.T. (2007) H-NS promotes looped domain formation in the bacterial chromosome. *Curr Biol* **17**: R913–4.

NRC (1992) Microbial threats to health in the united states. *Natl Acadamies Press*.

NRC (2010) Infectious disease movement in a borderless world: workshop summary. *Natl Acadamies Press*.

Nuss, A.M., Schuster, F., Pisano, F., Heroven, A.K. and Dersch, P. (2014) A direct link between the global regulator PhoP and the Csr regulon in Y. pseudo¬tuberculosis through the small regulatory RNA CsrC. *Prep*.

Oellerich, M.F., Jacobi, C.A., Freund, S., Niedung, K., Bach, A., Heesemann, J., and Trülzsch, K. (2007) Yersinia enterocolitica infection of mice reveals clonal invasion and abscess formation. *Infect Immun* **75**: 3802–11.

Olekhnovich, I.N., and Kadner, R.J. (2007) Role of Nucleoid-Associated Proteins Hha and H-NS in Expression of Salmonella enterica Activators HilD, HilC, and RtsA Required for Cell Invasion. *J Bacteriol* **189**: 6882–6890.

Ono, M., and Kuwano, M. (1979) A conditional lethal mutation in an Escherichia coli strain with a longer chemical lifetime of messenger RNA. *J Mol Biol* **129**: 343–57.

Opitz, W. (2013) Cell contact-dependent virulence gene expression in Yersinia pseudotuberculosis. .

Oshima, T., Ishikawa, S., Kurokawa, K., Aiba, H., and Ogasawara, N. (2006) Escherichia coli histone-like protein H-NS preferentially binds to horizontally acquired DNA in association with RNA polymerase. *DNA Res* **13**: 141–53.

Osipiuk, J., Xu, X., Cui, H., Savchenko, A., Edwards, A., and Joachimiak, A. (2011) Crystal structure of secretory protein Hcp3 from Pseudomonas aeruginosa. *J Struct Funct Genomics* **12**: 21–6.

Paff, J.R. and Triplett, D.A. (1976) Clinical and laboratory aspects of Yersinia pseudotuberculosis infections, with a report of two cases. *Am J Clin Pathol* **66**: 101 – 10.

Pannuri, A., Yakhnin, H., Vakulskas, C.A., Edwards, A.N., Babitzke, P., and Romeo, T. (2011) Translational Repression of NhaR, a Novel Pathway for Multi-Tier Regulation of Biofilm Circuitry by CsrA. *J Bacteriol* **194**: 79–89.

Pederson, K.J., Carlson, S., and Pierson, D.E. (1997) The ClpP protein, a subunit of the Clp protease, modulates ail gene expression in Yersinia enterocolitica. *Mol Microbiol* **26**: 99–107.

Perry, R.D., and Fetherston, J.D. (1997) Yersinia pestis--etiologic agent of plague. *Clin Microbiol Rev* **10**: 35–66.

Peters, K.N., Dhariwala, M.O., Hughes Hanks, J.M., Brown, C.R., and Anderson, D.M. (2013) Early apoptosis of macrophages modulated by injection of Yersinia pestis YopK promotes progression of primary pneumonic plague. *PLoS Pathog* **9**: e1003324.

Pfaffl, M.W. (2001) A new mathematical model for relative quantification in real-time RT-PCR. *Nucleic Acids Res* **29**: e45.

Pieper, R., Huang, S.-T., Robinson, J.M., Clark, D.J., Alami, H., Parmar, P.P., *et al.* (2009) Temperature and growth phase influence the outer-membrane proteome and the expression of a type VI secretion system in Yersinia pestis. *Microbiology* **155**: 498–512.

Porath, J., Carlsson, J., Olsson, I., and Belfrage, G. (1975) Metal chelate affinity chromatography, a new approach to protein fractionation. *Nature* **258**: 598–9.

Pukatzki, S., McAuley, S.B., and Miyata, S.T. (2009) The type VI secretion system: translocation of effectors and effector-domains. *Curr Opin Microbiol* **12**: 11–7.

Quade, N., Mendonca, C., Herbst, K., Heroven, A.K., Ritter, C., Heinz, D.W., and Dersch, P. (2012) Structural basis for intrinsic thermosensing by the master virulence regulator RovA of Yersinia. *J Biol Chem* **287**: 35796–803.

Reimmann, C., Valverde, C., Kay, E., and Haas, D. (2005) Posttranscriptional repression of GacS/GacA-controlled genes by the RNA-binding protein RsmE acting together with RsmA in the biocontrol strain Pseudomonas fluorescens CHA0. *J Bacteriol* **187**: 276–85.

Renzi, F., Rescalli, E., Galli, E., and Bertoni, G. (2010) Identification of genes regulated by the MvaT-like paralogues TurA and TurB of Pseudomonas putida KT2440. *Environ Microbiol* **12**: 254–63.

Rimsky, S., Zuber, F., Buckle, M., and Buc, H. (2002) A molecular mechanism for the repression of transcription by the H-NS protein. *Mol Microbiol* **42**: 1311–1323.

Robinson, J.B., Telepnev, M. V, Zudina, I. V, Bouyer, D., Montenieri, J.A., Bearden, S.W., *et al.* (2009) Evaluation of a Yersinia pestis mutant impaired in a thermoregulated type VI-like secretion system in flea, macrophage and murine models. *Microb Pathog* **47**: 243–51.

Rodriguez, R.C. and Tait, R.L. (1983) *Recombinant DNA techniques: an introduction, Addison-Wesley Publishing Company*.

Rodríguez, S., Nieto, J.M., Madrid, C., and Juárez, A. (2005) Functional replacement of the oligomerization domain of H-NS by the Hha protein of Escherichia coli. *J Bacteriol* **187**: 5452–9.

Romeo, T., Gong, M., Liu, M.Y., and Brun-Zinkernagel, A.M. (1993) Identification and molecular characterization of csrA, a pleiotropic gene from Escherichia coli that affects glycogen biosynthesis, gluconeogenesis, cell size, and surface properties. *J Bacteriol* **175**: 4744–55.

Romeo, T. (1997) Post-transcriptional regulation of bacterial carbohydrate metabolism: evidence that the gene product CsrA is a global mRNA decay factor. *Res Microbiol* **147**: 505–12.

Romeo, T. (1998) Global regulation by the small RNA-binding protein CsrA and the non-coding RNA molecule CsrB. *Mol Microbiol* **29**: 1321–30.

Romeo, T., Vakulskas, C.A., and Babitzke, P. (2013) Post-transcriptional regulation on a global scale: form and function of Csr/Rsm systems. *Environ Microbiol* **15**: 313–24.

Ruiz de los Mozos, I., Vergara-Irigaray, M., Segura, V., Villanueva, M., Bitarte, N., Saramago, M., *et al.* (2013) Base pairing interaction between 5'- and 3'-UTRs controls icaR mRNA translation in Staphylococcus aureus. *PLoS Genet* **9**: e1004001.

Russell, A.B., Hood, R.D., Bui, N.K., LeRoux, M., Vollmer, W., and Mougous, J.D. (2011) Type VI secretion delivers bacteriolytic effectors to target cells. *Nature* **475**: 343–7.

Saier, M.H. (1998) Multiple mechanisms controlling carbon metabolism in bacteria. *Biotechnol Bioeng* **58**: 170–4.

Sambrook, J. and Russel, D.W. (2001) *Molecular Cloning*.

Sandrini, S., Masania, R., Zia, F., Haigh, R., and Freestone, P. (2013) Role of porin proteins in acquisition of transferrin iron by enteropathogens. *Microbiology* **159**: 2639–50.

Sansonetti, P.J. (2004) War and peace at mucosal surfaces. *Nat Rev Immunol* **4**: 953–64.

Savin, C., Martin, L., Bouchier, C., Filali, S., Chenau, J., Zhou, Z., *et al.* (2014) The Yersinia pseudotuberculosis complex: Characterization and delineation of a new species, Yersinia wautersii. *Int J Med Microbiol* .

Schägger, H. (2006) Tricine-SDS-PAGE. *Nat Protoc* **1**: 16–22.

Schiano, C. A. and Lathem, W.W. (2012) Post-transcriptional regulation of gene expression in Yersinia species. *Front Cell Infect Microbiol* **2**: 129.

Schiemann, D.A. (1979) Synthesis of a selective agar medium for Yersinia enterocolitica. *Can J Microbiol* **25**: 1298–1304.

Schreiber, G., and Fersht, A.R. (1996) Rapid, electrostatically assisted association of proteins. *Nat Struct Biol* **3**: 427–31.

Schubert, M., Lapouge, K., Duss, O., Oberstrass, F.C., Jelesarov, I., Haas, D., and Allain, F.H.-T. (2007) Molecular basis of messenger RNA recognition by the specific bacterial repressing clamp RsmA/CsrA. *Nat Struct Mol Biol* **14**: 807–13.

Schubert, S., Rakin, A., and Heesemann, J. (2004) The Yersinia high-pathogenicity island (HPI): evolutionary and functional aspects. *Int J Med Microbiol* **294**: 83–94.

Schulte, R., Wattiau, P., Hartland, E.L., Robins-Browne, R.M., and Cornelis, G.R. (1996) Differential secretion of interleukin-8 by human epithelial cell lines upon entry of virulent or nonvirulent Yersinia enterocolitica. *Infect Immun* **64**: 2106–13.

Serganov, A., and Nudler, E. (2013) A decade of riboswitches. *Cell* **152**: 17–24.

Shin, S., Lu, G., Cai, M., and Kim, K.-S. (2005) Escherichia coli outer membrane protein A adheres to human brain microvascular endothelial cells. *Biochem Biophys Res Commun* **330**: 1199–204.

Silva, A.J., Sultan, S.Z., Liang, W., and Benitez, J.A. (2008) Role of the histone-like nucleoid structuring protein in the regulation of rpoS and RpoS-dependent genes in Vibrio cholerae. *J Bacteriol* **190**: 7335–45.

Simon, R., Priefer, U., and Pühler, A. (1983) A Broad Host Range Mobilization System for In Vivo Genetic Engineering: Transposon Mutagenesis in Gram Negative Bacteria. *Bio/Technology* **1**: 784–791.

Sorger-Domenigg, T., Sonnleitner, E., Kaberdin, V.R., and Bläsi, U. (2007) Distinct and overlapping binding sites of Pseudomonas aeruginosa Hfq and RsmA proteins on the non-coding RNA RsmY. *Biochem Biophys Res Commun* **352**: 769–73.

Soutourina, O., Kolb, A., Krin, E., Laurent-Winter, C., Rimsky, S., Danchin, A., and Bertin, P. (1999) Multiple control of flagellum biosynthesis in Escherichia coli: role of H-NS protein and the cyclic AMP-catabolite activator protein complex in transcription of the flhDC master operon. *J Bacteriol* **181**: 7500–8.

Starke, M. and Fuchs, T.M. (2014) YmoA negatively controls the expression of insecticidal genes in Yersinia enterocolitica. *Mol Microbiol* .

Steinmann, R. (2013) Characterization of temperature-dependent and feedback-controlled expression of the virulence activator LcrF in Yersinia pseudotuberculosis.

Sterzenbach, T., Nguyen, K.T., Nuccio, S.-P., Winter, M.G., Vakulskas, C.A., Clegg, S., *et al.* (2013) A novel CsrA titration mechanism regulates fimbrial gene expression in Salmonella typhimurium. *EMBO J* **32**: 2872–83.

Studier, F.W., and Moffatt, B.A. (1986) Use of bacteriophage T7 RNA polymerase to direct selective high-level expression of cloned genes. *J Mol Biol* **189**: 113–30.

Suzuki, K., Babitzke, P., Kushner, S.R., and Romeo, T. (2006) Identification of a novel regulatory protein (CsrD) that targets the global regulatory RNAs CsrB and CsrC for degradation by RNase E. *Genes Dev* **20**: 2605–17.

Takeshita, S., Sato, M., Toba, M., Masahashi, W., and Hashimoto-Gotoh, T. (1987) High-copy-number and low-copy-number plasmid vectors for lacZ alpha-complementation and chloramphenicol- or kanamycin-resistance selection. *Gene* **61**: 63–74.

Thomas, M.B. (2013) Creation of a viable csrA mutant in Vibrio cholerae.

Timmermans, J., and Melderen, L. Van (2009) Conditional essentiality of the csrA gene in Escherichia coli. *J Bacteriol* **191**: 1722–4.

Timmermans, J. and Melderen, L. Van (2010) Post-transcriptional global regulation by CsrA in bacteria. *Cell Mol Life Sci* **67**: 2897–908.

Towbin, H., Staehelin, T., and Gordon, J. (1992) Electrophoretic transfer of proteins from polyacrylamide gels to nitrocellulose sheets: procedure and some applications. 1979. *Biotechnology* **24**: 145–9.

Tran, H.J., Heroven, A.K., Winkler, L., Spreter, T., Beatrix, B., and Dersch, P. (2005) Analysis of RovA, a transcriptional regulator of Yersinia pseudotuberculosis virulence that acts through antirepression and direct transcriptional activation. *J Biol Chem* **280**: 42423–32.

Trülzsch, K., Oellerich, M.F., and Heesemann, J. (2007) Invasion and dissemination of Yersinia enterocolitica in the mouse infection model. *Adv Exp Med Biol* **603**: 279–85.

Tupper, A.E., Owen-Hughes, T.A., Ussery, D.W., Santos, D.S., Ferguson, D.J.P., Sidebotham, J.M., *et al.* (1994) The chromatin-associated protein H-NS alters DNA topology in vitro. *EMBO J* **13**: 258–268.

Viegas, S.C., and Arraiano, C.M. (2008) Regulating the regulators: How ribonucleases dictate the rules in the control of small non-coding RNAs. *RNA Biol* **5**: 230–243.

Viegas, S.C., Pfeiffer, V., Sittka, A., Silva, I.J., Vogel, J., and Arraiano, C.M. (2007) Characterization of the role of ribonucleases in Salmonella small RNA decay. *Nucleic Acids Res* **35**: 7651–64.

Vogel, J. and Luisi, B.F. (2011) Hfq and its constellation of RNA. *Nat Rev Microbiol* **9**: 578–89.

Wang, X., Dubey, A.K., Suzuki, K., Baker, C.S., Babitzke, P., and Romeo, T. (2005) CsrA post-transcriptionally represses pgaABCD, responsible for synthesis of a biofilm polysaccharide adhesin of Escherichia coli. *Mol Microbiol* **56**: 1648–63.

Wang, Y. (2002) The function of OmpA in Escherichia coli. *Biochem Biophys Res Commun* **292**: 396–401.

Wei, B.L., Brun-Zinkernagel, A.M., Simecka, J.W., Prüss, B.M., Babitzke, P., and Romeo, T. (2001) Positive regulation of motility and flhDC expression by the RNA-binding protein CsrA of Escherichia coli. *Mol Microbiol* **40**: 245–256.

Weilbacher, T., Suzuki, K., Dubey, A.K., Wang, X., Gudapaty, S., Morozov, I., *et al.* (2003) A novel sRNA component of the carbon storage regulatory system of Escherichia coli. *Mol Microbiol* **48**: 657–670.

White, D., Hart, M.E., and Romeo, T. (1996) Phylogenetic distribution of the global regulatory gene csrA among eubacteria. *Gene* **182**: 221–3.

Williams, S., Varcoe, L., Attridge, S., and Manning, P. (1996) Vibrio cholerae Hcp, a secreted protein coregulated with HlyA. *Infect Immun* **64**: 283–289.

Winkler, W.C. (2005) Riboswitches and the role of noncoding RNAs in bacterial metabolic control. *Curr Opin Chem Biol* **9**: 594–602.

Winnacker, E.L. (1990) *Gene und Klone - Eine Einführung in die Gentechnologie, VCH Weinheim.*

Wren, B.W. (2003) The yersiniae--a model genus to study the rapid evolution of bacterial pathogens. *Nat Rev Microbiol* **1**: 55–64.

Xiong, J.P., Stehle, T., Diefenbach, B., Zhang, R., Dunker, R., Scott, D.L., *et al.* (2001) Crystal structure of the extracellular segment of integrin alpha Vbeta3. *Science* **294**: 339–45.

Yakhnin, A. V, Baker, C.S., Vakulskas, C. a, Yakhnin, H., Berezin, I., Romeo, T., and Babitzke, P. (2013) CsrA activates flhDC expression by protecting flhDC mRNA from RNase E-mediated cleavage. *Mol Microbiol* **87**: 851–66.

Yakhnin, H., Pandit, P., Petty, T.J., Baker, C.S., Romeo, T., and Babitzke, P. (2007) CsrA of Bacillus subtilis regulates translation initiation of the gene encoding the flagellin protein (hag) by blocking ribosome binding. *Mol Microbiol* **64**: 1605–20.

Yakhnin, H., Yakhnin, A. V, Baker, C.S., Sineva, E., Berezin, I., Romeo, T., and Babitzke, P. (2011) Complex regulation of the global regulatory gene csrA: CsrA-mediated translational repression, transcription from five promoters by $E\sigma^{70}$ and Eσ(S), and indirect transcriptional activation by CsrA. *Mol Microbiol* **81**: 689–704.

Yersin, A. (1894) Sur la peste bubonique. *Ann Inst Pasteur Microbiol* **2**: 428–430.

Yoon, H., Hong, J., and Ryu, S. (2008) Effects of chaperones on mRNA stability and gene expression in Escherichia coli. *J Microbiol Biotechnol* **18**: 228–33.

Zhan, L., Yang, L., Zhou, L., Li, Y., Gao, H., Guo, Z., *et al.* (2009) Direct and negative regulation of the sycO-ypkA-ypoJ operon by cyclic AMP receptor protein (CRP) in Yersinia pestis. *BMC Microbiol* **9**: 178.

Zhang, A., Rimsky, S., Reaban, M.E., Buc, H., and Belfort, M. (1996) Escherichia coli protein analogs StpA and H-NS: regulatory loops, similar and disparate effects on nucleic acid dynamics. *EMBO J* **15**: 1340–9.

Zhang, W., Wang, Y., Song, Y., Wang, T., Xu, S., Peng, Z., *et al.* (2013) A type VI secretion system regulated by OmpR in Yersinia pseudotuberculosis functions to maintain intracellular pH homeostasis. *Environ Microbiol* **15**: 557–69.

Zhang, W., Xu, S., Li, J., Shen, X., Wang, Y., and Yuan, Z. (2011) Modulation of a thermoregulated type VI secretion system by AHL-dependent quorum sensing in Yersinia pseudotuberculosis. *Arch Microbiol* **193**: 351–63.

Zheng, D., Constantinidou, C., Hobman, J.L., and Minchin, S.D. (2004) Identification of the CRP regulon using in vitro and in vivo transcriptional profiling. *Nucleic Acids Res* **32**: 5874–93.

Zuker, M. (2003) Mfold web server for nucleic acid folding and hybridization prediction. *Nucleic Acids Res* **31**: 3406–15.

8. Supplementary material

Tab. S 1 Single components of DMEM medium. Components were dissolved in dem. water, sterile filtrated in Stericups (Millipore) and kept at 4°C.

Component	Concentration [mg/l]
Carbon source (6x)	
D-glucose · H_2O	11892
Sodium pyruvate	660
Mineral salts 1 (12x)	
NaCl	45594
KCl	1341.6
Na_2HPO_4 · $7H_2O$	1607.8
$NaHCO_3$	7056
Mineral salts 2 (12x)	
$CaCl_2$ · $2H_2O$	264
$MgCl_2$ · $6H_2O$	732
Amino acids (6x)	
L-Alanine	54
L-Arginine · HCl	1266
L-Asparagine · H_2O	90
L-Aspartic acid	79.8
L-Cysteine · HCl · H_2O	210.77
L-Glutamine	876
L-Glutamc acid	88.2
Glycine	45
L-Histidine · HCl · H_2O	126
L-Isoleucine	24
L-Leucine	78
L-Lysine · HCl	219
L-Methionine	26.8
L-Phenylalanine	30
L-Proline	207
L-Serine	63
L-Threonine	72
L-Tryptophane	12
L-Tyrosine	32.4
L-Valine	11.7
Trace elements (6x)	
$FeSO_4$ · $7H_2O$*	5.004
$CuSO_4$ · $5H_2O$*	0.01494
$ZnSO_4$ · $7H_2O$*	5.178

Component	Concentration [mg/L]
Vitamins (6x)	
Biotin	0.0436
Vitamine B_5	2.88
Folic acid	7.8
Nicotinamide	0.222
Vitamine B_6	0.372
Riboflavin	0.228
Vitamine B_1	2.04
Vitamin B_{12}	8.16
Rest (6x)	
Choline chloride	84
Myo-inositol	108
Hypoxanthine	24.6
Thymidine	4.38
Lipoic acid	1.26
Linoleic acid	0.504 (0.56 µl)
Putrescine · 2HCl	0.966 (1.1 µl)

Tab. S 2 Classification of YmoA-dependent genes

Gene ID	Gene locus	Fold change	Description	Category - class
Virulence genes				
Downregulated loci (YmoA-activated)				
YPK_0281	*bfr*	-2,5	bacterioferritin, persistence	virulence factor
YPK_1268	*ail*	-2	virulence-related outer membrane protein	virulence factor
YPK_1876	*rovA*	-2,5	virulence regulator, induces invasin	virulence regulation
YPK_3214	*ymoA*	-2	modulator of virulence	virulence regulation
YPK_3289	*crl*	-2,5	DNA transcriptional regulator, adhesion; sigma factor-binding protein	virulence regulation
Upregulated loci (YmoA-repressed)				
pYV0001	*ypkA/yopO*	2,7	effector protein, kinase	virulence factor, pYV
pYV0002	*sycO*	3,8	effector chaperone, increases solubility of YpkA/YopO	virulence factor, pYV
pYV0013	*yadA*	1,8	adhesin	virulence factor, pYV
pYV0024	*sycE, yerA*	3,7	effector chaperone, increases solubility of YopE	virulence factor, pYV
pYV0025	*yopE*	8,4	effector protein, GEF mimic, immune defense	virulence factor, pYV
pYV0040	*yopK/yopQ*	6	effector protein, immune defense	virulence factor, pYV
pYV0047	*yopM*	4	effector protein, leucine rich repeat protein	virulence factor, pYV
pYV0049		4,1	similarity with autotransporter proteins	virulence factor, pYV
pYV0054	*yopD*	4,9	effector protein, translocator protein	virulence factor, pYV
pYV0055	*yopB*	5,7	effector protein, translocator protein	virulence factor, pYV
pYV0056	*lcrH, sycD*	5,9	effector chaperone	virulence factor, pYV
pYV0057	*lcrV*	9	V antigen, antihost protein, immune defense	virulence factor, pYV

pYV0058	*lcrG*	7,5	type III secretion system, immune defense	virulence factor, pYV
pYV0059	*lcrR*	3,8	type III secretion system, regulator	virulence factor, pYV
pYV0061	*yscY, lcrD*	2,4	type III ecretion system, immune defense	virulence factor, pYV
pYV0062	*yscX*	2,2	type III secretion system, immune defense	virulence factor, pYV
pYV0063	*sycN*	2,1	effector chaperone, YopN chaperone	virulence factor, pYV
pYV0064	*tyeA*	2,2	Yop secretion and targeting protein, regulator	virulence factor, pYV
pYV0065	*yopN, lcrE*	3,3	type III secretion system, secretion control	virulence factor, pYV
pYV0068	*yscO*	2,9	type III secretion system, immune defense	virulence factor, pYV
pYV0069	*yscP*	2,5	type III secretion system, immune defense	virulence factor, pYV
pYV0070	*yscQ*	2,2	type III secretion system, immune defense	virulence factor, pYV
pYV0071	*yscR*	2	type III secretion system, immune defense	virulence factor, pYV
pYV0072	*yscS*	1,9	type III secretion system, immune defense	virulence factor, pYV
pYV0074	*yscU*	2	type III secretion system, immune defense	virulence factor, pYV
pYV0075	*virG, yscW*	7,3	putative Yop targeting lipoprotein	virulence factor, pYV
pYV0076	*lcrF, virF*	5,5	thermoregulatory virulence regulator protein	virulence factor, pYV
pYV0077	*yscA*	9,6	type III secretion system, immune defense	virulence factor, pYV
pYV0078	*yscB*	9	type III secretion system, chaperone, immune defense	virulence factor, pYV
pYV0079	*yscC*	5,5	type III secretion system, immune defense	virulence factor, pYV
pYV0080	*yscD*	4,6	type III secretion system, immune defense	virulence factor, pYV
pYV0081	*yscE*	8,1	type III secretion system, immune defense	virulence factor, pYV
pYV0082	*yscF*	8,5	type III secretion system, immune defense	virulence factor, pYV
pYV0083	*yscG*	5,3	type III secretion system, immune defense	virulence factor, pYV
pYV0084	*yscH,lcrP*	3,8	type III secretion system, immune defense	virulence factor, pYV
pYV0085	*yscI, lcrO*	5	type III secretion system, immune defense	virulence factor, pYV
pYV0086	*yscJ, ylpB*	4,2	type III secretion system, immune defense	virulence factor, pYV
pYV0087	*yscK*	3,9	type III secretion system, immune defense	virulence factor, pYV
pYV0088	*yscL*	5	type III secretion system, immune defense	virulence factor, pYV
pYV0089	*yscM, lcrQ*	3,9	type III secretion system, regulatory protein	virulence factor, pYV
pYV0094	*yopH*	5,9	effector protein, protein-tyrosine phosphatase	virulence factor, pYV
pYV0098	*yopP, yopJ*	14,8	effector protein, protease family, immune defense	virulence factor, pYV
YPK_0051	*yqiL*	6,3	fimbrial protein, colonization factor	virulence factor
YPK_0052	*yqiG*	1,8	fimbrial biogenesis outer membrane usher protein	virulence factor
YPK_0053	*ybgP*	2,4	pili assembly protein	virulence factor
YPK_0054	*ybgO*	1,8	fimbrial protein	virulence factor
YPK_0251		1,7	type VI secretion system effector, Hcp1 family	virulence factor
YPK_0386	*impB1*	2,8	type VI secretion system	virulence factor
YPK_0387	*impC1*	2,4	type VI secretion system	virulence factor
YPK_0479	*tcaB*	2,8	insecticidal toxin subunit	defense
YPK_0480	*tcaA*	2,7	insecticidal toxin subunit	defense
YPK_0694	*smfA1*	2,7	fimbrial protein, colonization factor	virulence factor
YPK_0792	*yspI/ytbI*	2,6	autoinducer synthesis protein	
YPK_0871	*yadF*	2	putative adhesin	virulence factor
YPK_1304		3,5	Hcp1 family type VI secretion system effector	virulence factor
YPK_1449	*csgG*	4,5	curli production assembly, colonization factor	virulence factor
YPK_1450		3,7	putative lipoprotein	virulence factor
YPK_1475	*fimA1*	3,4	fimbrial protein, colonization factor	virulence factor
YPK_1479	*impB3*	2,2	type VI secretion system	virulence factor

YPK_1480	*impC*	2,5	type VI secretion system, EvpB family	virulence factor
YPK_1481		5,7	Hcp1 family type VI secretion system effector, Hcp	virulence factor
YPK_1522	*smfA2*	2,6	fimbrial protein, colonization factor	virulence factor
YPK_1606	*ompX/ailD*	1,9	Ail-type outer membrane proteine, put. virulence factor	virulence factor
YPK_1644		2,1	CRISPR-associated Cas1 family protein	defense, immunity
YPK_1655	*sdiA/ypsR/yenR*	1,8	LuxR family transcriptional regulator	virulence regulation
YPK_1786	*fimA2*	3,7	fimbrial protein, colonization factor	virulence factor
YPK_1953	*srfB*	2	putative virulence factor	virulence factor
YPK_2061	*ailB*	2	Ail-type outer membrane proteine, put. virulence factor	virulence factor
YPK_2356	*uvrY*	1,9	response regulator	virulence regulation
YPK_2615	*cnf1*	9,6	cytotoxic necrotizing factor, bacterial toxin	virulence factor
YPK_2672	*yadC*	2,1	putative adhesin	virulence factor
YPK_2758	*psaB*	1,7	pili assembly chaperone, colonization factor	virulence factor
YPK_2759	*psaA*	2,7	pH6 antigen, adhesin, colonization factor	virulence factor
YPK_2760	*psaF*	2,1	regulator of psaABC operon	virulence factor
YPK_3060		6	Hcp1 family type VI secretion system effector	virulence factor
YPK_3177	*wzz*	3,8	chain length determinant protein, LPS/O-antigen	defense, persistence
YPK_3178	*manB*	3,1	phosphomannomutase, LPS/O-antigen	defense, persistence
YPK_3179	*gne*	3,4	NAD-dependent epimerase/hydratase, LPS/O-antigen	defense, persistence
YPK_3180	*wbyL*	3,4	glycosyl transferase family protein, LPS/O-antigen	defense, persistence
YPK_3181	*manC*	2,7	mannose-1-phosphate guanyltransferase/mannose-6-phosphate isomerase, LPS/O-antigen	defense, persistence
YPK_3182	*fcl*	2,4	NAD-dependent epimerase/dehydratase; GDP-L-fucose synthetase, LPS/O-antigen	defense, persistence
YPK_3183	*gmd*	2,3	GDP-mannose 4,6,-dehydratase, LPS/O-antigen	defense, persistence
YPK_3184	*wbyK*	2,3	mannoslytransferase, LPS/O-antigen	defense, persistence
YPK_3562	*impF*	1,7	type VI secretion system, lysozyme-related protein	virulence factor
YPK_3564	*impC2*	2,4	type VI secretion system, EvpB family	virulence factor
YPK_3565	*impB2*	2,4	type VI secretion system	virulence factor
YPK_3566	*impA*	2,5	type VI secretion system	virulence factor
YPK_3649	*lsrR*	2,1	transcriptional repressor	
YPK_3653	*lsrB*	1,8	autoinducer-2 (AI-2) ABC transporter, periplasmic	
YPK_3654	*lsrF*	2,2	autoinducer-2 (AI-2) modifying/degrading protein LsrF	
YPK_3655	*lsrG*	2,2	autoinducer-2 (AI-2) modifying protein LsrG	
YPK_3869	*fimC1*	1,9	periplasmic fimbrial chaperone protein	virulence factor
YPK_3870	*fimD1*	2	fimbrial biogenesis outer membrane usher protein	virulence factor
YPK_4042	*fimA3*	2,1	fimbrial protein, colonization factor	virulence factor
YPK_4085	*hasA*	8,2	heme-binding protein, heme acquisition, persistence	virulence factor
Motility				
Downregulated loci (YmoA-activated)				
YPK_2381	*fliC*	-2	flagellin	cell motility, flagellar assembly
Upregulated loci (YmoA-repressed)				
YPK_1745	*flhD*	2,9	transcriptional activator for flagellar/motility genes	cell motility, flagellar assembly
YPK_1746	*flhC*	2,2	transcriptional activator for flagellar/motility genes	cell motility, flagellar assembly
YPK_2378	*fliZ*	2,3	flagellar biosynthesis protein	cell motility, flagellar assembly

YPK_2383	*fliS*	1,8	flagellar protein	cell motility, flagellar assembly
YPK_2384	*fliT*	2,6	flagellar protein	cell motility, flagellar assembly
YPK_2390	*fliE*	2,5	hook basal body protein	cell motility, flagellar assembly
YPK_2391	*fliF*	2	flagellar MS-ring protein	cell motility, flagellar assembly
YPK_2392	*fliG*	1,8	flagellar motor switch protein	cell motility, flagellar assembly
YPK_2401	*fliO*	1,9	flagellar biosynthesis protein	cell motility, flagellar assembly
YPK_2418	*flgI*	1,8	flagellar basal body P-ring protein	cell motility, flagellar assembly
YPK_2419	*flgH*	1,8	flagellar basal body L-ring protein	cell motility, flagellar assembly
YPK_2423	*flgD*	2,5	flagellar basal body rod modification protein	cell motility, flagellar assembly
YPK_2424	*flgC*	2,1	flagellar basal body rod protein	cell motility, flagellar assembly
YPK_2425	*flgB*	2,1	flagellar basal body rod protein	cell motility, flagellar assembly
YPK_2426	*flgA*	1,8	flagellar basal body P-ring biosynthesis	cell motility, flagellar assembly

Stress adaptation

Downregulated loci (YmoA-activated)

YPK_0120	*uspA*	-2	universal stress protein	stress response
YPK_1140	*hdeB*	-3,3	acid-resistance protein	stress response, acid resistance
YPK_1602	*dps*	-2	DNA starvation/stationary phase protection	stress response, starvation
YPK_1863	*sodB*	-1,7	superoxide dismutase	stress response, oxidative stress
YPK_2017	*cstA*	-2	carbon starvation protein	stress response, starvation
YPK_2694	*cspD*	-3,3	cold shock protein, DNA binding protein	stress response
YPK_2855	*katA*	-2	catalase	stress response, oxidative stress
YPK_3388	*katY*	-2	catalase/peroxidase	stress response, oxidative stress
YPK_3445	*sodC*	-2,5	superoxide dismutase	stress response, oxidative stress
YPK_3632	*osmY*	-2	transport-associated	osmotic stress

Upregulated loci (YmoA-repressed)

YPK_0011	*ibpA*	8	heat shock chaperone	stress response, heat shock
YPK_0012	*ibpB*	5,4	heat shock chaperone	stress response, heat shock
YPK_0175	*hslO*	1,8	HSP33-like chaperonin	stress response, heat shock
YPK_0442	*cspA1*	3,1	cold shock regulator protein, CspA family	stress response, regulator
YPK_0443	*cspA2*	2,7	cold shock regulator protein, CspA family	stress response, regulator
YPK_0444	*cspA3*	2,1	cold shock regulator protein, CspA family	stress response, regulator
YPK_1124	*cspB*	1,9	cold shock regulator protein	stress response, regulator
YPK_1740	*cspC/cspA*	4,2	cold shock regulator protein	stress response, regulator
YPK_2355	*uvrC*	1,8	exinuclease ABC subunit C	stress response, repair
YPK_2974	*grpE*	2,7	heat shock chaperone	stress response, heat shock
YPK_3195	*htpG*	2,6	heat shock chaperone, Hsp90	stress response, heat shock

YPK_3232	*lon*	1,9	ATP dependent protease	stress response
YPK_3349	*clpB*	2,4	protein assembly disaggregation chaperone	stress response
YPK_3593	*dnaJ*	2,9	heat shock chaperone	stress response, heat shock
YPK_3594	*dnaK*	3,2	heat shock chaperone, assist RNA degradation	stress response, heat shock
YPK_3822	*groEL*	1,9	chaperonin, assist bacterial RNA degradation	stress response, heat shock
YPK_3823	*groES*	1,9	co-chaperonin	stress response, heat shock
YPK_4103	*hslV*	2,9	ATP dependent protease subunit	stress response
YPK_4104	*hslU*	2,4	ATP dependent protease subunit	stress response

Genetic information processing

Downregulated loci (YmoA-activated)

YPK_0273	*tusC*	-1,7	sulfur relay protein TusC, tRNA 2-thiouridine synthase	translation
YPK_0348	*rsd*	-2	regulator of sigma 70/RpoD	transcription
YPK_0504	*yhbH*	-2,5	putative sigma 54 modulation protein	transcription
YPK_1016		-1,7	putative transcription factor, CadC	transcription
YPK_1183	*rseA*	-1,7	anti-RNA polymerase sigma factor E/RpoE	transcription
YPK_1826	*ihfA*	-2	integration host factor	transcription
YPK_3425	*rpoS*	-2	RNA polymerase sigma factor	transcription
YPK_3673	*hsdS*	-1,7	restriction modification system DNA specificity subunit	DNA modification

Upregulated loci (YmoA-repressed)

YPK_0282	*rpsJ*	2,4	small subunit ribosomal protein S10	translation
YPK_0283	*rplC*	2	large subunit ribosomal protein L3	translation
YPK_0284	*rplD*	1,9	large subunit ribosomal protein L4	translation
YPK_0285	*rplW*	2	large subunit ribosomal protein L23	translation
YPK_0286	*rplB*	2	large subunit ribosomal protein L2	translation
YPK_0287	*rpsS*	2	small subunit ribosomal protein S19	translation
YPK_0288	*rplV*	2,1	large subunit ribosomal protein L22	translation
YPK_0289	*rpsC*	2,2	small subunit ribosomal protein S3	translation
YPK_0291	*rpmC*	2,4	large subunit ribosomal protein L29	translation
YPK_0292	*rpsQ*	1,7	small subunit ribosomal protein S17	translation
YPK_0299	*rplR*	1,8	large subunit ribosomal protein L18	translation
YPK_0300	*rpsE*	1,7	large subunit ribosomal protein S5	translation
YPK_0304	*rpmJ*	1,9	large subunit ribosomal protein L36	translation
YPK_0305	*rpsM*	1,9	small subunit ribosomal protein S13	translation
YPK_0309	*rplQ*	2,3	large subunit ribosomal protein L17	translation
YPK_0335	*rplK*	1,8	large subunit ribosomal protein L11	translation
YPK_0338	*rplL*	1,9	large subunit ribosomal protein L7/12	translation
YPK_0452	*fis*	1,8	DNA-binding protein Fis	transcription
YPK_0524	*rplM*	2	large subunit ribosomal protein L13	translation
YPK_0525	*rpsI*	1,9	small subunit ribosomal protein S9	translation
YPK_0603	*tdcF*	1,7	endoribonuclease L-PSP	RNA processing
YPK_0604		2,1	endoribonuclease L-PSP	RNA processing
YPK_0636	*rpsU*	2,3	small subunit ribosomal protein S21	translation
YPK_0725		2,8	putative transcription factor, CadC	transcription
YPK_1066	*rpsB*	1,8	small subunit ribosomal protein S2	translation

YPK_2385		2,2	AraC family transcription factor	transcription
YPK_2843	*rcsB*	2	two component system, capsular synthesis response regulator	transcription
YPK_3196	*recR*	1,9	recombination protein	DNA modification
YPK_3361	*rplS*	1,8	small subunit ribosomal protein L19	translation
YPK_3362	*trmD*	1,8	tRNA (guanine-N1-)-methyltransferase	translation
YPK_3363	*rimM*	1,8	16S rRNA processing protein	translation
YPK_3364	*rpsP*	1,9	small subunit ribosomal protein S16	translation
YPK_3590	*rpsT*	2,2	small subunit ribosomal protein S20	translation
YPK_3736	*hflB*	1,9	ATP-dependent metalloprotease, devision protease FtsH	translation
YPK_3737	*rrmJ*	2	23S rRNA methyltransferase, ribosomal RNA large subunit methyltransferase E	translation
YPK_3756	*rpmA*	2,2	large subunit ribosomal protein L27	translation
YPK_3757	*rplU*	2,1	large subunit ribosomal protein L21	translation
YPK_3781	*rplI*	2	large subunit ribosomal protein L9	translation
YPK_3782	*rpsR*	2,3	small subunit ribosomal protein S18	translation
YPK_3783	*priB*	1,8	primosomal replication protein N	replication, repair
YPK_4154	*rpmB*	2,1	large subunit ribosomal protein L28	translation
YPK_4248	*rnpA*	1,9	ribonuclease P protein component	RNA processing
YPK_4249	*rpmH*	1,8	large subunit ribosomal protein L34	translation

Metabolism

Downregulated loci (YmoA-activated)

YPK_0077	*hutH*	-2	histidine ammonia-lyase	N metabolism
YPK_0151	*glgP*	-1,7	glycogen/starch/alpha-glucan phosphorylase	C metabolism
YPK_0356	*purD*	-2	phosphoribosylamine glycine ligase	nucleotide/purine metabolism
YPK_0859	*serA*	-1,7	D-3-phosphoglycerate dehydrogenase	aa metabolism
YPK_1001	*cynT*	-3,3	carbonic anhydrase	N metabolism
YPK_1265	*glyA*	-2	glycine, serine, threonine metabolism	aa metabolism
YPK_1302	*guaB*	-2	inosine-5'-monophosphate dehydrogenase	nucleotide/purine metabolism
YPK_1351	*purI*	-2	phosphoribosylaminoimidazole synthetase	nucleotide/purine metabolism
YPK_1534	*cvpA*	-2	colicin production protein, holin	nucleotide/purine metabolism
YPK_1538	*hisJ*	-1,7	cationic amino acid ABC transporter, periplasmic binding protein	aa metabolism, transport
YPK_1846	*ydiI*	-2	thioesterase superfamily protein	metabolism
YPK_1883	*gst*	-2,5	glutathionine S-transferase	aa metabolism, transport
YPK_1983	*tpx*	-2	thiol peroxidase	metabolism
YPK_2070	*oppA*	-1,7	extracellular solute-binding protein	aa metabolism, transport
YPK_2229	*astC*	-2	bifunctional succinylornithine transaminase/acetyl-ornithine aminotransferase	aa metabolism
YPK_2363	*wrbA*	-2,5	TrpR repressor binding protein	metabolism, regulation
YPK_2447	*purT*	-2	phosphoribosylglycinamide formyltransferase 2	nucleotide/purine metabolism
YPK_2465	*manY*	-2	PTS system, mannose-specific IIC component	C metabolism, transport
YPK_2466	*manZ*	-2	PTS system, mannose-specific IID component	C metabolism, transport
YPK_3001	*asnB*	-1,7	asparagine synthase	N metabolism
YPK_3010	*gltI*	-5	glutamate and aspartate transport subunit substrate binding protein	aa metabolism, transport

YPK_3011	*gltJ*	-1,7	polar amino acid ABC transporter, inner membrane unit	aa metabolism, transport
YPK_3049	*mmsA/iolA*	-1,7	methylmalonate-semialdehyde dehydrogenase	aa metabolism
YPK_3219	*amtB*	-5	ammonium transporter	N metabolism
YPK_3220	*glnK*	-5	nitrogen regulator protein P-II	N metabolism
YPK_3368	*luxS*	-1,7	S-ribosylhomocysteinase, cysteine/methionine metabolism	aa metabolism
YPK_3582	*carB*	-2	carbamoyl-phosphate synthase, large subunit	nucleotide/pyrimidine metabolism
YPK_3813	*frdA*	-1,7	fumerate reductase flavoprotein subunit A	C metabolism, TCA
YPK_3848	*fucO*	-2	lactaldehyde reductase	metabolism
YPK_3923	*actP*	-2	acetate permease, Na+ symporter	C metabolism, transport
YPK_3950	*udp*	-2	uridine phosphorylase	nucleotide/pyrimidine metabolism
YPK_4189	*glnA*	-5	glutamine synthase	N metabolism, assimilation
YPK_4190	*glnL*	-2	nitrogen regulation protein NRII, histidine sensor kinase	N metabolism, assimilation
YPK_4191	*glnG*	-2	nitrogen regulation protein NRI, response regulator	N metabolism, assimilation
YPK_4214	*asnA*	-2	aspartate-ammonia ligase	N metabolism

Upregulated loci (YmoA-repressed)

YPK_0116	*opdA*	1,9	oligopeptidase A	metabolism
YPK_0378	*malE*	4	maltose ABC transporter periplasmic protein	C metabolism, transport
YPK_0379	*amyA*	4,1	glycosidase	C metabolism, transport
YPK_0380	*malK*	4,7	maltose/maltodextrin transporter ATP-binding protein	C metabolism, transport
YPK_0381	*lamB*	7,9	maltose/matodextrin outer membrane porine	C metabolism, transport
YPK_0382	*malM*	2,7	maltose regulon periplasmic protein	C metabolism, transport
YPK_0494	*treC*	2,1	trehalose(maltose) specific PTS system components IIBC	C metabolism, transport
YPK_0495	*treB*	2,2	trehalose-6 phosphate hydrolase	C metabolism, transport
YPK_0586		2	ABC transporter related	transport
YPK_0692	*cpbD-1*	2,1	chitin-binding protein, contains fibronectin type III domain	metabolism
YPK_0693	*chiC*	2	glycoside hydrolase family protein, chitinase	metabolism
YPK_0789		2,2	intradiol ring-cleavage dioxygenase	metabolism
YPK_0998		1,9	outer membrane autotransporter	transport
YPK_1134	*ureE*	1,8	urease accessory protein	purine, aa metabolism
YPK_1349	*speG*	1,8	GCN5-related N-acetyltransferase	metabolism
YPK_1385	*napF*	1,8	ferredoxin-type protein	N metabolism
YPK_1386	*napD*	2	assembly protein fpr periplasmic nitrate reductase	N metabolism
YPK_1388	*napB*	1,9	citrate reductase cytochrome c-type subunit	N metabolism
YPK_1389	*napC*	1,8	cytochrome c-type subunit	N metabolism
YPK_1394		1,9	putative acetyltransferase	metabolism
YPK_1400	*nanA*	1,9	dihydrodipicolinate synthase, N-acetylneuraminate lyase	metabolism
YPK_1547	*sgaB*	1,9	PTS system, ascorbate-specific IIB subunit	C metabolism, transport
YPK_1548	*cmtB*	1,9	PTS system, ascorbate-specific IIA subunit	C metabolism, transport
YPK_1575	*idnK*	2,3	gluconokinase	C metabolism, PPP
YPK_1576	*idnO*	3	gluconate 5-dehydrogenase	C metabolism, PPP
YPK_1980	*bioD*	2,5	dethiobiotin synthase	vitamin/cofactor metabolism

YPK_2072	*adhE*	2	acetaldehyde dehydrogenase/ alcohol dehydrogenase	C metabolism
YPK_2096	*gapA*	2,1	glyceraldehyde-3-phosphate dehydrogenase, glycolysis	C metabolism
YPK_2224	*ompC2*	2	porin	transport
YPK_2451	*sdaA*	1,8	L-serine dehydratase 1, serine <-> pyruvate	aa metabolism, transport
YPK_2565	*mglA*	1,9	methyl-galactoside transport system ATP-binding protein	transport
YPK_2576		2	ABC transporter-related	transport
YPK_2577		2,3	radical SAM domain-containing	metabolism
YPK_2603	*acpP*	3,6	putative acyl carrier protein	fatty acid metabolism
YPK_2605	*fabG7*	1,8	short chain dehydrogenase/reductase	metabolism
YPK_2674	*ansB*	2	L-asparaginase II, asparagine -> aspartate	aa metabolism
YPK_2676	*focA*	1,8	formate transporter	C metabolism, transport
YPK_2739	*sdaC*	3,9	serine transporter	aa metabolism, transport
YPK_2839	*ompC*	1,9	porin	transport
YPK_2885	*pbpG*	1,8	D-alanyl-D-alanine endopeptidase, penicillin binding protein	metabolism
YPK_3161	*ybbN*	2	putative thioredoxin	metabolism
YPK_3189	*rfbH/ddhC*	1,8	DegT/DnrJ/EryC1/StrS aminotransferase	C metabolism
YPK_3215	*ybaZ*	3,3	methylated DNA-protein cysteine-methyltransferase	metabolism, transport
YPK_3284	*yafE*	2,5	methyltransferase	metabolism
YPK_3285		2,1	hypothetical protein	metabolism
YPK_3293	*cpbD-2*	2,5	chitin-binding domain-containing domain	metabolism
YPK_3397	*fucR*	1,8	DeoR family transcriptional regulator, similar to fucose operon activator	C metabolism, transport
YPK_3398		3	carbohydrate ABC transporter periplasmic protein	C metabolism, transport
YPK_3399		2	simple sugar transport system ATP-binding protein	C metabolism, transport
YPK_3402	*sgbU*	2,8	putative L-xylose 5-phosphate 3-epimerase	C metabolism, transport
YPK_3403	*sgbK*	2,3	Hexulose-6-phosphate isomerase	C metabolism, transport
YPK_3658	*frwC*	1,8	PTS system, fructose-specific EIIC subunit	C metabolism, transport
YPK_3659	*ptsI/frwB*	1,9	PTS system, fructose-specific EIIB subunit	C metabolism, transport
YPK_3710		2,3	hypothetical protein	metabolism
YPK_3711		1,9	heparinase family II/III	metabolism
YPK_3894	*metC*	2,4	cystathionine beta-lyase, cysteine -> pyruvate homocysteine synthesis	S, N metabolism
YPK_3920	*gltP*	1,9	glutamate/aspartate proton symporter	aa metabolism, transport

Transport and secretion, structural proteins

Downregulated loci (YmoA-activated)

YPK_2048		-2	transport-associated, lipoprotein	transport
YPK_4237		-2	extracellular solute-binding protein family 3	transport

Upregulated loci (YmoA-repressed)

YPK_0303	*secY*	1,9	preprotein translocase subunit	protein export, secretion
YPK_1007	*gspG*	2,2	general secretion pathway protein G	protein export, secretion
YPK_1012	*gspL*	1,8	general secretion pathway protein L	protein export, secretion
YPK_1014	*gspO*	3,7	general secretion pathway protein O, prepilin peptidase	protein export,

Others

Downregulated loci (YmoA-activated)

YPK_0426	*yjcD/pbuG*	-2	Xanthine/uracil/vitamin C permease

Upregulated loci (YmoA-repressed)

YPK_0065	*hsdM*	1,8	N4/N6-methyltransferase family protein
YPK_0794		1,8	lipoprotein
YPK_1778		2	Spore coat U domain protein
YPK_2291		2	transposase
YPK_2293		1,9	hypothetical protein
YPK_2385		2,2	transcriptional regulator, AraC family
YPK_3091		1,9	tail assembly chaperone gp38
YPK_3824	*fxsA*	2	FxsA cytoplasmic membrane protein

Hypothetical proteins

Downregulated loci (YmoA-activated)

YPK_0631		-3,3	hypothetical protein
YPK_0856	*yggE*	-1,7	hypothetical protein
YPK_1062		-1,7	hypothetical protein
YPK_2018		-2,5	hypothetical protein
YPK_2101		-2	hypothetical protein
YPK_2185		-1,7	hypothetical protein
YPK_2282		-2	hypothetical protein
YPK_2290		-2	hypothetical protein
YPK_2412		-1,7	hypothetical protein
YPK_2441		-2	hypothetical protein
YPK_2483		-2	hypothetical protein
YPK_2723		-2	hypothetical protein
YPK_2879		-2	hypothetical protein
YPK_3148		-2	hypothetical protein
YPK_3218		-5	hypothetical protein
YPK_3281	*yaiE*	-2	hypothetical protein
YPK_3773		-2	hypothetical protein
YPK_3922		-2	hypothetical protein

Upregulated loci (YmoA-repressed)

pYV0017	1,8	putative resolvase
pYV0018	1,7	putative transposase
pYV0039	4,2	putative transposase
pYV0044	4,9	hypothetical protein
pYV0045	1,8	hypothetical protein
pYV0046	1,8	putative transposase remnant
pYV0048	2,6	hypothetical protein
pYV0056	5,9	hypothetical protein
pYV0066	3,9	putative Yops secretion ATP synthase
pYV0090	3,2	putative transposase
pYV0091	4,2	putative transposase

pYV0092	6,4	putative transposase
pYV0093	4,6	putative transposase
pYV0095	2,1	hypothetical protein
YPK_0044	2,1	hypothetical protein
YPK_0045	2,1	hypothetical protein
YPK_0062	2,1	hypothetical protein
YPK_0064	2,1	hypothetical protein
YPK_0154	2	hypothetical protein
YPK_0252	2,7	hypothetical protein
YPK_0411	2,4	hypothetical protein
YPK_0585	1,9	hypothetical protein
YPK_0602	1,8	hypothetical protein
YPK_0611	1,8	hypothetical protein
YPK_0612	2,8	hypothetical protein
YPK_0724	2,1	hypothetical protein
YPK_0759	1,9	hypothetical protein
YPK_0767	3,9	hypothetical protein
YPK_0768	3,3	hypothetical protein
YPK_0769	4,9	hypothetical protein
YPK_0770	1,9	hypothetical protein
YPK_0771	3,5	hypothetical protein
YPK_0772	4,4	hypothetical protein
YPK_0773	4,2	hypothetical protein
YPK_0774	1,8	hypothetical protein
YPK_0775	4,5	hypothetical protein
YPK_0776	4,1	hypothetical protein
YPK_0777	2,2	hypothetical protein
YPK_0999	2	hypothetical protein
YPK_1017	2,6	hypothetical protein
YPK_1413	1,9	hypothetical protein
YPK_1451	4,1	hypothetical protein
YPK_1574	2	hypothetic protein
YPK_1623	1,8	hypothetical protein
YPK_1731	2,8	hypothetical protein
YPK_1954	1,9	hypothetical protein
YPK_1971	1,9	hypothetical protein
YPK_2065	2,3	hypothetical protein
YPK_2200	2,5	hypothetical protein
YPK_2379	1,7	hypothetical protein
YPK_2405	2,5	hypothetical protein
YPK_2406	2,8	hypothetical protein
YPK_2471	6,1	hypothetical protein
YPK_2485	1,8	hypothetical protein
YPK_2500	1,8	hypothetical protein
YPK_2501	1,8	hypothetical protein
YPK_2573	2,2	hypothetical protein
YPK_2582	4,7	hypothetical protein

YPK_2604		2,3	hypothetical protein
YPK_2781		2	hypothetical protein
YPK_2874		2,5	hypothetical protein
YPK_2888		2	hypothetical protein
YPK_2892		2,5	hypothetical protein
YPK_2893		3,4	hypothetical protein
YPK_2894		2,6	hypothetical protein
YPK_3025		1,9	hypothetical protein
YPK_3061		4,8	hypothetical protein
YPK_3062		5,1	hypothetical protein
YPK_3212		5,7	hypothetical protein
YPK_3213		9	hypothetical protein
YPK_3555		1,8	hypothetical protein
YPK_3567		2,7	hypothetical protein
YPK_3576		3,2	hypothetical protein
YPK_3577		1,9	hypothetical protein
YPK_3579		1,8	hypothetical protein
YPK_3595	*yaaH*	1,9	hypothetical protein
YPK_3732		1,8	hypothetical protein
YPK_3836		3	hypothetical protein
YPK_3871		3	hypothetical protein
YPK_3897		2,4	hypothetical protein
YPK_3982		2,1	hypothetical protein
YPK_3983		2,4	hypothetical protein
YPK_4107		2,6	hypothetical protein
YPK_4108		2,1	hypothetical protein
YPK_4247		1,9	hypothetical protein

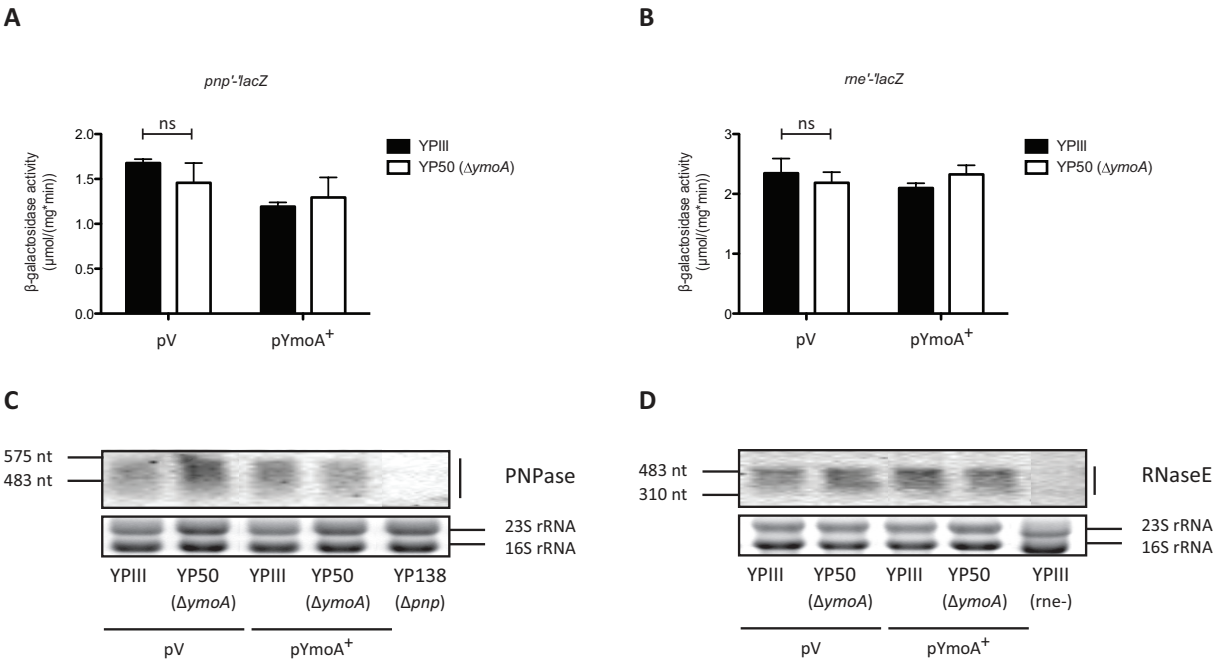

Fig. S 1 YmoA does not affect transcription and mRNA stability of the degradosome components
To assess, if YmoA affects components of the degradosome, promoter activity assays of PNPase (*pnp'-'lacZ* = pSSE51) (**A**) and RNase E (*rne'-'lacZ* = pSSE52) (**B**) were compared in *Y. pseudotuberculosis* YPIII (wildtype) and YP50 (Δ*ymoA*). Strains were transformed with the empty vector pACYC184 (pV) or its derivative pAKH71 (pYmoA$^+$). Strains were grown in LB medium at 25°C to stationary growth phase. Data are means and standard deviations of two independent experiments, each performed with biological duplicates. Data were analysed by Student's t test. Stars indicate the results that differed significantly from each other (ns = not significant). The same growth conditions were applied for the cultures used for northern blot sample preparation. PNPase (**C**) and RNase E (**D**) transcript levels were analysed by northern blotting. Total RNA was prepared from YPIII and YP50 (Δ*ymoA*), transformed with the empty vector pACYC184 (pV) or its derivative pAKH71 (pYmoA$^+$), separated on 0.7% MOPS agarose gels, transferred onto a nylon-membrane and probed with a digoxigenin (DIG)-labelled PCR fragment encoding the *pnp* or *rne* gene. Respective mutant strains YP138 (Δ*pnp*) or the dominant-recessive strain (YPIII+pRS40, *rne*$^-$) were used as negative controls. 16S and 23S rRNAs were used as loading controls.

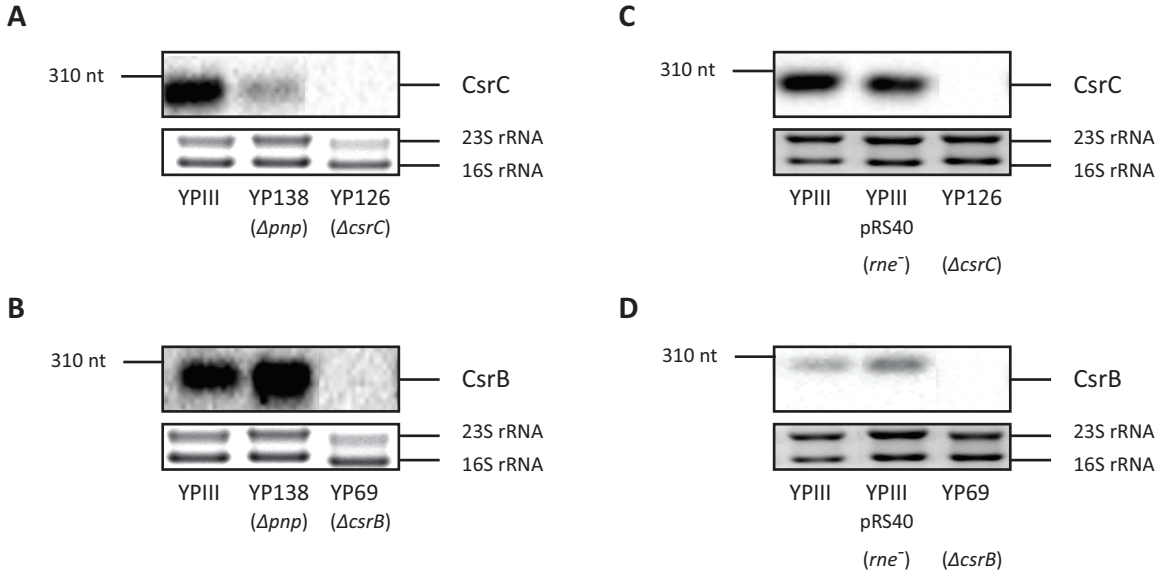

Fig. S 2 Impact of PNPase and RNase E on CsrC and CsrB RNA levels
To monitor whether PNPase (**A**+**B**) and RNase E (**C**+**D**) influence the cellular amount of CsrB and CsrC ncRNA, transcript levels were analysed by northern blotting. Total RNA was prepared from YPIII and YP138 (Δ*pnp*) transformed with pRS40 (dominant-recessive for *rne*) grown at 25°C for 16 h, separated on 0.7% MOPS agarose gels, transferred onto a nylon-membrane and probed with a digoxigenin (DIG)-labelled PCR fragment encoding the *csrC* or *csrB* gene. Respective mutant strains YP126 (Δ*csrC*) or the YP96 (Δ*csrB*) were used as negative controls. 16S and 23S rRNAs were used as loading controls.

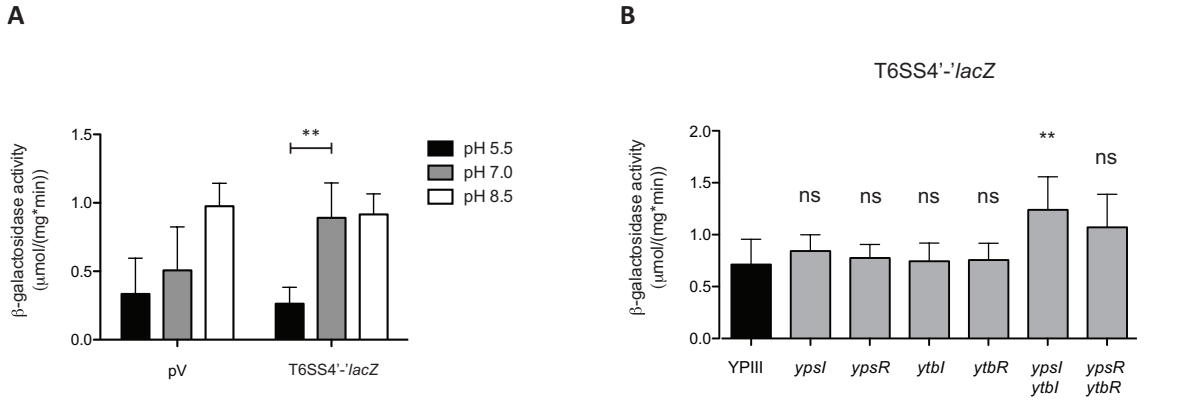

Fig. S 3 Expression of T6SS4 in response to pH and quorum-sensing mutant strains

A pH-dependent expression of a translational T6SS4'-*'lacZ* (pSSE64) fusion was monitored in *Y. pseudotuberculosis* YPIII wildtype. β-galactosidase activity (µmol/(mg*min)) was measured from overnight cultures grown at 25°C in LB medium with different pH values (pH 5.5. pH 7.0. pH 8.5). Data are means and standard deviations of two independent experiments, each performed at least in triplicates. Data were analysed by Student's t test. Stars indicate data that differed significantly from each other (** P<0.01**,** ns = not significant).

B Expression of T6SS4'-*'lacZ* (pSSE64) fusions was monitored in different quorum-sensing YPIII mutant strains (YPIII *ypsI, ypsR, ytbI, ytbR, ypsI/ytbI, ypsR/ytbR*). β-galactosidase activity (µmol/(mg*min)) was measured after strains were grown in LB medium at 25°C for 16 h. Data are means and standard deviations of two independent experiments, each performed at least in triplicates. Data were analysed by Student's t test. Stars indicate data that differed significantly from each other (** P<0.01**,** ns = not significant).

Appendix

Manuscript: The transcriptional regulator RovC controls *csrC* expression and is associated with type VI secretion in *Yersinia pseudotuberculosis*

Stephanie Seekircher, Tanja Krause, Ann Kathrin Heroven and Petra Dersch*

Dep. of Molecular Infection Biology, Helmholtz Centre for Infection Research, 38124 Braunschweig, Germany

* Corresponding author

Petra Dersch

Dep. of Molecular Infection Biology

Helmholtz Centre for Infection Research

38124 Braunschweig

Germany

Phone: +49-531-6181-5700

Fax: +49-531-6181-5709

E-Mail: petra.dersch@helmholtz-hzi.de

Running title: RovC represses *csrC* transcription

Keywords: *Yersinia*, regulatory RNA, gene regulation, Csr system, type VI secretion

Summary

The Carbon storage regulator (Csr) system controls bacterial virulence on the post-transcriptional level. Abundance of the non-coding Csr-type RNAs modulates the availability of active CsrA in the cell and therefore determines target gene regulation. We describe the identification and characterization of RovC - a transcriptional regulator of the Yersinia *csrC* gene. RovC represses *csrC* transcription and thereby controls expression of the downstream genes *rovM*, *rovA* and *invA* that are essential for the initial host colonization. Expression of *rovC* is upregulated at moderate temperatures during stationary growth and is under the control of Crp and CsrA, which are both involved in maintaining cellular CsrC levels. Both, Crp and CsrA repress *rovC* transcription, while CsrA further inhibits *rovC* translation by directly interacting with its 5'-UTR. Moreover, expression of *rovC* is activated in *Y. pseudotuberculosis* while it is barely detectable in *E. coli,* demonstrating the need for additional *Yersinia*-specific factors. In addition to *csrC*, we found that the virulence-associated type VI secretion system 4 (T6SS4) of *Y. pseudotuberculosis* is activated by RovC.

Introduction

The genus *Yersinia* encompasses 18 different species three of which are human pathogens (Carniel *et al*., 2006; Savin *et al.*, 2014). In contrast to *Y. pestis*, which is transmitted via the flea vector and causes bubonic plague, the two enteropathogenic species *Y. enterocolitica* and *Y. pseudotuberculosis* are taken up via contaminated food or water and provoke gut-associated diseases (Carniel *et al*., 2006). Adhesion to M-cells (multifaceted cells) of the intestinal epithelium is of central importance for a successful infection. Bacterial attachment is mediated via the outer membrane protein invasin (*invA*) (Marra and Isberg, 1997; Dersch and Isberg, 1999). Invasin expression is directly stimulated by the global MarR-type transcriptional regulator RovA (regulator of virulence A) (Nagel *et al.*, 2001) that is further controlled by a regulatory cascade, which is governed by the global carbon storage regulator (Csr) system (Heroven and Dersch, 2006; Heroven *et al.*, 2008).

The Csr system modulates gene expression on the post-transcriptional level in response to the metabolic state of the cell thereby affecting motility, the carbon flux and bacterial pathogenicity. It is composed of non-coding RNAs (ncRNAs) CsrB and CsrC in *Yersinia* and a protein antagonist referred to as CsrA. CsrA alters the stability and translation of its target mRNAs by direct interaction with GGA motifs within the Shine-Dalgarno (SD) sequence, while the ncRNAs possess high-affinity binding-sites for CsrA sequestration to antagonize its function and to control the availability of active CsrA proteins in the cell (Romeo, 1998; Heroven *et al.*, 2012a; Romeo *et al.*, 2013).

As the Csr-type RNAs determine the amount of active CsrA in the cell, homeostasis and expression of these structural RNAs is a tightly controlled process (Gudapaty *et al.*, 2001). Among the several different factors that appear to be involved, the *Yersinia* CsrA protein is indispensable to maintain integrity of the Csr-type RNAs CsrB and CsrC (Böhme, unpublished data). Furthermore the ncRNAs

are subject to counter-regulation, which implies upregulation of one RNA and subsequent downregulation of the other RNA and *vice versa* (Heroven *et al.*, 2008).

For *Y. pseudotuberculosis* it was shown that the regulatory RNA CsrB is controlled by the BarA/UvrY two-component system (TCS) in response to yet unknown environmental signals (Heroven *et al.*, 2008). Furthermore, the cAMP receptor protein Crp indirectly controls this TCS leading to repression of *csrB* expression and consequently induces *csrC* expression. Additionally, Crp exerts a positive effect on CsrC levels by a so far unknown mechanism, which is independent of the counter-regulation between both Csr-type RNAs (Heroven *et al.*, 2008; Heroven *et al.*, 2012b).

Recent findings from our group particularly highlight the importance of the CsrC RNA for expression of the global virulence regulator RovA that activates invasin synthesis. This observation prompted us to screen for *Yersinia*-specific regulators that affect *csrC* expression in *Y. pseudotuberculosis*. Here, we describe regulation of the CsrC RNA by the transcription factor RovC and characterize its expression pattern. Moreover, we identify a type VI secretion system (T6SS) as further RovC target that is potentially associated with *Yersinia* virulence.

Results

Identification and characterization of RovC - a new virulence-associated factor of Y. pseudotuberculosis

In order to identify regulatory factors that control *csrC* expression, a plasmid-borne gene library (pACYC184 backbone) from *Y. pseudotuberculosis* YPIII was introduced in the wildtype strain carrying a *csrC-lacZ* reporter plasmid (pKB46) harbouring the first 81 nucleotides of the *csrC* gene. By using this reporter construct, transcriptional and post-transcriptional regulators should be found. Approximately $2x10^3$ clones were screened on X-Gal agar plates at 25°C. Three candidates were isolated. Two formed darker blue colonies and exhibited significantly increased *csrC-lacZ* activity (>150%), while one candidate formed pale blue colonies and exhibited significantly reduced *csrC-lacZ* expression levels (< 60%) at 25°C (Fig. 1 A). The first two candidates harboured gene bank plasmids encoding either the Crp or the Hfq protein of *Y. pseudotuberculosis,* which were previously shown to positively affect CsrC levels in the cell (Böhme, unpublished data; Heroven *et al.*, 2012b), demonstrating that the selection procedure was successful and reliable. The latter clone, which bared a negative effect on *csrC-lacZ* expression, carried a single, common open reading frame (ORF), encoding a hypothetical protein of 247 amino acids (YPK_3567). *In silico* analyses using the BLAST algorithm showed that this gene is highly conserved in two pathogenic members of the genus - *Y. pestis* and *Y. pseudotuberculosis* but cannot be found in *Y. enterocolitica* or other *Yersinia* species. It does not exhibit homology to any known and characterized protein domain. The new protein was

named RovC for regulator of virulence associated with CsrC. It is located directly downstream of a type VI secretion system and upstream of YPK_3568 encoding for a pseudouridine synthase.

In order to evaluate the impact of RovC on the expression of *csrC*, a *rovC* mutant strain was generated. First, *csrC-lacZ* expression in *Y. pseudotuberculosis* YPIII (wildtype) and a *rovC* deletion mutant (YP148) was assessed. Furthermore, CsrC transcript levels were monitored. Interestingly, deletion of the *rovC* gene lead to a small, but not significant induction of *csrC* expression, whereas RovC overproduction significantly repressed *csrC* transcription (Fig. 1 B).

Northern blot analyses clearly demonstrated that a rovC deletion leads to increased CsrC levels (Fig. 1 C). Next, post-transcriptional effects of RovC on the CsrC RNA were analysed by comparing the CsrC RNA stability in Y. pseudotuberculosis YPIII (wildtype) and YP148 (ΔrovC). Transcription was stopped by the addition of rifampicin and samples were taken directly and after 80 min. The fold change of transcription levels was similar in the presence and absence of RovC. This indicated that neither RovC deletion nor overproduction lead to altered CsrC stability (Fig. 1 D), suggesting that RovC acts as a transcriptional repressor of CsrC.

RovC controls invasin expression through the Csr-RovM-RovA signalling cascade

Recently it was shown, that the *Y. pseudotuberculosis* Csr system controls a subset of genes (*rovM*, *rovA*), which in turn modulates expression of the primary internalization factor invasin (Heroven *et al.*, 2008). To analyse if RovC acts via CsrC on the whole Csr-cascade, we monitored *rovM, rovA* and *invA* expression levels in *Y. pseudotuberculosis* YPIII (wildtype) and YP148 (Δ*rovC*). As shown in Fig. 2, loss of *rovC* did not significantly change expression levels of *rovM* or *rovA*. In contrast, expression of a *rovM'-'lacZ* fusion and endogenous RovM levels were strongly induced upon RovC overproduction. Accordingly, *rovA'-'lacZ* fusions and endogenous RovA and InvA levels were significantly repressed, demonstrating that RovC modulates the whole Csr cascade.

In conclusion, RovC-dependent invasin synthesis was shown to occur via the Csr-RovM-RovA cascade, when RovC was overexpressed.

RovC is unique in Yersinia

BLAST analyses revealed that RovC is unique in *Y. pestis* and *Y. pseudotuberculosis*. Nevertheless it might be possible that factors, which are present in other bacterial strains, can modulate *rovC* expression. To test this hypothesis we monitored the expression of a translational *rovC'-'lacZ* fusion in *E. coli in comparison to Y. pseudotuberculosis.* While *rovC* expression was basal in *E. coli*, it was significantly induced in *Y. pseudotuberculosis*, but was still elevated in comparison to the empty vector control (pV) (Fig. 3). This strongly suggests that *Yersini*a-specific factors are required for full RovC activation.

The rovC *gene is activated during stationary growth at moderate temperatures*

During host-colonization bacteria face a rapidly changing environment regarding temperature, nutrient and oxygen supply, ion availability and the surrounding pH. Especially the temperature shift from a moderate tempered environment (15°C - 25°C) to the warm-blooded host (37°C) is a major factor that regulates virulence gene expression in *Yersinia.* In addition to temperature the growth phase and nutrient availability are crucial parameters in controlling gene regulation. In order to gain more information about RovC and its expression pattern we constructed *rovC* transcriptional and translational fusions. The transcriptional start site (TSS) of rovC was determined by *in vitro* transcriptome data (A. Nuss, unpublished data) and starts 39 nucleotides upstream of the translational start. Accordingly, the translational fusion harboured the first fifty nucleotides relative to the transcriptional start site of *rovC*, while the transcriptional fusion ended directly upstream of the Shine-Dalgarno sequence. Our data show that expression of the *rovC'-'lacZ* translational reporter fusion was slightly induced at 25°C during stationary growth (Fig. 4 B). This was confirmed by comparing RovC transcript levels (Fig. 4 C): RovC mRNA transcripts were detectable at 25°C but not at 37°C. *In vitro* transcriptome data could confirm the finding, that RovC mRNA is maximally expressed at 25°C during stationary growth (Nuss, unpublished data), suggesting that it might not be expressed *in vivo*/ in the mammalian host. Notably, RovC transcript levels were consistent with the translational fusion but not with the transcriptional fusion (Fig. 4 A), indicating that post-transcriptional regulation might be involved in RovC control. Although we detected high *rovC* expression levels with the translation fusion, the transcriptional fusion exhibited only basal expression and the RovC mRNA was barely detectable.

Crp and CsrA repress rovC *expression*

RovC is associated with the Csr system as it regulates *csrC* transcription and therefore has an impact on the downstream genes *rovM*, *rovA* and *invA*. So far, Crp and the CsrA protein itself were found to be important regulators that control the Csr system in *Yersinia* (Heroven *et al.*, 2012a; 2012b). To monitor whether these factors might also influence *rovC* expression, we introduced transcriptional and translational *rovC* reporter fusions (as described above) into the two different mutant strains and monitored their expression.

As shown in Fig.5 *rovC* expression was increased in a *crp* mutant background for both *rovC-lacZ* fusions. *In trans* complementation with a Crp^+ plasmid reduced the transcriptional *rovC-lacZ* to wildtype levels in the *crp* mutant strain, whereas the translational fusion was partially restored (Fig. 5 A+B). CsrA exhibited a strongly pronounced effect on *rovC* expression. Loss of the *csrA* leads to highly increased *rovC* transcription (Fig. 5 A), which can be complemented with a $csrA^+$ plasmid. The translational fusion also indicated CsrA-dependent *rovC* expression (Fig. 5 B). Herein, CsrA

overexpression even further repressed *rovC* translation. From these data we concluded that Crp and CsrA function as transcriptional repressors of RovC. In consideration of the enhanced repressional impact of CsrA on the translational fusion, CsrA-mediated repression might include additional sequences in the first nucleotides of the *rovC*- coding region.

Next, the impact of Crp and CsrA on the RovC mRNA transcript levels and on endogenous RovC protein concentration was monitored. Northern blot analyses in YPIII, YP89 (Δ*crp*) and YP53 (Δ*csrA*) indicated elevated RovC transcript levels in both mutant strains compared to the wildtype, whereby the repressional impact of CsrA was most pronounced (Fig. 5 C). Northern blot results confirmed the promoter-fusion experiments (Fig. 5 A+B) and demonstrated a negative impact of Crp and CsrA on *rovC* expression. Moreover, it became evident that there was nearly no RovC transcript detectable in the *Yersinia* wildtype strain.

In order to analyse if the elevated RovC mRNA levels lead to increased amounts of endogenous RovC protein, a plasmid-based His-tagged version of RovC (C-terminal His-tag), under control of its own promoter, was introduced into the cells. Immunoblotting with an anti-His antibody revealed increased amounts of endogenous RovC protein in the *csrA* and *crp* mutant strains compared to the wildtype (Fig. 5 D). Herein, loss of *csrA* exerted the strongest derepression on endogenous RovC, confirming the results obtained from the northern blot analysis.

CsrA directly interacts with RovC mRNA

Expression analysis of transcriptional and translation *rovC-lacZ* reporter constructs indicated that CsrA might act as transcriptional repressor of *rovC*. However, CsrA is well known as post-transcriptional regulator that controls the stability of its target mRNAs and usually induces rapid degradation (Romeo *et al.*, 2013). According to this, we examined the role of CsrA on *rovC* synthesis more closely.

First RovC transcript levels were compared in the *Y. pseudotuberculosis* wildtype strain (YPIII) and the *csrA* mutant strain (YP53). As shown by the northern blot (Fig. 6 C) RovC transcript levels were highly increased in a *csrA* mutant in comparison to the wildtype and could be complemented with a $csrA^+$ plasmid. CsrA homodimers preferentially bind RNA consensus sequences like 5'-$_A/_U$CANGGANG$_U/_A$-3' (N = any nucleotide) (Schubert *et al.*, 2007). With regard to a recently performed *in vitro* transcriptome analyses (A. Nuss, unpublished data) the transcriptional start site (TSS) of the *rovC* leader transcript was mapped 39 nucleotides upstream of the RovC translational start codon ($RovC_{AUG}$). Within this region, in addition to the GGA motif of the Shine-Dalgarno sequence, a second GGA motif was localized in close proximity to the TSS. Further 32 nucleotides downstream of the $RovC_{AUG}$ a third 5'-GGA-3' motif was present (Fig. 6 A).

In order to see whether CsrA interacts directly with the RovC 5'-UTR, electrophoretic mobility shift assays (EMSAs) were performed. RNA was *in vitro* transcribed from a PCR template, harbouring the T7 promoter for the bacteriophage T7 RNA polymerase. The *in vitro* transcribed RovC RNA fragment (overall length = 75 nt) harboured all three putative CsrA-binding sites. The CsrA protein was heterologously expressed in *E. coli* BL21λDE3 and affinity purified via a C-terminal His-tag. 10 pmol of RNA were incubated with increasing amounts of protein. EMSA analysis clearly demonstrated a direct interaction of CsrA with the 5'-UTR of *rovC* (Fig. 6 B). Initial interactions of the RovC transcript and the CsrA protein occurred, when a 2.4-fold excess of CsrA protein was applied (24 pmol CsrA protein). This corresponds to the model that CsrA binds to RNA as a homodimer (Schubert *et al.*, 2007). RovC mRNA is fully shifted in presence of 56 pmol to 75 pmol CsrA protein, indicating that at least two binding sites may exist. In comparison to the RovM negative control, which shows a slight, unspecific CsrA-binding, the CsrA-RovC interaction is clearly more specific, even at lower protein concentrations.

To analyse whether CsrA influences RovC mRNA degradation or stabilization, we compared the RovC mRNA stability in *Y. pseudotuberculosis* wildtype (YPIII) and the *csrA* mutant strain (YP53). Therefore both strains were transformed with a midi-copy plasmid harbouring RovC under control of its own promoter, as RovC mRNA is barely detectable in the wildtype background. Our data revealed, that two different phenomena can be observed. Like previously shown in the northern blot (Fig. 6 C) overall RovC mRNA levels were drastically increased in the *csrA* mutant strain in comparison to the wildtype (Fig. 6 D). Surprisingly, a reciprocal impact of CsrA on RovC mRNA stability was observed. When CsrA was absent, the transcript stability of RovC was reduced by more than 50%. In the wildtype background RovC had a half-life of about 41 minutes, while this was reduced to 13 minutes in the absence of CsrA, indicating that CsrA exerts a stabilizing effect on this mRNA target.

From these data we conclude that CsrA acts as repressor most presumably by indirectly repressing *rovC* transcription but by directly interfering with *rovC* translation. Surprisingly CsrA is absolutely required for RovC stabilization, which is mediated by direct CsrA-binding to the 5'-UTR of RovC.

Microarray analysis of RovC-dependent gene expression reveals activation of a virulence-associated type VI secretion system

To identify additional genes under control of RovC, a microarray was performed using total RNA from *Y. pseudotuberculosis* YPIII (wildtype) and YP148 (Δ*rovC*) grown at 25°C to stationary phase in DMEM-F12 medium. The impact of RovC on CsrB and CsrC levels was most pronounced under these conditions (data not shown). Mixed Cy3- (Δ*rovC*) and Cy5-(wildtype) labelled RNA was hybridized to an Agilent customized microarray carrying 4172 chromosomally-encoded and 92 plasmid-encoded genes of *Y. pseudotuberculosis*.

In total, 56 genes showed 1.7-fold or greater difference in transcript abundance between the wildtype and the *rovC* mutant strain (Tab. S). Majority of these genes was activated by RovC, whereas only two genes were repressed.

About fourteen of all RovC-dependent transcripts were related to metabolic adaptation processes and another twelve encoded for hypothetical proteins and other genes with unknown function. The remaining transcripts were related to virulence (ten genes), genetic information processing (ten genes), cellular processes and transport and secretion (ten genes) (Fig. 7 A). Accordingly, RovC seems to play a role in virulence but also in metabolic responses and is involved in information processing with regard to genetic and cellular relevance.

Remarkably, RovC activated nine genes belonging to one operon. BLAST analyses revealed that the whole cluster belongs to the type VI secretion operon-4 of *Y. pseudotuberculosis* YPIII (T6SS4, gene IDs from YPK_3550 to YPK_3566) (Fig. 7 C). This operon encompasses 16 genes with a total size of 23.6 kb. Especially the *hcp* gene (YPK_3563) is strongly down-regulated (19-fold) in a *rovC* mutant. This gene encodes for the hemolysin-coregulated protein. Hcp from *P. aeruginosa* forms hexameric nanotubules that resemble the bacteriophage T4 tail and is a major component of the bacteriophage-like subassembly of the T6SS, which contacts the target cells (Mougous *et al.*, 2006; Ballister *et al.*, 2008). These tubules emerge at the cell surface but can also be secreted into the surrounding medium (Osipiuk *et al.*, 2011; Jones *et al.*, 2014).

To validate the results obtained from the microarray analysis, we performed RT-PCR of four identified RovC targets (T6SS genes) and one unrelated gene. As shown in Fig. 7 B the unrelated gene YPK_3548 directly upstream of the T6SS cluster was not affected, while the other candidates that belonged to the T6SS4 were significantly downregulated when *rovC* was absent. Strikingly the *rovC* gene is located directly downstream of this operon (Fig. 7 C), encoded in the opposite direction. According to this characteristic organization, RovC might be a perfect candidate for a transcription factor assigned to this T6S system.

RovC activates T6SS4 expression in response to moderate temperatures

To verify that the identified T6SS4 is indeed activated by RovC, we constructed a translational reporter fusion that harboured the promoter region of the first gene (YPK_3566) of this operon. Expression of this reporter fusion was compared in YPIII and YP148 (Δ*rovC*). Results clearly demonstrated that RovC is crucial for the activation of this T6SS4 (Fig. 8). In *Y. pestis* and *Y. pseudotuberculosis* YPIII and IP31758 expression of the T6SS4 operon was found to be temperature-regulated. Accordingly, it is preferentially expressed at moderate temperatures, while it is inactive at elevated temperatures like 37°C (Pieper *et al.*, 2009; Zhang *et al.*, 2011; Gueguen *et al.*, 2013). To prove these findings, we compared the expression of the T6SS4 reporter fusions at 25°C

and 37°C in presence or absence of the *rovC* gene. We observed that expression of the T6SS was switched on at 25°C, whereas no activity was found at 37°C (Fig. 8 C). Herein, presence of RovC was absolutely required to activate T6SS expression. Furthermore overexpression of RovC could activate T6SS expression under non-inducing conditions at 37°C (Fig. 8 B), clearly demonstrating that RovC is absolutely required for T6SS4 activation.

Discussion

Genomic studies and experimental approaches revealed that almost all Csr/Rsm system encompass more than one Csr/Rsm RNA (Lenz *et al.*, 2005; Kulkarni *et al.*, 2006; Lapouge *et al.*, 2008). Especially *Vibrio cholerae* and *Pseudomonas fluorescence* possess three different Csr-type RNAs (Lenz *et al.*, 2005; Kay *et al.*, 2005). For several species it was shown that these ncRNAs can complement for one another (Cui *et al.*, 1996; Weilbacher *et al.*, 2003; Lenz *et al.*, 2005), whereas this was not the case in *Y. pseudotuberculosis.* This pathogen harbours at least two Csr-type RNAs, CsrB and CsrC, that seem to be differentially regulated and might serve diverse functions accordingly. For instance Crp controls CsrB expression via repression of the UvrY response regulator of the BarA/UvrY TCS (Heroven *et al.*, 2012b), while not much is known about CsrC control.

Screening of a genomic library of *Y. pseudotuberculosis* for additional CsrC regulators revealed a hypothetical protein (YPK_3567) that was found to control *csrC* expression and was designated as regulator of virulence associated with CsrC (RovC). Within this work, the novel factor was confirmed to be a protein that encompasses 247 amino acids and is highly conserved among *Y. pestis* and *Y. pseudotuberculosis*. However, it does not exhibit homology to any known protein or even contains a conserved DNA-binding domain. Furthermore, RovC overexpression lead to significant repression of *csrC* transcription, while deletion of this factor promoted increased expression of a transcriptional *csrC-lacZ* reporter fusion and elevated CsrC levels in the cell. So far, it is unclear whether RovC exerts a direct effect on CsrC, as attempts to overproduce and purify RovC protein for DNA-binding studies failed. Deletion of *rovC* exerts minor effects on the Csr downstream genes *rovM, rovA* and *invA,* whereas RovC overexpression leads to dramatic changes in the endogenous RoM, RovA and invasin levels, as RovA and hence invasin are only barely detectable in a *rovC*$^{+}$ strain.

Concluding, these results indicate that RovC might constitute an important additional regulator that controls the abundance of the CsrC RNA and therefore might affect the level of free CsrA molecules in response to certain environmental conditions, which in turn affect the early virulence genes.

The overall amount of RovC seems to be very low at laboratory growth conditions, as the RovC mRNA and the endogenous RovC protein were barely detectable via northern and western blotting. RovC is maximally synthesized at 25°C during stationary growth, while it is basally expressed at 25°C and 37°C in the exponential phase. *CsrC* is maximally expressed during the late stationary phase at

25°C and is mainly affected by the composition of the growth medium. This Csr-type RNA exerts low levels in minimal medium while it is highly activated in complex medium such as LB (Heroven *et al.*, 2008a). Recently Crp and UvrY were shown to be indirectly involved in *csrC* expression control (Heroven *et al.*, 2012b). However, neither Crp nor UvrY contribute to CsrC regulation in response to the nutrient-availability. As shown in this study, even RovC does also not participate in this nutrient-dependent control of CsrC, but it might be involved in the temperature- and growth phase-dependent regulation.

Interestingly, only basal expression of *rovC* was reported in an *E. coli* background, implicating that RovC is not only a *Yersinia* specific factor, but might also require a *Yersinia* specific activator. Nevertheless, negative regulators that were found to control *rovC* synthesis are also present in *E. coli:* the cAMP receptor protein Crp and the global regulator CsrA.

Under glucose-limiting conditions cAMP-Crp complexes bind their target DNA an thus control gene expression in response to the nutrient availability (Gunasekera *et al.*, 1992; Saier, 1998; Zheng *et al.*, 2004). Recently, a tight connection of the cAMP-Crp regulatory system and the Csr system was shown to link carbon metabolism and *Yersinia* virulence (Heroven *et al.*, 2012b). Accordingly, Crp activates *csrB* transcription via repression of the response regulator UvrY. Resulting from the counter-regulation of both Csr-type RNAs, *csrC* expression is abolished in a *crp* mutant strain. As shown in the present study, loss of *crp* leads to highly increased *rovC* expression, which is reflected by elevated levels of RovC mRNA and endogenous protein. Most interestingly, only the transcriptional fusions could be fully complemented by Crp overexpression. Contrary, the translational fusion was only partially complemented. In general, Crp could function as transcriptional *rovC* repressor. The Crp consensus sequence is described as TGTGA-N_6-TCACA (Kolb *et al.*, 1993; Busby and Ebright, 1999). The first consensus (TGTGA) of this region is found 141 nt upstream of the transcriptional start site of *rovC*, while the second half comprises CAACC instead of TCACA and hence differs from the proposed binding site. Nevertheless, it might be plausible that Crp directly represses *rovC* transcription, but prospective experimental evidence is indispensable.

Besides Crp, CsrA seems to be the most important regulator of RovC. Interestingly, CsrA bears both, transcriptional and post-transcriptional effects on *rovC* expression in *Y. pseudotuberculosis*. Upon loss of *csrA,* highly increased RovC mRNA levels and protein concentrations were denoted. CsrA is known to act via binding to its target mRNA thus influencing translation and/or stability of the mRNA (Romeo, 1998). Target recognition involves CsrA-binding to unpaired nucleotides (Schubert *et al.*, 2007). Since unpaired regions are typical features of RNA secondary structures and are not found in DNA duplexes, it is unlikely that CsrA directly affects *rovC* transcription. Nonetheless, CsrA-mediated transcriptional effects on other components of the Csr system have been reported previously. Weilbacher *et al.* (2003) revealed an indirect positive transcriptional effect of CsrA on *csrC* in *E. coli,*

which did not involve CsrA-mediated RNA stabilization. So far, the underlying mechanism is unknown but it is likely to occur indirectly. Moreover, CsrA was shown to indirectly activate its own transcription by activating the expression of σ^S, which in turn stimulates *csrA* transcription (Yakhnin *et al.*, 2011).

In addition to transcriptional repression, CsrA prevents *rovC* translation as the translational *rovC'-'lacZ* fusion was strongly repressed upon CsrA overexpression. *In vitro* gel shift assays indicate a direct interaction between CsrA and the RovC upstream region (5'-UTR +38 nt of *rovC* coding region). *In silico* analyses predict two distinct *rovC* secondary structures, which both possesses a base-paired ribosomal binding site. This would indicate that CsrA-binding to the GGA motif within the SD sequence is not possible. However, both predicted structures bear one accessible GGA motif, either in close proximity to the upstream or downstream site of the ribosomal binding site (RBS). With regard to this structure, one would assume that CsrA binds first to the exposed GGA motifs and has no access to the GGA motif within the SD sequence.

However, recent studies in *P. aeruginosa,* which harbours the CsrA homologue RsmE, could show that RsmE protein dimers bind to their RsmZ sRNA target (homologue to CsrB) in a sequential, specific and cooperative manner (Duss, 2012; Duss *et al*., 2013). The model shows that initial RsmE-binding leads to conformational changes in the RNA secondary structure, which then provides the structural basis for additional RsmE-binding. A related mechanism is proposed for RsmE-binding to the *hcnA* 5'-UTR in *P. fluorescence* (Schubert *et al.*, 2007) and CsrA-binding to the *glgC* 5'-upstream region in *E. coli* (Mercante *et al.*, 2009). RsmE-binding to HcnA implies additional GGA motifs in the SD upstream region. When these GGA sequences are tightly gripped by RsmE, they fold into a loop structure that is fixed by a 3 base-pair stem (Schubert *et al.*, 2007). GGA motifs upstream the *glgC* SD sequence represent a high affinity CsrA biding site that mediates CsrA-binding to the low-affinity binding site within the SD (Mercante *et al.*, 2009). Both experiments demonstrate initial CsrA-binding events to the terminal GGA motif, that provoke conformational changes in the RNA secondary structure to render the SD sequence accessible for the second RsmE/CsrA-binding surface. Sequential CsrA binding leading to changes in the RNA secondary structure might also be involved in RovC-CsrA interactions. Initial RsmE/CsrA-binding usually requires a high-affinity binding-site with a sequence motif of 5'-$^{A}/_{U}$CAN<u>GGA</u>NG$^{U}/_{A}$-3', that is located upstream of the SD sequence (Schubert *et al.*, 2007). Strikingly, the 5'-terminal GGA motif exhibits a nearly perfect high affinity RsmE/CsrA-binding site (as proposed by Schubert *et al.*, 2007), emphasizing the discussed hypothesis of CsrA-RovC interaction. The importance of the 5'- GGA motif is further stressed by the translational *rovC'-'lacZ* fusion, which exhibits strong CsrA dependency, but lacks the downstream GGA motif. Accordingly, the GGA located downstream of the RBS is supposed to play a minor role during CsrA-RovC interaction. Besides the sequential binding that goes along with structural rearrangements of the RNA, CsrA dimers

preferentially bind to recognition sites that are interspersed by ≥18 nt (Mercante *et al.*, 2009). Notably, the GGA motif in close proximity to the 5'-end of the RovC upstream region provides optimal spacing of exactly 18 nt to the SD site, further supports the involvement of conformational changes upon initial CsrA-binding to the first recognition site.

CsrA-binding to the SD sequence of target transcripts usually destabilizes the messenger, e.g. *pgaABCD* anf *glgCAP* mRNA in *E. coli* (Baker *et al.*, 2002; Pannuri *et al.*, 2011). In contrast, RovC mRNA stability assays indicate destabilization of the RovC mRNA when CsrA is absent. In exceptional cases CsrA-binding promotes protection of the 5'-end from RNase E-mediated cleavage and stabilizes the transcript (Yakhnin *et al.*, 2013). In particular, CsrA-binding to the extreme 5'-end of the *flhDC* leader RNA occupies RNase E cleavage sites (AU-rich sequence) and confers protection from this ribonuclease. *In silico* modelling of the RovC upstream region reveals a single stranded AU-rich sequence that might constitute a putative RNase E target site. CsrA-binding could render this target site inaccessible for RNase E-mediated cleavage, leading to transcript stabilization. In absence of CsrA, translation of the *rovC* transcript is highly increased. Despite of representing RNase E cleavage sites, AU-rich sequences in the 5'-UTRs of mRNAs represent target sites for the ribosomal protein S1 (Arnold *et al.*, 1998). Moreover, a high degree of mRNA occupancy by ribosomes in the 5'-UTR represents a physical hindrance of RNase E-binding and protects the messenger from degradation (Arnold *et al.*, 1998; Komarova *et al.*, 2002; Komarova *et al.*, 2005). In the presence of CsrA, ribosomes could be replaced by the homodimer leading to translational blockage (as seen with the translational reporter fusion). Whether CsrA-binding to RovC mRNA really leads to degradation or is protective still needs to be elucidated. However, with regard to the binding model presented above and the strong CsrA-mediated repressional impact on the translational *rovC'-'lacZ* fusion, it seems likely that CsrA-binding to the RovC mRNA blocks translation.

Taken together, the *rovC* expression analysis with regard to the two regulators Crp and CsrA could also represent an interconnected network that is involved in fine-tuning the *csrC* expression level (Fig. 9). Crp might either directly bind to the *rovC* promoter region or might indirectly act on *rovC* expression by modulating the CsrB levels in the cell (via UvrY). Loss of *crp* leads to dramatic increases in CsrB concentration, which might in turn sequester CsrA proteins from RovC RNA, relieving the repressional effect. All these connections might resemble an interdependency of the three regulators that are all involved in maintaining CsrC levels in the cell and hence tightly control the global Csr system. DNA-binding and epistasis studies will help to unravel these hypotheses.

Expression analysis of RovC revealed a very limited transcript and protein abundance in the *Y. pseudotuberculosis* YPIII wildtype strain under standard growth conditions (complex medium, 25°C stationary phase). The strongest influence of RovC was observed upon overproduction e.g. on the Csr-RovM-RovA cascade.

Microarray analysis, comparing the transcriptome of the *Yersinia* wildtype and its isogenic *rovC* mutant, identified a relatively small regulon of 54 RovC-activated genes, indicating that even a low *rovC* expression suffices to induce target gene expression. Among the 56 differentially regulated genes only two were repressed by RovC (a holin-family protein and one 4-oxalocrotonate tautomerase family enzyme). No impact was denoted for proteins belonging to the flagella, motility or chemotaxis apparatus of the cell or the stress adaptation machineries. Differential expression of some ribosomal proteins was denoted in a *rovC* mutant strain, which is accompanied by upregulation of distinct genes that are involved in amino acid metabolism and energy production. Also, RovC regulates proteins involved in cell wall biogenesis. For instance, RovC activates the *ompA* gene that encodes for a porin, which is required for diffusion of small solutes, plays a role as phage receptor molecule, maintains the structural integrity of the bacterial cell and mediates host cell attachment of *E. coli* (Wang, 2002; Shin *et al.*, 2005; Sandrini *et al.*, 2013).

Most remarkably, the present data show that RovC is not only a repressor of CsrC but is further an activator of the type VI secretion system T6SS4 in *Y. pseudotuberculosis*. Most recently, type VI secretion systems have been discovered as versatile nanomachines, which structurally resemble the puncturing device of bacteriophages. Although the overall architecture and structural components of T6SSs are well conserved among the different species, their functionality and regulation is multifaceted and adopted to the specialised needs of the particular organism and its biological niche. To reduce the energetic costs that go along with assembly, contraction and disassembly of the organelle in response to the diverse stimuli, T6S is tightly controlled on the transcriptional and post-transcriptional level (Mougous *et al.*, 2007; Kitaoka *et al.*, 2011).

Comparative genome analysis in *Yersinia* revealed the presence of four complete and two incomplete T6SS loci (T6SS1-T6SS6) in *Y. pseudotuberculosis* YPIII (Zhang *et al.*, 2011). The four complete clusters are composed of 13 core components as defined by Boyer *et al.* (2009), and are organized in huge operons and possibly serve different functions in dependence on the surrounding conditions (Bingle *et al.*, 2008; Pukatzki *et al.*, 2009). The T6SS4 belongs to a special cluster that is unique in *Y. pestis* (YPO0499-YPO0516 or y3658-y3677) and *Burkholderia spp* in concern of sequence and organization homologies (Zhang *et al.*, 2011). In contrast to the other T6SS clusters found in *Yersinia*, it appears to be controlled from a single promoter and is strongly influenced by the surrounding temperature (Han *et al.*, 2004; Cathelyn *et al.*, 2006; Pieper *et al.*, 2009).

Interestingly, RovC is genetically linked to the T6SS4 of *Y. pseudotuberculosis* as it is located immediately downstream of the T6SS4 operon in the opposite direction (Fig. 7). Expression analyses of the T6SS4 indicated a temperature-dependent regulation. T6SS4 is expressed at 25°C but not at elevated temperatures like 37°C. This is in-line with the findings that RovC is maximally induced at moderate temperatures and hence can activate expression of its associated T6SS4 operon. This

thermally controlled synthesis has also been observed by Zhang et al., (2011; 2013). Additionally, they could demonstrate that the effector protein Hcp is released, indicating that T6SS4 is not only expressed but also functional at 25°C. Hcp is the hallmark of a functional T6SS. Hcp orthologs are found throughout the organisms that carry T6SS gene clusters and seem to be crucial structural components on the one hand and vital effectors with regard to bacterial virulence (Pukatzki *et al.*, 2009). For instance, the human pathogen *Burkholderia pseudomallei,* defective for *hcp,* reveals an attenuated phenotype in the mouse model of infection (Hopf *et al.*, 2014). Most strikingly, *hcp* expression is 20-fold reduced in a Δ*rovC* background (Tab. S), whereas the remaining T6SS genes are affected to a lesser extent. This might point towards post-transcriptional modifications (e.g. separation of distinct mRNAs by RNases), as all genes of this operon are transcribed as one polycistronic RNA. With regard to bacterial virulence the precise role of the Hcp protein has not been described yet and will be subject of future analysis. Nonetheless, as suggested by Gueguen and co-workers expression of T6SS4 might be beneficial to *Y. pseudotuberculosis* YPIII in the environmental reservoir or during competition with the gut-microbiota rather than in the mammalian host.

In a nutshell, RovC was discovered as transcriptional repressor of CsrC, that affects the downstream genes *rovM*, *rovA* and *invA* via the Csr cascade. Furthermore RovC activates expression of the type VI secretion system T6SS4, which might be beneficial during environmental survival of the bacteria or during competition with the host microbiota.

RovC itself is expressed at moderate temperatures and tightly controlled by Crp and CsrA - two factors that govern the Csr system. The RNA-binding protein CsrA directly interacts with the RovC 5'-UTR to administer its turnover and indirectly controls its transcription. The explicit RovC working-model is summarized in Fig. 9.

Experimental procedures

Bacterial strains, media and growth conditions

All strains are listed in Tab. . *E. coli* strains were routinely grown at 37°C in LB (Luria-Bertani) medium, while *Y. pseudotuberculosis* was incubated at 25°C in LB (if not indicated otherwise) and grown to stationary phase. If necessary antibiotics were added in the following concentrations: carbenicillin 100 µg ml^{-1}, chlormaphenicol 30 µg ml^{-1}, kanamycin 50 µg ml^{-1}, tetracycline 5 µg ml^{-1}.

Construction of the Y. pseudotuberculosis *gene bank and screening for factors that influence* csrC-lacZ *expression in* Y. pseudotuberculosis

The *Y. pseudotuberculosis* gene bank was constructed as described previously (Nagel *et al.*, 2001) and introduced into *Y. pseudotuberculosis* YPIII harbouring a plasmid-based *csrC-lacZ* fusion (pKB46). Gene bank plasmids of clones that either showed increased or decreased *csrC-lacZ* expression on agar plates supplemented with X-Gal, were isolated and retransformed into the YPIII reporter strain to verify their influence on *csrC-lacZ* expression. Finally, the plasmids were sequenced; the respective ORF was subcloned and again verified in the YPIII reporter strain.

DNA manipulation and plasmid construction

All DNA manipulations, restriction digests, ligations and transformations were performed according to standard genetic and molecular techniques (Miller, 1992; Sambrook, 2001). The plasmids used in this work are listed in Tab. . Oligonucleotides used for PCR, sequencing, RT-PCR and probe generation were purchased from Metabion (Martinsried, Germany) and are indicated in Tab. 2. PCR reactions were performed in 100 µl aliquots for 29 cycles using *Taq* polymerase (NEB) or Phusion High-Fidelity DNA polymerase (Finnzymes) according to the manufacturer's instructions. PCR products were purified with the QIAquick PCR purification kit (Qiagen, Germany) before and after digestion of the amplicon. Plasmid DNA was purified using a Qiagen kit. Restriction and DNA-modifying enzymes were obtained from Roche, Promega or NEB. Sequencing reactions were performed at the GMAK in-house facility.

Plasmids used in this study are listed in Tab. 1 and primers for plasmid generation are indicated in Tab. 2. The *rovC*$^{+}$ fragment of *Y. pseudotuberculosis* YPIII from plasmid pSSE11 was generated by PCR using primers III286 and III287, digested with *Sal*I and *Bam*HI and inserted into pACYC184. Plasmids pSSE32 and pSSE64 carry PCR generated fragments harbouring the *rovC* promoter region encompassing 618 nt upstream of the translational start site (primer III779-III780) and the T6SS4 promoter region harbouring 503 nt upstream of the translational start site (primer IV735-IV736), respectively. The fragments were digested with *Bam*HI or *Bam*HI and *Sal*I respectively and cloned into the corresponding sites in pTS02. The *rovC* transcriptional fusion (pSSE67) harboured a PCR

generated fragment that encompassed 629 nt upstream of the ribosomal binding site (primer IV923-III779), was digested with *Bam*HI and cloned into the respective site in pTS03. The second transcriptional *rovC* fusion encompassed 604 nt upstream of the *rovC* transcriptional start site and was PCR amplified using primer pair III779 and V819. The resulting fragment was digested with *Bam*HI and *Sal*I and cloned into the respective site in pTS03. The transcriptional *csrC-lacZ* fusion (pKB46) was generated by PCR amplification of the *csrC* upstream region harbouring the first 81 nt of the gene (primer pair II65 and II67), digested with PstI and ligated into the respective site in pTS03. The plasmid harbouring a RovC C-terminal His-tag (pSSE68) was constructed by insertion of a PCR fragment amplified with primer III286 and V655 encoding for a hexa histidin-tag at the C-terminal part of RovC into pACYC184 digested with *Sal*I. The plasmid harbouring the CsrA protein with an N-terminal hexa histidin-tag (pAKH172) was constructed as follows: the complete *csrA* gene (180bp) was PCR amplified with primer pairs IV783-IV784 and digested with *Nco*I and *Xho*I and ligated into the respective site in pET28a(+).

The *rovC* deletion plasmid pSSE35 was generated by three-step PCR. First the upstream region was amplified by primers III920-III921 and the downstream region was amplified with primers III844-III845. Next, the kanamycin resistance cassette was amplified with primers I661-I662 from pKD4 as template. Then up- and downstream fragments were mixed with the kanamycin resistance cassette fragment to generate the rovC deletion fragment with primers III845-III920. The amplicon was digested with SacI and inserted into the corresponding site in pAKH3. In principle the invA deletion plasmid pRG06 was generated as described above. The upstream region was amplified using primer pair III992-III997, while the downstream region was amplified by primer pair III996-III994. Subsequently, the three-step PCR was performed with primer pairs III992 and III994, digested with SacI and ligated into the respective site in pAKH03.

The *Y. pseudotuberculosis* YP148 and YP191 mutant strains were constructed via homologous recombination with the pSSE35 and pRG06 suicide plasmids and derive from the wildtype strain YPIII. Plasmids were transferred via conjugation from *E. coli* S17-1λpir (*tra*$^{+}$) into *Y. pseudotuberculosis* YPIII. Transconjugants and mutant strains resulting from excision of the integrated plasmid were selected as described earlier (Nagel *et al.*, 2001). Strains harbouring the desired phenotype were confirmed by PCR and sequencing.

β-*Galactosidase assays*

The β-galactosidase activity of the *lacZ* reporter fusion constructs was measured in permeabilized cells as described previously (Nagel *et al.*, 2001) and was calculated as follows: OD_{420} * 6.75 *OD_{600}^{-1} * t $(min)^{-1}$ *Vol $(ml)^{-1}$

Western blotting

For detection of the regulatory proteins RovM, RovA, InvA and RovC-His_6 cultures of the *Y. pseudotuberculosis* strains were grown at the indicated environmental growth conditions. Whole cell extracts were prepared from equal amounts of bacteria and separated by Tris-TRICINE PAGE and blotted onto nitrocellulose membranes (Sambrook, 2001). Subsequently, membranes were blocked in 1x TBST-M (20 mM Tris/Hcl pH 7.5, 150 mM NaCl, 0.05% TWEEN-20, 5% non-fat dry milk). Primary polyclonal rabbit IgG antibodies (anti-RovM, anti-RovA) were diluted 1:8,000 in 1x TBST-M; primary monoclonal mouse IgG antibodies (anti-InvA, anti-His) were diluted 1:10,000 or 1:2,000 respectively in 1x TBST-M. Primary polyclonal rabbit IgG antibody against H-NS was used as loading control and diluted 1:10,000 in 1x TBST-M. The secondary antibodies, either anti-rabbit IgG conjugated with horseradish peroxidase or anti-mouse IgG conjugated with alkaline-phosphatase were supplied in 1:10,000 or 1:5,000 dilutions in 1x TBST-M. Immunological detection was performed as described earlier (Heroven *et al.*, 2008a; Heroven *et al.*, 2012b).

Northern blotting

For isolation of total RNA bacteria were cultured under the indicated conditions. Subsequently, 2 ml were harvested by centrifugation, mixed with 0.2 volumes of stop solution (5% phenol, 95% ethanol) and snap-frozen in liquid nitrogen. Bacteria were pelleted by centrifugation (1 min 12,000 rpm) and RNA was isolated using the SV total RNA purification kit (Promega) as indicated by the manufacturer. RNA concentration and quality was determined photometrically by measuring A_{260} and A_{280}.

For northern blotting RNA (5 µg) was mixed with loading buffer (0.03% (w/v) bromophenol blue, 4 mM EDTA pH 7.5, 0.1 mg/ml ethidium bromide, 2.7% (v/v) formaldehyde, 31% (v/v) formamide, 20% (v/v) glycerol in 4x MOPS buffer) and separated on agarose gels (0.7%), transferred onto positively charged nylon-membranes (GE Healthcare) by vacuum blotting for 1.5 h in 10x SSC and UV cross-linked. Prehybridization, hybrodization to DIG-labelled DNA probes and membrane washing was performed using the DIG luminescent Detection kit (Roche) according to the manufacturer's instructions. Primer pairs used for DIG-labelled probe amplification (DIG-PCR nucleotide mix, Roche) are listed in Tab. 2.

Expression and purification of CsrA

E. coli BL21λDE3 pAKH172 was grown at 37°C to exponential growth phase (OD_{600} = 0.4-0.6). Bacterial cultures were shifted to 18°C and expression of His-tagged CsrA (His_6-CsrA) was induced by adding 1 mM IPTG (isopropyl-β-D-thiogalactoside). After five hours of incubation cells were harvested by centrifugation (4°C, 10 min 6000 g) and resuspended in lysis buffer (50 mM Tris/HCl pH 8.0, 250 mM NaCl, 20 mM imidazol). Bacterial cells were lysed with a French Pressure cell (G.

Heinemann) and soluble His_6-CsrA protein was purified by a Ni-NTA agarose column (Macherey&Nagel). Unbound protein was removed by washing with two column volumes of wash buffer I (50 mM Tris/HCl pH 8.0, 250 mM NaCl, 20 mM imidazol) followed by washing with two column volumes of wash buffer II (50 mM Tris/HCl pH 8.0, 250 mM NaCl, 40 mM imidazol). The His_6-CsrA protein was eluted by applying elution buffer (50 mM Tris/HCl pH 8.0, 250 mM NaCl, 250 mM imidazol). The purity (>95%) was verified by SDS-PAGE and protein concentration was assessed by the Bradford assay (Bradford, 1976).

Electrophoretic Mobility Shift Assay

For RNA-binding studies the respective RovC and RovM RNA fragments were *in vitro* transcribed using the TranscriptAid™ T7 High Yield Transcription kit (Fermentas) from DNA templates. Templates were generated by PCR amplification with primers V773/V777 (*rovC*) and I523/I524 (*rovM*) that harboured the T_7 promoter from chromosomal DNA of YPIII. The run-off transcripts were purified by phenol:chloroform extraction, precipitated with ethanol and stored in RNAse-free water. RNA-binding reactions included 10 pmol RovC or RovM respectively, 1x RNA-binding buffer and increasing concentrations of CsrA protein. RNA was denatured for 10 min at 70°C and cooled down to room temperature to allow refolding of the RNA. RNA-protein mixtures were incubated at 25°C for 20 min and subsequently separated on 4% native TBE gels. Afterwards RNA-protein complexes were transferred onto nitrocellulose membranes by semi-dry blotting. RNA cross-linking and immunological detection was carried out as described elsewhere (Heroven *et al.*, 2012b).

Microarray analysis and data evaluation

Custom Microarray 8x15K slides from Agilent Technologies were designed by the webdesign application eArray available at (http://www.genomics.agilent.com). Sequences of the oligonucleotide probes were designed according to the NCBI Genome Genbank (NC_010465 and NC_006153) and encompassed 60 nt in length. The array covered three different probes for the 4172 chromosomal open reading frames (ORFs > 30 codons) from *Y. pseudotuberculosis* YPIII and six different probes for the 92 virulence plasmid (pYV) encoded ORFs from *Y. pseudotuberculosis* IP32953 (Heroven et al., 2012b).

RNA was prepared using the SV total RNA isolation kit (Promega) according to the manufacturer's instructions. Therefore 16 independent cultures of *Y. pseudotuberculosis* YPIII and the *rovC* mutant (YP148) were grown in DMEM-F12 medium at 25°C for 16h. Contaminating chromosomal DNA was removed by an additional DNaseI-step and checked for remaining DNA by PCR. RNA concentration and quality was assessed by means of an Agilent 2100 Bioanalyzer using the RNA 6000 Nano kit according to the manufacturer's instructions. A RIN (RNA integrity number) between 9 to 10 was

indicative for high quality RNA without degradation. Subsequently total RNA from four independent cultures was pooled and appr. 1 µg of pooled RNA was used for Cy5-labelling (red, wildtype RNA) or Cy3-labelling (green, *rovC* mutant RNA) using the ULS^{TM} Fluorescent labelling kit for Agilent Arrays (Kreatech). Non-incorporated dyes were removed by KREA*pure* purification columns as described by the manufacturer. RNA concentration and the degree of labelling (DoI) were determined using a Nanodrop (PEQLAB) and the DoI calculation sheet (www.kreatech.com). 300 ng of each labelled-RNA were mixed, fragmented and hybridized to the customized microarray slides (Agilent 8x15K) using the Agilent Gene expression hybridization kit (Agilent) and a Microarray Hybridization Chamber kit (Agilent) as indicated by the manufacturer. Hybridization was carried out for 17 h at 65°C. Afterwards the microarray slide was washed and dried and data were scanned using the Axon GenePix Personal 4100A scanner. Array images were captured using the software package GenePix Pro 6.015. Data processing, bioinformatic evaluation, normalization and statistical analysis was performed as described by Heroven et al. (2012b).

Quantitative RT-PCR

RT-PCR analysis was performed with the Bioline SensiFast SYBR no-ROX One-step kit. A master mix was prepared for each primer-pair based on a standard 12.5 µl final reaction volume. Gene-specific primers are listed in Tb.XX and were designed to amplify 150-200 bp amplicons with *Y. pseudotuberculosis* YPIII cDNA. The amount of PCR product was quantified by measuring the fluorescence intensity of the SYBR Green dye in a Rotor-Gene Q real-time PCR cycler (Qiagen, Germany) using the three-step cycling programme as recommended by the manufacturer. Expression levels were normalized to the *sopB* gene since it exhibited identical expression levels in the wildtype strain and the *rovC* mutant strain. Relative transcription levels were calculated according to (Pfaffl, 2001), assuming an optimal primer efficiency of 2 (one duplication per cycle).

Acknowledgements

We thank members of our group for fruitful discussions and Sandra Stengel for her supportive performance in the lab. This work was funded by grants of the Deutsche Forschungsgemeinschaft DE616/3 (SPP 1258) and by grants of the International Graduate School for Infection Research.

References

Arnold, T.E., Yu, J., and Belasco, J.G. (1998) mRNA stabilization by the ompA 5' untranslated region: two protective elements hinder distinct pathways for mRNA degradation. *RNA* **4**: 319–30.

Baker, C.S., Morozov, I., Suzuki, K., Romeo, T., and Babitzke, P. (2002) CsrA regulates glycogen biosynthesis by preventing translation of glgC in Escherichia coli. *Mol Microbiol* **44**: 1599–1610.

Ballister, E.R., Lai, A.H., Zuckermann, R.N., Cheng, Y., and Mougous, J.D. (2008) In vitro self-assembly of tailorable nanotubes from a simple protein building block. *Proc Natl Acad Sci U S A* **105**: 3733–8.

Bingle, L.E., Bailey, C.M., and Pallen, M.J. (2008) Type VI secretion: a beginner's guide. *Curr Opin Microbiol* **11**: 3–8.

Böhme, K. (2010) Identification and characterization of regulatory factors and regulatory RNA elements controlling the expression of the primary invasion factors invasin and YadA in Yersinia pseudotuberculosis.

Boyer, F., Fichant, G., Berthod, J., Vandenbrouck, Y., and Attree, I. (2009) Dissecting the bacterial type VI secretion system by a genome wide in silico analysis: what can be learned from available microbial genomic resources? *BMC Genomics* **10**: 104.

Bradford, M.M. (1976) A rapid and sensitive method for the quantitation of microgramm quantities of protein utilizing the prinziple of protein-dye binding. *Anal Biochem* **72**: 248–254.

Busby, S., and Ebright, R.H. (1999) Transcription activation by catabolite activator protein (CAP). *J Mol Biol* **293**: 199–213.

Carniel, E., Autenrieth, I., Cornelis, G., Fukushima, H., Guinet, F., Isberg, R., Pham, J., Prentice, M., Simonet, M., Skurnik, M. and Wauters, G. (2006) Y. enterocolitica and Y. pseudotuberculosis. In *Prokaryotes*. pp. 270–398.

Cathelyn, J.S., Crosby, S.D., Lathem, W.W., Goldman, W.E., and Miller, V.L. (2006) RovA, a global regulator of Yersinia pestis, specifically required for bubonic plague. *Proc Natl Acad Sci U S A* **103**: 13514–13519.

Cui, Y., Madi, L., Mukherjee, A., Dumenyo, C.K., and Chatterjee, A.K. (1996) The RsmA- mutants of Erwinia carotovora subsp. carotovora strain Ecc71 overexpress hrpNEcc and elicit a hypersensitive reaction-like response in tobacco leaves. *Mol Plant Microbe Interact* **9**: 565–573.

Dersch, P., and Isberg, R.R. (1999) A region of the Yersinia pseudotuberculosis invasin protein enhances integrin-mediated uptake into mammalian cells and promotes self-association. *EMBO J* **18**: 1199–1213.

Duss, O.P. (2012) Assembly, 70 kDa solution structure and mechanism of action of the bacterial non-coding RNA RsmZ in complex with the global regulatory protein RsmE. .

Gudapaty, S., Suzuki, K., Wang, X., Babitzke, P., and Romeo, T. (2001) Regulatory interactions of Csr components: the RNA binding protein CsrA activates csrB transcription in Escherichia coli. *J Bacteriol* **183**: 6017–27.

Gueguen, E., Durand, E., Zhang, X.Y., d'Amalric, Q., Journet, L., and Cascales, E. (2013) Expression of a Yersinia pseudotuberculosis Type VI Secretion System Is Responsive to Envelope Stresses through the OmpR Transcriptional Activator. *PLoS One* **8**: e66615.

Gunasekera, A., Ebright, Y.W., and Ebright, R.H. (1992) DNA sequence determinants for binding of the Escherichia coli catabolite gene activator protein. *J Biol Chem* **267**: 14713–14720.

Han, Y., Zhou, D., Pang, X., Song, Y., Zhang, L., Bao, J., *et al.* (2004) Microarray analysis of temperature-induced transcriptome of Yersinia pestis. *Microbiol Immunol* **48**: 791–805.

Heroven, A.K., and Dersch, P. (2006) RovM, a novel LysR-type regulator of the virulence activator gene rovA, controls cell invasion, virulence and motility of Yersinia pseudotuberculosis. *Mol Microbiol* **62**: 1469–1483.

Heroven, A.K., Bohme, K., Rohde, M., and Dersch, P. (2008) A Csr-type regulatory system, including small non-coding RNAs, regulates the global virulence regulator RovA of Yersinia pseudotuberculosis through RovM. *Mol Microbiol* **68**: 1179–1195.

Heroven, A.K., Bohme, K., and Dersch, P. (2012a) The Csr/Rsm system of Yersinia and related pathogens: A post-transcriptional strategy for managing virulence. *RNA Biol* **9**.

Heroven, A.K., Sest, M., Pisano, F., Scheb-Wetzel, M., Steinmann, R., Böhme, K., *et al.* (2012b) Crp induces switching of the CsrB and CsrC RNAs in Yersinia pseudotuberculosis and links nutritional status to virulence. *Front Cell Infect Microbiol* **2**: 158.

Hopf, V., Göhler, A., Eske-Pogodda, K., Bast, A., Steinmetz, I., and Breitbach, K. (2014) BPSS1504, a cluster 1 type VI secretion gene, is involved in intracellular survival and virulence of Burkholderia pseudomallei. *Infect Immun* .

Jones, C., Hachani, A., Manoli, E., and Filloux, A. (2014) An rhs Gene Linked to the Second Type VI Secretion Cluster Is a Feature of the Pseudomonas aeruginosa Strain PA14. *J Bacteriol* **196**: 800–10.

Kay, E., Dubuis, C., and Haas, D. (2005) Three small RNAs jointly ensure secondary metabolism and biocontrol in Pseudomonas fluorescens CHA0. *Proc Natl Acad Sci U S A* **102**: 17136–41.

Kitaoka, M., Miyata, S.T., Brooks, T.M., Unterweger, D., and Pukatzki, S. (2011) VasH is a transcriptional regulator of the type VI secretion system functional in endemic and pandemic Vibrio cholerae. *J Bacteriol* **193**: 6471–82.

Kolb, A., Busby, S., Buc, H., Garges, S., and Adhya, S. (1993) Transcriptional regulation by cAMP and its receptor protein. *Annu Rev Biochem* **62**: 749–95.

Komarova, A. V., Tchufistova, L.S., Dreyfus, M., and Boni, I. V. (2005) AU-Rich Sequences within 5' Untranslated Leaders Enhance Translation and Stabilize mRNA in Escherichia coli. *J Bacteriol* **187**: 1344–1349.

Komarova, A. V., Tchufistova, L.S., Supina, E. V., and Boni, I. V. (2002) Protein S1 counteracts the inhibitory effect of the extended Shine-Dalgarno sequence on translation. *RNA* **8**: 1137–1147.

Kulkarni, P.R., Cui, X., Williams, J.W., Stevens, A.M., and Kulkarni, R. V (2006) Prediction of CsrA-regulating small RNAs in bacteria and their experimental verification in Vibrio fischeri. *Nucleic Acids Res* **34**: 3361–9.

Lapouge, K., Schubert, M., Allain, F.H.-T., and Haas, D. (2008) Gac/Rsm signal transduction pathway of gamma-proteobacteria: from RNA recognition to regulation of social behaviour. *Mol Microbiol* **67**: 241–53.

Lenz, D.H., Miller, M.B., Zhu, J., Kulkarni, R. V, and Bassler, B.L. (2005) CsrA and three redundant small RNAs regulate quorum sensing in Vibrio cholerae. *Mol Microbiol* **58**: 1186–202.

Marra, A., and Isberg, R. (1997) Invasin-dependent and invasin-independent pathways for translocation of Yersinia pseudotuberculosis across the Peyer's patch intestinal epithelium. *Infect Immun* **65**: 3412–3421.

Mercante, J., Edwards, A.N., Dubey, A.K., Babitzke, P., and Romeo, T. (2009) Molecular geometry of CsrA (RsmA) binding to RNA and its implications for regulated expression. *J Mol Biol* **392**: 511–28.

Miller, J.H. (1992) *A Short Course in Bacterial Genetics. Cold Spring Harbor, NY: Cold Spring Harbour Laboratory Press.* .

Mougous, J.D., Cuff, M.E., Raunser, S., Shen, A., Zhou, M., Gifford, C.A., *et al.* (2006) A virulence locus of Pseudomonas aeruginosa encodes a protein secretion apparatus. *Science* **312**: 1526–30.

Mougous, J.D., Gifford, C.A., Ramsdell, T.L., and Mekalanos, J.J. (2007) Threonine phosphorylation post-translationally regulates protein secretion in Pseudomonas aeruginosa. *Nat Cell Biol* **9**: 797–803.

Nagel, G., Lahrz, a, and Dersch, P. (2001) Environmental control of invasin expression in Yersinia pseudotuberculosis is mediated by regulation of RovA, a transcriptional activator of the SlyA/Hor family. *Mol Microbiol* **41**: 1249–69.

Osipiuk, J., Xu, X., Cui, H., Savchenko, A., Edwards, A., and Joachimiak, A. (2011) Crystal structure of secretory protein Hcp3 from Pseudomonas aeruginosa. *J Struct Funct Genomics* **12**: 21–6.

Pannuri, A., Yakhnin, H., Vakulskas, C.A., Edwards, A.N., Babitzke, P., and Romeo, T. (2011) Translational Repression of NhaR, a Novel Pathway for Multi-Tier Regulation of Biofilm Circuitry by CsrA. *J Bacteriol* **194**: 79–89.

Pfaffl, M.W. (2001) A new mathematical model for relative quantification in real-time RT-PCR. *Nucleic Acids Res* **29**: e45.

Pieper, R., Huang, S.-T., Robinson, J.M., Clark, D.J., Alami, H., Parmar, P.P., *et al.* (2009) Temperature and growth phase influence the outer-membrane proteome and the expression of a type VI secretion system in Yersinia pestis. *Microbiology* **155**: 498–512.

Pukatzki, S., McAuley, S.B., and Miyata, S.T. (2009) The type VI secretion system: translocation of effectors and effector-domains. *Curr Opin Microbiol* **12**: 11–7.

Romeo, T. (1998) Global regulation by the small RNA-binding protein CsrA and the non-coding RNA molecule CsrB. *Mol Microbiol* **29**: 1321–30.

Romeo, T., Vakulskas, C.A., and Babitzke, P. (2013) Post-transcriptional regulation on a global scale: form and function of Csr/Rsm systems. *Environ Microbiol* **15**: 313–24.

Saier, M.H. (1998) Multiple mechanisms controlling carbon metabolism in bacteria. *Biotechnol Bioeng* **58**: 170–4.

Sambrook, J. and Russel, D.W. (2001) *Molecular Cloning*.

Sandrini, S., Masania, R., Zia, F., Haigh, R., and Freestone, P. (2013) Role of porin proteins in acquisition of transferrin iron by enteropathogens. *Microbiology* **159**: 2639–50.

Savin, C., Martin, L., Bouchier, C., Filali, S., Chenau, J., Zhou, Z., *et al.* (2014) The Yersinia pseudotuberculosis complex: Characterization and delineation of a new species, Yersinia wautersii. *Int J Med Microbiol* .

Schubert, M., Lapouge, K., Duss, O., Oberstrass, F.C., Jelesarov, I., Haas, D., and Allain, F.H.-T. (2007) Molecular basis of messenger RNA recognition by the specific bacterial repressing clamp RsmA/CsrA. *Nat Struct Mol Biol* **14**: 807–13.

Shin, S., Lu, G., Cai, M., and Kim, K.-S. (2005) Escherichia coli outer membrane protein A adheres to human brain microvascular endothelial cells. *Biochem Biophys Res Commun* **330**: 1199–204.

Wang, Y. (2002) The function of OmpA in Escherichia coli. *Biochem Biophys Res Commun* **292**: 396–401.

Weilbacher, T., Suzuki, K., Dubey, A.K., Wang, X., Gudapaty, S., Morozov, I., *et al.* (2003) A novel sRNA component of the carbon storage regulatory system of Escherichia coli. *Mol Microbiol* **48**: 657–670.

Yakhnin, A. V, Baker, C.S., Vakulskas, C. a, Yakhnin, H., Berezin, I., Romeo, T., and Babitzke, P. (2013) CsrA activates flhDC expression by protecting flhDC mRNA from RNase E-mediated cleavage. *Mol Microbiol* **87**: 851–66.

Yakhnin, H., Yakhnin, A. V, Baker, C.S., Sineva, E., Berezin, I., Romeo, T., and Babitzke, P. (2011) Complex regulation of the global regulatory gene csrA: CsrA-mediated translational repression, transcription from five promoters by $E\sigma^{70}$ and Eσ(S), and indirect transcriptional activation by CsrA. *Mol Microbiol* **81**: 689–704.

Zhang, W., Wang, Y., Song, Y., Wang, T., Xu, S., Peng, Z., *et al.* (2013) A type VI secretion system regulated by OmpR in Yersinia pseudotuberculosis functions to maintain intracellular pH homeostasis. *Environ Microbiol* **15**: 557–69.

Zhang, W., Xu, S., Li, J., Shen, X., Wang, Y., and Yuan, Z. (2011) Modulation of a thermoregulated type VI secretion system by AHL-dependent quorum sensing in Yersinia pseudotuberculosis. *Arch Microbiol* **193**: 351–63.

Zheng, D., Constantinidou, C., Hobman, J.L., and Minchin, S.D. (2004) Identification of the CRP regulon using in vitro and in vivo transcriptional profiling. *Nucleic Acids Res* **32**: 5874–93.

1

Figure Legends

Fig. 1 RovC represses *Y. pseudotuberculosis* CsrC RNA

A A genomic library was introduced into *Y. pseudotuberculosis* YPIII harbouring a plasmid-based *csrC-lacZ* fusion (pKB46). β-galactosidase activity (µmol/(mg*min)) was monitored in strains either harbouring different gene bank plasmids (pRovC$^+$, pCrp$^+$, pHfq$^+$) or the empty vector pACYC184 (control). Data are means and standard deviations of one experiment, performed with technical duplicates. Data were analysed by Student's t test. Stars indicate the results that differed significantly from the control (*** P<0.001).

B Expression of a transcriptional *csrC-lacZ* (pKB46) fusion was measured in *Y. pseudotuberculosis* YPIII (wildtype) and YP148 (Δ*rovC*). Strains were transformed with the empty vector pAKH85 (pV) and complemented or overexpressed with pSSE11 (pRovC$^+$). β-galactosidase activity (µmol/(mg*min)) was measured after cells were grown at 25°C in LB_{BD} medium for 16h. Data are means and standard deviations of three independent experiments, each performed at least in duplicates. Data were analysed by Student's t test. Stars indicate the results that differed significantly from each other (*** P<0.001, ** P<0.05, ns = not significant).

C Transcript levels of CsrC were analysed by northern blotting. *Y. pseudotuberculosis* YPIII (wildtype) and YP148 (Δ*rovC*) were used without any plasmid or they were transformed with the empty vector pAKH85 (pV) or the complementation plasmid pSSE11 (pRovC$^+$). YP126 (Δ*csrC)* was used as control strain. Overnight cultures were grown at 25°C in LB_{BD} medium. Total RNA was prepared, separated on 0.7 % MOPS agarose gels, transferred to a nylon-membrane and probed with a digoxigenin (DIG)-labelled PCR fragment encoding the gene. 16S and 23S rRNAs were used as loading controls.

D Transcript stability of CsrC was monitored by northern blot analysis in *Y. pseudotuberculosis* YPIII (wildtype) and YP148 (Δ*rovC*). Strains were transformed with the empty vector pAKH85 (pV) and complemented with its derivative pSSE11 (pRovC$^+$). Overnight cultures were grown at 25°C in LB_{BD} medium. To stop transcription, rifampicin was added to the stationary phase cells in a final concentration of 1 mg/ml. Samples were taken directly after rifampicin addition (0 min) or after 80 min. Total RNA was prepared, separated on 0.7 % MOPS agarose gels, transferred to a nylon-membrane and probed with a digoxigenin (DIG)-labelled PCR fragment encoding the *csrC* gene. 16S and 23S rRNAs were used as loading controls. The relative band intensity was documented and the relative mRNA concentrations were normalized to the 23S and 16S rRNAs. The fold change is given as rel. intensity t_0/rel. intensity t_{80} for each strain.

E Recently the Csr system was discovered as global virulence regulator system. Within the last decades several transcriptional and post-transcriptional regulators were identified. The major players, namely the CsrBC non- coding RNAs are stabilized by CsrA-binding and counter-regulate each

other. Moreover CsrB transcription is activated by the response regulator UvrY of the two-component system BarA/UvrY in response to (yet unknown) environmental stimuli. Moreover, Crp represses UvrY. Herein, Crp responds to the nutrient composition of the surrounding medium. In addition, Crp positively affects CsrC transcript levels in a CsrB-independent manner. Upregulation of one or both ncRNAs sequesters CsrA, whereby RovM is repressed and RovA is activated leading to *invA* expression (dashed lines = indirect effect, solid lines = direct interaction).

Fig. 2 RovC controls invasin synthesis via the CsrBC-RovM-RovA cascade

Expression of translational *rovM'-'lacZ* (pAKH63) (**A**) and *rovA'-'lacZ* (pAKH47) (**B**) fusions was monitored in *Y. pseudotuberculosis* YPIII (wildtype) and YP148 (Δ*rovC*). Strains were transformed with the empty vector pAKH85 (pV) and complemented or overexpressed with its derivative pSSE11 (pRovC$^+$). β-galactosidase activity (µmol/(mg*min)) was measured after cells were grown at 25°C in LB_{BD} medium for 16h. Data are means and standard deviations of three independent experiments, each performed at least in duplicates. Data were analysed by Student's t test. Stars indicate the results that differed significantly from each other (*** P<0.001, ns = not significant). **C** Protein concentrations of RovM, RovA and invasin (InvA) in YPIII und YP148 were compared by western blot analysis. Strains were transformed with the empty vector pAKH85 (pV) and complemented or overexpressed with pSSE11 (pRovC$^+$). Whole cell extracts were prepared from cultures grown at 25°C in LB_{BD} medium for 16h, separated on 12 % Tris-TRICINE gels (RovM, RovA) or 10% SDS-PAA gels (InvA) and transferred to an Immobilon membrane. Proteins were detected by immunoblotting with polyclonal antibodies directed against RovM, RovA and InvA. The respective mutant (Δ*rovM* = YP72, Δ*rovA* = YP102, Δ*invA* = YP191) served as negative control. Immunoblotting with a polyclonal antibody against H-NS served as loading control.

Fig. 3 Expression of *rovC* is unique to *Yersinia*

Expression of a translational *rovC'-'lacZ* (pSSE32) fusion was monitored in *Y. pseudotuberculosis* YPIII (wildtype) and *E. coli* DH10β. The empty vector pTS02 in *E. coli* served as control (pV). β-galactosidase activity (µmol/(mg*min)) was measured after strains were grown in LB_{BD} medium at 25°C and 37°C for 16h. Data are means and standard deviations of two independent experiments, each performed at least in triplicates. Data were analysed by Student's t test. Stars indicate the results that differed significantly from each other (*** P<0.001, ** P<0.01)

Fig. 4 Expression of *rovC* is favoured at 25°C during stationary growth

Expression of transcriptional *rovC-lacZ* (pSSE67) (**A**) and translational *rovC'-'lacZ* (pSSE32) (**B**) fusions was monitored in *Y. pseudotuberculosis* YPIII (wildtype). β-galactosidase activity (µmol/(mg*min))

was measured after strains were grown in LB_{BD} medium at 25°C or 37°C for 4h (exponential) or 16h (stationary). Data are means and standard deviations of two independent experiments, each performed at least in triplicates. Data were analysed by Student's t test. Stars indicate the results that differed significantly from each other. **C** RovC transcript levels were analysed by northern blotting. Strains were grown in LB_{BD} medium at 25°C or 37°C for 4h (exponential) or 16h (stationary). Total RNA was prepared, separated on 0.7 % MOPS agarose gels, transferred to a nylon-membrane and probed with a digoxigenin (DIG)-labelled PCR fragment encoding the *rovC* gene. 16S and 23S rRNAs were used as loading controls. The *rovC* mutant strain YP148 served as negative control. exp = exponential, stat = stationary growth.

Fig. 5 Crp and CsrA govern *rovC* expression

Expression of a transcriptional *rovC-lacZ* (pAKH189) (**A**) and a translational *rovC'-'lacZ* (pSSE32) fusion (**B**) was monitored in *Y. pseudotuberculosis* YPIII (wildtype), YP53 (Δ*csrA*) and YP89 (Δ*crp*). Strains were transformed with the empty vector pAKH85 (pV) and complemented or overexpressed with the midi-copy plasmid pAKH37 ($pCrp^+$). β-galactosidase activity (µmol/(mg*min)) was measured after strains were grown in LB_{BD} medium at 25°C for 16h. Data are means and standard deviations of two independent experiments, each performed at least in triplicates. Data were analysed by Student's t test. Stars indicate the results that differed significantly from each other (*** $P<0.001$, * $P<0.05$, ns = not significant).

C RovC transcript levels were analysed by northern blotting. Strains were grown in LB_{BD} medium at 25°C to stationary growth phase. Total RNA was prepared from YPIII, YP89 (Δ*crp*) and YP53 (Δ*csrA*), separated on 0.7 % MOPS agarose gels, transferred to a nylon-membrane and probed with a digoxigenin (DIG)-labelled PCR fragment encoding the *rovC* gene. 16S and 23S rRNAs were used as loading controls.

D Protein concentrations of RovC-His in from YPIII, YP89 (Δ*crp*) and YP53 (Δ*csrA*) were compared by western blot analysis. Strains were transformed with pSSE68, harbouring a C-terminal RovC-His-tag under control of its own promoter. Whole cell extracts were prepared from cultures grown at 25°C in LB_{BD} medium for 16h, separated on 8 % TRIS-Tricine gels and transferred onto an Immobilon membrane. Proteins were detected by immunoblotting with a monoclonal antibody directed against the His-tag. YPIII served as negative control (ctrl). Immunoblotting with a polyclonal antibody against H-NS served as loading control.

Fig. 6 CsrA represses *rovC* synthesis and directly interacts with its RNA

A Schematic representation of the first 79 nt of the RovC mRNA. The transcriptional start (TSS) is marked as +1, the ribosomal binding site is denoted by a dashed line. GGA motifs are highlighted in red.

B To show that CsrA can directly bind RovC mRNA transcripts, electrophoretic mobility shift assays (EMSAs) were performed. RovC mRNA was *in vitro* transcribed (RovC mRNA starts at +1 and harbours 38 nt of the coding region). 10 pmol RNA were denatured, cooled down at RT to refold the RNA and incubated with increasing amounts of CsrA protein (7.5 pmol to 75 pmol protein) at 25°C. Complexes were separated on a 4% TBE gel, transferred onto nitrocellulose membranes and probed with digoxigenin (DIG)-labelled PCR fragments encoding the *rovC* or *rovM* gene. Herein RovM *in vitro* transcribed RNA served as negative control.

C RovC transcript levels were analysed by northern blotting. YPIII and YP53 (Δ*csrA*) were transformed with the empty vector pAKH85 (pV) or with its derivative pAKH56 (pCsrA^{+}). Strains were grown in LB_{BD} medium at 25°C to stationary growth phase. Total RNA was prepared, separated on 0.7 % MOPS agarose gels, transferred to a nylon-membrane and probed with a digoxigenin (DIG)-labelled PCR fragment encoding the *rovC* gene. 16S and 23S rRNAs were used as loading controls.

D To compare RovC transcript stability in *Y. pseudotuberculosis* wildtype (YPIII) and YP53 (Δ*csrA*) a stability assay was performed. Strains were transformed with pSSE11, increasing the copy number of RovC transcript especially in the wildtype. Cultures were grown in LB medium at 25°C for 16h. Transcription was stopped by adding rifampicin to a final concentration of 1mg/ml. Samples were taken directly after rifampicin addition (0 min) and after 20 min, 40 min, 60 min and 80 minutes. Total RNA was isolated, separated on 0.7 % MOPS agarose gels, transferred to a nylon-membrane and probed with a digoxigenin (DIG)-labelled PCR fragment encoding the *rovC* gene. 16S and 23S rRNAs were used as loading controls and YP148 (Δ*rovC*) was used as negative control.

E The northern blots were documented and the relative band intensity was calculated in relation to the 23S and 16S rRNAs. The graph represents the remaining percentage of RNA (y-axis) over time (x-axis) on a half-logarithmic scale. The half-life of the RovC mRNA transcript was calculated via the exponential regression (dashed lines).

Fig. 7 RovC is genetically linked to the T6SS4

A Schematic representation of the differentially expressed genes (>1.7 fold) identified by microarray analyses between *Y. pseduotuberculosis* YPIII (wildtype) and the *rovC* mutant (YP148). The diagram indicates the absolute number of differentially regulated genes. Gene categories are given on the right hand side.

B To verify the results from the microarray, one-step real-time RT-PCR analyses were performed with specific primer pairs for selected genes of the T6SS4. RNA was isolated from 8 independent cultures for the *Y. pseudotuberculosis* wildtype (YPIII) reference strain and from 3 independent cultures of the Δ*rovC* candidate strain. Gene expression levels were normalized to the *sopB* reference transcript for YPIII and YP148 respectively (according to (Pfaffl, 2001)) and are given as relative expression of the respective gene in relation to *sopB*. Data are given as means ± standard deviation. Data were analysed by Student's t test. Stars indicate the results that differed significantly from each other (*** P<0.001, * P<0.05, ns = not significant).

C The T6SS4 cluster is composed of 16 genes (YPK_3550 to YPK_3566), encompassing a size of 23.6 kb. The *rovC* gene is found directly downstream of this cluster.

Fig. 8 T6SS4 is induced at 25°C and exhibits RovC-dependency

RovC-dependent expression of a translational T6SS4*'-'lacZ* (pSSE64) fusion was monitored in *Y. pseudotuberculosis* YPIII wildtype and YP148 (Δ*rovC*). Strains were transformed with the empty vector pAKH85 (pV) and complemented or overexpressed with pSSE11 ($RovC^+$). β-galactosidase activity (µmol/(mg*min)) was measured after strains were grown in LB_{BD} medium at 25°C (**A**) or 37°C (**B**) for 16h. Data are means and standard deviations of two independent experiments, each performed at least in triplicates. Data were analysed by Student's t test. Stars indicate the results that differed significantly from each other (*** P<0.001, ns = not significant). **C** Temperature dependent expression of a translational T6SS*4'-'lacZ* (pSSE64) fusion was monitored in *Y. pseudotuberculosis* YPIII wildtype at 25°C and 37°C. β-galactosidase activity (µmol/(mg*min)) was measured after strains were grown in LB_{BD} medium. Data are means and standard deviations of two independent experiments, each performed at least in triplicates. Data were analysed by Student's t test. Stars indicate the results that differed significantly from each other (*** P<0.001, ns = not significant).

Fig. 9 Putative connection of CsrC regulatory factors in *Y. pseudotuberculosis*

Dashed lines = indirect regulation, solid lines = direct interactions, bars = repression, arrows = activation, blue colour represents connections identified in this work.

Figures

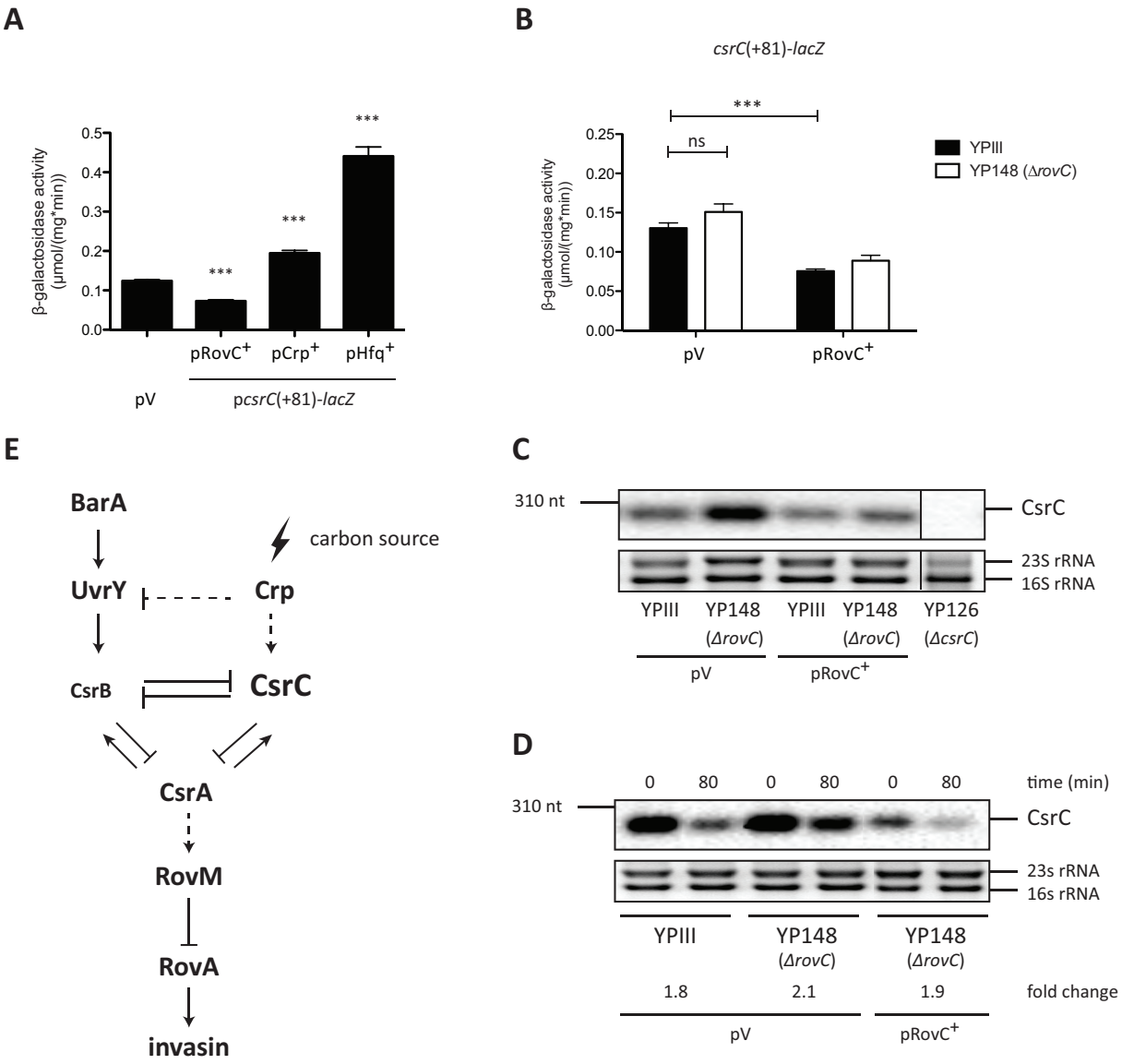

Fig. 1 Seekircher *et al*. 2014

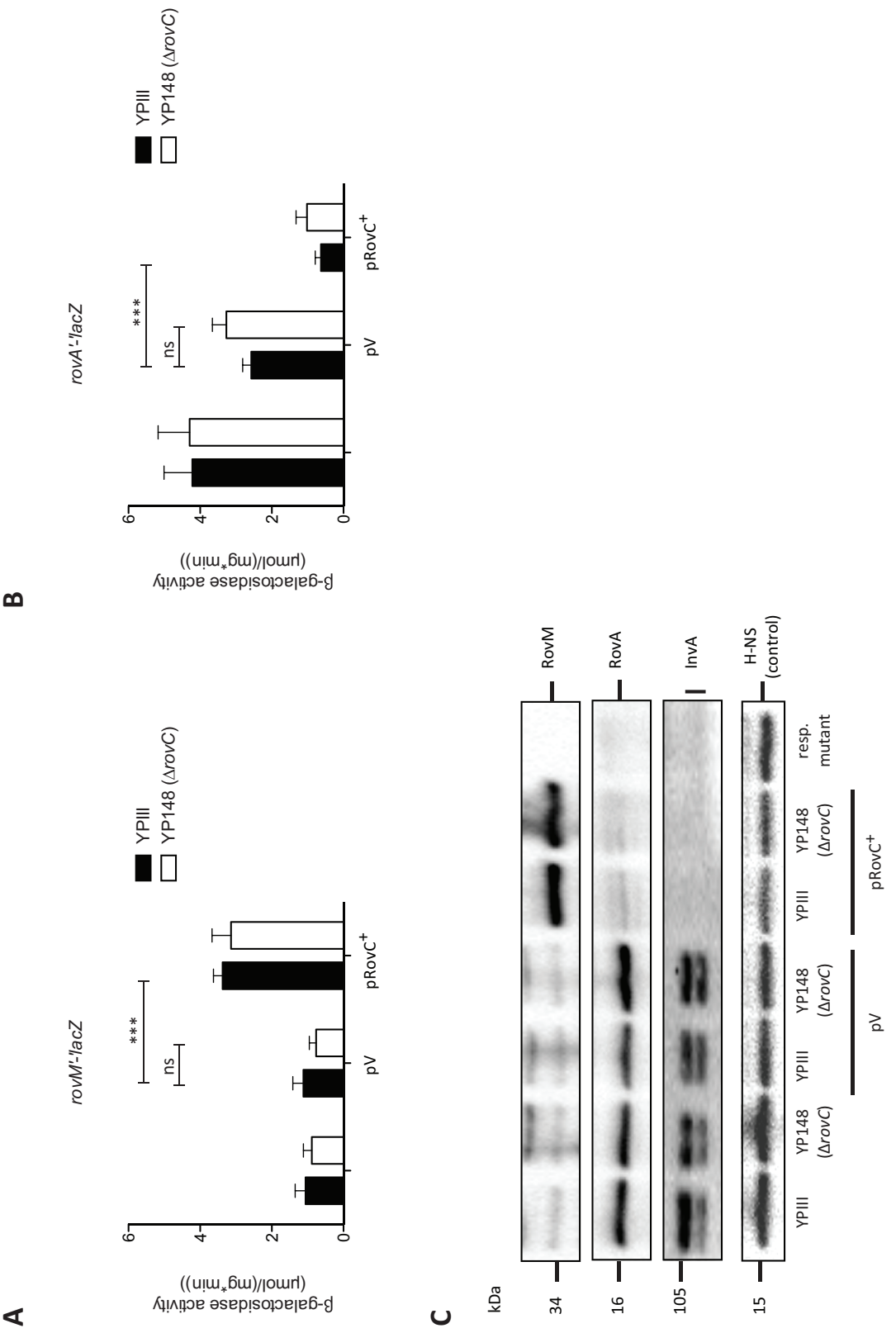

Fig. 2 Seekircher *et al*. 2014

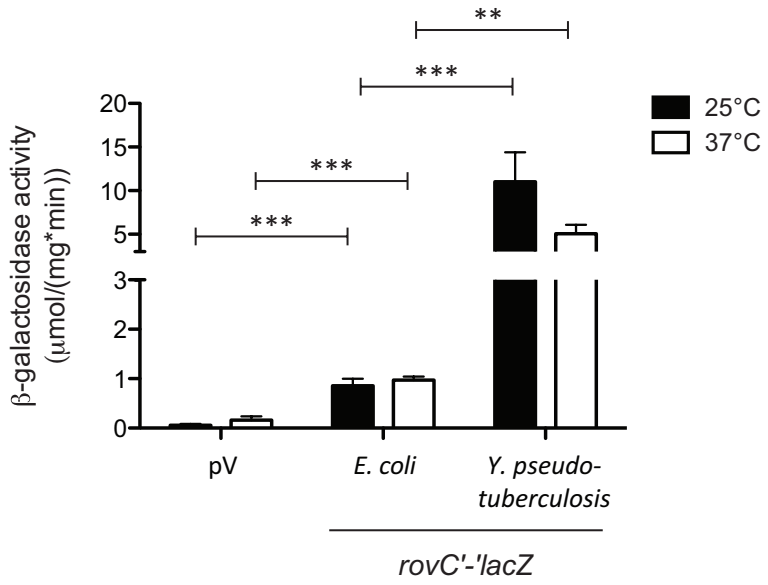

Fig. 3 Seekircher *et al*. 2014

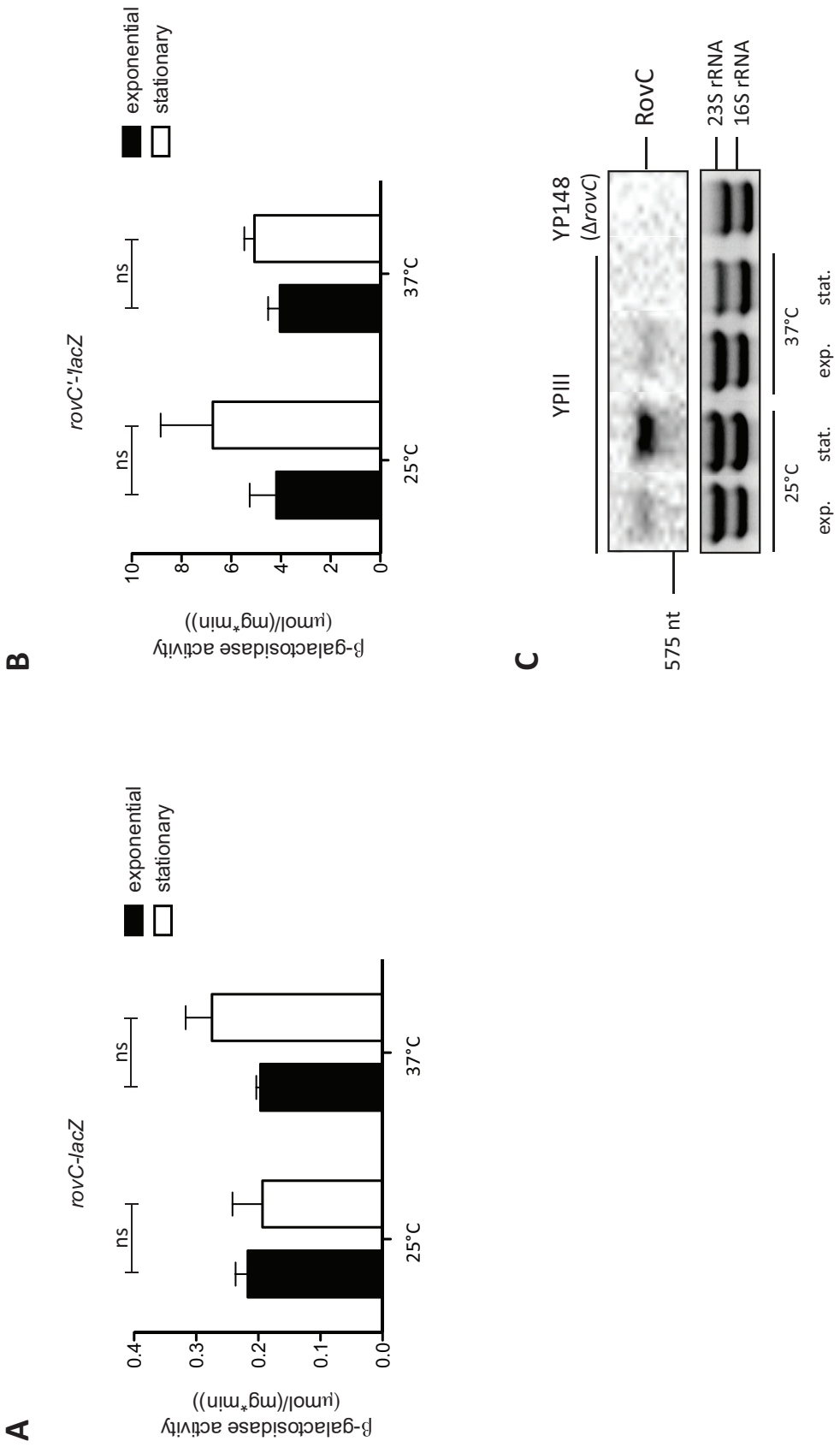

Fig. 4 Seekircher *et al*. 2014

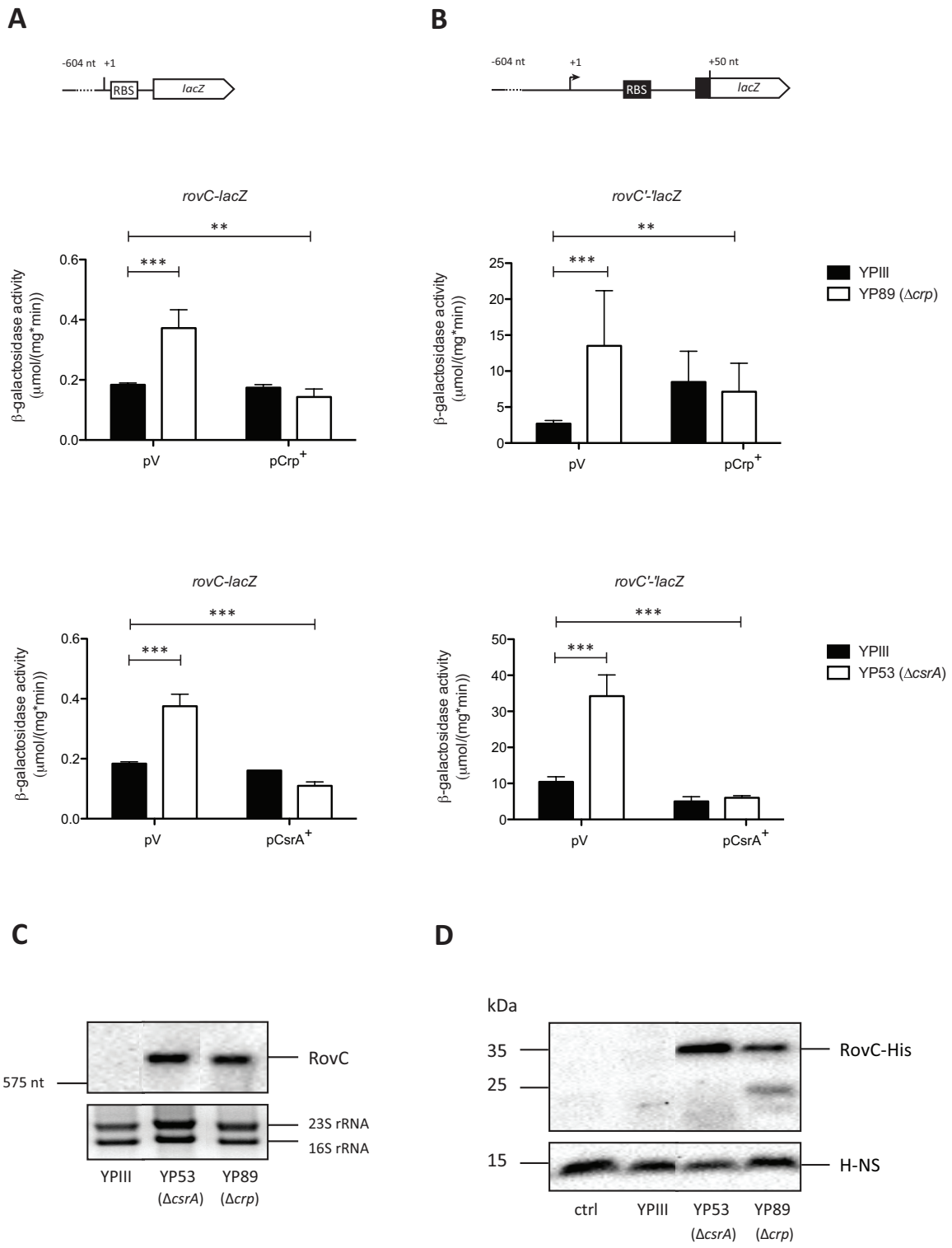

Fig. 5 Seekircher *et al*. 2014

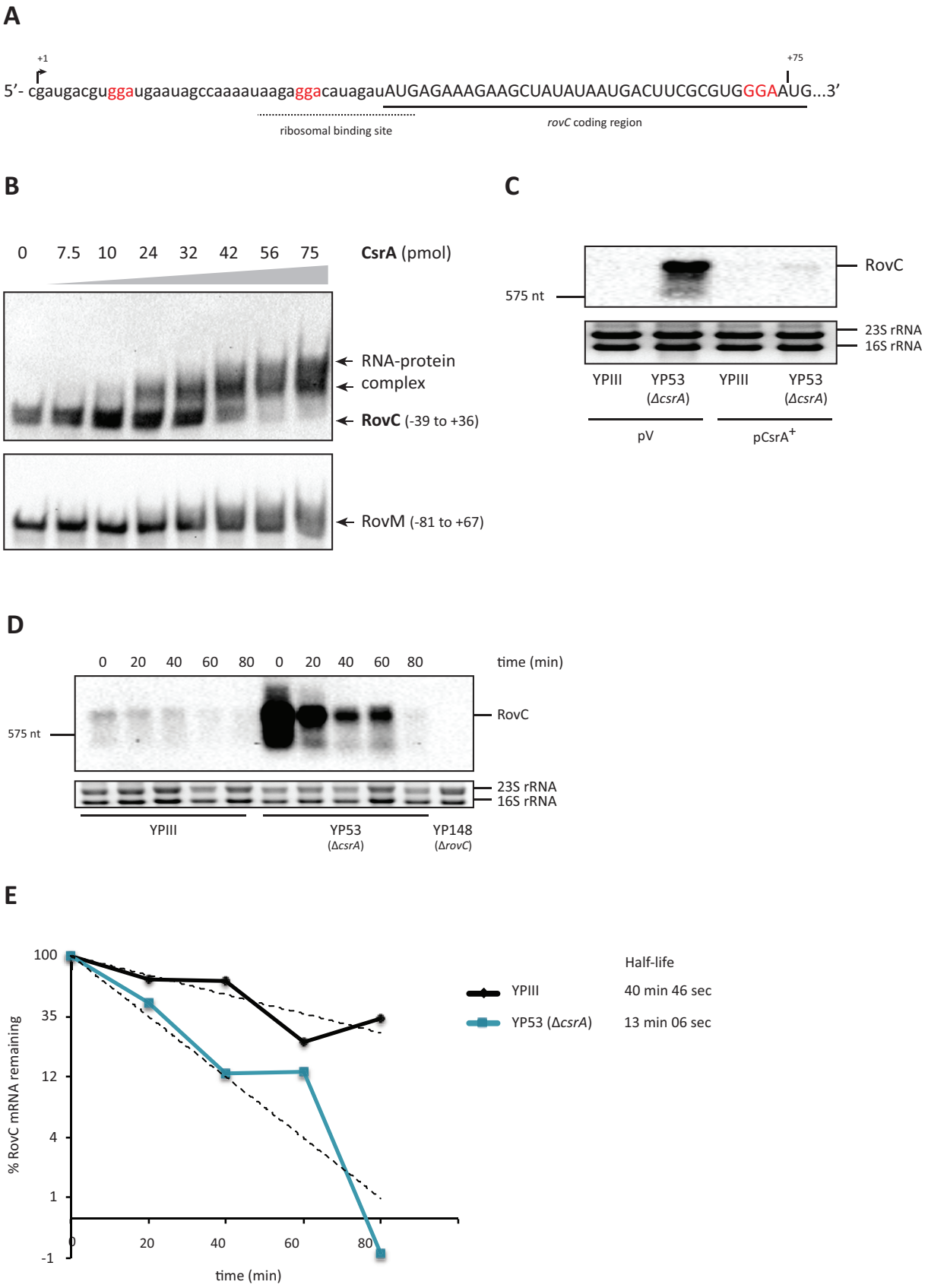

Fig. 6 Seekircher *et al*. 2014

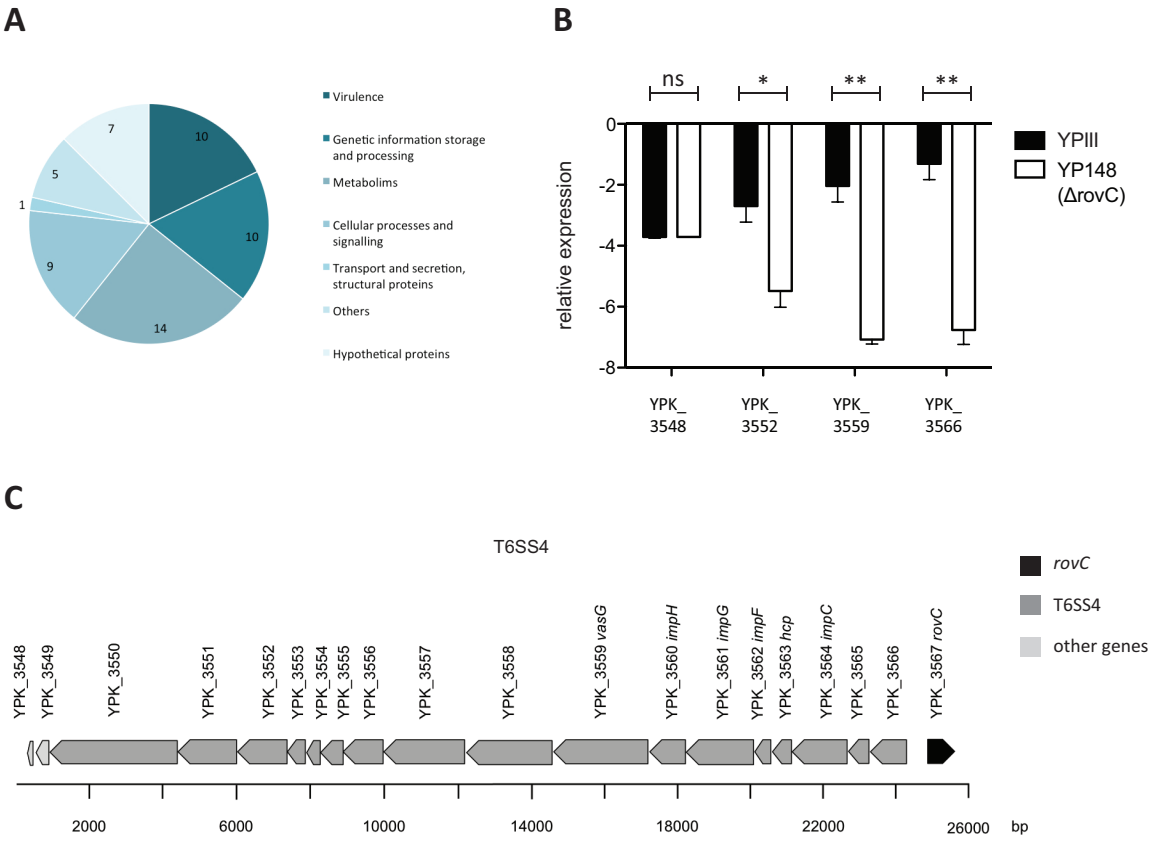

Fig. 7 Seekircher *et al*. 2014

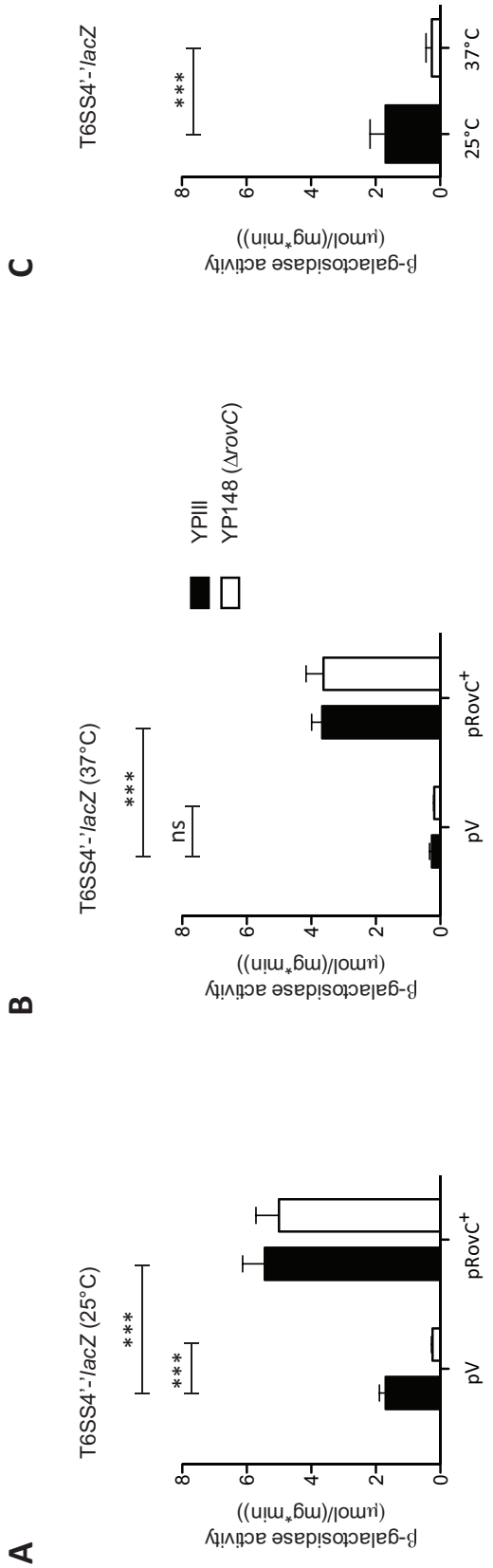

Fig. 8 Seekircher *et al*. 2014

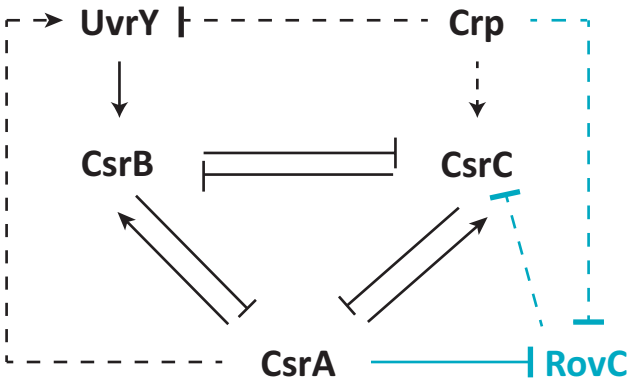

Fig. 9 Seekircher *et al*. 2014

Tables

Tab. 1 Strains and plamids

Strains, plasmids	Description	Primer pair
***E. coli* K12**		
BL21 λ DE3	F⁻ *ompT gal dcm lon hsdSB*(rB - mB -) λDE3	(Studier *et al*., 1990)
DH10β	F⁻ *endA1 recA1 galE15 galK16 nupG rpsL* Δ*lacX74* Φ80*lacZ* Δ*M15 araD139* Δ(*ara,leu*)*7697 mcrA* Δ(*mrr hsdRMS⁻mcrBC*), λ⁻	(Casadaban and Cohen, 1980)
S17-1λpir	*recA thi pro hsdR*⁻ M1⁺(RP4--2Tc::Mu--Km::Tn7), λpir	(Simon *et al*., 1983)
Y. pseudotuberculosis		
YPIII	pIB1, wildtype	(Bolin *et al*., 1982)
YP53	YPIII, Δ*csrA*, Kn^R	(Heroven *et al*., 2008)
YP72	YPIII, Δ*rovM*	A. K. Heroven
YP89	YPIII, Δ*crp*	A. K. Heroven
YP107	YPIII, Δ*rovA*	(Quade et al., 2012)
YP126	YPIII, Δ*csrC*	(Heroven *et al*., 2012b)
YP148	YPIII, Δ*rovC*, Kn^R	This study
YP191	YPIII, Δ*invA*, Kn^R	R. Geyer
Plasmids		
pTS02	pGP20, ori pSC101, *lacZ*$^+$, Amp^R	T. Stolz
pGB4	pACYC184, p15A, *hfq*$^+$, Cm^R	This study
pGB9	pACYC184, p15A, *rovC*$^+$, Cm^R	This study
pGB176	pACYC184, p15A, *crp*$^+$, Cm^R	This study
pAKH37	pACYC184, p15A, *crp*$^+$, Cm^R	(Heroven *et al*., 2012b)
pAKH47	pGP20, ori pSC101, *rovA'-'lacZ* (17)[c], Tet^R	(Heroven and Dersch, 2006)
pAKH56	pACYC184, p15A, *csrA*$^+$, Cm^R	(Heroven *et al*., 2012)
pAKH63	pGP20, ori pSC101, *rovM'-'lacZ* (41)[c], Tet^R	(Heroven and Dersch,2006)
pAKH85	pACYC184, p15A, Δ*tet*, Cm^R	(Heroven and Dersch, 2006)
pAKH172	pET28a(+), ori 3286 ,*csrA*$^+$, Kan^R	A. K. Heroven
pAKH189	pTS03, ori pSC101, *rovC-lacZ* (-618 to -39)[b], Amp^R	A. K. Heroven
pKB46	pTS03, ori pSC101, *csrC-lacZ* (-355 to +81)[a], Amp^R	K. Böhme
pSSE11	pACYC184, p15A, *rovC*$^+$, Cm^R	This study
pSSE32	pTS02, ori pSC101, *rovC*'-'*lacZ* (3)[c], Amp^R	This study
pSSE35	pAKH3, Δ*rovC*, Amp^R	This study
pSSE64	pTS02, ori pSC101, YPK_3566'-'*lacZ* (3)[c], Amp^R	This study
pSSE67	pTS03, ori pSC101, *rovC-lacZ* (-618 to -14)[b], Amp^R	This study
pSSE68	pACYC184, p15A, *rovC-his*$^+$, Cm^R	This study

[a] relative to transcriptional start

[b] relative to translational start

[c] amino acids

Tab. 2 Oligonucleotides

Oligonucleotide	Sequence (5'>3')	Feature
Oligonucleotides for plasmid generation		**Restriction site**
III108	GCG GCG GGA TCC GAG GAT ATA TCA TGA AGT CAG	*Bam*HI
III286	CGC GCG GTC GAC CAT ATT CAA CGC CGA ATA ATG C	*Sal*I
III287	CGC GCG GGA TCC CTA GAG GAA GTT CAG GTA GCC	*Bam*HI
III585	GCG CGG ATC CAA ACG TAA CTC CCT AGG AAA T	*Bam*HI
III654	GCG CGG ATC CGG TAG AGT TTA TCG CTC GC	*Bam*HI
III655	GCG CGG ATC CAC TGA CTT CAT GAT ATA TCC TC	*Bam*HI
III656	GCG CGG ATC CCG TCT ATT CAT GAT AAC TCT CC	*Bam*HI
III662	GCG CGG ATC CGG AGT TAA CAA ACG TAA CTC C	*Bam*HI
III773	GCG CGG ATC CTA GTC GTT CTA ACG ATG ATA GT	*Bam*HI
III774	GCG CGG ATC CTT AGC TGC CAT TGG TAT TTC C	*Bam*HI
III775	GCG CGG ATC CGG CCG ACT AAG CTT AAC CA	*Bam*HI
III776	GCG CGG ATC CAT TTT ACC CAT CTA AAA CGC CT	*Bam*HI
III777	GCG CGG ATC CGG CGA AGC GGT CAT CAA TA	*Bam*HI
III778	GCG CGG ATC CTT ACT ACT CAT GGA TAT CTC C	*Bam*HI
III779	GCG CGG ATC CGC ATA AAG CCA TCA TAG AG	*Bam*HI
III780	GCG CGG ATC CTT CTT TCT CAT ATC TAT GTC C	*Bam*HI
IV455	GCG CGT CGA CGG AGT CAG CAA AAT TGT ACC	*Sal*I
IV458	GCG CGT CGA CAT TCT TTT CAT CTT TAA CTT ACT C	*Sal*I
IV459	GCG CGG ATC CGC ACT ACT GGA TTA TTC GTT	*Bam*HI
IV464	GCG CGG ATC CCA CGG CCT GCC TTG CGA TC	*Bam*HI
IV735	GCG CGG ATC CCA GCT CTG ATT GGA TTA ATT CAG	*Bam*HI
IV736	GCG CGT CGA CAT GTC ACT CAT ATT ATT GTC CAT C	*Sal*I
IV923	GCG CGT CGA CAT TTT GGC TAT TCA TCC ACG TC	*Bam*HI
V655	CGC GCG GGA TCC CTA *GTG ATG ATG ATG ATG ATG* GAG GAA GTT CAG GTA GCC	*Sal*I
Oligonucleotides for mutagenesis		
III844	**CAT ATG AAT ATC CTC CTT AGT** TGT CCT ATC TGA CAT GC	
III845	GCG CGA GCT CGG CAG AGT TAA TGT AAT GTT CC	*Sac*I
III920	GCG CGA GCT CGG CTT GCT CAC TGA TAT G	*Sac*I
III921	**GAA GCA GCT CCA GCC TAC AC**A TCT ATG TCC TCT TAT TTT GGC	
III992	CCG GGG AGC TCG GAT TAA TGC GGA TAT TGC GGA GTA ACA C	*Sac*I
III994	CCG GGG AGC TCC GCC AGC TCA CGC TTA TCG C	*Sac*I
III996	**GGA ACT AAG GAG GAT ATT CAT ATG** CCA GAT AAC AGA TAG CAA TAA GAA CAG TTT AAT GAG C	
III997	**GA AGC AGC TCC AGC CTA CAC** TCC CGC ATT CCT TAT CAA GAG AAA CTC A	
Oligonucleotides for probe generation		**Transcript**
V4 V5	TGA TTG GCG ATG AGG TTA CGG TTC TGC TTG GAT GCG CTG GT	*csrA*
555 556	CGG CGC GGA TCC CTC TCA CAC CAG CTG TG GGG GGC GTC GAC GGC AAA CTC AAT ATC CTG	*csrB*
582 583	GCG GCG GTC GAC CCT TCA TCC CGT GGT AGG GGG CGC GGA TCC GAT TGG GCC GGA ATC TAG C	*csrC*
I521 I522	GGG CGC GTA ATA CGA CTC ACT ATA GGA GCG AAT TTT GTA AAG TGG C CCA GTG TCC TAA CAT CCC T	csrC (+1 to +151)[a]
III286 IV91	CGC GCG GTC GAC CAT ATT CAA CGC CGA ATA ATG C GCG CGA GCT CGC TCC TCT TTG CAT TCC AC	*rovC*

V773	GTA ATA CGA CTC ACT ATA GGA TGA CGT GGA TGA ATA GCC	*rovC* (+1 to +77)[a]
V777	CAT TCC CAC GCG AAG TCA TTA T	
I523	GGG CGC GTA ATA CGA CTC ACT ATA GGC GTT GTC CTT TAT TGA TAA C	*rovM* (-81 to +67)[b]
I524	GCA ACA GCT ACA AAG GTT C	
IV527	TTG CTG ACT CCG ATT ATT CG	*pnp*
IV528	GAA GAC GAC CGC GCC CAA C	
IV529	CGC GAC TCA GCA AGA AGA G	*rne*
IV530	GCC GAT GTC TGG GCG CAG	
Oligonucleotides for RT-PCR		**Transcript**
III393	CCG ACG TAA AGC CGC GAT AC	*sopB*
III394	CCT CGT TCA TAA GCA CTC GTC	
III923	GTG GCA TGG AAT GCC AAT GGC	YPK_0604
III924	GAC GTA CAA CAT CAG CAG GCG	
V647	ATG TAT TTA CGG CGT CTT TAC GAT C	YPK_3548
V648	TTA GAT GCT ATC CGG CTG GTG G	
V649	GCT CAC CTT ACG TGC CAG CGT	YPK_3552
V650	CCG CAT TAT CGA TCC ACC CTA TG	
V651	CGG CCC AAC TGG ATG TGC TC	YPK_3559
V652	CAT GCA GAT GGC GGC TTT GC	
V653	CAT CTT CGA CAT TAT TTT TAA CTG TC	YPK_3566
V654	GTT CAC AAT GCA GTT GGT AAC TC	

underlined = restriction site, **bold** sequence homologous to kan resistance cassette, *italic* = His-tag, grey bar = T7 promoter

[a] nucleotides relative to transcriptional start
[b] nucleotides relative to translational start

Supplementary material

Tab. S 1 Classification of RovC-dependent genes

Gene ID	Gene locus	Fold change	Description	Category - class
Virulence genes				
Downregulated loci (YPK_3567 activated)				
YPK_1268	*ail*	-1,9	virulence-related outer membrane protein	virulence factor
YPK_3552		-1,8	type VI secretion protein, VC_A0114 family	virulence factor
YPK_3553		-2,2	putative lipoprotein	virulence factor
YPK_3554		-2,2	conserved hypothetical protein	virulence factor
YPK_3555		-1,8	conserved hypothetical protein	virulence factor
YPK_3561	*impG*	-1,9	type VI secretion protein, VC_A0110 family	virulence factor
YPK_3562	*impF*	-3,7	type VI secretion system lysozyme-related protein	virulence factor
YPK_3563	*hcp*	-19,9	protein of unknown function DUF796	virulence factor
YPK_3564	*impC*	-3,3	type VI secretion protein, EvpB/VC_A0108 family	virulence factor
YPK_3565		-3,6	type VI secretion protein, VC_A0107 family	virulence factor
Genetic information storage and processing				
Downregulated loci (YPK_3567 activated)				
YPK_0282	*rpsJ*	-1,8	ribosomal protein S10	Translation
YPK_0284	*rplD*	-2,1	ribosomal protein L4/L1e	Translation
YPK_0285	*rplW*	-1,9	Ribosomal protein L25/L23	Translation
YPK_0288	*rplV*	-1,8	ribosomal protein L22	Translation
YPK_0337	*rplJ*	-1,8	ribosomal protein L10	Translation
YPK_0338	*rplL*	-2,0	ribosomal protein L7/L12	Translation
YPK_0354	*hupA*	-1,8	histone family protein DNA-binding protein	Replication
YPK_3231	*hupB*	-1,8	histone family protein DNA-binding protein	Replication
YPK_3757	*rplU*	-1,8	ribosomal protein L21	Translation
YPK_4249		-1,7	ribosomal protein L34	Translation
Metabolism				
Downregulated loci (YPK_3567 activated)				
YPK_0025	*yiaF*	-2,1	putative lipoprotein	Amino acid transport
YPK_0076	*hutU*	-2,3	urocanate hydratase	Amino acid transport
YPK_0077	*hutH*	-3,5	histidine ammonia-lyase	Amino acid transport
YPK_0078	*hutT*	-2,6	amino acid permease-associated region	Energy production and conversion
YPK_0364	*aceB*	-2,2	malate synthase A	Energy production and conversion
YPK_0365	*aceA*	-1,7	isocitrate lyase	Energy production and conversion
YPK_1375		-3,1	extracellular solute-binding protein family 1	Inorganic ion transport and metabolism
YPK_1377		-1,8	ABC transporter related	Amino acid transport
YPK_1463	*sfuA*	-1,8	extracellular solute-binding protein family 1	Inorganic ion transport and metabolism
YPK_1520	*fabB*	-1,8	beta-ketoacyl synthase	Lipid transport and metabolism
YPK_2070	*oppA*	-1,8	extracellular solute-binding protein family 5	Amino acid transport
YPK_3445	*sodC*	-1,9	superoxide dismutase	Inorganic ion transport and metabolism
YPK_4225	*atpG*	-1,8	ATP synthase F1, gamma subunit	Energy production and conversion
Upregulated loci (YPK_3567 repressed)				
YPK_0906		1,8	holin family 2	Amino acid transport Inorganic ion transport
Cellular processes and signaling				
Downregulated loci (YPK_3567 activated)				
YPK_1760		-2,1	N-acetylmuramyl-L-alanine amidase, negative regulator of AmpC, AmpD	Defense mechanisms
YPK_1917	*hslJ*	-1,8	protein of unknown function DUF306 Meta and HslJ	Posttranslational modification

YPK_2017	*cstA*	-1,8	carbon starvation protein CstA	Signal transduction mechanisms
YPK_2630	*ompA*	-2,0	OmpA domain protein transmembrane region-containing protein	Cell wall/membrane/envelope biogenesis
YPK_2649			porin Gram-negative type	Cell wall/membrane/envelope biogenesis
YPK_2784	*spr*		NLP/P60 protein	Cell wall/membrane/envelope biogenesis
YPK_0270	*fkpA*	-1,7	peptidylprolyl isomerase	Posttranslational modification
YPK_3452	*htrA*	-1,8	protease Do	Posttranslational modification
Transport and secretion, structural proteins				
Upregulated loci (YPK_3567 repressed)				
YPK_0702	*flhA*	1,8	type III secretion FHIPEP protein	Cell motility; Intracellular trafficking, secretion, and vesicular transport
Others (no described function)				
Downregulated loci (YPK_3567 activated)				
YPK_0547		-1,8	protein of unknown function DUF883 ElaB	
YPK_1772		-1,8	protein of unknown function DUF1480	
YPK_2643		-1,8	protein of unknown function DUF1379	
YPK_4187		-1,9	HAD-superfamily hydrolase, subfamily IA, variant 3	General function prediction only
Upregulated loci (YPK_3567 repressed)				
YPK_0102		1,9	4-oxalocrotonate tautomerase family enzyme	General function prediction only
Hypothetical Proteins				
Downregulated loci (YPK_3567 activated)				
YPK_0497		-3,7	conserved hypothetical protein	
YPK_2025		-1,8	conserved hypothetical protein	
YPK_2200		-2,9	hypothetical protein YPK_2200	
YPK_3549		-6,2	conserved hypothetical protein	
YPK_3567		-6,2	conserved hypothetical protein	
YPK_4107		-2,0	conserved hypothetical protein	
YPK_4108		-2,4	conserved hypothetical protein	

Danksagung

Großer Dank geht an Prof. Dr. Petra Dersch für die Vergabe meines interessanten Themas und ihr konstantes Interesse am Fortgang meiner Arbeit.

Ich danke Prof. Dr. André Fleissner für die unkomplizierte Übernahme des Koreferats und die damit verbundene Begutachtung meiner Arbeit.

Herzlicher Dank geht an Dr. Ann Kathrin Heroven für ein stets offenes Ohr und hilfreiche Diskussionen bezüglich meiner Experimente. Ganz besonders möchte ich mich für den Einsatz während der intensiven Zeit meiner Promotion bedanken, während der sie keine Mühen scheute und meine Arbeit trotz Gipsarm korrigiert hat.

Weiterhin bedanke ich mich bei Dr. Susanne Talay und PD Dr. Simone Bergmann, für die konstruktive Teilnahme an meinen Thesis Komitees. Simone Bergmann danke ich darüber hinaus für die Übernahme des Prüfungsvorsitzes.

Außerdem danke ich der Graduierten Schule für meine Teilfinanzierung und die Organisation verschiedener Aktivitäten, die im Rahmen der Promotion den wissenschaftlichen Austausch innerhalb der Doktoranden ermöglichten.

Mein größter Dank gilt meiner Familie und meinen Freunden, die mich während der gesamten Promotionszeit begleitet, mit Rat und Tat unterstützt und besonders meine Launen toleriert haben.

Ein herzliches Dankeschön an alle "MIBIs", die mir immer ein großartiges Kollegium gewesen sind, meine Ergebnisse kritisch begutachtet haben, meine Stimmungen toleriert und ertragen haben, mich zum Lachen brachten, mich stetig zum Weitermachen motivierten und unterstützten wo sie konnten.

Hierbei gilt mein besonderer Dank dem "irRNA Labor" mit Rebekka und Babsi - wir hatten eine ganz besondere Zeit, die mit vielen schönen Erinnerungen einhergeht.

In diesem Zuge geht auch ein großes Dankeschön an Tanja Krause, die mich von Anfang an herzlich willkommen geheißen hat und mir eine gute Freundin geworden ist.

Last but not least danke ich Rebecca, die mir eine "Konstante" während der gesamten Zeit gewesen ist, mich immer und immer unterstützt und motiviert und mit mir zusammen den Traum vom Surfen in die Tat umgesetzt hat 🤙